MICROBIAL BIOFILMS IN CHRONIC AND RECURRENT INFECTIONS

EDITED BY: Axel Cloeckaert, Karl Kuchler, Enea Gino Di Domenico, Fiorentina Ascenzioni, Catherine Dunyach-Remy and María Guembe

PUBLISHED IN: Frontiers in Microbiology

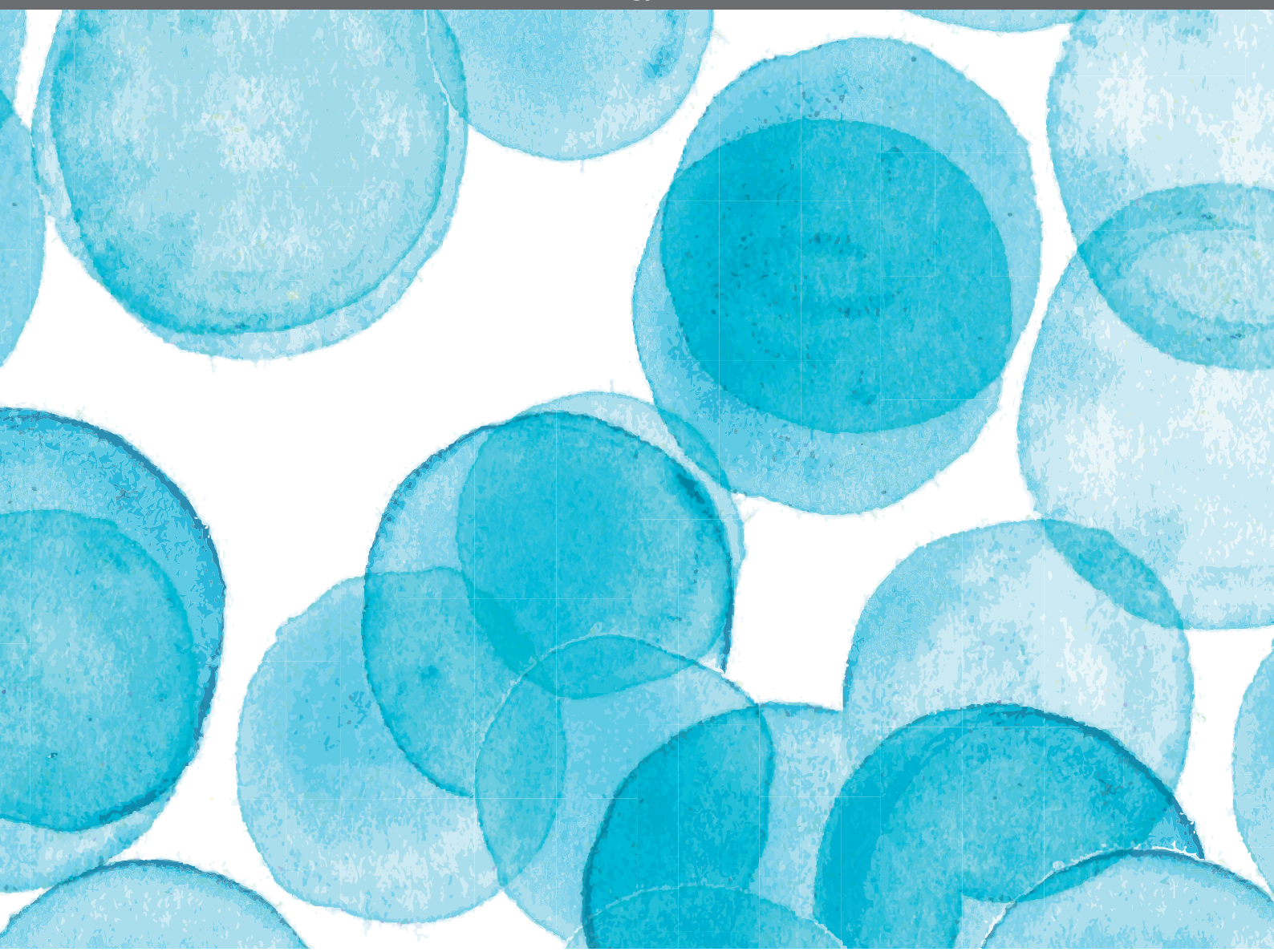

frontiers Research Topics

frontiers

ISSN 1664-8714
ISBN 978-2-88974-099-4
DOI 10.3389/978-2-88974-099-4

About Frontiers

Frontiers is more than just an open-access publisher of scholarly articles: it is a pioneering approach to the world of academia, radically improving the way scholarly research is managed. The grand vision of Frontiers is a world where all people have an equal opportunity to seek, share and generate knowledge. Frontiers provides immediate and permanent online open access to all its publications, but this alone is not enough to realize our grand goals.

Frontiers Journal Series

The Frontiers Journal Series is a multi-tier and interdisciplinary set of open-access, online journals, promising a paradigm shift from the current review, selection and dissemination processes in academic publishing. All Frontiers journals are driven by researchers for researchers; therefore, they constitute a service to the scholarly community. At the same time, the Frontiers Journal Series operates on a revolutionary invention, the tiered publishing system, initially addressing specific communities of scholars, and gradually climbing up to broader public understanding, thus serving the interests of the lay society, too.

Dedication to Quality

Each Frontiers article is a landmark of the highest quality, thanks to genuinely collaborative interactions between authors and review editors, who include some of the world's best academicians. Research must be certified by peers before entering a stream of knowledge that may eventually reach the public - and shape society; therefore, Frontiers only applies the most rigorous and unbiased reviews.
Frontiers revolutionizes research publishing by freely delivering the most outstanding research, evaluated with no bias from both the academic and social point of view. By applying the most advanced information technologies, Frontiers is catapulting scholarly publishing into a new generation.

What are Frontiers Research Topics?

Frontiers Research Topics are very popular trademarks of the Frontiers Journals Series: they are collections of at least ten articles, all centered on a particular subject. With their unique mix of varied contributions from Original Research to Review Articles, Frontiers Research Topics unify the most influential researchers, the latest key findings and historical advances in a hot research area! Find out more on how to host your own Frontiers Research Topic or contribute to one as an author by contacting the Frontiers Editorial Office: frontiersin.org/about/contact

MICROBIAL BIOFILMS IN CHRONIC AND RECURRENT INFECTIONS

Topic Editors:
Axel Cloeckaert, l'alimentation et l'environnement (INRAE), France
Karl Kuchler, Medical University of Vienna, Austria
Enea Gino Di Domenico, Hospital Physiotherapy Institutes (IRCCS), Italy
Fiorentina Ascenzioni, Sapienza University of Rome, Italy
Catherine Dunyach-Remy, INSERM U1047 Virulence Bactérienne et Maladies Infectieuses, France
María Guembe, Gregorio Marañón Hospital, Spain

Citation: Cloeckaert, A., Kuchler, K., Di Domenico, E. G., Ascenzioni, F., Dunyach-Remy, C., Guembe, M., eds. (2022). Microbial Biofilms in Chronic and Recurrent Infections. Lausanne: Frontiers Media SA.
doi: 10.3389/978-2-88974-099-4

Table of Contents

frontiers in Microbiology

EDITORIAL
published: 30 November 2021
doi: 10.3389/fmicb.2021.803324

Editorial: Microbial Biofilms in Chronic and Recurrent Infections

Fiorentina Ascenzioni[1], *Axel Cloeckaert*[2], *Enea Gino Di Domenico*[3]*, *Catherine Dunyach-Remy*[4] *and María Guembe*[5,6]

[1] Department of Biology and Biotechnology "Charles Darwin", Sapienza University of Rome, Rome, Italy, [2] INRAE, Université de Tours, UMR, ISP, Nouzilly, France, [3] Microbiology and Virology, IRCCS San Gallicano Institute, Rome, Italy, [4] VBIC, INSERM U1047, Université de Montpellier, Service de Microbiologie et Hygiène Hospitalière, CHU Nîmes, Nîmes, France, [5] Instituto de Investigación Sanitaria Gregorio Marañón, Madrid, Spain, [6] Department of Clinical Microbiology and Infectious Diseases, Hospital General Universitario Gregorio Marañón, Madrid, Spain

Keywords: biofilm, infection, inflammation, resistance, antibiotic

Editorial on the Research Topic

Microbial Biofilms in Chronic and Recurrent Infections

Biofilm plays a significant role in the pathogenesis of most chronic infections in humans, either tissue-specific or involving medical implants (Lebeaux et al., 2014). Biofilm-associated infections exhibit high resistance to host defenses, often contributing to an excessive or inappropriate inflammatory response leading to further tissue damage and spreading of the infection (Jensen et al., 2010). On the other hand, biofilms are highly tolerant to antimicrobial therapy (Römling and Balsalobre, 2012; Di Domenico et al., 2019). Biofilms can tolerate up to 100–1,000 times higher minimal inhibitory concentration (MIC) than the same bacterial cells in planktonic growth (Macià et al., 2014). Unfortunately, the effective antibiotic MIC *in vivo* for biofilm eradication may be impossible to reach due to the drugs' toxicity and side effects, including limitations imposed by renal and/or hepatic functions (Ciofu et al., 2015). However, *in vitro* experiments showed that an aggressive antibiotic treatment can effectively eradicate biofilm during the initial stage of colonization (Lebeaux et al., 2014; Ciofu et al., 2015). Despite their importance, the early recognition of biofilm-associated infections still represents an unmet need in clinical microbiology. Therefore, the development of novel diagnostic and therapeutic strategies is urgently needed to manage biofilm-associated infections effectively.

We thank all the authors who contributed with their relevant works to this Research Topic by analyzing different aspects of the pathogenesis and therapeutic management of chronic biofilm-related infections.

In their review paper, Huang et al., examined the most recent metagenomic and metatranscriptomic evidence to study the links between microbial dysbiosis and periodontitis. It has been well-established that polymicrobial biofilms play an essential role in the initiation and progression of periodontitis. In particular, an imbalanced microbial community alters the host response, leading to inappropriate inflammation, further damaging periodontal tissues. In turn, the inflammatory response affects the oral microbiome and modulates the expression of bacterial virulence factors. The authors concluded that assessing the correlation between the dynamic changes in the functional behaviors of the periodontal microbiome and the progression and outcome of periodontitis might provide valuable information for developing effective prevention and treatment strategies.

Dental caries is another typical biofilm-related disease of the oral cavity, and the acidification of biofilm pH is central in diseases development. Zhang et al. showed that pH-responsive core-shell nano micelle loaded with bedaquiline, can potently inhibit the growth of *Streptococcus mutans*

OPEN ACCESS

Edited and reviewed by:
Daniel Pletzer,
University of Otago, New Zealand

***Correspondence:**
Enea Gino Di Domenico
enea.didomenico@ifo.gov.it

Specialty section:
This article was submitted to Infectious Agents and Disease, a section of the journal Frontiers in Microbiology

Received: *27 October 2021*
Accepted: *12 November 2021*
Published: *30 November 2021*

Citation:
Ascenzioni F, Cloeckaert A, Di Domenico EG, Dunyach-Remy C and Guembe M (2021) Editorial: Microbial Biofilms in Chronic and Recurrent Infections. Front. Microbiol. 12:803324. doi: 10.3389/fmicb.2021.803324

biofilm in an acidic environment (pH 5) without cytotoxic effect on the periodontal cells. Therefore, this pH-responsive micelle showed great potential in preventing dental caries.

Biofilm formation on implant surfaces is considered the main risk factor for inflammatory tissues processes and implant failure. However, in many cases, traditional cultures have proven poor sensitivity in pathogen isolation. In their paper, Oliva, Miele et al. provided a critical overview on the principal culture-based methods, sonication technique molecular testing used in the clinical practice for the most effective identification of the causative agents of implant-associated infections.

Biofilm-growing *Staphylococcus aureus* is a prominent cause of implant-associated infections. The study conducted by Yu et al. showed that *S. aureus* nucleases nuc1 and nuc2 are complementary genes involved in biofilm formation in implant-associated infections, with nuc2 contributing less to virulence and immune evasion.

S. aureus is also the most feared pathogen in another clinically relevant infection like a prosthetic joint infection. The study presented by Lamret et al. has hypothesized that the periprosthetic bone environment is stressful for *S. aureus*, influencing biofilm development. The authors assessed several parameters to mimic bone environment, such as lack of oxygen, casamino acids and glucose starvation, and high magnesium concentration. In the classic *in vitro* model, the *S. aureus* strains formed various biofilm structures. However, in the bone-like environment, these strains shared common responses, including the increase in biofilm biomass and number of adherent cells proportion with a similar production of extracellular DNA and engagement of the SOS response. By mimicking the highly challenging bone-like conditions, this model may provide the base for future anti-biofilm strategies.

In an *in vitro* model simulating a prosthetic joint infection, Scheper et al. evaluated the effects of antimicrobial peptides on Methicillin-resistant *S. aureus* (MRSA) persisters exposed to antibiotics. The combined activity of rifampicin and ciprofloxacin alone did not eliminate persister cells within mature biofilms grown on polystyrene plates, titanium/aluminum/niobium disks, and prosthetic joint liners. However, SAAP-148, a synthetic peptide based on LL-37, eradicated persisters within mature biofilms on different abiotic surfaces. Based on these data, SAAP-148 resulted in a promising candidate for further development as an agent for the treatment of biofilm-associated prosthetic joint infection.

MRSA isolates are of particular concern in patients with cystic fibrosis. Biofilm formation is a common characteristic of pathogenic MRSA strains representing a critical barrier to eradication treatment and host defenses. In their study, Boudet et al. investigated, by the Antibiofilmogram®, the ability of MRSA isolates from patients with cystic fibrosis to form a biofilm with and without antibiotics. They highlighted that ceftaroline and ceftobiprole were remarkably active in hampering the biofilm formation of certain strains adapted to the lung environment of patients with cystic fibrosis. In addition, the authors concluded that the Antibiofilmogram® could be a promising tool for guiding the choice of the most effective drugs against biofilm-growing MRSA in CF airways.

The lipoglycopeptide dalbavancin emerged as another promising agent for treating biofilm-related infections. In the review article presented by Oliva, Stefani et al. the authors outlined the mechanisms regulating biofilm development in *Staphylococcus* and *Enterococcus* species and the clinical impact of biofilm-related infections. Thus, the authors conclude that the use of dalbavancin may represent a valuable option for the treatment of skin and soft tissues infections and other invasive Gram-positive infections.

Biofilm plays a significant role in the progression and chronicity of diabetic foot ulcers. In their review article, Pouget et al. discussed current knowledge and the contribution of biofilms on diabetic foot ulcers. In particular, the authors focused on preventive strategies to hinder the establishment of microbial biofilms and wound chronicity to support or eventually replace the current approach for managing diabetic foot ulcers.

Biofilms contribute to the pathogenesis of several otorhinolaryngologic chronic infective disorders, including otitis media, chronic rhinosinusitis, and cholesteatoma. Patients with acquired cholesteatoma generally present with chronic otorrhea and progressive conductive hearing loss. Jiang et al. highlighted by next-generation sequencing (NGS)-based approach that the severity of the patient's pathological condition worsens the more complex the types of microbes' infections. The results obtained from this study revealed that the most commonly detected microbial genus was *Aspergillus*, particularly in patients with severe bone erosion. In summary, NGS help to identify pathogens of cholesteatoma patients and *Aspergillus* infections in acquired cholesteatoma.

Finally, we would like to thank the people that supported this Research Topic and the reviewers for their time and comments that helped to improve the manuscripts.

AUTHOR CONTRIBUTIONS

All authors have contributed substantially to the manuscript, providing a direct, and intellectual contribution to the work. All authors approved the final version of the manuscript.

REFERENCES

Ciofu, O., Tolker-Nielsen, T., Jensen, P. Ø., Wang, H., and Høiby, N. (2015). Antimicrobial resistance, respiratory tract infections and role of biofilms in lung infections in cystic fibrosis patients. *Adv. Drug Deliv. Rev.* 85, 7–23. doi: 10.1016/j.addr.2014.11.017

Di Domenico, E. G., Rimoldi, S. G., Cavallo, I., D'Agosto, G., Trento, E., Cagnoni, G., et al. (2019). Microbial biofilm correlates with an increased antibiotic tolerance and poor therapeutic outcome in infective endocarditis. *BMC Microbiol.* 19:228. doi: 10.1186/s12866-019-1596-2

Jensen, P. Ø., Givskov, M., Bjarnsholt, T., and Moser, C. (2010). The immune system vs. Pseudomonas aeruginosa biofilms. *FEMS Immunol. Med. Microbiol.* 59, 292–305. doi: 10.1111/j.1574-695X.2010.00706.x

Lebeaux, D., Ghigo, J. M., and Beloin, C. (2014). Biofilm-related infections: Bridging the gap between clinical management and fundamental aspects of recalcitrance toward antibiotics. *Microbiol. Mol. Biol. Rev*. 78, 510–543. doi: 10.1128/MMBR.00013-14

Macià, M. D., Rojo-Molinero, E., and Oliver, A. (2014). Antimicrobial susceptibility testing in biofilm-growing bacteria. *Clin. Microbiol. Infect*. 20, 981–990. doi: 10.1111/1469-0691.12651

Römling, U., and Balsalobre, C. (2012). Biofilm infections, their resilience to therapy and innovative treatment strategies. *J. Intern. Med*. 272, 541–561. doi: 10.1111/joim.12004

Conflict of Interest: The authors declare that the research was conducted in the absence of any commercial or financial relationships that could be construed as a potential conflict of interest.

Publisher's Note: All claims expressed in this article are solely those of the authors and do not necessarily represent those of their affiliated organizations, or those of the publisher, the editors and the reviewers. Any product that may be evaluated in this article, or claim that may be made by its manufacturer, is not guaranteed or endorsed by the publisher.

frontiers in Microbiology

ORIGINAL RESEARCH
published: 29 January 2021
doi: 10.3389/fmicb.2021.625952

SAAP-148 Eradicates MRSA Persisters Within Mature Biofilm Models Simulating Prosthetic Joint Infection

Henk Scheper[1], Julia M. Wubbolts[1], Joanne A. M. Verhagen[1], Adriëtte W. de Visser[1], Robert J. P. van der Wal[2], Leo G. Visser[1], Mark G. J. de Boer[1] and Peter H. Nibbering[1]*

[1] Department of Infectious Diseases, Leiden University Medical Center, Leiden, Netherlands, [2] Department of Orthopedic Surgery, Leiden University Medical Center, Leiden, Netherlands

OPEN ACCESS

Edited by:
Catherine Dunyach-Remy, INSERM U1047 Virulence Bactérienne et Maladies Infectieuses, France

Reviewed by:
Deirdre Fitzgerald-Hughes, Royal College of Surgeons in Ireland, Ireland
Fany Reffuveille, Université de Reims Champagne-Ardenne, France

***Correspondence:**
Henk Scheper
h.scheper@lumc.nl

Specialty section:
This article was submitted to Infectious Diseases, a section of the journal Frontiers in Microbiology

Received: 04 November 2020
Accepted: 12 January 2021
Published: 29 January 2021

Citation:
Scheper H, Wubbolts JM, Verhagen JAM, de Visser AW, van der Wal RJP, Visser LG, de Boer MGJ and Nibbering PH (2021) SAAP-148 Eradicates MRSA Persisters Within Mature Biofilm Models Simulating Prosthetic Joint Infection. Front. Microbiol. 12:625952. doi: 10.3389/fmicb.2021.625952

Prosthetic joint infection (PJI) is a severe complication of arthroplasty. Due to biofilm and persister formation current treatment strategies often fail. Therefore, innovative anti-biofilm and anti-persister agents are urgently needed. Antimicrobial peptides with their broad antibacterial activities may be such candidates. An *in vitro* model simulating PJI comprising of rifampicin/ciprofloxacin-exposed, mature methicillin-resistant *Staphylococcus aureus* (MRSA) biofilms on polystyrene plates, titanium/aluminium/niobium disks, and prosthetic joint liners were developed. Bacteria obtained from and residing within these biofilms were exposed to SAAP-148, acyldepsipeptide-4, LL-37, and pexiganan. Microcalorimetry was used to monitor the heat flow by the bacteria in these models. Daily exposure of mature biofilms to rifampicin/ciprofloxacin for 3 days resulted in a 4-log reduction of MRSA. Prolonged antibiotic exposure did not further reduce bacterial counts. Microcalorimetry confirmed the low metabolic activity of these persisters. SAAP-148 and pexiganan, but not LL-37, eliminated the persisters while ADEP4 reduced the number of persisters. SAAP-148 further eradicated persisters within antibiotics-exposed, mature biofilms on the various surfaces. To conclude, antibiotic-exposed, mature MRSA biofilms on various surfaces have been developed as *in vitro* models for PJI. SAAP-148 is highly effective against persisters obtained from the biofilms as well as within these models. Antibiotics-exposed, mature biofilms on relevant surfaces can be instrumental in the search for novel treatment strategies to combat biofilm-associated infections.

Keywords: MRSA, prosthetic joint infection, biofilms, persisters, antimicrobial peptides, SAAP-148, ADEP4

INTRODUCTION

Yearly over one million prosthetic joints are implanted in patients in the United States. Prosthetic joint infection (PJI) is a severe complication occurring in 1–3% of patients and has a high economic burden on health care systems. Most PJIs are caused by staphylococci (Tande and Patel, 2014; Zeller et al., 2018). Treatment of patients with an acute PJI consists of thorough surgical debridement of the implant and the infected tissue around it, followed by 6–12 weeks of antibiotic therapy.

Nevertheless, failure rates for this treatment strategy are considerable, ranging from 10 to 45% in some of the largest studies (Lora-Tamayo et al., 2013, 2017). An important cause of treatment failure is the formation of a biofilm on the surface of the implant. A biofilm is formed by bacteria that, after adherence to the implant, form a matrix of extrapolymeric substances (EPS) that protect bacteria against the actions of antibiotics and effectors of host's immune systems (Lewis, 2010). Within biofilms bacteria may switch phenotypically to a metabolically inactive, non-dividing, dormant state, called persisters (Balaban et al., 2004; Lewis, 2010). Persisters are defined as metabolically inactive, dormant bacteria that survive lethal concentrations of antibiotics without induction of resistance. The formation of persisters is triggered by stress factors like lack of nutrients and exposure to antibiotics (Harms et al., 2016). Persisters within biofilms are tolerant to antibiotic therapy, which contributes to PJI treatment failures (Conlon et al., 2013). Based on these considerations, innovative anti-biofilm and anti-persister treatment strategies are urgently needed. For evaluation of such candidates an *in vitro* biofilm model that approximates a PJI as closely as possible is instrumental.

Antimicrobial peptides are considered promising candidates to combat biofilm-associated infections. For instance, the human cathelicidin LL-37 has broad-spectrum antibacterial activities, including antibiofilm activity, together with immune modulating capabilities (van der Does et al., 2010). SAAP-148, a synthetic peptide based on LL-37, has shown to be more effective in eradicating bacteria than LL-37 (de Breij et al., 2018). Acyldepsipeptide 4 (ADEP4) activates bacterial proteases in an ATP-independent manner resulting in cell death. In combination with rifampicin, ADEP4 eradicates biofilms in a mouse model with a chronic *S. aureus* infection (Conlon et al., 2013). Pexiganan, an analog of magainin isolated from the skin of the African clawed frog, exhibited *in vitro* broad-spectrum antibacterial activity (Ge et al., 1999; Haisma et al., 2016).

For the current study we developed an *in vitro* biofilm model approximating a PJI as closely as possible. With this model the efficacy of four promising antimicrobial peptides on persisters and bacteria in other growth modes in mature biofilms was assessed.

MATERIALS AND METHODS

Antibiotics and Antimicrobial Peptides

Ciprofloxacin hydrochloride (Sigma-Aldrich, PHR 1044-1G) and rifampicin (Sigma-Aldrich, R3501-250 mg) at concentrations corresponding to 10x the minimal bactericidal concentration (MBC) for MRSA LUH14616 were used (1.28 mg/mL ciprofloxacin, 10 μg/mL rifampicin). The MBC was defined as the lowest concentration that killed 99.9% of the bacteria compared to untreated control bacteria. SAAP-148 (LKRVWKRVFKLLKRYWRQLKKPVR), LL 37 (LLGDFFRKSKEKIGKEFKRIVQRIKDFLRNLVPRTES), and pexiganan (GIGKFLKKAKKFGKAFVKILKK), all N-terminal acetylated, C-terminal amidated, were synthesized by solid phase strategies on an automated multiple peptide synthesizer (SyroII, MultiSyntech, Witten, Germany) as described elsewhere (Nell et al., 2006; Haisma et al., 2014; de Breij et al., 2018). The molecular mass of the peptides was confirmed by mass spectrometry and the purity of the peptide exceeded 95%, as determined by reverse phase high-performance liquid chromatography. The lyophilized peptides were stored at −20°C until use. The Clp protease activator acyldepsipeptide 4 (ADEP4) was purchased from ABGENT, a WuXi AppTec company (China); the purity of this commercial peptide was >98%. Peptide stocks were stored in 0.01% acetic acid (pexiganan), dimethyl sulphoxide (ADEP4), and milliQ (SAAP-148 and LL-37). For experiments, peptide stocks were diluted in phosphate-buffered saline (PBS) to the desired concentrations.

Methicillin-Resistant *Staphylococcus aureus*

Methicillin-resistant *Staphylococcus aureus* (MRSA) LUH14616 sequence type 247, was collected by a nasal swab from a patient without an infection. It was preserved in nutrient broth supplemented with 20% glycerol at −80°C. Prior to experiments, inocula from the frozen stocks were grown overnight at 37°C on sheep blood agar plates (BioMerieux). Thereafter, bacteria were cultured to mid-log phase in tryptic soy broth for 2.5 h at 37°C. Finally, the bacteria were harvested by centrifugation (1,000 × *g* for 10 min) and then resuspended in PBS to the desired inoculum concentration (10^7 CFU/mL), based on the optical density at 600 nm.

In vitro Biofilm Model Simulating Biofilm Associated Infection

Mid-log phase MRSA were diluted to 10^7 CFU/mL in brain heart infusion (BHI) medium. Next, 100 μl of this suspension were cultured in 96-wells polystyrene plates covered with breathable seals and incubated at 37°C for 7 days in a humidified environment. Thereafter, the medium was removed and the wells were washed twice with PBS (140 mM NaCl and pH 7.4). Next, 100 μL of fresh BHI medium containing ciprofloxacin and rifampicin, both 10x MBC, was carefully added to each well in order not to disrupt the biofilm. The medium containing antibiotics was refreshed daily for 72 h. In the second model TAN disks (consisting of titanium7%-aluminium6%-niobium; ISO5832/11) were inserted in the 96-well plates and mature biofilms were developed on these metal disks using the protocol as above. A third model comprised of bacterial biofilms developed on the bottom of the cup of a prosthetic hip liner. Twelve ultra-high-molecular-weight polyethylene acetabular cups were provided by Waldemar Link GmbH & Co., KG (Germany). During formation of the biofilm and antibiotic exposure, the liner was covered with aluminium foil to prevent contamination and dehydration of the biofilm. Liners were re-used due to the limited number of liners provided. Prior to re-use, the liner was, after rinsing with 70% ethanol, submerged in 70% ethanol overnight after which the liner was rinsed again with 70% ethanol and autoclaved thereafter. The experiments with the liners were done twice. In the first dose-finding experiment liners were tested per increasing SAAP-148

concentration. Thereafter, the experiment was repeated for the concentrations with the highest effectivity in the first experiment. A schematic overview of the different models is provided in **Figure 1**.

Assessment of the Effects of Antimicrobial Peptides on Persisters in Antibiotics-Exposed Mature Biofilms

The activity of antimicrobial peptides against bacteria, i.e., persisters and possibly other bacterial subpopulations with a long lag time, in antibiotics-exposed mature biofilms was assessed by exposure of the biofilms to increasing concentrations of antimicrobial peptides in PBS for 2 or 24 h after removal of the supernatant. Prior to and at the indicate interval after exposure to the peptide, biofilms were sonicated in PBS and the number of surviving bacteria was determined microbiologically. In case of complete eradication bacterial plates were inspected again after 5 days in the incubator for possible regrowth of persisters and/or bacteria with a long lag time. To assess the direct effects of the peptides on these bacterial subpopulations, antibiotics-exposed mature biofilms from multiple wells were sonicated, pooled and diluted in PBS and then exposed to increasing concentrations of antimicrobial peptides. The possibility that not all bacteria could be obtained from biofilms by sonication was investigated microbiologically and we did not find viable bacteria (even up to 5 days of maintaining the bacterial plates in the incubator) remaining in the wells. In addition, the viability of bacteria was also not affected by the sonication procedure used in these experiments.

Isothermal Microcalorimetric Assay

Isothermal microcalorimetry (IMC) was used to monitor heat flow (μW) by MRSA in four different stages during the formation of antibiotics-exposed mature biofilms on TAN disks in real time for 30 h using a Calscreener (Symcel Sverige, Spånga, Sweden). BHI broth was used as a reference to calibrate the Calscreener. Mature biofilms and antibiotics-exposed mature biofilms were developed in this model as described above. After removal of the supernatant by two washes with PBS the inserts containing the biofilms were transferred to metal microcontainers and then exposed to 100 μL of BHI with or without 51.2 μM SAAP-148 peptide. In addition, 100 μL of 1×10^7 CFU planktonic MRSA/mL was transferred to metal microcontainers. Furthermore, microcontainers with 100 μL of BHI served as a control. All metal microcontainers were maintained in the Calscreener for 4 days at 37°C for continuous monitoring of the heat production by the various bacterial populations. At the end of the experiments the microcontainers were sonicated for 10 min and the number of persisters was determined microbiologically and cultured for 5 days afterward.

Statistical Analysis

The non-parametric Mann–Whitney *U* test was performed to determine statistical significance when comparing medians of antibiotics and/or antimicrobial peptide treated biofilms using GraphPad prism (GraphPad software, La Jolla, CA, United States). *P* values ≤ 0.05 were considered to be statistically significant different.

RESULTS

Effect of Antibiotics on Bacteria Within Mature Biofilms on Polystyrene

A constant bacterial load of 8 log CFU/ml was present during the seven days of biofilm maturition (**Figure 2A**). Results revealed a time-dependent reduction in bacterial counts in seven-day mature antibiotics-exposed MRSA biofilms on polystyrene plates with a maximum 4 log reduction at day three-four (**Figure 2B**), indicating that the surviving bacteria were antibiotic-tolerant. Therefore, antibiotic exposure of mature biofilms for more than 3 days was considered sufficient for persister enrichment.

MRSA in Antibiotics-Exposed Mature Biofilms Are Dormant

To further characterize these antibiotic-tolerant bacteria their metabolic activity was measured by isothermal calorimetry. Results revealed that heat flow of these bacteria in antibiotics-exposed, mature biofilms was almost zero (**Figures 3A–C**), indicating that these bacteria are metabolically inactive, i.e., persisters. Of note, an initial modest peak of 7 μW upon incubation of these cells with BHI confirms their ability to revive. For comparison, we also assessed heat flow by planktonic MRSA and bacteria in mature biofilms. Results revealed two peaks in the heat flow curve of planktonic bacteria: the first peak occurred after 2.5 h of incubation and the second peak at 6–8 h (**Figure 3A**). Thereafter, heat flow dropped to a value of approximately 10 μW, probably due to the evolution to stationary phase bacteria with less metabolic activity. MRSA within mature biofilms supplemented with BHI (bacterial load $> 5 \times 10^8$ MRSA) showed a peak in heat production around 6 h after which the level decreased to a continuous level of 10 μW, which was equal to heat production by stationary phase bacteria (**Figure 3B**), indicating that heat production by bacteria within a biofilm is considerably less than by mid log phase bacteria.

Effect of SAAP-148, ADEP4, LL-37, and Pexiganan on MRSA Persisters

To select the most promising antimicrobial peptide, the direct effect of SAAP-148, ADEP4, LL-37, and pexiganan on persisters obtained from antibiotics-exposed, mature MRSA biofilms on polystyrene plates was assessed (**Figure 4**). Within 2 h SAAP-148 (at doses $\geq$ 1.6 μM; **Figure 4A**) and pexiganan (at doses $\geq$ 12.8 μM; **Figure 4B**) eradicated all bacteria, whereas bacterial counts were reduced by LL-37 (**Figure 4C**) and ADEP4 (**Figure 4D**). In agreement with the expectation that ADEP4 requires more time to exert its effects, we found that at 24 h of exposure all persisters were eliminated by ADEP4 (at doses $\geq$ 12.8 μM; **Figure 4E**). Of note, bacterial samples obtained after exposure to the peptides were cultured up to 5 days to ascertain that all

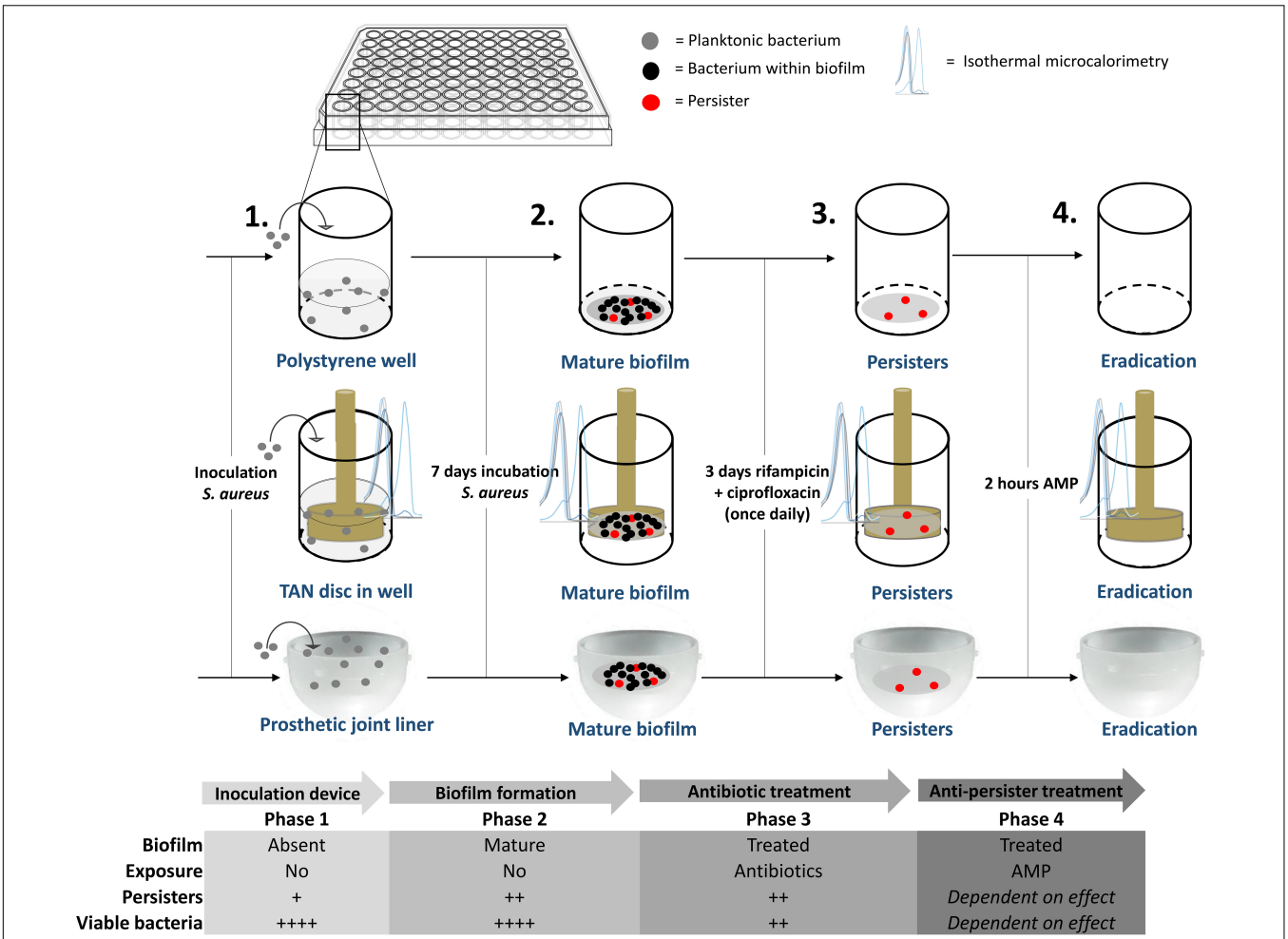

FIGURE 1 | Overview of the mature, antibiotics-exposed biofilm model. Briefly, methicillin-resistant *Staphylococcus aureus* (MRSA) were inoculated into a well, on a metal implant device within a well and into a sterile acetabular hip liner, incubated for 7 days, exposed to rifampicin and ciprofloxacin and subsequently exposed to antimicrobial peptide. AMP: antimicrobial peptide. Estimated proportion of persisters/viable bacteria: +, < 0.1%, ++, > 0.1% and < 1%; ++++, 10–100%.

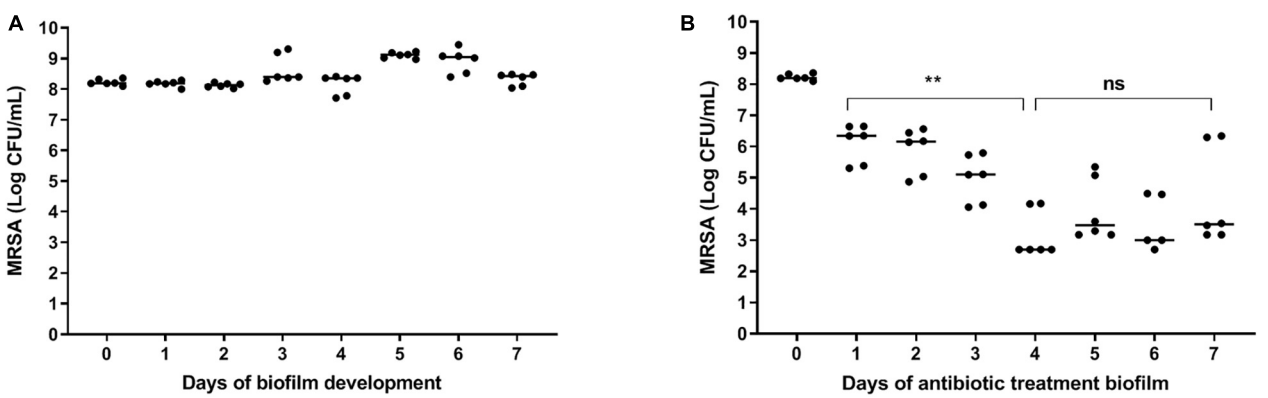

FIGURE 2 | | Effect of antibiotics on bacteria within mature biofilms on polystyrene. **(A)** The number of bacteria within biofilms on 96-well polystyrene plates remained constant for 7 days. **(B)** Exposure of a seven-day mature biofilm on 96-well polystyrene plates to rifampicin/ciprofloxacin daily for 3 days, significantly reduced the bacterial load ($p = 0.002$). Prolonged exposure to rifampicin/ciprofloxacin did not result in further reduction of bacterial counts. The solid line denotes the median log CFU/mL. $n = 3$ experiments, each in duplicate. ns, not significant.

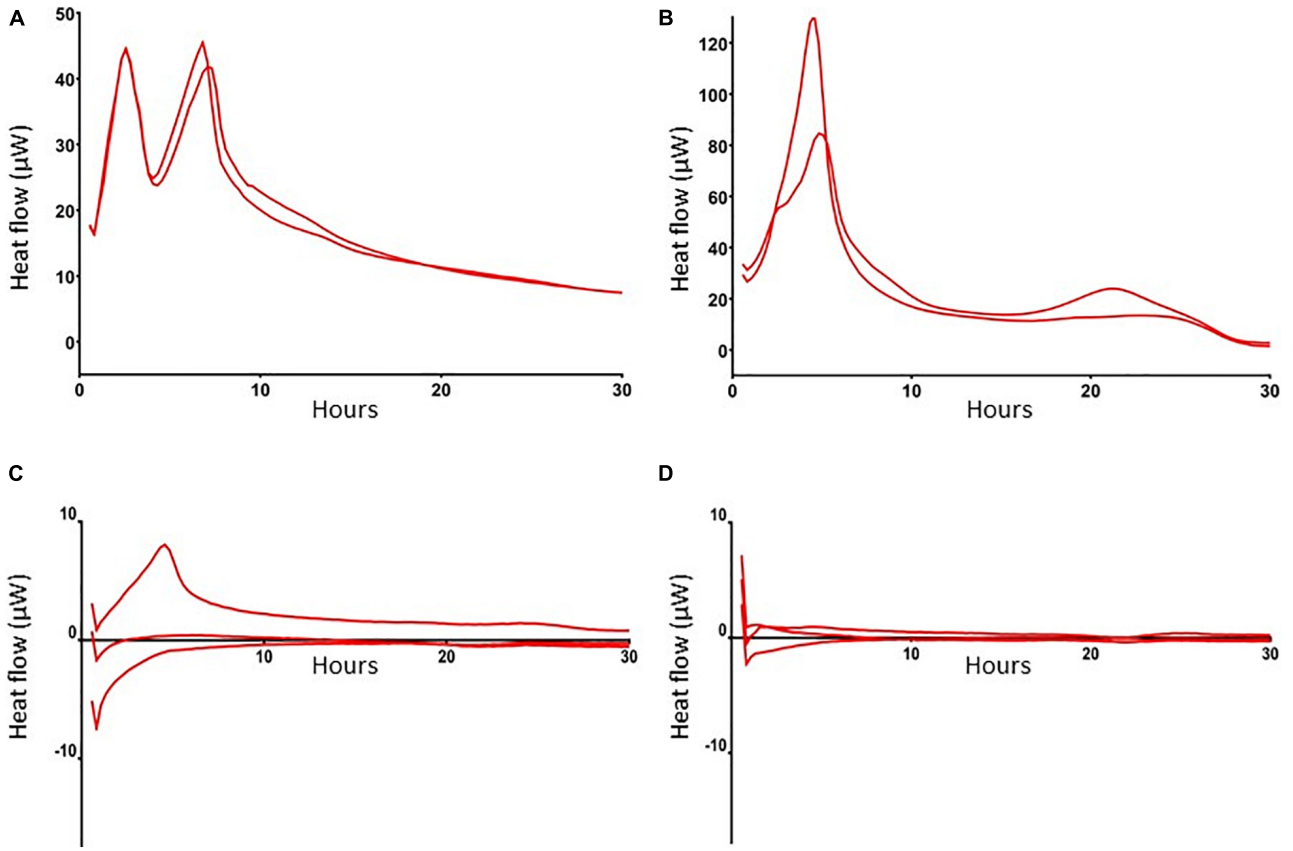

FIGURE 3 | Heat flow by MRSA in log phase, in mature biofilms and in mature, antibiotics-exposed biofilms with and without exposure to SAAP-148. Heat flow by 1×10^6 log phase MRSA **(A)**, $>5 \times 10^8$ MRSA in a mature biofilm **(B)**, 1×10^4 persisters in antibiotics-exposed biofilms upon exposure to BHI broth **(C)**, and antibiotics-exposed mature biofilms to BHI supplemented with 51.2 μM SAAP-148 **(D)**. Log-phase MRSA, MRSA in mature biofilms and antibiotics-exposed biofilms were maintained in microcontainers in a Calscreener during 30 h. There was no heat flow in the persister subpopulation apart from a small peak after addition of BHI **(C)**. Persisters exposed to SAAP-148 did not display any detectable heat flow **(D)**. Results are from two replicates of a representative experiment (n = 2–3 experiments).

persisters were killed. In addition, SAAP-148 was also highly effective in eliminating persisters residing in antibiotics-exposed, mature biofilms with complete eradication seen at ≥1.6 μM (**Figure 3F**). Based on these data SAAP-148 was selected for further experiments.

Effect of SAAP-148 on MRSA Persisters Obtained From and Residing in Antibiotics-Exposed Mature Biofilms on TAN Disks

Next, seven-days mature MRSA biofilms were produced on TAN disks and then exposed for 3 days to rifampicin and ciprofloxacin. SAAP-148 eliminated all persisters obtained from these antibiotics-exposed mature MRSA biofilms in a dose-dependent fashion with complete eradication already seen at ≥1.6 μM (**Figure 5A**). Exposure of the persisters residing in antibiotics-exposed mature biofilms to SAAP-148 also resulted in complete eradication, but at higher doses (≥51.2 μM; **Figure 5B**). Prolonged exposure of the persisters in biofilms to SAAP-148 did not improve the efficacy of the peptide (eradication at doses ≥ 51.2 μM; **Figure 5C**). To rule out the possibility that SAAP-148 was in fact effective against persisters which became metabolically active again after quitting antibiotic therapy, the experiment was repeated with addition of the antibiotics together with SAAP-148 on the fourth day of antibiotic exposure. This also resulted (in five out of six experiments) in elimination of all biofilm-embedded bacteria from a dose of 51.2 μM (**Figure 5D**). In agreement, calorimetry showed that SAAP-148 reduced heat production of bacteria residing in the biofilm on TAN disks to undetectable levels (**Figure 3D**). Together, these data indicate that higher doses of SAAP-148 are required to eliminate bacteria within the mature biofilm than when directly in contact with the persisters.

Effect of SAAP-148 on MRSA Biofilms Formed on a Polyethylene Insert of a Prosthetic Hip Joint

To simulate a PJI more closely, the effect of different SAAP-148 concentrations was assessed on persisters in antibiotics-exposed,

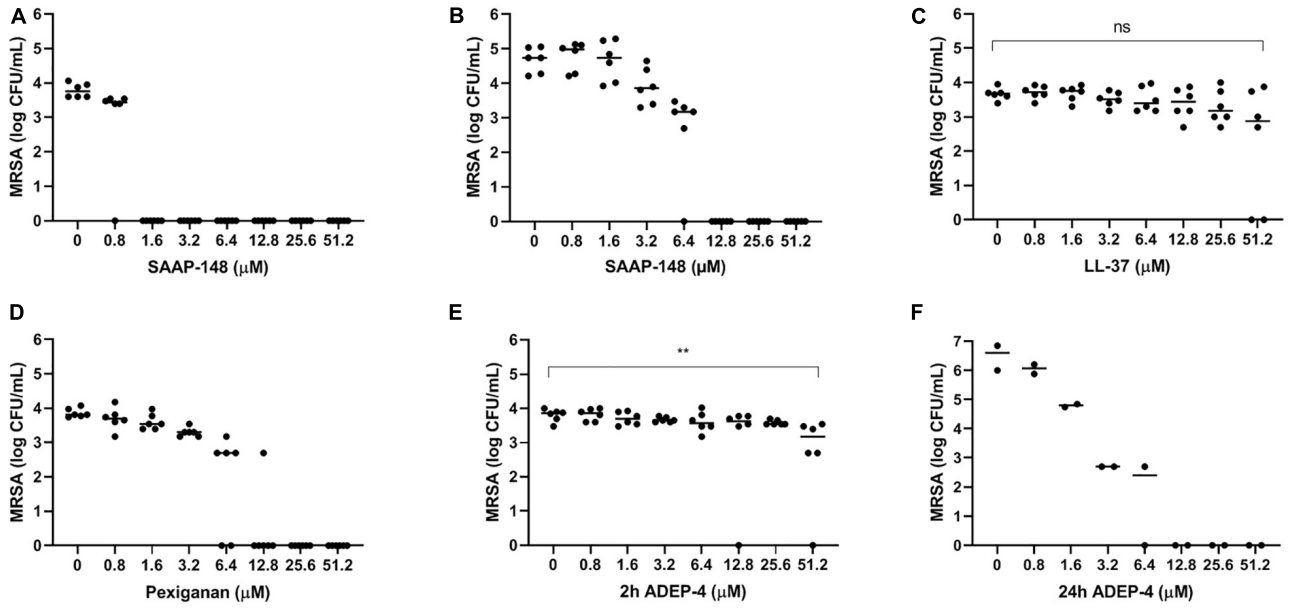

FIGURE 4 | Effect of SAAP-148, ADEP4, LL-37, and pexiganan on MRSA originating from antibiotics-exposed seven-day mature biofilms. SAAP-148 resulted in complete eradication of bacteria sonicated from antibiotics-exposed seven-day mature biofilms on polystyrene at doses ≥1.6 μM **(A)**. Exposure of the intact biofilm without sonication to SAAP-148 resulted in complete eradication at doses ≥12.8 μM **(B)**. Pexiganan resulted in complete eradication of sonicated bacteria at doses ≥6.4 μM **(C)**. Acyldepsipeptide 4 (ADEP4) **(D)** reduced the bacterial counts by 1 log. Exposing the bacteria for 24 h to ADEP4 **(E)** resulted in compete eradication at doses ≥12.8 μM. Human cathelicidin LL-37 **(F)** reduced the bacterial counts by 1 log. Solid lines denote the median log CFU/mL. **Figures 3A–E**: *n* = 3 experiments (each in duplicate) **Figure 3F**: *n* = 1 experiment in duplicate. ns, not significant.

mature biofilms on sterile acetabulum liners of a hip prosthesis. Results revealed eradication of the bacteria by peptide at all concentrations ≥25.6 μM except for three outliers (**Figure 6**). The results indicate that SAAP-148 is also effective against persisters in mature biofilms on acetabular hip liners.

DISCUSSION

Importance of an *in vitro* Mature Biofilm Model Simulating PJI and Other Foreign Material Infections

As antibiotic treatment of PJI often fails novel agents that eradicate persisters in mature biofilms are urgently needed. In this study we compared the anti-persister activities of synthetic antimicrobial peptides as potential candidates. For this purpose, we first developed innovative *in vitro* models simulating a PJI. These models were based on the following considerations. First, in most clinical biofilm-associated infections like PJI a mature biofilm has developed. The heterogeneous biofilm structure with extracellular polymers substances, eDNA and proteins makes drug penetration more difficult (Wolcott et al., 2010). Also, the subpopulation of persisters in mature biofilms is denser than in immature biofilms (that are often used in biofilm studies) due to antibiotic treatment and nutrient starvation. To avoid outcomes that may not be optimal for translation to clinical biofilm-associated infections, we used seven-day matured MRSA biofilms followed by 3 days of antibiotic exposure. Second, we developed the biofilms on acetabular hip liners and metal alloys (titanium, niobium, and aluminum) that are used in prosthetic joints. Third, to avoid awakening of persisters, exposure of the persisters to antimicrobial peptides is initiated immediately after termination of antibiotic exposure. Finally, we ruled out late regrowth of surviving persisters in biofilms after SAAP-148 exposure by inspecting the bacterial agar plates after 5 days in the incubator. These *in vitro* models can be used to screen other anti-biofilm and anti-persister agents, although limitations in simulating PJI should be taken into account, such as the absence of host cells and inflammatory mediators.

Antibiotic Tolerance of Persisters to Rifampicin and Ciprofloxacin

We exposed mature biofilms to high doses of rifampicin and ciprofloxacin. These antibiotics are widely used as treatment for staphylococcal PJI, penetrate well in biofilms, and reduce bacterial counts within biofilms significantly (Zimmerli and Sendi, 2019). We found that the antibiotics reduced the bacterial load in mature biofilms by >99.9% with the remaining bacteria displaying tolerance for high doses of rifampicin and ciprofloxacin. Microcalorimetry confirmed the dormant state of these antibiotics-tolerant bacterial cells as well as their ability to revive upon addition of bacterial growth medium. A limitation of microcalorimetry is its lower limit of detection being approximately 1×10^4 bacteria (Braissant et al., 2010), which is close to the number of persisters in the mature

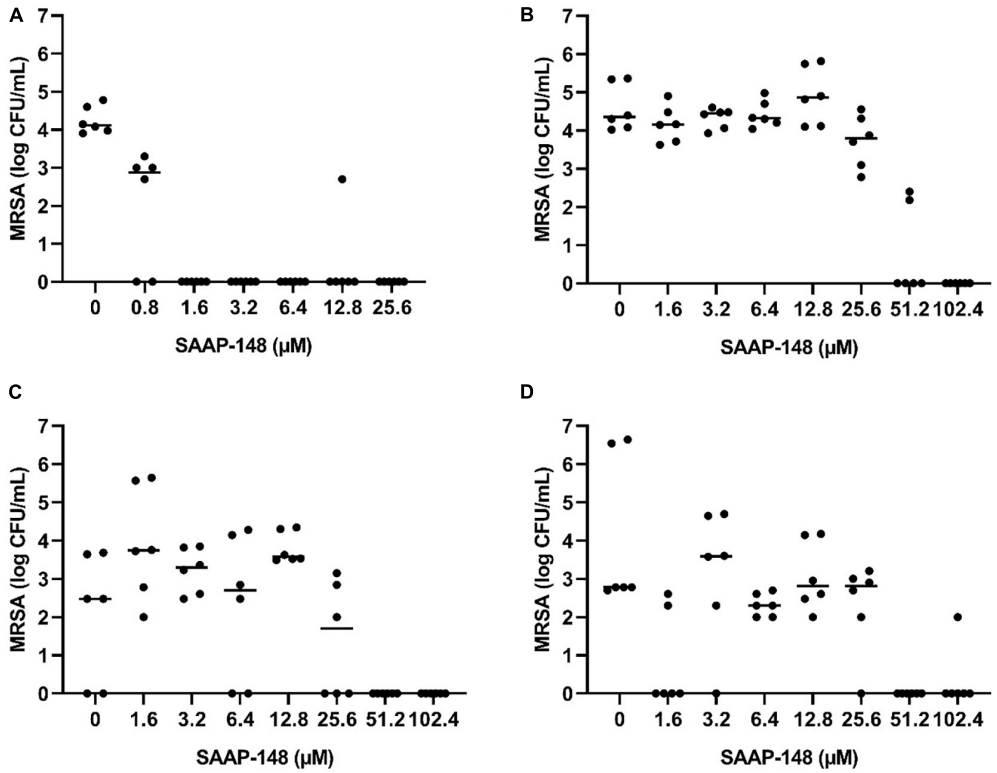

FIGURE 5 | Effect of SAAP-148 on MRSA persisters in antibiotics-exposed mature biofilms on TAN disks. Bacteria obtained by sonication from antibiotics-exposed mature biofilms on TAN disks were exposed for 2 h to SAAP-148. This resulted in eradiation of the bacteria at SAAP-148 doses of ≥1.6 μM **(A)**. SAAP-148 dose-dependently reduced bacterial counts in intact biofilms (without sonication) on TAN disks at doses ≥51.2 μM **(B)**. Prolonging the exposure of the biofilms to SAAP 148 to 24 h resulted in similar eradication of bacteria at doses ≥51.2 μM **(C)**. Addition of SAAP 148 for 24 h during an additional fourth day of antibiotic exposure on the intact biofilm also resulted in eradication of bacteria **(D)**. Solid lines denote the median log CFU/mL (n = 3 experiments, each in duplicate).

biofilms. Also, the measured heat flow is the sum of all chemical and physical processes that take place within the bacterial community. Obviously, additional and more sensitive methods, for example transcriptome analysis, cryo-electron microscopy and/or measurement of ATP levels in bacteria within biofilms, should be implicated to further characterize the persisters. Nevertheless, we can conclude that substantial numbers of persisters are present in the current antibiotics-exposed, mature biofilms. We cannot exclude that bacteria with a long lag time or small colony variants (SCVs) also survived antibiotic exposure. SCVs differ from the normal phenotype in their small colony size and reduced growth rate. However, complete elimination of all bacterial cells that were not affected by the antibiotics indicates that these SCVs, if present, were also killed by the antimicrobial peptides (Lewis and Shan, 2016; Vulin et al., 2018). The inability of rifampicin and ciprofloxacin to eradicate persisters is in line with other studies that showed incomplete eradication (Dunne et al., 1993; Reiter et al., 2012; Conlon et al., 2013; Molina-Manso et al., 2013; Jorgensen et al., 2016) or even induction of persisters (Kwan et al., 2013). Interestingly, rifampicin in combination with a fluoroquinolone eliminated all bacteria in several experimental animal models with foreign-body infections (Widmer et al., 1990; Zimmerli et al., 1994; Trampuz et al., 2007; Zimmerli and Sendi, 2019). The strong innate immune response in these animals may have contributed to this favorable outcome. The favorable outcome may also be related to the maturation state of the biofilms as the rifampicin combination was not effective in 2-week MRSA biofilms in a rat model (Lucet et al., 1990). In a guinea pig tissue-cage infection model rifampicin eradicated implant-adhering *S. aureus* after a 12 h treatment delay but not after a 24–48 h treatment delay (Tshefu et al., 1983). Together, results from studies on elimination of bacteria in immature biofilms in animals with a strong innate immune response may not be representative for mature biofilms in human biofilm-associated infections.

Effectivity of Antimicrobial Peptides

The main conclusion from this study pertains to the efficacy of four promising antimicrobial peptides to eradicate persisters within antibiotics-exposed, mature biofilms. Both SAAP-148 and pexiganan rapidly eliminated biofilm-derived bacteria in a dose-dependent fashion with SAAP-148 being the most effective peptide. The required concentration of SAAP-148 to eliminate persisters within biofilms was considerably higher than for direct killing of the persisters, indicating that peptide's antibacterial and antipersister activities are hampered by the

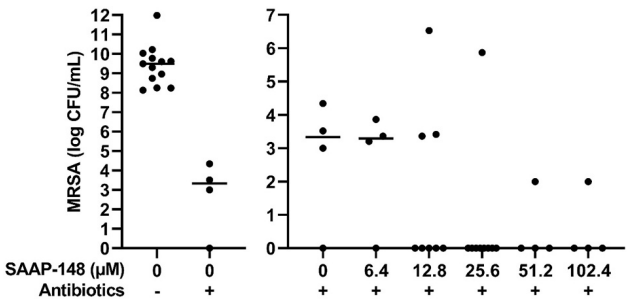

FIGURE 6 | Effect of SAAP-148 on mature antibiotics-exposed MRSA biofilms on an acetabular hip liner. From a SAAP-148 dose of 25.6 μM, bacteria were eradicated from the majority of liners. This experiment was performed twice. In the second experiment, more liners were used for the concentrations with the highest effectivity in the first experiment. Controls and 6.4 μM: $n = 4$ liners; 12.8 μM: $n = 8$ liners; 25.6 μM: $n = 9$ liners; 51.2 and 102.4 μM: $n = 4$ liners. Outliers were present in both experiments. Antibiotics-, before exposure to antibiotics; Antibiotics+, after exposure to antibiotics. Solid lines denote the median log CFU/mL.

extracellular matrix of the biofilm. Interestingly, higher SAAP-148 concentrations were needed for biofilms on TAN disks and hip liners, indicating that the surface of the implant may play a role in the development of the biofilm that protects bacteria within it. Despite displaying good antibiofilm activity in earlier studies, LL-37 reduced the bacterial counts in the antibiotics-exposed, mature biofilms only moderately (Haisma et al., 2014). ADEP4 eliminated the bacteria in the biofilms in a dose-dependent fashion at 24 h, but not at 2 h of exposure. This was expected as it takes more time before bacteria die from massive protein breakdown due to activation of the ATP-independent caseinolytic protease Clp, the proteolytic core of a major bacterial protein degradation machinery, by ADEP (Brotz-Oesterhelt et al., 2005; Conlon et al., 2016; Shan et al., 2017). Together, SAAP-148, ADEP4, LL-37, and pexiganan all exerted activity against MRSA persisters obtained from mature antibiotics-exposed, mature biofilms as well as persisters in such biofilms. The most effective peptide, SAAP-148, eliminated all persisters within mature biofilms on polystyrene, TAN disks, and on most prosthetic hip liners. Unexpected survival of bacteria was seen in the experiments with the TAN disks and in both liner experiments (**Figures 5**, **6**). Given the high bacterial load we presumed that these bacteria had not been exposed to the antimicrobial peptide in these experiments. Therefore, we regarded those as outliers related to outgrowth of untreated persisters. Of note, SAAP-148 killed the persisters as well as log phase bacteria within 2 h, indicating that peptide's toxic effect on bacteria is independent of the metabolic activity of bacteria. SAAP-148 kills bacteria by binding to the phospholipid bilayer of the bacterial membrane and the subsequent conformational change of the peptide that causes direct leakage of bacteria resulting in cell death.

Antibiofilm effects of SAAP-148 were evaluated on only one clinical MRSA isolate here. However, the model can be extended to the investigation of further isolates including those of clinical relevance in device-associated infections such as Coagulase-negative staphylococci and enterococci. Of note, the effectiveness of SAAP-148 against Gram-positive and Gram-negative bacteria in mature biofilms has been confirmed in another study (Nibbering et al., personal communication). SAAP-148 formulated in an ointment was also highly effective against an established biofilm-associated infection on wounded *ex vivo* human skin models (de Breij et al., 2018). Together, SAAP-148 is the most promising peptide for further development as novel agent to combat biofilm-associated infections. In order to prevent PJI, a SAAP-148 formulation may be developed as a coating for prosthetic joints and/or for application to the tissues surrounding the implant. SAAP-148 could also be used as adjunctive treatment during surgical debridement to rapidly kill any surviving bacteria after debridement.

Other Strategies to Combat Persisters

In addition to the application of antimicrobial peptides, mechanic or enzymatic disruption of the matrix of the biofilms may also prevent the subsequent awakening of persisters rendering them susceptible to antibiotics again. Other innovative strategies, like bacteriophages and heat induction, should be further explored as viable approaches to combat clinical device-associated infections (Pijls et al., 2018; Morris et al., 2019). The biofilm model described in this study is well suited to investigate the possibilities and limitations of these strategies in more detail. Finally, combinations of various strategies may have the largest clinical effect on biofilm-associated infections.

CONCLUSION

Novel *in vitro* models simulating PJI have been developed to evaluate the effects of antimicrobial peptides on persisters residing in antibiotics-exposed, mature biofilms. Combined rifampicin/ciprofloxacin treatment did not eliminate all biofilm-embedded bacteria, indicating the presence of persisters within mature biofilms. Microcalorimetry confirmed the dormant state of these bacteria. SAAP-148 eliminated persisters within mature biofilms on abiotic surfaces. SAAP-148 was more effective than LL-37, pexiganan, and ADEP4. Based on these data, SAAP-148 is a promising candidate for further development as agent to treat patients suffering from biofilm-associated infections like PJI.

DATA AVAILABILITY STATEMENT

The original contributions presented in the study are included in the article/supplementary material, further inquiries can be directed to the corresponding author/s.

AUTHOR CONTRIBUTIONS

HS designed the experiments and wrote draft version of the manuscript, contributed to the experiments, and integrated all

comments in manuscript. JW, JV, and AV performed the most experiments and reviewed draft versions of the manuscript. LV and RW reviewed draft versions of the manuscript. MB and PHN designed experiments, reviewed draft version of the manuscript, and supervised the project. All authors contributed to the article and approved the submitted version.

ACKNOWLEDGMENTS

We thank Willem van Wamel and Valerie Baede (Department of Medical Microbiology, Erasmus Medical Center, Rotterdam, Netherlands) for their assistance with the heat flow measurements using microcalorimetry.

REFERENCES

Balaban, N. Q., Merrin, J., Chait, R., Kowalik, L., and Leibler, S. (2004). Bacterial persistence as a phenotypic switch. *Science* 305, 1622–1625. doi: 10.1126/science.1099390

Braissant, O., Wirz, D., Gopfert, B., and Daniels, A. U. (2010). Use of isothermal microcalorimetry to monitor microbial activities. *FEMS Microbiol. Lett.* 303, 1–8. doi: 10.1111/j.1574-6968.2009.01819.x

Brotz-Oesterhelt, H., Beyer, D., Kroll, H. P., Endermann, R., Ladel, C., Schroeder, W., et al. (2005). Dysregulation of bacterial proteolytic machinery by a new class of antibiotics. *Nat. Med.* 11, 1082–1087. doi: 10.1038/nm1306

Conlon, B. P., Nakayasu, E. S., Fleck, L. E., LaFleur, M. D., Isabella, V. M., Coleman, K., et al. (2013). Activated ClpP kills persisters and eradicates a chronic biofilm infection. *Nature* 503, 365–370. doi: 10.1038/nature12790

Conlon, B. P., Rowe, S. E., Gandt, A. B., Nuxoll, A. S., Donegan, N. P., Zalis, E. A., et al. (2016). Persister formation in *Staphylococcus aureus* is associated with ATP depletion. *Nat. Microbiol.* 1:16051. doi: 10.1038/nmicrobiol.2016.51

de Breij, A., Riool, M., Cordfunke, R. A., Malanovic, N., de Boer, L., Koning, R. I., et al. (2018). The antimicrobial peptide SAAP-148 combats drug-resistant bacteria and biofilms. *Sci. Transl. Med.* 10:eaan4044. doi: 10.1126/scitranslmed.aan4044

Dunne, W. M. Jr., Mason, E. O. Jr., and Kaplan, S. L. (1993). Diffusion of rifampin and vancomycin through a *Staphylococcus epidermidis* biofilm. *Antimicrob. Agents Chemother.* 37, 2522–2526.

Ge, Y., MacDonald, D. L., Holroyd, K. J., Thornsberry, C., Wexler, H., and Zasloff, M. (1999). In vitro antibacterial properties of pexiganan, an analog of magainin. *Antimicrob. Agents Chemother.* 43, 782–788.

Haisma, E. M., de Breij, A., Chan, H., van Dissel, J. T., Drijfhout, J. W., Hiemstra, P. S., et al. (2014). LL-37-derived peptides eradicate multidrug-resistant *Staphylococcus aureus* from thermally wounded human skin equivalents. *Antimicrob. Agents Chemother.* 58, 4411–4419. doi: 10.1128/AAC.02554-14

Haisma, E. M., Goblyos, A., Ravensbergen, B., Adriaans, A. E., Cordfunke, R. A., Schrumpf, J., et al. (2016). Antimicrobial Peptide P60.4Ac-Containing Creams and Gel for Eradication of Methicillin-Resistant Staphylococcus aureus from Cultured Skin and Airway Epithelial Surfaces. *Antimicrob. Agents Chemother.* 60, 4063–4072. doi: 10.1128/AAC.03001-15

Harms, A., Maisonneuve, E., and Gerdes, K. (2016). Mechanisms of bacterial persistence during stress and antibiotic exposure. *Science* 354:aaf4268. doi: 10.1126/science.aaf4268

Jorgensen, N. P., Skovdal, S. M., Meyer, R. L., Dagnaes-Hansen, F., Fuursted, K., and Petersen, E. (2016). Rifampicin-containing combinations are superior to combinations of vancomycin, linezolid and daptomycin against *Staphylococcus aureus* biofilm infection *in vivo* and *in vitro*. *Pathog. Dis.* 74:ftw019. doi: 10.1093/femspd/ftw019

Kwan, B. W., Valenta, J. A., Benedik, M. J., and Wood, T. K. (2013). Arrested protein synthesis increases persister-like cell formation. *Antimicrob. Agents Chemother.* 57, 1468–1473. doi: 10.1128/AAC.02135-12

Lewis, K. (2010). Persister cells. *Annu. Rev. Microbiol.* 64, 357–372. doi: 10.1146/annurev.micro.112408.134306

Lewis, K., and Shan, Y. (2016). Persister awakening. *Mol. Cell* 63, 3–4. doi: 10.1016/j.molcel.2016.06.025

Lora-Tamayo, J., Murillo, O., Iribarren, J. A., Soriano, A., Sanchez-Somolinos, M., Baraia-Etxaburu, J. M., et al. (2013). A large multicenter study of methicillin-susceptible and methicillin-resistant *Staphylococcus aureus* prosthetic joint infections managed with implant retention. *Clin. Infect. Dis.* 56, 182–194. doi: 10.1093/cid/cis746

Lora-Tamayo, J., Senneville, E., Ribera, A., Bernard, L., Dupon, M., Zeller, V., et al. (2017). The not-so-good prognosis of streptococcal periprosthetic joint infection managed by implant retention: the results of a large multicenter study. *Clin. Infect. Dis.* 64, 1742–1752. doi: 10.1093/cid/cix227

Lucet, J. C., Herrmann, M., Rohner, P., Auckenthaler, R., Waldvogel, F. A., and Lew, D. P. (1990). Treatment of experimental foreign body infection caused by methicillin-resistant *Staphylococcus aureus*. *Antimicrob. Agents Chemother.* 34, 2312–2317. doi: 10.1128/aac.34.12.2312

Molina-Manso, D., del Prado, G., Ortiz-Perez, A., Manrubia-Cobo, M., Gomez-Barrena, E., Cordero-Ampuero, J., et al. (2013). In vitro susceptibility to antibiotics of staphylococci in biofilms isolated from orthopaedic infections. *Int. J. Antimicrob. Agents* 41, 521–523. doi: 10.1016/j.ijantimicag.2013.02.018

Morris, J. L., Letson, H. L., Elliott, L., Grant, A. L., Wilkinson, M., Hazratwala, K., et al. (2019). Evaluation of bacteriophage as an adjunct therapy for treatment of peri-prosthetic joint infection caused by *Staphylococcus aureus*. *PLoS One* 14:e0226574. doi: 10.1371/journal.pone.0226574

Nell, M. J., Tjabringa, G. S., Wafelman, A. R., Verrijk, R., Hiemstra, P. S., Drijfhout, J. W., et al. (2006). Development of novel LL-37 derived antimicrobial peptides with LPS and LTA neutralizing and antimicrobial activities for therapeutic application. *Peptides* 27, 649–660. doi: 10.1016/j.peptides.2005.09.016

Pijls, B. G., Sanders, I., Kuijper, E. J., and Nelissen, R. (2018). Segmental induction heating of orthopaedic metal implants. *Bone Joint Res.* 7, 609–619. doi: 10.1302/2046-3758.711.BJR-2018-0080.R1

Reiter, K. C., Sambrano, G. E., Villa, B., Paim, T. G., de Oliveira, C. F., and d'Azevedo, P. A. (2012). Rifampicin fails to eradicate mature biofilm formed by methicillin-resistant *Staphylococcus aureus*. *Rev. Soc. Bras. Med. Trop.* 45, 471–474.

Shan, Y., Brown Gandt, A., Rowe, S. E., Deisinger, J. P., Conlon, B. P., and Lewis, K. (2017). ATP-dependent persister formation in *Escherichia coli*. *mBio* 8:e02267-16. doi: 10.1128/mBio.02267-16

Tande, A. J., and Patel, R. (2014). Prosthetic joint infection. *Clin. Microbiol. Rev.* 27, 302–345. doi: 10.1128/CMR.00111-13

Trampuz, A., Murphy, C. K., Rothstein, D. M., Widmer, A. F., Landmann, R., and Zimmerli, W. (2007). Efficacy of a novel rifamycin derivative, ABI-0043, against *Staphylococcus aureus* in an experimental model of foreign-body infection. *Antimicrob. Agents Chemother.* 51, 2540–2545. doi: 10.1128/AAC.00120-07

Tshefu, K., Zimmerli, W., and Waldvogel, F. A. (1983). Short-term administration of rifampin in the prevention or eradication of infection due to foreign bodies. *Rev. Infect. Dis.* 5(Suppl. 3), S474–S480.

van der Does, A. M., Beekhuizen, H., Ravensbergen, B., Vos, T., Ottenhoff, T. H., van Dissel, J. T., et al. (2010). LL-37 directs macrophage differentiation toward macrophages with a proinflammatory signature. *J. Immunol.* 185, 1442–1449. doi: 10.4049/jimmunol.1000376

Vulin, C., Leimer, N., Huemer, M., Ackermann, M., and Zinkernagel, A. S. (2018). Prolonged bacterial lag time results in small colony variants that represent a sub-population of persisters. *Nat. Commun.* 9:4074. doi: 10.1038/s41467-018-06527-0

Widmer, A. F., Frei, R., Rajacic, Z., and Zimmerli, W. (1990). Correlation between *in vivo* and *in vitro* efficacy of antimicrobial agents against foreign body infections. *J. Infect. Dis.* 162, 96–102.

Wolcott, R. D., Rumbaugh, K. P., James, G., Schultz, G., Phillips, P., Yang, Q., et al. (2010). Biofilm maturity studies indicate sharp debridement opens a time-

dependent therapeutic window. *J. Wound Care* 19, 320–328. doi: 10.12968/jowc.2010.19.8.77709

Zeller, V., Kerroumi, Y., Meyssonnier, V., Heym, B., Metten, M. A., Desplaces, N., et al. (2018). Analysis of postoperative and hematogenous prosthetic joint-infection microbiological patterns in a large cohort. *J. Infect.* 76, 328–334. doi: 10.1016/j.jinf.2017.12.016

Zimmerli, W., Frei, R., Widmer, A. F., and Rajacic, Z. (1994). Microbiological tests to predict treatment outcome in experimental device-related infections due to *Staphylococcus aureus*. *J. Antimicrob. Chemother.* 33, 959–967.

Zimmerli, W., and Sendi, P. (2019). Role of Rifampin against Staphylococcal biofilm infections *in vitro*, in animal models, and in orthopedic-device-related infections. *Antimicrob. Agents Chemother.* 63:e01746-18. doi: 10.1128/AAC.01746-18

Conflict of Interest: PHN is co-inventor on patent WO-2015088344 relating to the SAAP-148 peptide studied in this paper.

The remaining authors declare that the research was conducted in the absence of any commercial or financial relationships that couldbe construed as a potential conflict of interest.

frontiers in Microbiology

ORIGINAL RESEARCH
published: 24 June 2021
doi: 10.3389/fmicb.2021.687888

Thermonucleases Contribute to *Staphylococcus aureus* Biofilm Formation in Implant-Associated Infections–A Redundant and Complementary Story

Jinlong Yu[1], Feng Jiang[1], Feiyang Zhang[1], Musha Hamushan[1], Jiafei Du[1], Yanjie Mao[1], Qiaojie Wang[1], Pei Han[1], Jin Tang[2]* and Hao Shen[1,3]**

[1] Department of Orthopedics, Shanghai Jiao Tong University Affiliated Sixth People's Hospital, Shanghai, China,
[2] Department of Clinical Laboratory, Shanghai Jiao Tong University Affiliated Sixth People's Hospital, Shanghai, China,
[3] Department of Orthopedics, Jinjiang Municipal Hospital, Fujian, China

OPEN ACCESS

Edited by:
Catherine Dunyach-Remy,
INSERM U1047 Virulence Bactérienne et Maladies Infectieuses, France

Reviewed by:
Angela Maria Oliveira de Sousa França,
University of Minho, Portugal
Anders P. Hakansson,
Lund University, Sweden

***Correspondence:**
Pei Han
hanpei_cn@163.com
Jin Tang
tangjin6ph@163.com;
tangjin6ph@126.com
Hao Shen
shenhao7212@sina.com

Specialty section:
This article was submitted to Infectious Diseases, a section of the journal Frontiers in Microbiology

Received: 30 March 2021
Accepted: 27 May 2021
Published: 24 June 2021

Citation:
Yu J, Jiang F, Zhang F, Hamushan M, Du J, Mao Y, Wang Q, Han P, Tang J and Shen H (2021) Thermonucleases Contribute to Staphylococcus aureus Biofilm Formation in Implant-Associated Infections–A Redundant and Complementary Story. Front. Microbiol. 12:687888. doi: 10.3389/fmicb.2021.687888

Biofilms formed by *Staphylococcus aureus* are one of the predominant causes of implant-associated infections (IAIs). Previous studies have found that *S. aureus* nucleases *nuc1* and *nuc2* modulate biofilm formation. In this study, we found low *nuc1/nuc2* expression and high biofilm-forming ability among IAI isolates. Furthermore, in a mouse model of exogenous IAIs, Δ*nuc1/2* exhibited higher bacterial load on the surface of the implant than that exhibited by the other groups (WT, Δ*nuc1*, and Δ*nuc2*). Survival analysis of the hematogenous IAI mouse model indicated that *nuc1* is a virulence factor related to mortality. We then detected the influence of *nuc1* and *nuc2* on biofilm formation and immune evasion *in vitro*. Observation of *in vitro* biofilm structures with scanning electron microscopy and evaluation of bacterial aggregation with flow cytometry revealed that both *nuc1* and *nuc2* are involved in biofilm structuring and bacterial aggregation. Unlike *nuc1*, which is reported to participate in immune evasion, *nuc2* cannot degrade neutrophil extracellular traps. Moreover, we found that *nuc1/nuc2* transcription is negatively correlated during *S. aureus* growth, and a possible complementary relationship has been proposed. In conclusion, *nuc1/nuc2* are complementary genes involved in biofilm formation in exogenous IAIs. However, *nuc2* contributes less to virulence and is not involved in immune evasion.

Keywords: *Staphylococcus aureus*, biofilm, thermonuclease, implant associated infections, periprosthetic joint infection

INTRODUCTION

Orthopedic implants are mainly used for bone fixation and joint replacement. Owing to locally compromised host defense, implanted foreign structures are highly susceptible to microbial colonization (Zimmerli and Moser, 2012; Zimmerli, 2014). As a devastating complication after arthroplasty or internal fixation, implant-associated infections (IAIs) frequently lead to the failure

Abbreviations: MRSA/MSSA, methicillin-resistant/methicillin-sensitive *Staphylococcus aureus*; EPS, extracellular polymeric substances; SEM, scanning electronic microscope; IAIs, implant-associated infections; MIC, minimum inhibitory concentration; TSB, tryptic soy broth.

of the prosthetic device or requirement of implant replacement and are associated with substantial patient morbidity (Kapadia et al., 2016; Depypere et al., 2020). Orthopedic IAIs are often caused by *Staphylococcus aureus*, although many other pathogens can lead to such infections (Arciola et al., 2005; Pulido et al., 2008). IAIs can be classified as exogenous or hematogenous (Zimmerli, 2014; Wang et al., 2017; Arciola et al., 2018). Exogenous infections, which are the most common type, occur as a consequence of direct seeding from external contaminants or contiguous spread during the perioperative period. Hematogenous infections involve bacterial seeding on implants through the bloodstream. Although hematogenous infections occur less frequently, they represent up to 20% of prosthetic joint infections (PJIs) (Sendi et al., 2011; Konigsberg et al., 2014; Tande et al., 2016).

In contrast to other infections such as bacteremia and skin abscess, microbes in IAIs generally form biofilms, which are aggregated structured bacterial communities encased in an extracellular matrix. Biofilms are responsible for the recalcitrance of implant infection to therapy and serve as a source of bacterial dissemination (Arciola et al., 2018). Biofilms are characterized by the production of extracellular polymeric substances (EPSs), which commonly comprise lipids, extracellular proteins, extracellular DNA (eDNA), and exopolysaccharides (Hobley et al., 2015; Schilcher and Horswill, 2020). EPSs typically account for 90% or more of the biofilm dry weight and perform various functions for the inhabitants, such as providing structural rigidity or protecting them from external environmental stress (Flemming and Wingender, 2010; Flemming, 2016). Researchers found that methicillin-sensitive *S. aureus* (MSSA) strains commonly produce polysaccharide intercellular adhesin (PIA)-dependent biofilms. In contrast, the release of eDNA and cell surface expression of a number of sortase-anchored proteins have been implicated in the biofilm phenotype of methicillin-resistant *S. aureus* (MRSA) (Mccarthy et al., 2015).

Extracellular DNA has been recognized as a component of the EPS matrix for a long time. However, its role in the EPS was underestimated until the discovery that it is an essential component in *Pseudomonas aeruginosa* biofilms (Whitchurch et al., 2002). Further investigation revealed that eDNA stabilizes the biofilm matrix and promotes antimicrobial resistance (Hall-Stoodley et al., 2012). In addition, two clinical studies have recently reported a relationship between the presence of eDNA in the biofilm and the outcome of orthopedic IAIs (Zatorska et al., 2017, 2018).

Extracellular DNA is released through bacterial autolysis and digested by nucleases (Okshevsky et al., 2015). According to previous reports, *S. aureus* secretes thermonuclease enzymes to regulate biofilm formation by modulating eDNA (Kiedrowski et al., 2011; Tang et al., 2011). To our knowledge, the chromosome of *S. aureus* encodes two thermonucleases, *nuc1* and *nuc2* (Tang et al., 2008; Hu et al., 2012). *nuc1*, also called micrococcal nuclease, was the first documented thermonuclease, and it is a secreted virulence factor controlled by the *SaeRS* two-component system (Olson et al., 2013). *nuc2* is a cell surface-binding protein with functional nuclease activity (Kiedrowski et al., 2014). Previous studies have reported that *S. aureus* secretes *nuc1* to degrade neutrophil extracellular traps (NETs) and kill phagocytes (Berends et al., 2010; Thammavongsa et al., 2013; Sultan et al., 2019). Interestingly, the two abovementioned phenotypes (biofilm formation and immune evasion) seem incompatible because *nuc1* upregulation contributes to immune evasion, whereas *nuc1* downregulation leads to biofilm formation. The mechanism by which nucleases regulate the survival of *S. aureus* in the IAI microenvironment remains unknown. In addition, the contribution of *nuc2* to *S. aureus* pathogenesis in biofilm-related infections and whether *nuc2* contributes to immune evasion are particularly unclear because this nuclease was more recently discovered than *nuc1* and has received limited attention.

In this study, we evaluated the activity of thermonucleases in IAI isolates. We also examined the impact of *nuc1* and *nuc2* on biofilm formation and immune evasion under *in vitro* and *in vivo* conditions. Finally, we discussed the relationship between the two nucleases and their function in *S. aureus* survival and adaptation in the IAI microenvironment.

RESULTS

Low Thermonuclease Expression and High Biofilm-Forming Ability in IAI Strains

We analyzed the transcription levels of *S. aureus* thermonucleases among 28 clinical isolates using quantitative PCR (qPCR; **Figures 1A,B**). Significantly lower transcription levels of both *nuc1* ($p < 0.01$) and *nuc2* ($p < 0.05$) were observed in IAI strains ($n = 14$) than in non-IAI strains ($n = 14$). *nuc1* and *nuc2* transcription levels in the IAI group were 2.57- and 2.47-fold lower than those in the non-IAI groups, respectively. Since gene expression is highly dependent on the involved environment, we included human synovial fluid to mimic the environment encountered by the bacteria in the host, and the results were similar to isolates grown in TSB (**Supplementary Figure 1**).

To determine whether there were differences in nuclease enzyme activity between the two groups, thermonuclease activity was measured directly using toluidine blue DNA agar, and the zones of clearing were measured. The majority of strains from the IAI group had smaller zones of clearing than those of the strains from the non-IAI group ($p < 0.01$), which indicated lower thermonuclease activity. Representative images for each group are shown in **Figure 1C**.

Previous reports demonstrated that *S. aureus* nuclease (*nuc1*) could affect biofilm formation by modulating eDNA (Kiedrowski et al., 2011). Here, we noted an increased biofilm eDNA in the IAI group (**Supplementary Figure 2A**). By relating the eDNA amount to *nuc1* and *nuc2* expression levels, we found a moderate correlation between *nuc1* and eDNA (Pearson $R = -0.4592$; **Supplementary Figure 2B**), but no significant correlation was found between *nuc2* and eDNA (Pearson $R = -0.2983$, $p > 0.05$). Then, we wonder if the IAI isolates with low thermonuclease activity also have higher biofilm-forming ability. Static microtiter biofilm assay found that IAI isolates had higher biofilm-forming ability (**Figure 1D**). Considering that

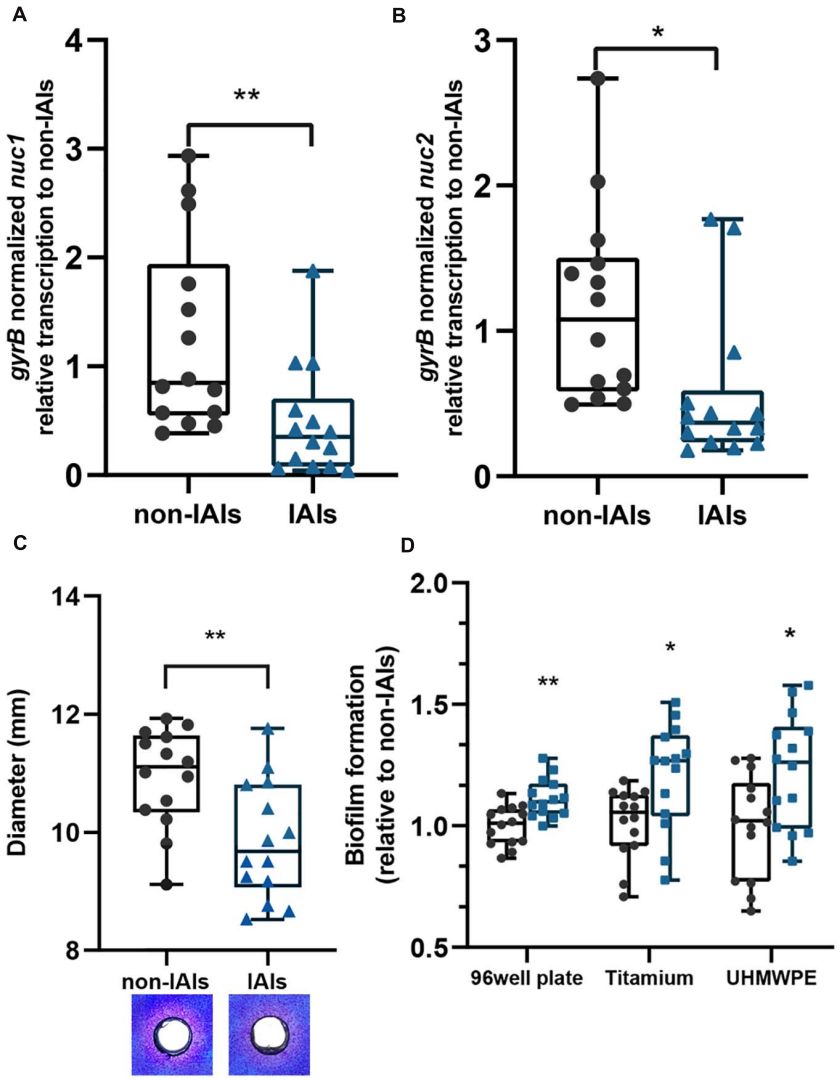

FIGURE 1 | The expression levels of thermonucleases and biofilm-forming ability in clinical isolates. Expression of *nuc1* **(A)** and *nuc2* **(B)** in IAI and non-IAI isolates (n = 14/group) determined by qPCR. **(C)** Nuclease activity in toluidine blue DNA agar represented in the diameter of red zones. Representative images are also presented. Red zones indicate nuclease activity. **(D)** Biofilm formation of IAI (n = 14) and non-IAI isolates (n = 14) on different materials including polypropylene 96-well plates (non-IAIs = 1.334 ± 0.103), titanium disk (non-IAIs = 1.664 ± 0.229), and UHMWPE (non-IAI = 1.407 ± 0.284). Biofilm biomass was stained with crystal violet. Statistical significance was calculated using two-tail Student's t-test in panels **(A–C)**; the multiple t-test (Bonferroni–Dunn's test) was used in panel **(D)**. $^{*}p < 0.05$; $^{**}p <$ 0.01 vs. non-IAI strains.

the most used materials in orthopedic implants are titanium alloy and ultra-high-molecular-weight polyethene (UHMWPE), we further performed biofilm formation assay on titanium disk and UHMWPE, and similar results were obtained (**Figure 1D**). These data together showed that IAI strains are more prone to form biofilms on the surface of various materials than their non-IAI counterparts.

Construction and Characterization of *nuc1*/*nuc2* Mutant Strains

To study the pathogenesis of *S. aureus nuc1* and *nuc2* in IAIs, we constructed *nuc1* and/or *nuc2* mutants using the clinical IAI isolate ST1792, which we termed Δ*nuc1*, Δ*nuc2*, and Δ*nuc1/2*. After in-frame mutation, the strain genotypes were validated by Sanger sequencing (**Supplementary Figure 3A**). Interestingly, the colony formed by Δ*nuc1/2* was much stickier (**Supplementary Figure 3B**) than that formed by wild type (WT), Δ*nuc1*, and Δ*nuc2*. The same phenomenon was also observed in the USA300 *nuc1*/*nuc2* isogenic mutant (BD1281).

Nuclease activity was then compared among the four strains (Δ*nuc1*, Δ*nuc2*, Δ*nuc1/2*, and WT) using toluidine blue DNA agar (**Figure 2A**). No observable difference was found between Δ*nuc2* and WT with a wide area of the clearing zone. In contrast, no detectable nuclease activity was

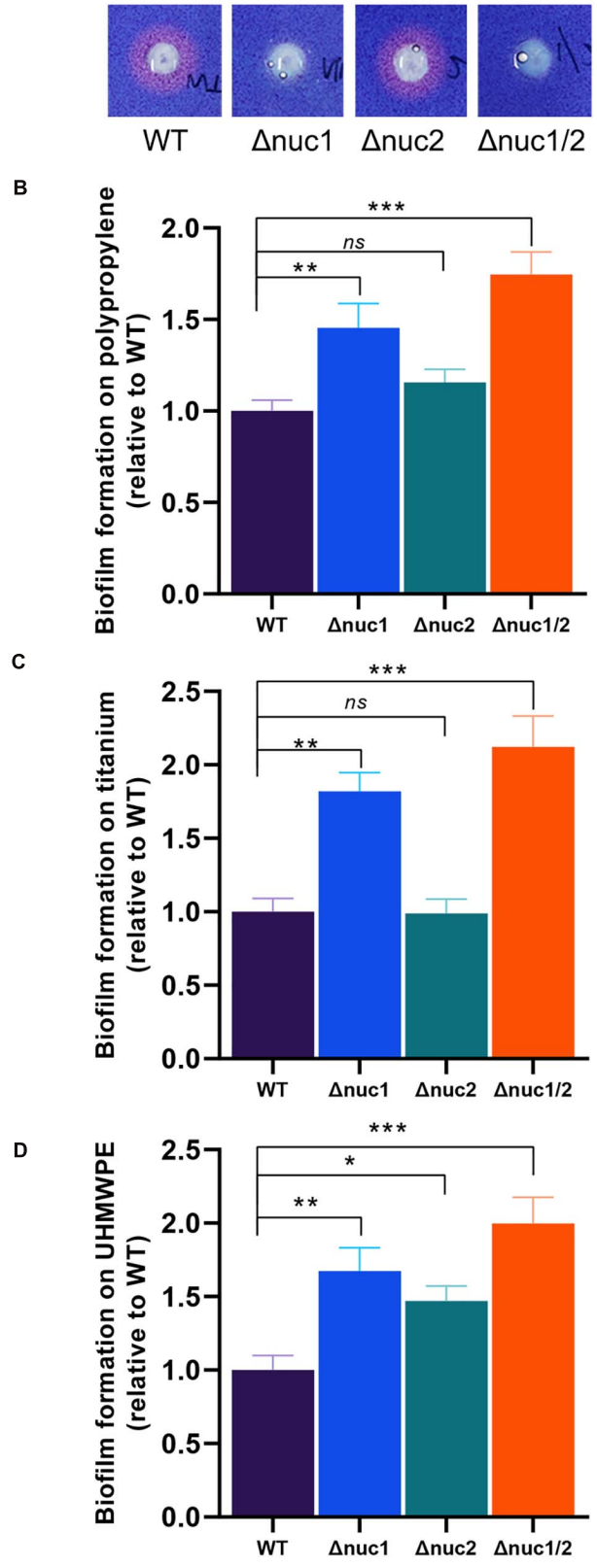

FIGURE 2 | Continued

FIGURE 2 | *In vitro* nuclease activity and biofilm-forming ability of ST1792 and its isogenic mutant strains. **(A)** Toluidine blue DNA agar test with red zones representing nuclease activity. **(B–D)** Biofilm-forming ability of tested strains on polypropylene 96-well plates (**B**, WT = 1.135 ± 0.055), titanium disk (**C**, WT = 1.237 ± 0.091), and UHMWPE disk (**D**, WT = 1.457 ± 0.119). Biofilm biomass was stained with crystal violet. Statistical significance was calculated using ANOVA with Dunnett multiple column comparisons. n = 3/group for each experiment. $^{*}p < 0.05$; $^{**}p < 0.01$; $^{***}p < 0.001$ vs. WT.

observed for Δ*nuc1* and Δ*nuc1/2*. We also quantified the biofilm-forming capacity of these strains. Following crystal violet staining, we observed that the biomass of Δ*nuc1* and Δ*nuc1/2* increased significantly (**Figures 2B–D**, Δ*nuc1*: $p < 0.01$, Δ*nuc1/2*: $p < 0.001$) in various materials, including titanium, UHMWPE, and polypropylene 96-well plates. However, the biomass of the Δ*nuc2* biofilm varied with the materials. For example, when grown in UHMWPE, Δ*nuc2* bacteria developed a more robust biofilm than developed by the WT bacteria. However, biofilms grown on titanium disks and 96-well plates were comparable to the WT biofilms. In addition to quantifying biofilm biomass, the number of culturable cells was also assessed. The results showed that Δ*nuc1/2* biofilms contained more bacterial cells than the other genotypes (**Supplementary Figure 4**).

Δ*nuc1/2* Has Higher Biofilm-Forming Capacity in the Exogenous IAI Mouse Model

By inoculating bacteria around the implant locally, we constructed an exogenous IAI mouse model. All mice were euthanized 7 days after infection. No significant differences were found among the groups (WT, Δ*nuc1*, Δ*nuc2*, and Δ*nuc1/2*) when evaluating the bacterial load in the peri-implant tissues (**Figures 3A,B**). However, when quantifying adherent bacteria on the implant, a higher bacterial load was exhibited by Δ*nuc1/2* than by the WT (**Figures 3C,D**). Interestingly, the adherent bacterial load showed no statistical difference among the Δ*nuc1*, Δ*nuc2*, and WT groups.

To investigate the effect of nucleases on environmental adaptations *in vivo*, a competitive assay was conducted. Bacteria with different genotypes and fluorescent labels were mixed and inoculated *in vivo*. The implants were harvested on day 7 and observed under a fluorescence microscope. Groups infected with a mixture of Δ*nuc1* and Δ*nuc2* presented overlapping red and green fluorescence, and no difference was detected between them (**Figure 4**). The Pearson correlation test showed a strong correlation (R = 0.83) between Δ*nuc1* (green) and Δ*nuc2* (red) signals (**Supplementary Figure 5A**). However, in groups infected with a mixture of WT and Δ*nuc1/2*, a difference in bacterial distribution (**Figure 4B**) and a low Pearson correlation (**Supplementary Figure 5B**) were observed. Specifically, Δ*nuc1/2* strains labeled with mCherry exhibited broad and even distribution, whereas WT strain labeled with superfolder GFP (sfGFP) was distributed in clusters with less area covered.

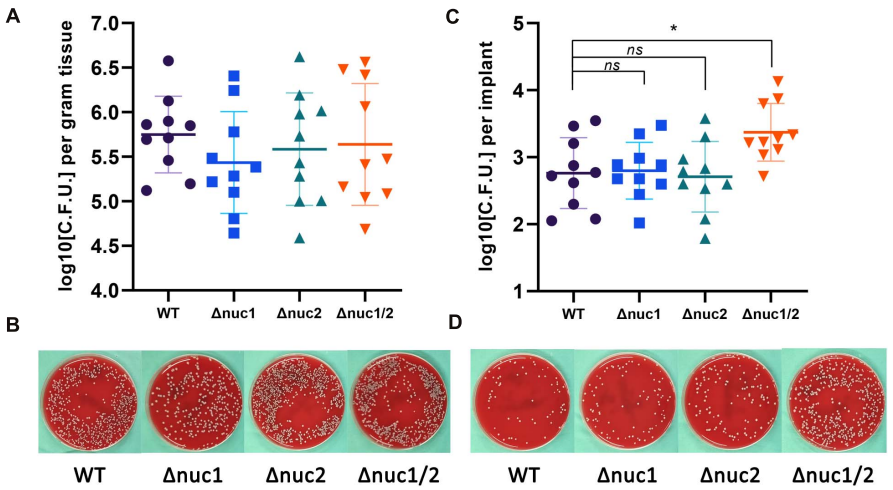

FIGURE 3 | Bacterial burden in an exogenous IAI mouse model. CFU for peri-implant tissue and biofilms on implant was determined 7 days after infection. **(A)** Bacterial count for peri-implant tissues and representative photos **(B)**. **(C)** Bacterial count for biofilms on implant and representative photos **(D)**. Statistical significance was calculated using ANOVA with Dunnett multiple column comparisons. n = 10/group. *$p < 0.05$ vs. WT.

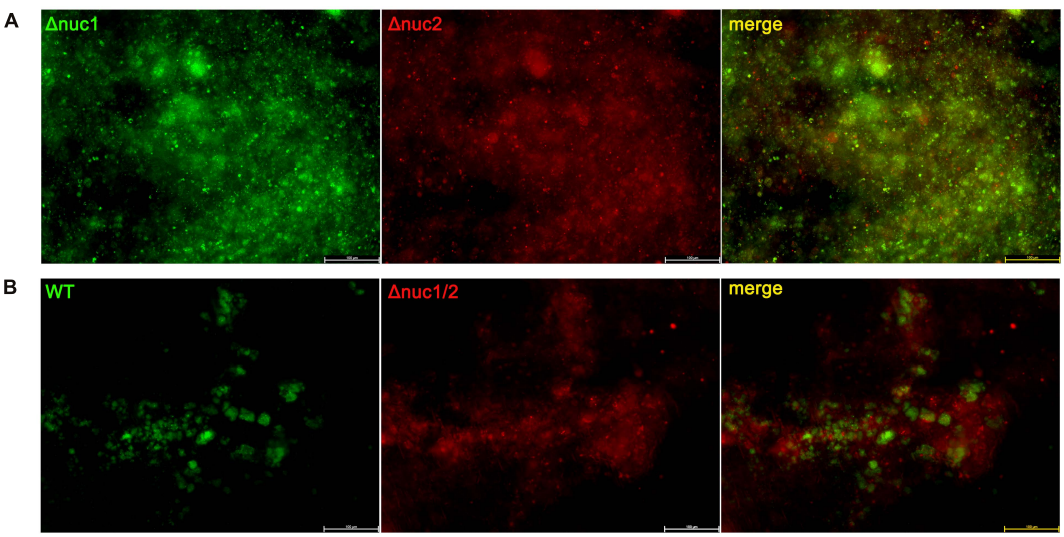

FIGURE 4 | Implant from a competition infection mouse model observed with a fluorescent microscope. Implants were harvested on the seventh day since infection and observed with a fluorescence microscope. **(A)** Implant from mice infected with a ∼1:1 mixture of Δ*nuc1* (green) and Δ*nuc2* (red). **(B)** Implant from mice infected with a ∼1:1 mixture of WT (green) and Δ*nuc1/2* (red). Scale bar = 100 μm, n = 3/group.

Δ*nuc1/2* Affects Bacterial Aggregation and Biofilm Structure *in vitro*

Next, we examined biofilm structure, *in vitro*, using scanning electronic microscopy (SEM). The biofilm structure of Δ*nuc1/2* was different from that of the other three genotypes (**Figure 5A**). Δ*nuc1/2* bacteria developed "valley and mountain-like" structures, whereas the other bacterial strains did not. However, this difference was only observed at ×50 magnification. When the biofilm was observed at ×2,000 magnification, no difference was detected (**Supplementary Figure 6**). In order to observe the extracellular matrix, we used a confocal microscope. We noticed that the biofilms formed by Δ*nuc1/2* were thicker and had higher PI signals, which represent both eDNA and dead cells.

We also measured the percentage of bacterial aggregation using flow cytometry (**Figures 5B,C**). Δ*nuc1/2* was more likely to aggregate between bacterial cells ($p < 0.01$). No statistical difference was observed among the remaining groups (Δ*nuc1*, Δ*nuc2*, and WT).

nuc2 Is Not a Virulence Factor Like *nuc1* in a Hematogenous Mice Model

The work mentioned above was based on an IAI mouse model induced by surgical site contamination. However, hematogenous

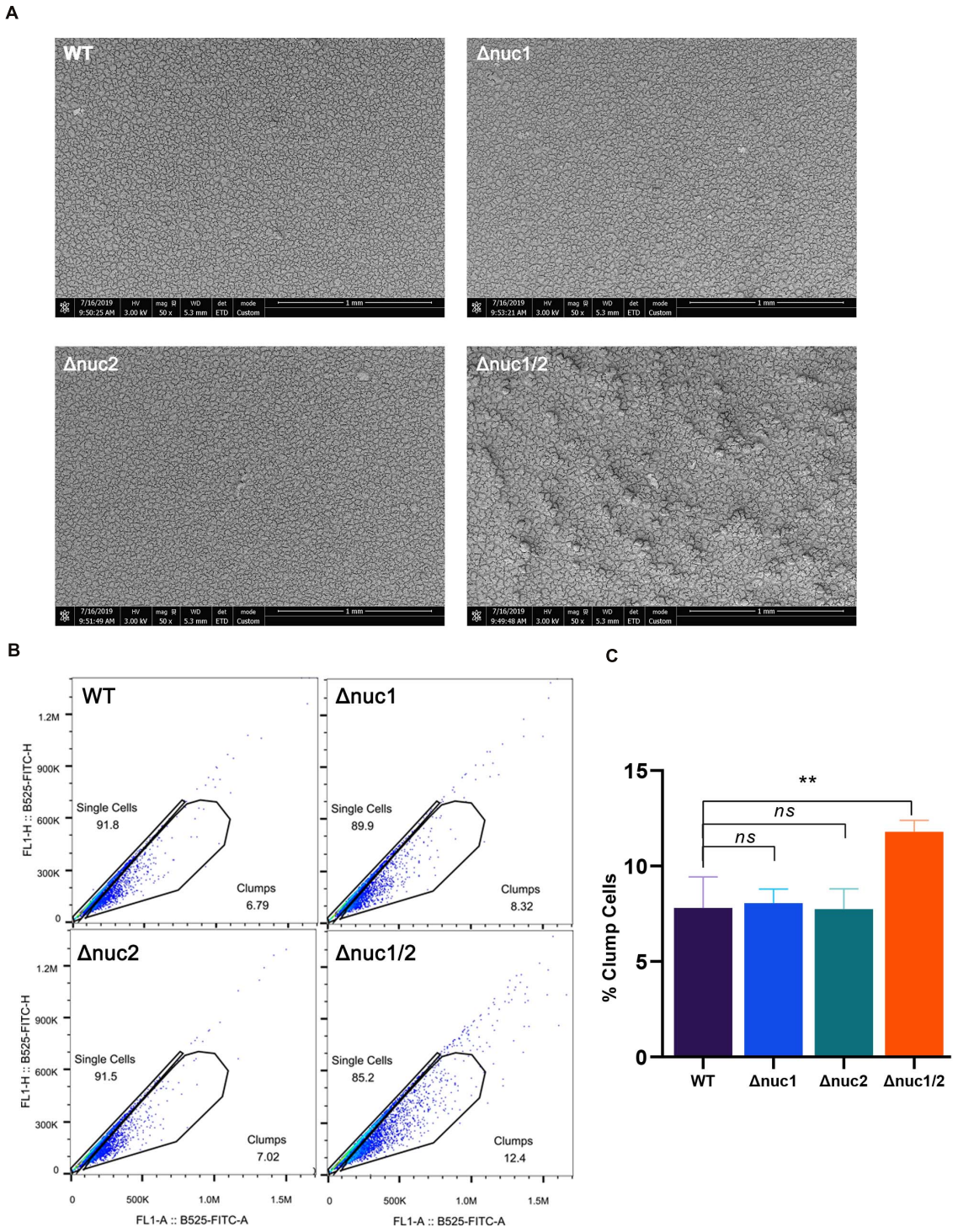

FIGURE 5 | Role of *nuc1* and *nuc2* on bacterial aggregation and biofilm structure *in vitro*. **(A)** Biofilm formed by ST1792 and its isogenic mutant on titanium disk observed with SEM (scale bar = 1 mm). **(B)** Flow cytometry was used to determine bacterial aggregation. **(C)** Quantification result for the flow cytometry experiment. Statistical significance was calculated using ANOVA with Dunnett multiple column comparisons. n = 3/group. $^{**}p < 0.01$ vs. WT.

infections represent up to 20% of IAIs (Wang et al., 2017). Therefore, we investigated the pathogenesis of Δ*nuc1* and/or Δ*nuc2* strains in a hematogenous IAI mouse model. Based on our observations, the group infected with WT and its isogenic *nuc2* mutant had significantly higher mortality rates ($p < 0.05$, **Figure 6A**). Mutual comparisons of survival curves among

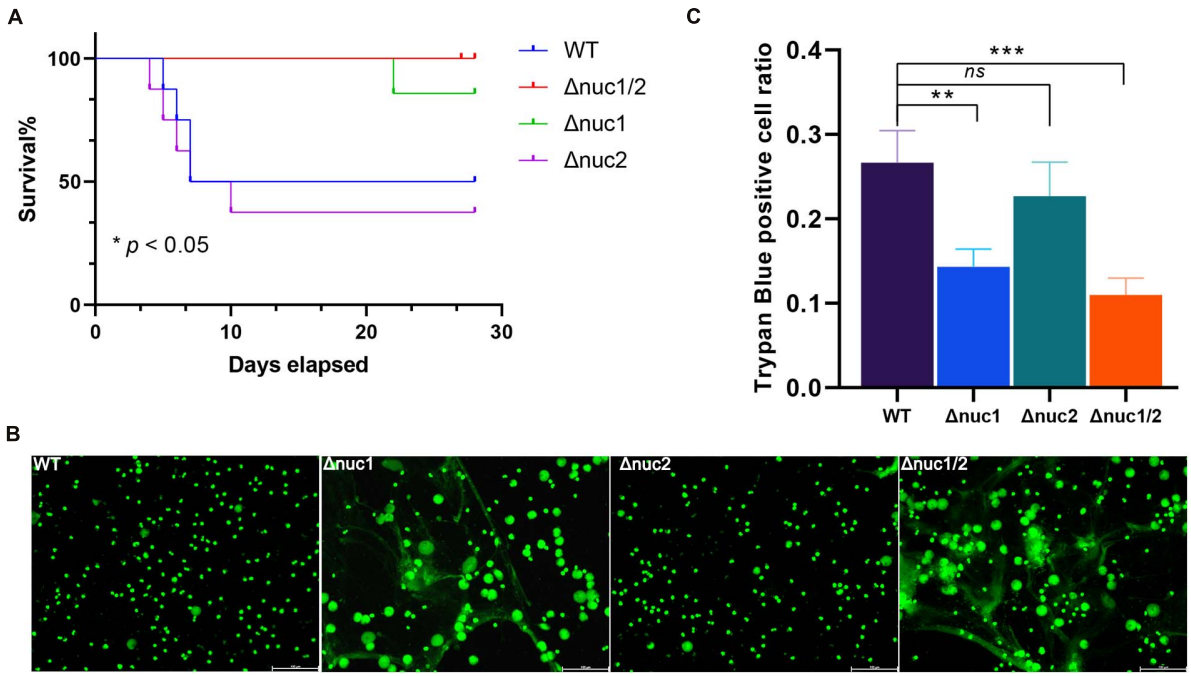

FIGURE 6 | *nuc1* and *nuc2* involvement in immune evasion. **(A)** Survival curve for a hematogenous IAI mouse model infected with ST1792 WT, Δ*nuc2* (n = 8 each), and Δ*nuc1* and Δ*nuc1/2* (n = 7 each). **(B)** Representative fluorescent images for NET degradation assay. *S. aureus* were incubated with PMA-stimulated neutrophils (n = 3/group). A green signal represents NETs and cell nucleus, scale bar = 100 μm. **(C)** THP-1 macrophages were incubated with DNA and *S. aureus*. Cell viability was determined by trypan blue staining (n = 3/group). The survival curve was analyzed with a log-rank (Mantel–Cox) test. ANOVA with Dunnett multiple column comparisons was used in panel **(C)**. $^{**}p < 0.01$; $^{***}p < 0.001$ vs. WT.

the four groups are presented in **Supplementary Figure 8**. Interestingly, most of the death events occurred within 7 days of infection. However, no difference was detected in the bacterial load in peri-implant tissue and on the implant among the four groups (**Supplementary Figure 9**).

According to previous reports, *nuc1* is involved in immune evasion (Tang et al., 2011; Thammavongsa et al., 2013). Hence, we speculated whether *nuc2* had the same function. In the NET degradation assay, in which WT and Δ*nuc1/2* were considered positive and negative controls, respectively, we did not detect any difference when comparing Δ*nuc1* with Δ*nuc1/2* (**Figure 6B**). A previous study reported that *nuc1* could lead to immune cell death (Thammavongsa et al., 2013). In line with this result, the trypan blue staining assay (**Figure 6C**) showed increased THP-1 cell viability in the Δ*nuc1* and Δ*nuc1/2* groups when compared with the WT. However, there was no difference in cell viability between the WT and Δ*nuc2* groups or between the Δ*nuc1* and Δ*nuc1/2* groups.

Staphylococcus aureus Sequentially Expresses *nuc1* and *nuc2* for Environmental Adaptation

Our study indicates that *nuc1* and *nuc2* are both essential for biofilm formation. However, the redundancy of thermonucleases in the *S. aureus* chromosome prompted us to investigate the underlying mechanism. By analyzing the public microarray dataset GSE25454, we found that *nuc1* and *nuc2* were negatively correlated (**Figure 7A**, $R = -0.59$, $p < 0.001$). Our qPCR results confirmed this phenomenon: during *S. aureus* growth in tryptic soy broth (TSB), *nuc2* was upregulated in 2–4 h and then decreased. In contrast, *nuc1* transcription peaked in the post-exponential stage (**Figure 7B**). Also, the correlation between *nuc1* and *nuc2* in our study was similar to what we found in the dataset GSE25454 (**Figure 7C**, $R = -0.8520$, $p < 0.001$). To exclude the possible regulation between the two genes, we also investigated *nuc1*/*nuc2* transcription in Δ*nuc2*/Δ*nuc1* (**Figure 7D**), and the data obtained showed no regulation between *nuc1* and *nuc2*. Such a negative correlation led to our hypothesis that *nuc1* and *nuc2* are complementary. Therefore, it is possible that *nuc2* functions in the early growth phase and that *nuc1* plays its role during the later phase.

Staphylococcus aureus Modulates Nuclease Transcription When Exposed to Antibiotics

In the first part of our study, we found low expression of nucleases in IAI isolates. Considering patients with IAIs generally require long-term antibiotic administration, we further speculated whether antibiotics would affect *nuc1/2* expression. We then exposed MRSA (USA300) and MSSA (ST1792) to several of the most commonly used antibiotics at sub-minimum inhibitory concentration (MIC) levels. First, we determined the

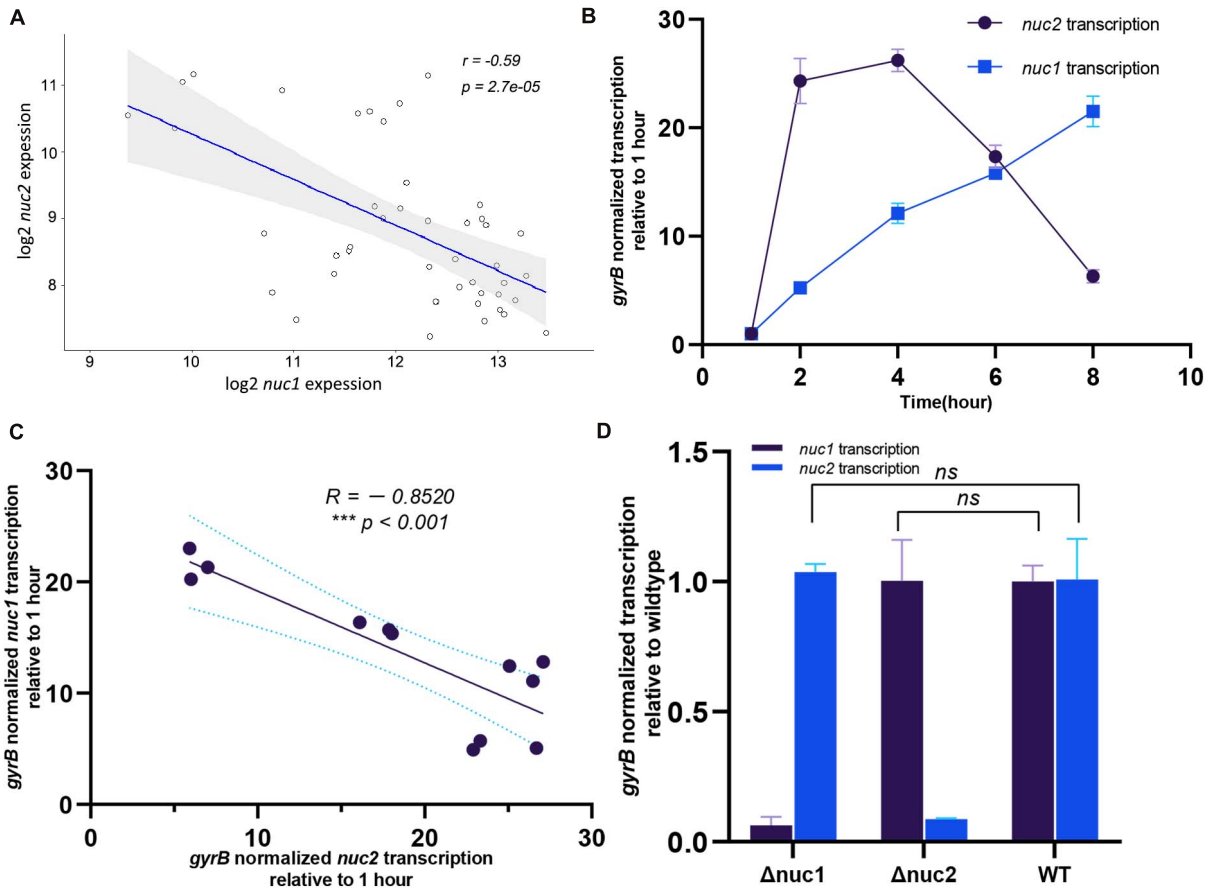

FIGURE 7 | Transcription relationship between *nuc1* and *nuc2*. **(A)** *nuc1* and *nuc2* correlation found by analyzing the publicly available data GSE25454. **(B)** Transcription levels of *nuc1* and *nuc2* in WT ST1792 at various time points determined through qPCR (n = 3/time point). **(C)** Transcription levels of *nuc2* at various time points (2, 4, 6, and 8 h) were related to *nuc1*. **(D)** *nuc1* and *nuc2* transcription levels in ST1792 WT, Δ*nuc1*, and Δ*nuc2* determined using qPCR (n = 3/group). A Pearson correlation test was performed in panels **(A,C)**, and unpaired Student's t test was performed in panel **(D)**.

TABLE 1 | Minimum Inhibitory Concentration and sub-MIC for strains tested#.

Strain	(μ g/ml)	Ciprofloxacin	Ceftriaxone	Daptomycin	Linezolid	Vancomycin
ST1792	MIC	0.25	2	>16	1	2
USA300	MIC	0.25	>8	>16	1	2
ST1792	sub-MIC*	0.125	1	8	0.5	1
USA300	sub-MIC*	0.125	4	8	0.5	1

*#MIC level was determined based on three technical replicates. *Sub-MIC was equal to 1/2 MIC.*

MIC and sub-MIC of both strains, and the results are listed in **Table 1**. Following sub-MIC exposure, qPCR was used to measure *nuc1* and *nuc2* transcriptions (**Figure 8**).

We found that MSSA and MRSA had different responses to antibiotics. Fewer differences in expression patterns were seen for *nuc1* in the two strains with only a major shift seen for vancomycin (decreased in MRSA but increased in MSSA). In both ST1792 and USA300, *nuc1* was upregulated when exposed to ciprofloxacin and downregulated after exposure to ceftriaxone and daptomycin. However, for *nuc2* expression, an increase was observed in both MRSA and MSSA strains after linezolid. Ciprofloxacin, ceftriaxone, and daptomycin increased *nuc2* expression only in the MRSA strain. Finally, *nuc2* expression increased in response to vancomycin for the MSSA strain, which is similar to *nuc1*.

DISCUSSION

To our knowledge, this is the first study reporting that *S. aureus* IAI isolates have low nuclease (*nuc1* and *nuc2*) expression levels, which may be relevant for the high biofilm-forming capacity of IAI isolates. By constructing nuclease mutant strains, we found that Δ*nuc1/2* exhibited higher biofilm-forming capacity

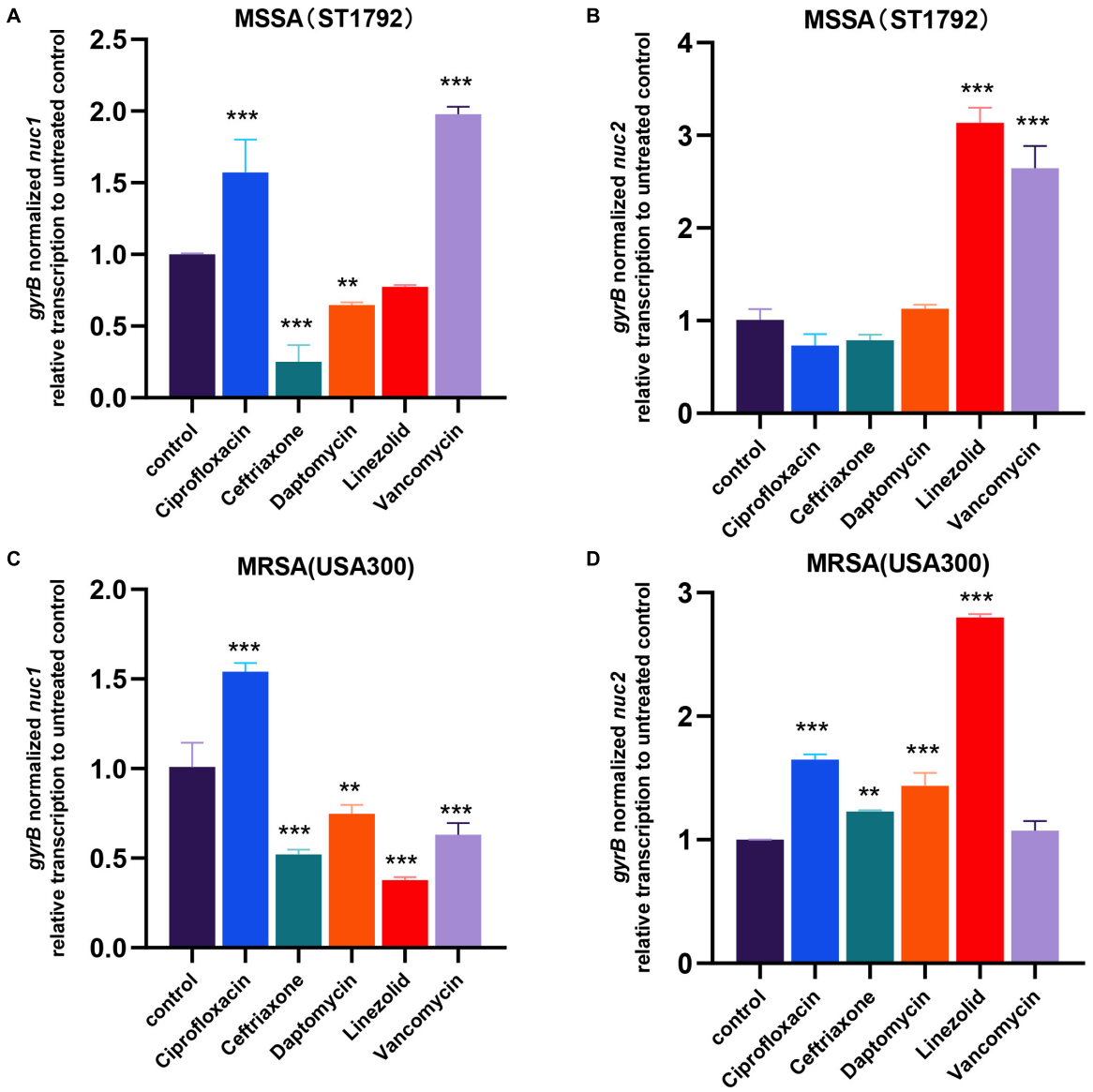

FIGURE 8 | *nuc1* and *nuc2* transcription changes when exposed to antibiotics in MRSA (USA300) and MSSA (ST1792). **(A,B)** *nuc1* **(A)** and *nuc2* **(B)** transcription changes in MSSA (ST1792). **(C,D)** *nuc1* **(C)** and *nuc2* **(D)** transcriptional changes in MRSA (USA300). Statistical significance was calculated using ANOVA with Dunnett multiple column comparisons. $^{**}p < 0.01$; $^{***}p < 0.001$ vs. non-treated control.

in an exogenous IAI mouse model. However, a previous study reported that *nuc1* and *nuc2* had no significant impact on biofilm formation using a murine model of catheter-associated biofilm formation (Beenken et al., 2012). Although the reason underlying this discrepancy with our results is unclear, we noticed that the strain used is different, which could explain, in part, the discrepancies observed.

According to previous reports, *nuc1* regulates biofilm formation by modulating eDNA in the biofilm matrix (Kiedrowski et al., 2011; Tang et al., 2011). However, the impact of *nuc2* on biofilms has received limited attention. In this study, we noticed that Δ*nuc1/2* strains formed sticky colonies and distinct biofilm morphology. One possible explanation for this phenomenon is that the mutation of both *nuc1* and *nuc2* leads to the accumulation of eDNA, which in turn may increase colony and biofilm viscosity. This hypothesis is partially corroborated by a previous study (Kaito et al., 2011), where it was reported that the presence of eDNA increases extracellular matrix viscosity. Also, biofilms observed with confocal microscopy showed that Δ*nuc1/2* formed thicker biofilms with higher PI signal. According to a previous report, eDNA degradation is involved in the "exodus" and "dispersal" steps during biofilm maturation (Moormeier et al., 2014). Their study prompted us to speculate that a high eDNA content in the biofilm matrix may make both live and dead bacteria unable to egress from the biofilm and get trapped, thus resulting in a

thicker biofilm with a higher PI signal. Nevertheless, we cannot exclude other possible mechanisms accounting for the observed phenotypes. Since previous studies have not determined if *nuc1* and *nuc2* have an influence on other biofilm-related genes, the detected phenomenon could also be caused by the regulation between nucleases and other genes.

By analyzing *nuc1* and *nuc2* transcription levels at different time points, we found that *nuc1* and *nuc2* transcription levels were temporally regulated during *S. aureus* growth, and this was also reported in a previous study (Hu et al., 2012). It seems *nuc2* was expressed when cell density was low, and *nuc1* was prone to be expressed at high cell density. Such temporal gene regulation was most likely dependent on a quorum-sensing system. However, *agr*, the most well-studied quorum sensing, is not directly associated with *nuc1* or *nuc2* regulation (Olson et al., 2013; Kiedrowski et al., 2014). Hence, other quorum-sensing systems (e.g., LuxS) and stimuli rather than population density might be involved in the temporal regulation of thermonucleases. Meanwhile, it should be noted that biofilms are not synchronized in terms of growth phase and that it would lead to special difference in gene expression. Previous studies found that *nuc1* and *nuc2* are highly expressed in the peripheral colony, highlighting the need to study in more detail the spatial regulation of *nuc1* and *nuc2* in biofilms (Kaito et al., 2011).

The redundancy of *nuc1* and *nuc2* does not mean equal contribution to *S. aureus* virulence. For instance, *nuc1* in hematogenous IAIs contributed to the mortality rate of infection while *nuc2* did not. Interestingly, we observed that most deaths, in the hematogenous IAI model, occurred during the first 7 days of infection. Based on the knowledge that adaptive immunity takes 4–7 days to mount a response (Iwasaki and Medzhitov, 2010), we speculated that *nuc1* may be relevant for innate immune evasion instead of adaptive immune evasion. This was consistent with published researches which demonstrated that *S. aureus* escapes innate immune defense through NET degradation and phagocyte apoptosis (Berends et al., 2010; Thammavongsa et al., 2013; Winstel et al., 2018). However, concerning *nuc2*, no observable immune evasion function was detected in our study. It may be due to its reported low enzymic activity (Kiedrowski et al., 2014), and thus, NETs could not be sufficiently degraded with *nuc2*.

Considering patients with IAIs require long-term administration of antibiotics, our study also examined the impact of antibiotics on nuclease expression. Although MSSA and MRSA had different responses to antibiotics, ceftriaxone and daptomycin reduced *nuc1* levels in both MSSA and MRSA. Because MRSA strains are resistant to ceftriaxone, which seems to downregulate *nuc1* expression, the use of this antibiotic could lead to increased biofilm formation. As such, caution should be taken when adopting ceftriaxone for IAI treatment before the antibiotic sensitivity testing is clear.

Our study has some limitations. First, the higher biofilm-forming capacity of IAI groups cannot be fully explained by the low expression of thermonucleases, as other factors such as *sarA*, *clfA/B*, *srtA*, and *agr* loci also contribute to biofilm formation regulation (Paharik and Horswill, 2016; Otto, 2018). Second, the regulation mechanism of *nuc2* transcription in *S. aureus* remains unknown. Finally, in our hematogenous IAI mouse model, we did not check the bacterial load in other systemic organs, which could help us understand the capacity of these strains to disperse to distant sites. Also, the bacterial load in the hematogenous IAI mouse model showed no significant differences even in the Δ*nuc1/2* group. Although the mechanism underlying the discrepancy observed between the two mouse models remains unclear, we speculated that the virulence adopted by *S. aureus* to colonize bone implants and develop biofilms might vary depending on how they invade the human body.

In summary, we identified temporal regulation for *nuc1* and *nuc2*. The pathogenesis of both nucleases was explored using two types of infection models. Low expression of both *nuc1* and *nuc2* is essential in *S. aureus* IAIs caused by surgical site contamination. However, in hematogenous IAIs, upregulation of *nuc1*, rather than *nuc2*, contributes to *S. aureus* pathogenesis. Our study may provide new insights into the prevention and treatment of IAIs.

MATERIALS AND METHODS

Bacterial Strains and Growth Conditions

Staphylococcus aureus strains used in this study were either strains that were maintained in our laboratory or clinically isolated. To construct a fluorescence-labeled strain, pRN11 and pCM29 plasmids (Pang et al., 2010; de Jong et al., 2017) expressing mCherry and sfGFP, respectively, were introduced into *S. aureus* competent cells RN4220 via electroporation using a MicroPulser (Bio-Rad, United States). After adding 0.5 μg of plasmid into 50 μl of RN4220 competent cells, the default Staph program was performed (2-mm gap, 1.8 kV, 2.5 ms). Then, the cells were immediately resuspended in 1 ml of TSB (Haibo, Qingdao, China) and cultured on a shaking incubator at 200 rpm for 1 h at 37°C. A total of 100 μl of the recovery culture was grown overnight at 37°C on a TSB-chloramphenicol (10 μg/ml) agar plate. Next morning, a single chloramphenicol-resistant colony harboring pRN11 or pCM29 plasmids was selected and grown overnight in 4 ml of TSB with chloramphenicol (10 μg/ml). Next, according to a previously described bacteriophage transformation method (Olson, 2014), the plasmid was transformed into *S. aureus* ST1792, which was isolated from an infected prosthesis, with bacteriophage 11.

Thermonuclease Activity Detection

Bacterial cultures were grown in TSB on a shaking incubator at 37°C and 200 rpm for 6 h and then heat-inactivated at 100°C for 10 min. Toluidine blue DNase agar was used to detect thermonuclease activity according to the manufacturer's instructions (Haibo, Qingdao, China). A total of 80 μl of inactivated culture was added into a 5-mm-diameter hole in the agar plate made with a sterile pellet tip. The plate was incubated for 6 h at 37°C, and the diameter of the clearing zone was measured.

Construction of Thermonuclease Mutants

In-frame deletion of *nuc1* and *nuc2* genes in clinical isolate ST1792 was performed by allelic replacement using the plasmid

pKOR1 as previously described elsewhere (Bae and Schneewind, 2006). The primers used are listed in **Supplementary Table 1**. Briefly, after amplifying the upstream and downstream regions of the target gene, we used SOE-PCR to ligate the upstream and downstream fragments. The PCR product was cloned into pKOR1, and the resulting recombinant plasmids pKOR1-*nuc1* and pKOR1-*nuc2* were further transformed into *S. aureus* competent cells RN4220 via electroporation and maintained using chloramphenicol (10 μg/ml). Next, the plasmid was transformed into *S. aureus* ST1792 using bacteriophage 11. *S. aureus* ST1792 containing the plasmid constructed was used for construction of mutants by allele replacement with temperature shifting as described previously (Bae and Schneewind, 2006). Candidate mutant strains were validated by Sanger sequencing.

In vitro Static Biofilm Assays

All bacterial strains involved in this experiment were cultured overnight at 37°C in TSB supplemented with 0.25% glucose (TSBG). The overnight culture was serially diluted to a concentration of $\sim 1 \times 10^6$ CFU/ml, and then, 100 μl of the culture was inoculated into a 96-well plate with a flat bottom (BIOFIL, Guangzhou, China). UHMWPE disks (5-mm diameter) were sterilized and placed on a 96-well plate with a round bottom (BIOFIL) and then inoculated with 100 μl of the bacterial culture followed by incubation. Titanium disks (10-mm diameter) were sterilized and placed on a 24-well plate with a flat bottom (BIOFIL) and then inoculated with 1 ml of bacterial culture followed by incubation. After incubation at 37°C for 24 h, the culture medium was aspirated from each well, and wells were washed three times with either 200 μl of PBS in case of the 96-well plate or 1 ml of PBS in case of the 24-well plate. After fixation with methanol, the plate was air-dried, and the biofilm was stained with 200 μl of crystal violet. The crystal violet bound at the bottom of the well was dissolved in 200 μl of 33% acetic acid, and 100 μl aliquots from each well were transferred into a new 96-well plate with a flat bottom. Optical absorbance was measured at 590 nm using a microplate reader (BioTek Instruments, Inc., United States) to quantify the biofilm biomass.

Biofilm eDNA Content Measurement

Staphylococcus aureus biofilms were grown as described above in a six-well plate (1.5 ml TSBG per well). After gently removing the supernatant, biofilm cells were resuspended with 1 ml of PBS and then filtered using a 0.2-μm filter. To measure eDNA content, 100 μl of filtered resuspension was mixed with 100 μl of 2 μM SYTOX Green (Invitrogen, United States). Fluorescence was measured by using a plate reader (BIOTEK, ELX 800, United States) with excitation and emission wavelengths of 485 and 520 nm.

Staphylococcus aureus RNA Isolation and Quantitative PCR

To investigate the transcription levels of thermonucleases between an IAI strain and a non-IAI strain, *S. aureus* was cultured in TSB (or TSB supplied with 20% human synovial fluid) in a shaking incubator at 37°C and 200 rpm for 6 h. To investigate thermonuclease expression at different time points, ST1792 was cultured in TSB (37°C/200 rpm) and collected at several time points (1, 2, 4, 6, and 8 h). To determine *nuc1/2* expression in ST1792 and its isogenic mutants (Δ*nuc1* and Δ*nuc2*), bacteria were cultured in TSB and incubated at 37°C and 200 rpm for 6 h. To explore *nuc1/nuc2* transcription changes after exposure to antibiotic, ST1792 and USA300 were cultured in TSB supplied with sub-MIC antibiotics for 6 h (37°C/200 rpm). The abovementioned bacteria were harvested and transferred to a tissue lyser (Scientz^{TM}, Ningbo, China), and the cell wall was physically disrupted for 30 s at a frequency of 50 Hz. RNA was isolated using the EZ-press RNA Purification Kit (EZBioscience, United States) according to the manufacturer's instructions. The quality of the RNA was measured using a Nanodrop device (Thermo Fisher Scientific, United States), and RNA samples with absorbance ratios of 260 nm/280 nm and 260 nm/230 nm higher than 2.0 were selected for reverse transcription. After adding DNase to remove gDNA, 1 μg fresh RNA was immediately reverse-transcribed into cDNA using an RT-PCR kit (EZBioscience, United States). cDNA was diluted with ddH_2O (1:5 dilution) and subsequently used as the DNA template for qPCR, performed with the kit 2 × SYBR Green qPCR Master Mix (EZBioscience). DNA amplification was performed by thermal cycling: initial denaturation at 95°C for 5 min, followed by 40 amplification cycles at 95°C for 10 s and at 60°C for 30 s using a Roche LightCycler 480 (Roche, Switzerland). The primers used in this study and other related information such as product size, primer efficiency, and cycling parameters are provided in **Supplementary Table 1**. Relative gene expression levels were quantified using the $2^{-\Delta\Delta CT}$ method, with the expression levels of *gyrB* as the internal reference.

Biofilm Structure Observation Using SEM and Confocal Microscopy

Overnight-grown ST1792 biofilms were formed on a titanium disk as described above. After gently being washed with PBS, the samples were fixed with 2.5% glutaraldehyde at 4°C for 4 h, dehydrated using a graded ethanol series (50, 70, 80, 90, 95, and 100% v/v) for 10 min, freeze-dried, coated with platinum, and visualized using SEM (Magellan 400, FEI, United States).

For confocal microscopy observation, biofilms grown on titanium disk were stained with a Live/Dead BacLight bacterial viability kit (Invitrogen, United States) according to the instructions of the manufacturer. Stained biofilms were observed immediately using a confocal microscope (Leica TCS SP8, Germany). The optimal exposure time and laser intensity for both channels (excitation: 488 and 555 nm) were manually set to ensure no overexposure among groups. Then, all of the images were acquired with the same setting for comparability among groups. Raw data were imported into Imaris 9.0.1 for biovolume and biofilm thickness calculation.

Detection of Bacterial Clumps Through Flow Cytometry

sfGFP-labeled ST1792 and its isogenic mutants were incubated in TSB at 37°C and 200 rpm overnight in the presence of

chloramphenicol. Then, overnight bacterial cultures were used for flow cytometry (Beckman Coulter CytoFLEX, United States). The sample flow rate was 10 μl/min, and 20,000 events were recorded for further analysis. First, the GFP+ cell population, comprising the bacteria, was selected. Then, single/clumping populations were labeled using the correlation between FITC-H and FITC-A.

Neutrophil Extracellular Traps Degradation Assay

Neutrophils were isolated from the blood of healthy donors. The anti-coagulated whole blood (5 ml) was carefully layered over 5.0 ml of Polymorphprep™ (Alere Technologies, Norway) in a 15-ml centrifuge tube. Tubes were centrifuged at 500×*g* for 30 min at 18–22°C. PMNs were gently separated, and 3 ml of RPMI medium was added to restore normal osmolality. Samples were centrifuged at 400×*g* for 10 min to collect cells. Finally, the cells were resuspended in the RPMI medium containing 10% fetal bovine serum (FBS). For NET induction, phorbol-12-myristate-13-acetate (PMA, Sigma, United States) was added to the culture medium to reach a final concentration of 90 nM, and samples were incubated at 37°C with 5% CO_2 for 4 h. Then, heat-inactivated bacterial culture (ST1792 and its isogenic mutants) was added (MOI = 100) and incubated for 2 h to degrade the NETs. After fixation with 4% paraformaldehyde, NETs were stained with SYTOX Green (Invitrogen, United States) and observed using a Leica DMI8 microscope (Leica, Germany).

Cellular Cytotoxicity Assays Using Trypan Blue Staining

Human monocytic THP-1 cells were obtained from the Institute of Biochemistry and Cell Biology (Shanghai, China). A total of 1×10^5 THP-1 cells were cultured, overnight, in an RPMI medium containing 10% FBS and penicillin/streptomycin together with heat-inactivated WT, Δ*nuc1*, Δ*nuc2*, or Δ*nuc1/2* bacterial suspensions (MOI = 10) and DNA (final concentration of 100 ng/μl). Subsequently, cells were stained with trypan blue and visualized using light microscopy.

Bacterial MIC Assay

We adopted a macrodilution method to determine the MIC of different antibiotics for MRSA and MSSA, and 1 ml of twofold serial dilutions of antibiotics dissolved in TSB was added to 1 ml of TSB, which contained nearly 10^6 CFU/ml, in separate tubes. After overnight incubation at 37°C, the turbidity of the test tubes was visually inspected, as turbid test tubes were indicative of bacterial growth, whereas tubes that remained clear indicated no growth. The MIC of the antibiotics tested was considered to be the lowest concentration that inhibited growth. Gentamycin, linezolid, daptomycin, ciprofloxacin, and ceftriaxone were purchased from Aladdin (Shanghai, China).

GEO Microarray Data Analysis

Public microarray dataset GSE25454 including 74 samples was selected. First, we downloaded the raw data (.CEL files) from the GEO database (GSE25454). Then, the following process was performed in R (4.0.1). We used the readAffy function (limma package; Ritchie et al., 2015) to import the .CEL files and performed background correction with the gcrma function (GCRMA package; Lim et al., 2007). Note that the resulting expression data were represented as intensity and transformed into log-2 scale according to descriptions in the GCRMA package manual. After that, we used the "normalizeWithinArray" function (from the limma package; Ritchie et al., 2015) to normalize the data among samples to remove batch effects. Finally, we extracted the *nuc1* and *nuc2* expression values for each sample at various time points and performed a Pearson correlation test. The scatter plot was presented with the ggscatter function (ggpubr package).

Implant-Associated Infections Mouse Model

Mice Model of Exogenous IAIs

Twenty BALB/c mice (6 weeks old) were randomly divided into four groups (WT, Δ*nuc1*, Δ*nuc2*, and Δ*nuc1/2*). Mice were intraperitoneally anesthetized with 1% pelltobarbitalum natricum (provided by the animal center), and both knees were shaved and disinfected. Then, the distal femur was exposed through a medial parapatellar incision, and a narrow channel was created at the femoral end using a 25G needle. Subsequently, the prepared sterile titanium wires (0.5-mm diameter) were inserted in a retrograde direction into the intramedullary canal. The overlying subcutaneous tissue and skin were closed using absorbable subcuticular sutures. Finally, 25 μl of the corresponding bacterial inoculum (ST1792 and its isogenic mutants, $\sim 1 \times 10^7$/ml) was injected intraarticularly into the knee joint space. All mice were anesthetized and euthanized by cervical dislocation 7 days after the infection. Peri-implant tissues were harvested and homogenized in 1 ml of sterile saline before CFU counting. The biofilm on the titanium wires together with 1 ml of sterile saline was subjected to sonication (30 kHz, 10 min) in an ultrasound bath (CQ-200B-DST, Yuejin, China), and the resulting sonicated fluid was used for further bacterial load quantification.

Competition Infection Model

To observe the *in vivo* biofilm structure and explore the adaptability of different *S. aureus* genotypes, a titanium disk was implanted subcutaneously into the dorsal area of the mice, and $\sim 1 \times 10^6$ CFU of the strain mixture was inoculated around the implant. We labeled Δ*nuc1*/WT with sfGFP and Δ*nuc2*/Δ*nuc1/2* with mCherry. Mice were infected with either a WT/Δ*nuc1/2* mixture or a Δ*nuc1*/Δ*nuc2* mixture. All mice were euthanized by cervical dislocation and anesthetized 7 days after the infection. The biofilm on the titanium disks was observed using a fluorescence microscope (Leica DMI8, Germany).

Mouse Model of Hematogenous IAIs

Thirty-two adult BALB/c mice were randomly divided into four groups (WT, Δ*nuc1*, Δ*nuc2*, and Δ*nuc1/2*). After the implantation surgery performed as described previously, mice were infected via tail vein injection (ST1792 and its isogenic mutants, 1×10^7 CFU/100 μl). Survival was recorded daily. All

mice were anesthetized and euthanized by cervical dislocation 28 days after the infection. Peri-implant tissues and biofilm cells on the implant were prepared as described above. Bacterial load enumeration was performed according to the protocol listed in Section "Bacterial Load Enumeration."

Bacterial Load Enumeration

The bacterial suspension or sonicated fluid was serially diluted tenfold. A total of 100 μl of the diluted suspension was spread on sheep blood agar plates. After incubation at 37°C overnight, CFU counts were performed according to the National Standard of China GB/T 4789.2 protocol. The resulting bacterial load for peri-implant tissues was normalized to tissue weight, and all bacterial loads were presented on a $\log_{10}$ scale.

Statistical Analysis

The GEO microarray was analyzed with R 4.0.1. The fluorescence distribution pattern in **Figure 4** was quantified with a Pearson correlation test using Coloc 2, a program in ImageJ (1.53c, Fiji). The remaining data analysis was performed using GraphPad Prism 8.3.0. Statistical significance was indicated as a two-sided $p < 0.05$. Results are represented as mean ± SD unless stated otherwise.

DATA AVAILABILITY STATEMENT

The raw data supporting the conclusions of this article will be made available by the authors, without undue reservation.

ETHICS STATEMENT

Neutrophils were isolated from the blood of healthy donors. Human synovial fluid was collected from osteoarthritis patients before they received intra-articular injection of hyaluronic acid. The procedures were approved by the Ethics Committee of the Shanghai Sixth Peoples Hospital. The handling of mice and related procedures in this study were approved by the Animal Care and Experiment Committee of the Medical College of Shanghai Jiao Tong University affiliated Sixth People's Hospital.

AUTHOR CONTRIBUTIONS

JY contributed to the concept of the study and wrote the manuscript. JD and FZ contributed to the qPCR experiment. YM and JY performed *S. aureus* mutant construction. JT and MH collected clinical strains and performed antibiotic susceptibility testing. JY, FJ, and FZ performed the *in vivo* experiment. QW and PH contributed to data analysis and data interpretation. HS contributed to the study design, manuscript editing and revision. All authors contributed to the article and approved the submitted version.

FUNDING

This study was supported by the National Natural Science Foundation of China (Grant No. 81772364) and Medical Guidance Scientific Research Support Project of Shanghai Science and Technology Commission (Grant No. 19411962600).

ACKNOWLEDGMENTS

We thank Diep BA for the gift of USA300 and its isogenic mutants (BD1276, BD1280, and BD1281).

SUPPLEMENTARY MATERIAL

The Supplementary Material for this article can be found online at: https://www.frontiersin.org/articles/10.3389/fmicb.2021.687888/full#supplementary-material

Supplementary Figure 1 | Transcription levels of thermonucleases in clinical isolates cultured in TSB (supplied with 20% human synovial fluid). Expression of *nuc1* **(A)** and *nuc2* **(B)** in IAI and non-IAI isolates (n=14/group) determined by qPCR. Statistical significance was calculated using two-tailed Student's t-test; $^{*}p < 0.05$; $^{**}p < 0.01$ vs. non-IAI strains.

Supplementary Figure 2 | Biofilm eDNA measurement for clinical isolates and its relation to *nuc1* or *nuc2* transcription. **(A)** Biofilm eDNA content in IAI and non-IAI biofilms was measured by with SYTOX green staining and presented as fluorescence signals (n=14/group). Two-tailed Student's t-test was adopted; $^{*}p < 0.05$ vs. the non-IAI group. **(B)** Biofilm eDNA content was related to *nuc1* or *nuc2* expression using the Pearson correlation test.

Supplementary Figure 3 | (A) Sanger sequence results of *nuc1* and *nuc2* mutations with alignment to WT ST1792. **(B)** ST1792 *nuc1* and *nuc2* double mutation leads to the sticky characteristic of the bacterial colony.

Supplementary Figure 4 | Bacterial load enumeration for biofilms formed *in vitro* by ST1792 and its isogenic mutants. Statistical significance was calculated using ANOVA with Dunnett multiple column comparisons. n=3/group. $^{**}p < 0.01$ vs. WT.

Supplementary Figure 5 | Fluorescence co-localization test using ImageJ. **(A)** Δ*nuc1* and Δ*nuc2* co-localization 2D intensity plot. **(B)** WT and Δ*nuc1/2* co-localization 2D intensity plot. A Pearson correlation test was performed in this study.

Supplementary Figure 6 | Biofilms formed on titanium disk *in vitro* by ST1792 and its isogenic mutant strains observed using SEM with ×2,000 magnification. Scale bar=10 μ m.

Supplementary Figure 7 | Biofilms formed by ST1792 and its isogenic mutant strains observed using a confocal microscope. Green represents live cells, and red represents eDNA and dead cells. Scale bar=50 μ m.

Supplementary Figure 8 | Mutual comparison of survival curves among four groups. **(A)** Survival analysis between WT (n=8) and Δ*nuc1* (n=7); **(B)** survival analysis between WT (n=8) and Δ*nuc2* (n=8); **(C)** survival analysis between WT (n=8) and Δ*nuc1/2* (n=7); **(D)** survival analysis between Δ*nuc1* (n=7) and Δ*nuc2* (n=8); **(E)** survival analysis between Δ*nuc1/2* (n=7) and Δ*nuc2* (n=8). Statistical significance was analyzed with a log-rank (Mantel–Cox) test.

Supplementary Figure 9 | Bacterial count for implant (right) and peri-implant tissues (left) in a hematogenous IAI mouse model (n=8, 12, 6, and 16 h for WT, Δ*nuc1*, Δ*nuc2*, and Δ*nuc1/2*, respectively). Statistical significance was calculated using ANOVA with Dunnett multiple column comparisons.

REFERENCES

Arciola, C. R., An, Y. H., Campoccia, D., Donati, M. E., and Montanaro, L. (2005). Etiology of implant orthopedic infections: a survey on 1027 clinical isolates. *Int. J. Artif. Organs* 28, 1091–1100. doi: 10.1177/039139880502801106

Arciola, C. R., Campoccia, D., and Montanaro, L. (2018). Implant infections: adhesion, biofilm formation and immune evasion. *Nat. Rev. Microbiol.* 16, 397–409. doi: 10.1038/s41579-018-0019-y

Bae, T., and Schneewind, O. (2006). Allelic replacement in *Staphylococcus aureus* with inducible counter-selection. *Plasmid* 55, 58–63. doi: 10.1016/j.plasmid.2005.05.005

Beenken, K. E., Spencer, H., Griffin, L. M., and Smeltzer, M. S. (2012). Impact of extracellular nuclease production on the biofilm phenotype of *Staphylococcus aureus* under in vitro and in vivo conditions. *Infect. Immun.* 80, 1634–1638. doi: 10.1128/IAI.06134-11

Berends, E. T., Horswill, A. R., Haste, N. M., Monestier, M., Nizet, V., and von Kockritz-Blickwede, M. (2010). Nuclease expression by Staphylococcus aureus facilitates escape from neutrophil extracellular traps. *J. Innate Immun.* 2, 576–586. doi: 10.1159/000319909

de Jong, N. W., van der Horst, T., van Strijp, J. A., and Nijland, R. (2017). Fluorescent reporters for markerless genomic integration in *Staphylococcus aureus*. *Sci. Rep.* 7:43889. doi: 10.1038/srep43889

Depypere, M., Morgenstern, M., Kuehl, R., Senneville, E., Moriarty, T. F., Obremskey, W. T., et al. (2020). Pathogenesis and management of fracture-related infection. *Clin. Microbiol. Infect.* 26, 572–578. doi: 10.1016/j.cmi.2019.08.006

Flemming, H. C. (2016). EPS-then and now. *Microorganisms* 4:41. doi: 10.3390/microorganisms4040041

Flemming, H. C., and Wingender, J. (2010). The biofilm matrix. *Nat. Rev. Microbiol.* 8, 623–633. doi: 10.1038/nrmicro2415

Hall-Stoodley, L., Stoodley, P., Kathju, S., Hoiby, N., Moser, C., Costerton, J. W., et al. (2012). Towards diagnostic guidelines for biofilm-associated infections. *FEMS Immunol. Med. Microbiol.* 65, 127–145. doi: 10.1111/j.1574-695X.2012.00968.x

Hobley, L., Harkins, C., MacPhee, C. E., and Stanley-Wall, N. R. (2015). Giving structure to the biofilm matrix: an overview of individual strategies and emerging common themes. *FEMS Microbiol. Rev.* 39, 649–669. doi: 10.1093/femsre/fuv015

Hu, Y., Xie, Y., Tang, J., and Shi, X. (2012). Comparative expression analysis of two thermostable nuclease genes in *Staphylococcus aureus*. *Foodborne Pathog. Dis.* 9, 265–271. doi: 10.1089/fpd.2011.1033

Iwasaki, A., and Medzhitov, R. (2010). Regulation of adaptive immunity by the innate immune system. *Science* 327, 291–295. doi: 10.1126/science.1183021

Kaito, C., Hirano, T., Omae, Y., and Sekimizu, K. (2011). Digestion of extracellular DNA is required for giant colony formation of *Staphylococcus aureus*. *Microb. Pathog.* 51, 142–148. doi: 10.1016/j.micpath.2011.04.007

Kapadia, B. H., Berg, R. A., Daley, J. A., Fritz, J., Bhave, A., and Mont, M. A. (2016). Periprosthetic joint infection. *Lancet* 387, 386–394. doi: 10.1016/S0140-6736(14)61798-0

Kiedrowski, M. R., Crosby, H. A., Hernandez, F. J., Malone, C. L., McNamara, J. O. II, and Horswill, A. R. (2014). Staphylococcus aureus Nuc2 is a functional, surface-attached extracellular nuclease. *PLoS One* 9:e95574. doi: 10.1371/journal.pone.0095574

Kiedrowski, M. R., Kavanaugh, J. S., Malone, C. L., Mootz, J. M., Voyich, J. M., Smeltzer, M. S., et al. (2011). Nuclease modulates biofilm formation in community-associated methicillin-resistant Staphylococcus aureus. *PLoS One* 6:e26714. doi: 10.1371/journal.pone.0026714

Konigsberg, B. S., Della Valle, C. J., Ting, N. T., Qiu, F., and Sporer, S. M. (2014). Acute hematogenous infection following total hip and knee arthroplasty. *J. Arthroplasty.* 29, 469–472. doi: 10.1016/j.arth.2013.07.021

Lim, W. K., Wang, K., Lefebvre, C., and Califano, A. (2007). Comparative analysis of microarray normalization procedures: effects on reverse engineering gene networks. *Bioinformatics* 23, i282–i288. doi: 10.1093/bioinformatics/btm201

Mccarthy, H., Rudkin, J. K., Black, N. S., Gallagher, L., O'Neill, E., and O'Gara, J. P. (2015). Methicillin resistance and the biofilm phenotype in Staphylococcus aureus. *Front. Cell. Infect. Microbiol.* 5:1. doi: 10.3389/fcimb.2015.00001

Moormeier, D. E., Bose, J. L., Horswill, A. R., and Bayles, K. W. (2014). Temporal and stochastic control of *Staphylococcus aureus* biofilm development. *mBio* 5:e01341–14. doi: 10.1128/mBio.01341-14

Okshevsky, M., Regina, V. R., and Meyer, R. L. (2015). Extracellular DNA as a target for biofilm control. *Curr. Opin. Biotechnol.* 33, 73–80. doi: 10.1016/j.copbio.2014.12.002

Olson, M. E. (2014). "Bacteriophage transduction in *Staphylococcus aureus*," in *Methods in Molecular Biology*, ed. J. L. Bose (New York, NY: Springer), 69–74. doi: 10.1007/7651_2014_186

Olson, M. E., Nygaard, T. K., Ackermann, L., Watkins, R. L., Zurek, O. W., Pallister, K. B., et al. (2013). *Staphylococcus aureus* nuclease is an SaeRS-dependent virulence factor. *Infect. Immun.* 81, 1316–1324. doi: 10.1128/IAI.01242-12

Otto, M. (2018). Staphylococcal biofilms. *Microbiol. Spectr.* 6:6.4.27. doi: 10.1128/microbiolspec.GPP3-0023-2018

Paharik, A. E., and Horswill, A. R. (2016). The *Staphylococcal Biofilm*: adhesins, regulation, and host response. *Microbiol. Spectr.* 4:4.2.06. doi: 10.1128/microbiolspec.VMBF-0022-2015

Pang, Y. Y., Schwartz, J., Thoendel, M., Ackermann, L. W., Horswill, A. R., and Nauseef, W. M. (2010). agr-Dependent interactions of *Staphylococcus aureus* USA300 with human polymorphonuclear neutrophils. *J. Innate Immun.* 2, 546–559. doi: 10.1159/000319855

Pulido, L., Ghanem, E., Joshi, A., Purtill, J. J., and Parvizi, J. (2008). Periprosthetic joint infection: the incidence, timing, and predisposing factors. *Clin. Orthop. Relat. Res.* 466, 1710–1715. doi: 10.1007/s11999-008-0209-4

Ritchie, M. E., Phipson, B., Wu, D., Hu, Y., Law, C. W., Shi, W., et al. (2015). limma powers differential expression analyses for RNA-sequencing and microarray studies. *Nucleic Acids Res.* 43, e47. doi: 10.1093/nar/gkv007

Schilcher, K., and Horswill, A. R. (2020). Staphylococcal biofilm development: structure, regulation, and treatment strategies. *Microbiol. Mol. Biol. Rev.* 84:e00026–19. doi: 10.1128/MMBR.00026-19

Sendi, P., Banderet, F., Graber, P., and Zimmerli, W. (2011). Periprosthetic joint infection following *Staphylococcus aureus* bacteremia. *J. Infect.* 63, 17–22. doi: 10.1016/j.jinf.2011.05.005

Sultan, A. R., Hoppenbrouwers, T., Lemmens-den Toom, N. A., Snijders, S. V., van Neck, J. W., Verbon, A., et al. (2019). During the early stages of *Staphylococcus aureus* biofilm formation, induced neutrophil extracellular traps are degraded by autologous thermonuclease. *Infect. Immun.* 87, e00605–19. doi: 10.1128/IAI.00605-19

Tande, A. J., Palraj, B. R., Osmon, D. R., Berbari, E. F., Baddour, L. M., Lohse, C. M., et al. (2016). Clinical presentation, risk factors, and outcomes of hematogenous prosthetic joint infection in patients with *Staphylococcus aureus* bacteremia. *Am. J. Med.* 129:221 e211–e220. doi: 10.1016/j.amjmed.2015.09.006

Tang, J., Kang, M., Chen, H., Shi, X., Zhou, R., Chen, J., et al. (2011). The staphylococcal nuclease prevents biofilm formation in *Staphylococcus aureus* and other biofilm-forming bacteria. *Sci. China Life Sci.* 54, 863–869. doi: 10.1007/s11427-011-4195-5

Tang, J., Zhou, R., Shi, X., Kang, M., Wang, H., and Chen, H. (2008). Two thermostable nucleases coexisted in *Staphylococcus aureus*: evidence from mutagenesis and in vitro expression. *FEMS Microbiol. Lett.* 284, 176–183. doi: 10.1111/j.1574-6968.2008.01194.x

Thammavongsa, V., Missiakas, D. M., and Schneewind, O. (2013). *Staphylococcus aureus* degrades neutrophil extracellular traps to promote immune cell death. *Science* 342, 863–866. doi: 10.1126/science.1242255

Wang, Y., Cheng, L. I., Helfer, D. R., Ashbaugh, A. G., Miller, R. J., Tzomides, A. J., et al. (2017). Mouse model of hematogenous implant-related Staphylococcus aureus biofilm infection reveals therapeutic targets. *Proc. Natl. Acad. Sci. U.S.A.* 114, E5094–E5102. doi: 10.1073/pnas.1703427114

Whitchurch, C. B., Tolker-Nielsen, T., Ragas, P. C., and Mattick, J. S. (2002). Extracellular DNA required for bacterial biofilm formation. *Science* 295:1487. doi: 10.1126/science.295.5559.1487

Winstel, V., Missiakas, D., and Schneewind, O. (2018). Staphylococcus aureus targets the purine salvage pathway to kill phagocytes. *Proc. Natl. Acad. Sci. U.S.A.* 115, 6846–6851. doi: 10.1073/pnas.1805622115

Zatorska, B., Arciola, C. R., Haffner, N., Segagni Lusignani, L., Presterl, E., and Diab-Elschahawi, M. (2018). Bacterial extracellular DNA production is associated with outcome of prosthetic joint infections. *Biomed. Res. Int.* 2018:1067413. doi: 10.1155/2018/1067413

Zatorska, B., Groger, M., Moser, D., Diab-Elschahawi, M., Lusignani, L. S., and Presterl, E. (2017). Does extracellular DNA production vary in staphylococcal biofilms isolated from infected implants versus controls? *Clin. Orthop. Relat. Res.* 475, 2105–2113. doi: 10.1007/s11999-017-5266-0

Zimmerli, W. (2014). Clinical presentation and treatment of orthopaedic implant-associated infection. *J. Intern. Med.* 276, 111–119. doi: 10.1111/joim.12233

Zimmerli, W., and Moser, C. (2012). Pathogenesis and treatment concepts of orthopaedic biofilm infections. *FEMS Immunol. Med. Microbiol.* 65, 158–168. doi: 10.1111/j.1574-695X.2012.00938.x

Conflict of Interest: The authors declare that the research was conducted in the absence of any commercial or financial relationships that could be construed as a potential conflict of interest.

frontiers in Microbiology

ORIGINAL RESEARCH
published: 07 September 2021
doi: 10.3389/fmicb.2021.714994

Staphylococcus aureus Strain-Dependent Biofilm Formation in Bone-Like Environment

*Fabien Lamret[1], Jennifer Varin-Simon[1], Frédéric Velard[1], Christine Terryn[2], Céline Mongaret[1,3], Marius Colin[1,4], Sophie C. Gangloff[1,4] and Fany Reffuveille[1,4]**

[1] Université de Reims Champagne-Ardenne, Laboratory BIOS EA 4691, Reims, France, [2] Plateforme en Imagerie Cellulaire et Tissulaire, Université de Reims Champagne-Ardenne, Reims, France, [3] Service Pharmacie, Centre Hospitalier Universitaire de Reims, Reims, France, [4] Université de Reims Champagne-Ardenne, UFR de Pharmacie, Reims, France

Staphylococcus aureus species is an important threat for hospital healthcare because of frequent colonization of indwelling medical devices such as bone and joint prostheses through biofilm formations, leading to therapeutic failure. Furthermore, bacteria within biofilm are less sensitive to the host immune system responses and to potential antibiotic treatments. We suggested that the periprosthetic bone environment is stressful for bacteria, influencing biofilm development. To provide insights into *S. aureus* biofilm properties of three strains [including one methicillin-resistant *S. aureus* (MRSA)] under this specific environment, we assessed several parameters related to bone conditions and expected to affect biofilm characteristics. We reported that the three strains harbored different behaviors in response to the lack of oxygen, casamino acids and glucose starvation, and high concentration of magnesium. Each strain presented different biofilm biomass and live adherent cells proportion, or matrix production and composition. However, the three strains shared common responses in a bone-like environment: a similar production of extracellular DNA and engagement of the SOS response. This study is a step toward a better understanding of periprosthetic joint infections and highlights targets, which could be common among *S. aureus* strains and for future antibiofilm strategies.

Keywords: MSSA, MRSA, biofilms, prosthetic joint infection, bone microenvironment

OPEN ACCESS

Edited by:
Enea Gino Di Domenico, Istituti Fisioterapici Ospitalieri, Scientific Institute for Research, Hospitalization and Healthcare, Italy

Reviewed by:
Mukesh Kumar Yadav, Mizoram University, India
Matthias Reiger, University of Augsburg, Germany

****Correspondence:***
Fany Reffuveille
fany.reffuveille@univ-reims.fr

Specialty section:
This article was submitted to Infectious Diseases, a section of the journal Frontiers in Microbiology

Received: *26 May 2021*
Accepted: *30 July 2021*
Published: *07 September 2021*

Citation:
Lamret F, Varin-Simon J, Velard F, Terryn C, Mongaret C, Colin M, Gangloff SC and Reffuveille F (2021) Staphylococcus aureus Strain-Dependent Biofilm Formation in Bone-Like Environment. Front. Microbiol. 12:714994. doi: 10.3389/fmicb.2021.714994

INTRODUCTION

Environmental parameters such as nutrient availability, oxygen level, dynamic flow, or static culture represent different stresses for bacteria. One adaptive response is the formation of biofilm with various organizations (Bjarnsholt, 2013; Haney et al., 2018). Into the biofilm state, bacteria adopt a different level of metabolic activity and can be phenotypically different from their planktonic counterpart (O'Toole et al., 2000; Hall-Stoodley et al., 2004). Furthermore, biofilm structure and more precisely the biofilm matrix reduces molecule permeability, and a reduced metabolism allows bacteria to escape the immune system and to be tolerant to antibiotics (Flemming and Wingender, 2010; Stewart, 2015). Moreover, the surface nature has a strong impact on the biofilm structure (Feng et al., 2015; Forson et al., 2020). These bacterial communities can grow on both biotic and abiotic supports, such as medical implants (i.e., catheters, pacemakers, or

bone and joint prostheses) (Donlan, 2001; Ahmed et al., 2019). Their implantation leads to a host biological response: chronic inflammation, foreign-body response, and host-protein adsorption like fibronectin cover, which also facilitates biofilm development (Fischer et al., 1996; Gibon et al., 2017a,b; Masters et al., 2019). According to the infection site, the proportion of viable adherent bacteria, dead cells, and matrix within the biofilm could be very variable (Nandakumar et al., 2013; Liu et al., 2020). Focusing on bone context, primary periprosthetic joint infections (PJIs) after surgery represent approximately 2% of total joint arthroplasty (Grammatico-Guillon et al., 2012; Springer et al., 2017; Shoji and Chen, 2020). As a consequence, this problem is a major concern with an increasing need of bone and joint prosthesis due to population aging (Levack et al., 2018; Li et al., 2018; Masters et al., 2019; Shoji and Chen, 2020).

Staphylococcus aureus, including methicillin-sensitive (MSSA) and methicillin-resistant (MRSA) strains, is mainly involved in PJIs with biofilm development in the periprosthetic environment (Masters et al., 2019; Shoji and Chen, 2020). *S. aureus* biofilm matrix is mainly composed of polysaccharides, extracellular DNA (eDNA), and proteins (Flemming and Wingender, 2010). Among polysaccharides involved in the biofilm, the polysaccharide intercellular adhesin (PIA), also named poly-ββ(1-6)-N-acetylglucosamine (PNAG), is largely predominant (Karygianni et al., 2020). eDNA originates from bacterial lysis or release by live bacteria (Rice et al., 2007; DeFrancesco et al., 2017). *S. aureus* produces considerable amount of proteins in the biofilm matrix such as enzymes or structural proteins, but it is also able to integrate host plasma proteins such as fibrinogen to its matrix (Flemming and Wingender, 2010; Zapotoczna et al., 2015). All these components stabilize the biofilm structures since enzymes such as dispersin B, DNAse, and protease disrupt biofilm by targeting these components (Sadovskaya et al., 2006; Tetz and Tetz, 2010; Lister and Horswill, 2014; Karygianni et al., 2020). MSSA strains produce PIA-dependent matrix mediated by *ica* operon, whereas MRSA strain biofilms are mainly dependent on surface proteins and eDNA (McCarthy et al., 2015). Those differences underline the fact that antibiofilm strategies cannot be universal but need to be adapted according to the bacterial strain and to the biofilm environment.

Thus, biofilm model choice is of utmost importance and has to be relevant and adapted to studied infection conditions (Bjarnsholt et al., 2013; Coenye et al., 2020). It could be suggested that developing new adapted models for each infection site is at least as important as investigating new antibacterial molecules. Models have been developed to improve the clinical relevance for biofilm studies, but to date, there is no existing *in vitro* bone biofilm model (Muthukrishnan et al., 2019). In order to develop new antimicrobial molecules adapted to control PJIs, study of specific bone environment influence on biofilm initiation is needed. Thus, the identification of bone factors affecting biofilms will allow the creation of an *in vitro* bone-biofilm model, close to clinic infection parameters.

Based on preliminary study, some factors were identified to strongly contribute to MSSA adherence and biofilm maturation: anaerobic growth, absence of nutritional molecules (glucose, amino acids), and high concentration of magnesium (Reffuveille et al., 2018). In this present study, we analyzed three different *S. aureus* strain (including one MRSA) behaviors in response to those identified bone microenvironment factors. We evaluated biofilm biomass, live adherent bacteria, matrix composition, and genes expression. A bone-like environment medium was proposed, and specific parameters were identified like influencing conditions for biofilm formation.

MATERIALS AND METHODS

Bacterial Strains and Culture Media

Three commercially available *S. aureus* strains were used in this study: CIP 53.154, SH1000, and USA300. *S. aureus* CIP 53.154 (sensitivity test organism quality control strain for European Pharmacopeia) equivalent to ATCC9144 or NCTC 6571 was first isolated in Oxford, UK, in 1944 and possess the "Set1 gene cluster" (Heatley, 1944). This strain is methicillin sensitive, whereas two mutations are known in *pbp2* gene (Fuller et al., 2005). SH1000 is another methicillin-sensitive strain and originated from 8325-4 strain with *rsbU* gene repaired (Horsburgh et al., 2002). USA300 strain, meanwhile, emerged first as community-associated MRSA in the United States in the late 1990s and become endemic pathogens worldwide. This strain is known to be implicated in osteomyelitis and was first reported in the United States as a cause of skin and soft issue infection (Diep et al., 2008; Tenover and Goering, 2009).

A minimal medium (MM) [62 mM potassium phosphate buffer, pH 7.0, 7 mM $(NH4)_2SO_4$, 2 mM $MgSO_4$, 10 μM $FeSO_4$) containing 0.4% (w/v) glucose and 0.1% (w/v) casamino acids] was used in all biofilm models. This medium was modified according to the conditions tested: $MgSO_4$ concentration was modified by increasing the amount of added $MgSO_4$ (10-folds). Experiments under hypoxic conditions were performed using the GenBag system (Biomérieux, Marcy-l'Étoile, France). For all experiments, the absorbance of overnight cultures was measured at 600 nm to dilute the overnight culture in appropriate and fresh medium to obtain an inoculum with a final absorbance of 0.01, except for real-time quantitative PCR (RT-qPCR); overnight cultures were diluted in the appropriate medium in order to get a final absorbance of 0.1. Media containing bacteria inoculated in microtiter plates were incubated at 37°C for 24 h.

Light Microscopy

Diluted bacteria are inoculated into a 24-well microtiter plate (Corning, New York, NY, United States) (500 μl per well) and incubated for 24 h. Wells were washed twice with distilled water before imaging. Light microscopy images of the well's bottom was performed by a Zeiss Axiovert 200 M using 20 × objective.

Crystal Violet Staining

As previously described, biofilm biomass was evaluated by crystal violet staining (Reffuveille et al., 2014). Briefly, inocula were adjusted to absorbance of 0.01, and 500 μl was distributed in a 48-well plate (Corning, New York, NY, United States). After 24 h of incubation, the planktonic growth was evaluated by measuring the absorbance at 600 nm. The

wells were gently washed three times with water, and 500 µl of 0.2% crystal violet was added to each well. Plates were incubated for 20 min in the dark at room temperature. Wells were washed three times with water, and 500 µl of 95% ethanol was added to each well. The absorbance at 595 nm was measured to evaluate the amount of biofilm biomass, which is proportional to the absorbance value. Four biological replicates were conducted, and each included three technical replicates.

Counting Method

To assess the number of live adherent bacteria, inocula were prepared as previously described with an adjusted absorbance of 0.01, and 500 µl was distributed in 24-well plates with a Thermanox™ coverslip (Thermo Fisher Scientific, New York, NY, United States) placed to stay vertically in the well. After 24 h of incubation, the coverslips were washed with minimal medium and transferred to a 15-ml tube containing 2 ml of minimal medium. Biofilm-embedded bacteria attached to coverslips were then detached by placing the tube in ultrasonic bath (40 kHz) for 5 min. A volume of 100 µl from serial dilutions was plated on nutrient agar plates to determine the quantity of initially attached bacteria. The results of counting method are expressed as the ratio of live adherent bacteria on total bacteria (live adherent and planktonic bacteria). Four biological replicates were conducted, and each included two technical replicates.

Scanning Electron Microscopy

To prepare the samples, inocula were prepared as previously described with an adjusted OD of 0.01, and 500 µl was distributed in 24-well plates on a Thermanox™ coverslip placed at the bottom of 24-well plates (cell culture treated side up). After 24 h of incubation, the coverslips were washed twice in phosphate-buffered saline (PBS), then fixed in 2.5% (w/v) glutaraldehyde (Sigma-Aldrich, St. Louis, MO, United States) at room temperature for 1 h. After two distilled water rinses, biofilms were dehydrated in graded ethanol solutions (50, 70, 90, and 100% twice) for 10 min. Biofilms were finally desiccated in a drop of hexamethyldisilazane (Sigma-Aldrich, St. Louis, MO, United States). After air drying at room temperature, samples were sputtered with a thin gold–palladium film using a JEOL ion sputter JFC 1100 instrument. Biofilms were observed using a Schottky Field Emission Scanning Electron Microscope (JEOL JSM-7900F). Images were obtained at a primary beam energy of 2 kV (SM-EXG65 electron emitter).

Confocal Laser Scanning Microscopy

To prepare the samples, inocula were prepared as previously described with an adjusted OD of 0.01, and 500 µl were distributed in 24-well plates on a Thermanox™ coverslip placed at the bottom of 24-well plates (cell culture treated side up). After 24 h of incubation, the coverslips were washed twice in PBS and stained with SYTO™ 9 at 1 µM and (i) propidium iodide (Thermo Fisher Scientific, Waltham, MA, United States) at 20 µM to label live and damaged or "dead" bacteria, (ii) SYPRO® Ruby (Thermo Fisher Scientific, Waltham, MA, United States) (v/v) to label proteins, or (iii) wheat germ agglutinin (WGA) associated with the Alexa Fluor™ 350 conjugate (Thermo Fisher Scientific, Waltham, MA, United States) at 100 µg/ml to label PIA with TOTO™-3 iodide (Thermo Fisher Scientific, Waltham, MA, United States) at 2 µM to label extracellular DNAs. Each label was diluted in 0.9% NaCl. After 30 min of incubation in the dark at room temperature, each coverslip was washed two times with PBS and placed in a 24-well Krystal plate with glass bottom (Dutscher, Porvair, United Kingdom) with the biofilm-side lower before observation with confocal laser scanning microscopy (CLSM) (LSM 710 NLO, Zeiss, Germany). Fluorochromes-labeled matrix compounds were imaged and their volume quantified using IMARIS software (Imaris, RRID:SCR_007370).

RT-qPCR (RNA Purification and Reverse Transcription)

To prepare the sample, inocula were prepared as previously described with an adjusted OD of 0.1, and 1 ml was distributed in six-well plates (Corning, New York, NY, United States). After 24 h of incubation, the wells were washed twice in PBS to discard planktonic cells, and total RNAs were extracted and cleaned up from *S. aureus* biofilms with MasterPure™ RNA Purification Kit (Lucigen, Middleton, WI, United States) in accordance with the manufacturer's protocol. Total RNAs were reverse transcribed into complementary DNA (cDNA) using a high-capacity cDNA reverse transcription kit (Lucigen, Middleton, WI, United States) following the manufacturer's instructions. Transcription products were amplified by RT-qPCR using different primers (Eurogentec, Seraing, Belgium) (**Table 1**) on a StepOne Plus™ system (Applied Biosystems, Villebon-sur-Yvette, France). The SYBR™ Green Master Mix (Applied Biosystems, Foster City, United States) was used for amplification. After a first denaturation step at 95°C for 10 min, RT-qPCR reactions were performed according to a thermal profile that corresponds to 40 cycles of denaturation at 95°C for 15 s, annealing and extension at 60°C for 1 min. Data collection was performed at the end of each annealing/extension step. The third step that consists in a dissociation process is performed to ensure the specificity of the amplicons by measuring their melting temperature (Tm). Data analysis was performed with the StepOne™ Software v2.3 (Applied Biosystems, Villebon-sur-Yvette, France). Target transcript levels (N-target) were normalized to the housekeeping gene transcript levels, and messenger RNA (mRNA) level with the equation N-target = $2.\delta Ct$, where δCt is the Ct value of the target gene after subtraction of Ct for the housekeeping gene (Ayciriex et al., 2017). *gyrB* was used as housekeeping gene for CIP 53.154; *rho* was used for SH1000 and USA300 strains.

Statistical Methods

The statistical significance of the results was assessed using the exact non-parametric Wilcoxon–Mann–Whitney test for independent samples (GraphPad Prism, RRID:SCR_002798). Differences were considered significant at $p < 0.05$.

TABLE 1 | Nucleotide sequences of primers used for RT-qPCR and efficiency for each primer couple.

Target gene	Sequences		Efficiency
	Forward primer (5′→3′)	Reverse primer (5′→3′)	
gyrB	CACGTGAAGGTATGACAGCA	ACAACTTGACGCACTTCAGA	2
rho	AACGTGGGGATAAAGTAACTGG	TTCACTTCTTCTGCGTTATGGT	1.9
icaC	TCGTATATTTACGTGCCATTATATGTG	AAGCAAGGTGTACCAAAAATGAC	1.9
recA	ATAGGTCGCCGAGTTTCAAC	GCGCTACTGTTGTCTTACCA	1.9
lexA	TCAATATTTTCTACTGCGGTAATAGG	GAAACGATTCATGTGCCAGTT	2
sarA	TTTCTCTTTGTTTTCGCTGATGT	TGTTATCAATGGTCACTTATGCTG	2
rsh	CGAAACCTAATAACGTATCAAATGC	TGTATGTAGATCGAAAACCATCACT	2
cidA	GATTGTACCGCTAACTTGGGT	GCGTAATTTCGGAAGCAACAT	1.8
nuc	TCGAGTTTGACAAAGGCCAA	AAGCAACTTTAGCCAAGCCT	1.9
fnbpB	AATTAAATCAGAGCCGCCAGT	AATGGTACCTTCTGCATGACC	2.0
srrA	AGCAAGTAATGGCCAAGAGG	TAGTTGCCACCTGGATACCA	2.0

RESULTS

Different *S. aureus* Strains Basically Harbor Different Biofilm Formation Patterns

In this study, we investigated 24-h-old biofilms to understand initiation of *S. aureus* biofilm formation in early stages of the periprosthetic infection outcome. Three strains of *S. aureus*, naive to bone environment, were selected. Two strains are methicillin-susceptible *S. aureus* (MSSA), namely, CIP 53.154 and SH1000, and the last one is a methicillin-resistant *S. aureus* (MRSA) strain, namely, USA300. Although these strains belong to the same species, their biofilms formed in aerobic condition in minimal medium (MM) presented a different organization, revealed by light microscopy (**Figure 1**). CIP 53.154 developed three-dimensional aggregates, and only few bacteria were individually adherent between aggregates. The second MSSA strain, namely, SH1000, formed smaller but more numerous aggregates. USA300 displayed a third organization, different from the two previous strains, without any aggregates but a homogeneous colonization of the bottom of the well.

Impact of Oxygen on Biofilm Biomass and Matrix Formation

The three different strains of *S. aureus* were grown in MM in the presence or absence of oxygen to mimic the hypoxic bone environment (Xu et al., 2016). Both MSSA (CIP 53.154 and SH1000 strains) presented planktonic growth default under hypoxic condition (CIP 53.154, 2.06-fold, $p < 0.0001$; SH1000, 1.57-fold, $p < 0.0001$; **Supplementary Material**). When cultured with oxygen, CIP 53.154 strain displayed a ratio of biofilm biomass on planktonic growth of 0.3, whereas SH1000 strain presented a ratio of 2.1, and USA300 had the higher ratio of 2.9 (**Figure 2A**). The three strains differently responded to the lack of oxygen. Indeed, hypoxic condition increased the biofilm proportion formed by CIP 53.154 strain by 21-fold ($p < 0.001$). We did not found statistical difference between the biofilm proportion ratio of aerobic and hypoxic incubation of SH1000 strain (increased by 1.08-fold in hypoxic condition). USA300 strain presented a third behavior: a decrease in biofilm proportion by threefold ($p < 0.001$).

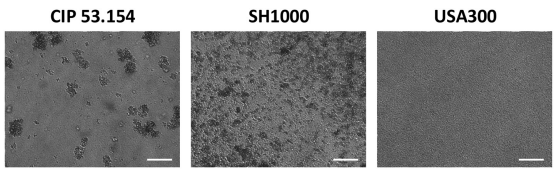

FIGURE 1 | Different biofilm structures according to *S. aureus* strains. Biofilms were grown aerobically for 24 h in minimal medium and imaged by light microscopy. Representative images are shown. The scale bars indicate 40 μm.

Next, the effect of hypoxic condition on adherent viable *S. aureus* cells was investigated. As seen in **Figure 2B**, in the presence of oxygen, 16% of viable bacteria were in biofilm state for CIP 53.154 strain, 6% for SH1000 strain, and <1% for USA300 strain. After 24 h of biofilm formation under hypoxic condition, the proportion of adherent viable bacteria was increased by 1.4-fold for CIP 53.154 strain, decreased by 3.4-fold for SH1000 strain, and increased by 3.6-fold for USA300 strain with no statistical differences due to highly dispersed results.

In order to explain results observed with crystal violet coloration and counting method, 24-h-old biofilm samples were observed by scanning electron microscopy (SEM) (**Figure 2C**). The three strains of this study produced few matrix structures under aerobic culture, sticking bacteria to each other. We observed a different matrix aspect, such as slime or granular structures. Oxygen-depleted culture led to a loss of matrix production for SH1000 strain and MRSA strain, whereas CIP 53.154 strain produced more matrix, which reinforced adherence between bacteria.

We next focused our attention on CIP 53.154 strain owing to the large increase in biofilm proportion due to hypoxic condition. When cultured with minimal medium and oxygen, 22% of bacteria included in the biofilm were dead or damaged (**Figure 3A**). Oxygen deprivation led to a decrease in dead

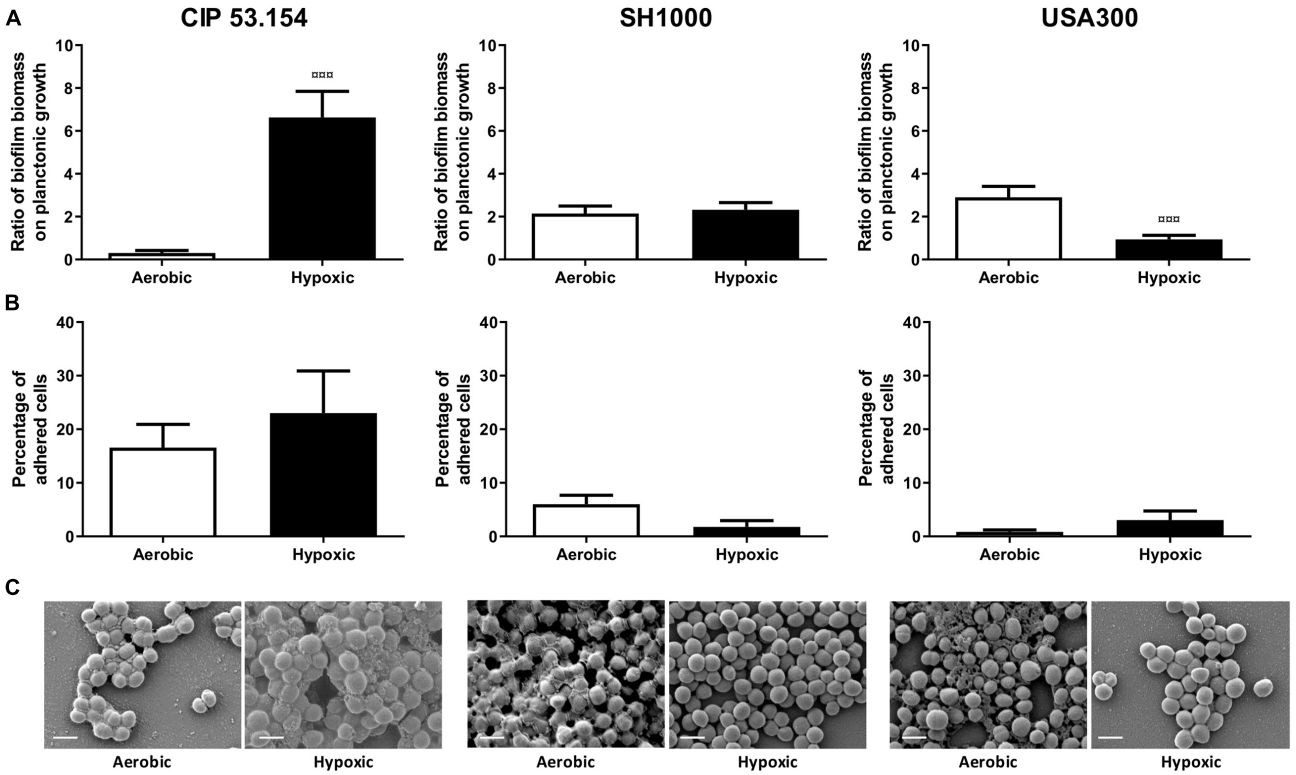

FIGURE 2 | Impact of hypoxia on *S. aureus* biofilm formation. Biofilms were grown in minimal medium with (white histograms) or without (black histograms) oxygen for 24 h before absorbance measurement, live adherent bacteria numeration, and scanning electron microscopy acquisition. **(A)** Results represent the ratio of crystal violet absorbance (biofilm biomass) on planktonic growth absorbance. Experiments were performed at least four independent times with three technical replicates for each. **(B)** Results represent the percentage of live adherent bacteria among all bacteria. Experiments were performed at least four independent times with two technical replicates for each. Error bars represent standard errors for each average value. **(C)** Representative images of scanning electronic microscopy acquisitions at 15,000 × are shown. Statistical analyses were performed using the exact non-parametric Wilcoxon–Mann–Whitney test for independent samples: ¤¤¤Statistically different from aerobic culture condition ($p < 0.001$). The scale bars indicate 1 μm.

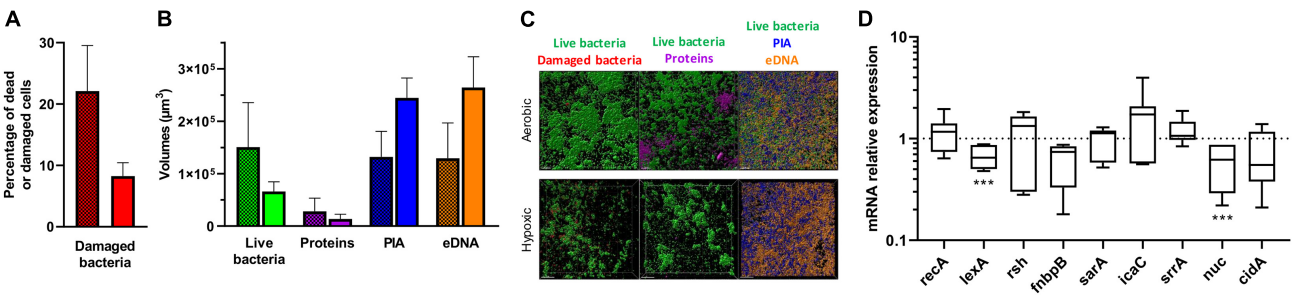

FIGURE 3 | Effect of hypoxia on matrix formation and gene regulation of *S. aureus* CIP 53.154. Biofilms were grown in minimal medium with or without oxygen for 24 h before staining and confocal laser scanning microscopy acquisitions or RT-qPCR analysis. **(A)** Results represent the percentage of dead or damaged bacteria (stained by PI) among live bacteria (stained by SYTO^{TM} 9) acquired by confocal microscopy. Grid histograms represent biofilm growth with oxygen, whereas non-grid histogram represents growth without oxygen. **(B)** Results represent the volume measurement of SYTO^{TM} 9 (green histograms, live bacteria), SYPRO® Ruby (magenta, protein), WGA (blue, PIA), and TOTO^{TM}-3 (orange, extracellular DNA) acquired by confocal microscopy. Grid histograms represent biofilm growth with oxygen, whereas non-grid histogram represents growth without oxygen. **(C)** Representative images of confocal microscopy acquisitions are shown. The scale bars indicate 20 μm. Experiments were performed two independent times with three representative acquisitions for each coverslip. **(D)** Results represented relative mRNA expressions of bacteria within biofilms grown hypoxically vs. those grown aerobically. Experiments were performed eight independent times with two technical replicates for each. Results are presented as box and whiskers: whiskers represent minimum and maximum, the bottom and top of the box are the 15th and 85th percentiles, and the black band inside the box stands for the median. Statistical analyses were performed using the exact non-parametric Wilcoxon–Mann–Whitney test for independent samples: ***Statistically different from aerobic culture condition ($p < 0.001$).

and damaged bacteria proportion, which reached 8%. Live bacteria volume reached 1.5×10^5 μm^3 in aerobic culture and was decreased to 0.6×10^4 μm^3 for culture without oxygen, without any statistical significance (**Figure 3B**). Protein-labeled volume represented the lowest matrix component stained (2.8×10^4 μm^3), and the oxygen deprivation induced a twofold decrease. PIA and eDNA volumes were instead increased by oxygen depletion by 1.8-fold (of 1.3×10^5 μm^3) and twofold (of 1.3×10^5 μm^3), respectively (**Figure 3C**).

To better understand these results, gene regulation was monitored by RT-qPCR analysis. Stress-responses-related genes (*recA*, *lexA*, and *rsh*), adhesion-related gene (*fnbpB*), and biofilm formation and matrix production-related genes (*sarA*, *icaC*, *srrA*, *nuc*, and *cidA*) were thus studied (Rice et al., 2007; Buck et al., 2010; Archer et al., 2011; Geiger et al., 2014; Josse et al., 2017; Mashruwala et al., 2017; Podlesek and Žgur Bertok, 2020). When CIP 53.154 strain was cultured without oxygen, *lexA* and *nuc* were statistically downregulated to 0.65- and 0.62-fold ($p < 0.001$), respectively (**Figure 3D**). Without statistical difference, *rsh* and *icaC* were upregulated by 1.33- and 1.73-fold, *fnbpB* and *cidA* were downregulated to 0.74- and 0.55-fold. *recA*, *sarA*, and *srrA* displayed no changes in their expression.

Impact of Bone Condition on Biofilm Biomass, Matrix Formation, and Gene Expression

In a second approach, based on a previous study, we modified MM to mimic bone environment parameters (Reffuveille et al., 2018). For this, amino acids and glucose were removed during preparation to mimic starvation, whereas magnesium was added in excess (10-fold initial concentration) to approach the parameters of the bone context. In order to investigate common staphylococcal responses, we selected conditions for which biofilm proportion was similar for all studied strains. In this way, three combinations demonstrated an impact on biofilms: the paucity of casamino acids alone (no CAA) or with magnesium excess (no CAA, 10 × Mg) and a third condition bringing together the lack of amino acids and glucose, with magnesium excess (no CAA, 10 × Mg, no Gluc), which better represented a bone-like environment (BLE). As shown in **Figure 4A**, casamino acids removal led to an increase in CIP 53.154 strain biofilm proportion by 1.2-fold ($p < 0.01$), SH1000 strain by 4.5-fold ($p < 0.001$), and USA300 strain by 9.9-fold ($p < 0.01$). In addition to the lack of amino acids, high concentration of magnesium reinforced the biofilm proportion, giving the highest biofilm proportion observed for each strain: CIP 53.154, SH1000, and USA300 biofilm proportion were enhanced by 2-fold ($p < 0.01$), 6.7-fold ($p < 0.01$), and 19.1-fold ($p < 0.01$), respectively. The last condition, bringing together the lack of amino acids, glucose, and 10 times the magnesium concentration, increased biofilm proportion of the three strains but in a smaller proportion than the previous condition: CIP 53.154 by 1.4-fold ($p < 0.001$),S H1000 by 2.5-fold ($p < 0.001$), and USA300 by 9.7-fold ($p < 0.01$).

All strains showed an increase in live adherent cell percentages, grown in the three tested conditions (**Figure 4B**). CIP 53.154 strain initially displayed 23% of bacteria in biofilm

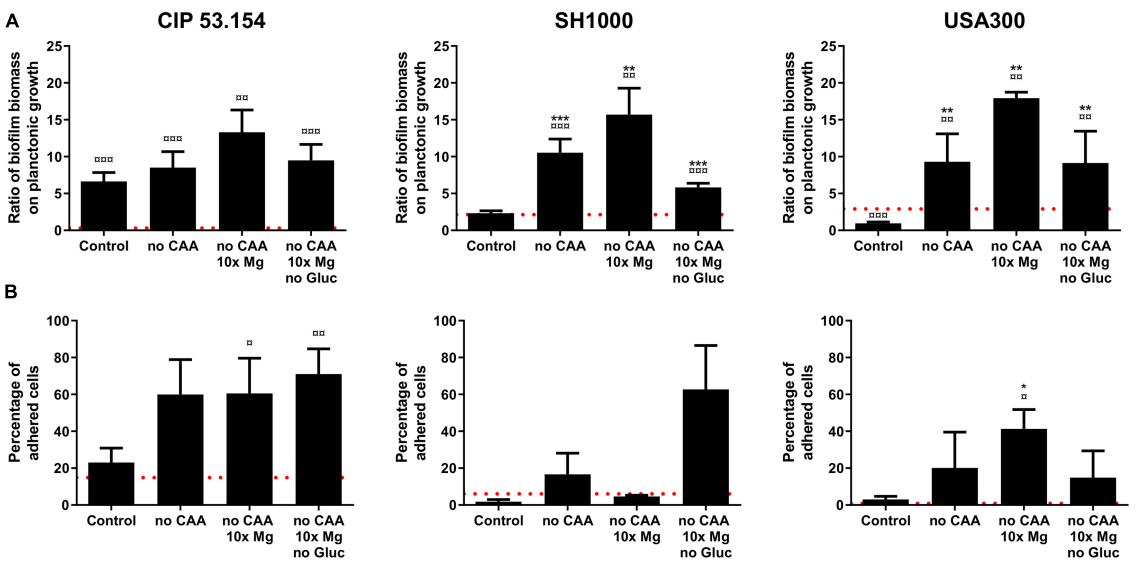

FIGURE 4 | Impact of starvation, magnesium excess, and hypoxia on *S. aureus* biofilm formation. Biofilms were grown in minimal medium (control) or modified minimal medium (no CAA, without casamino acids; 10 × Mg, 10 × minimal medium concentration; no Gluc, without glucose) without oxygen for 24 h before absorbance measurement and live adherent bacteria numeration. **(A)** Results represent the ratio of crystal violet absorbance (biofilm biomass) on planktonic growth absorbance. Experiments were performed at least four independent times with three technical replicates for each. **(B)** Results represent the percentage of live adherent bacteria among all bacteria. Experiments were performed at least four independent times with two technical replicates for each. Error bars represent standard errors for each average value. Red grid line represents results of biofilms grown with oxygen in minimal medium. Statistical analyses were performed using the exact non-parametric Wilcoxon–Mann–Whitney test for independent samples: ¤,¤¤,¤¤¤Statistically different from aerobic control ($p < 0.05$; $p < 0.01$; $p < 0.001$); *, **, ***Statistically different from hypoxic control ($p < 0.05$; $p < 0.01$; $p < 0.001$).

state in hypoxic control medium, which increased to 71% in BLE condition. The other MSSA, SH1000 strain, increased its biofilm-embedded bacteria percentage from 1.7 to 62% in BLE condition, whereas MRSA USA300 strain initially displayed 3% of cells under adherent state with control, which increased to 14% in BLE condition.

As seen before, when biofilms were grown in MM, CIP 53.154 strain produced an important matrix under oxygen deprivation. SH1000 and USA300 did not seem to produce matrix within the same condition. Casamino acids depletion (no CAA) led to an important decrease in matrix production for CIP 53.154, whereas SH1000 strain produced more matrix, which formed aggregates (**Figure 5**). MRSA strain USA300 still did not produce any detectable matrix. If magnesium was added in excess (no CAA, 10 × Mg), the aspect and amount of matrix were similar than in the previous condition (no CAA). The last condition bringing together the lack of both amino acids and glucose and magnesium excess (no CAA, 10 × Mg, no Gluc) led to biofilm matrix production for the three strains in variable amount but with a common granular aspect.

Grown in MM, all strains presented few dead or damaged cells within their biofilms: 8, 3, and 3% for CIP 53.154, SH1000, and USA300 strains, whereas the bone-like environment induced an increase in dead or damaged cells, which reached 56, 21, and 34%, respectively (**Figure 6A**). As previously mentioned in **Figure 3B**, the biofilm formed by CIP 53.154 strain in MM and hypoxic culture was mainly composed of eDNA and PIA. SH1000 strain biofilm incubated in MM in hypoxic condition was mainly composed of PIA as volumes of WGA reached 1.6×10^5 μm^3 (**Figure 6B**). The second main component was eDNA, which reached 0.5×10^5 μm^3. We observed opposite results with USA300 strain, as the matrix of this bacterial strain was mainly composed of eDNA (6.1×10^4 μm^3) and less PIA (3.8×10^4 μm^3). Incubation with BLE led to the reduction in almost every studied component of each strain. CIP 53.154 strain dramatically modified the composition of its matrix under BLE condition with a slight increase in matrix proteins and an important decrease in PIA (44-fold) and eDNA (35-fold) and proportionally to live bacteria (**Figure 6C**). Raw volumes of stained matrix components are equal for MSSA strains despite a higher amount of SYTO^{TM} 9 stained volumes for SH1000, whereas USA300 present the same amount of eDNA, but an important decrease in protein amount and almost no PIA was detected (**Figure 6D**).

Next, we compared gene expressions of bacteria within biofilms grown in BLE vs. MM, both in the absence of oxygen. Four genes were upregulated among CIP 53.154, SH1000, and USA300 strains: *recA* (1.33-fold, $p < 0.01$; 2.64-fold, $p < 0.001$; 2.80-fold, $p < 0.01$), *lexA* (3.92-fold, $p < 0.01$; 2.37-fold, $p < 0.001$; 2.03-fold, $p < 0.01$), *rsh* (2.88-fold, $p < 0.05$; 2.08-fold, $p < 0.001$; 1.30-fold), and *sarA* (2.51-fold, $p < 0.001$; 3.05-fold, $p < 0.05$, 9.87-fold, $p < 0.01$) (**Figure 7**). Focusing on *fnbpB* relative expression, the three strains behaved differently when cultured in BLE: an increase of 2.01-fold ($p < 0.001$) for CIP 53.154 strain, spread results for SH1000, and a decrease to 0.53-fold ($p < 0.05$) for USA300. Regarding the production of polysaccharides involved in matrix composition through *icaC* and *srrA*, exclusively USA300 strain had a downregulation of *icaC* expression (to 0.62-fold, $p < 0.01$), and *srrA* was upregulated for CIP 53.154 strain (1.49-fold, $p < 0.05$) and USA300 strain (1.51 fold, $p<0.01$) only. Finally, concerning genes involved in eDNA regulation, *nuc* was enhanced by 1.6-fold ($p < 0.001$) for CIP 53.154 strain, remained constant for SH1000, and downregulated to 0.76-fold ($p<0.01$) for USA300 strain; *cidA*, on the other hand, was downregulated for both SH1000 and USA300 strains to 0.72-fold ($p < 0.05$) and 0.45-fold ($p < 0.01$), respectively.

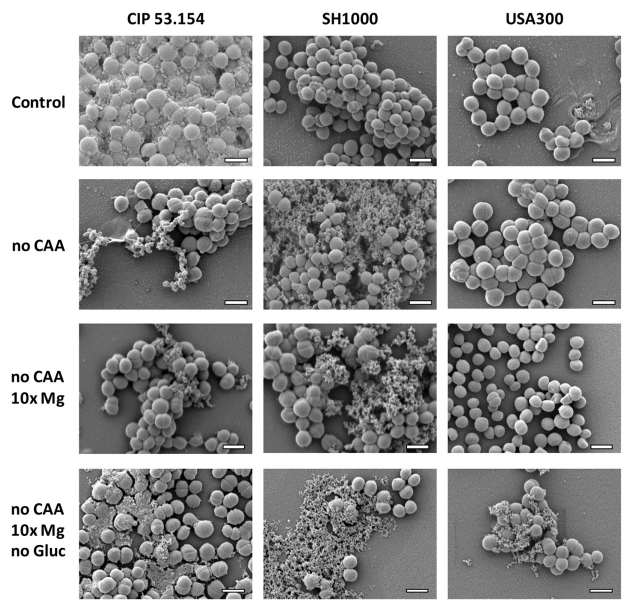

FIGURE 5 | Impact of starvation, magnesium excess, and hypoxia on *S. aureus* biofilm matrix. Biofilms were grown in minimal medium (control) or modified minimal medium (no CAA, without casamino acids; 10 × Mg, 10 × minimal medium concentration; no Gluc, without glucose) without oxygen for 24 h before imaging. Representative images of scanning electronic microscopy acquisitions at 15,000 × are shown. The scale bar indicates 1 μm.

DISCUSSION

Despite many preventive actions, the number of prosthetic infections cannot decrease without a better knowledge on bacterial biofilm development in bone context. Biofilm structure and composition are dependent on many environmental parameters. Biofilm kinetic and biomass can also vary according to *S. aureus* clonal lineage (Tasse et al., 2018). Methicillin susceptibility is also a key factor, as MSSA and MRSA expressed different levels of exopolysaccharides, protein, and eDNA (McCarthy et al., 2015). Thus, even before being influenced by environmental stress, different strains of the same species form different biofilm structures, probably by responding in a different way to stimuli.

Our data confirmed that different *S. aureus* strains formed various biofilm structures in classic *in vitro* model. Interestingly,

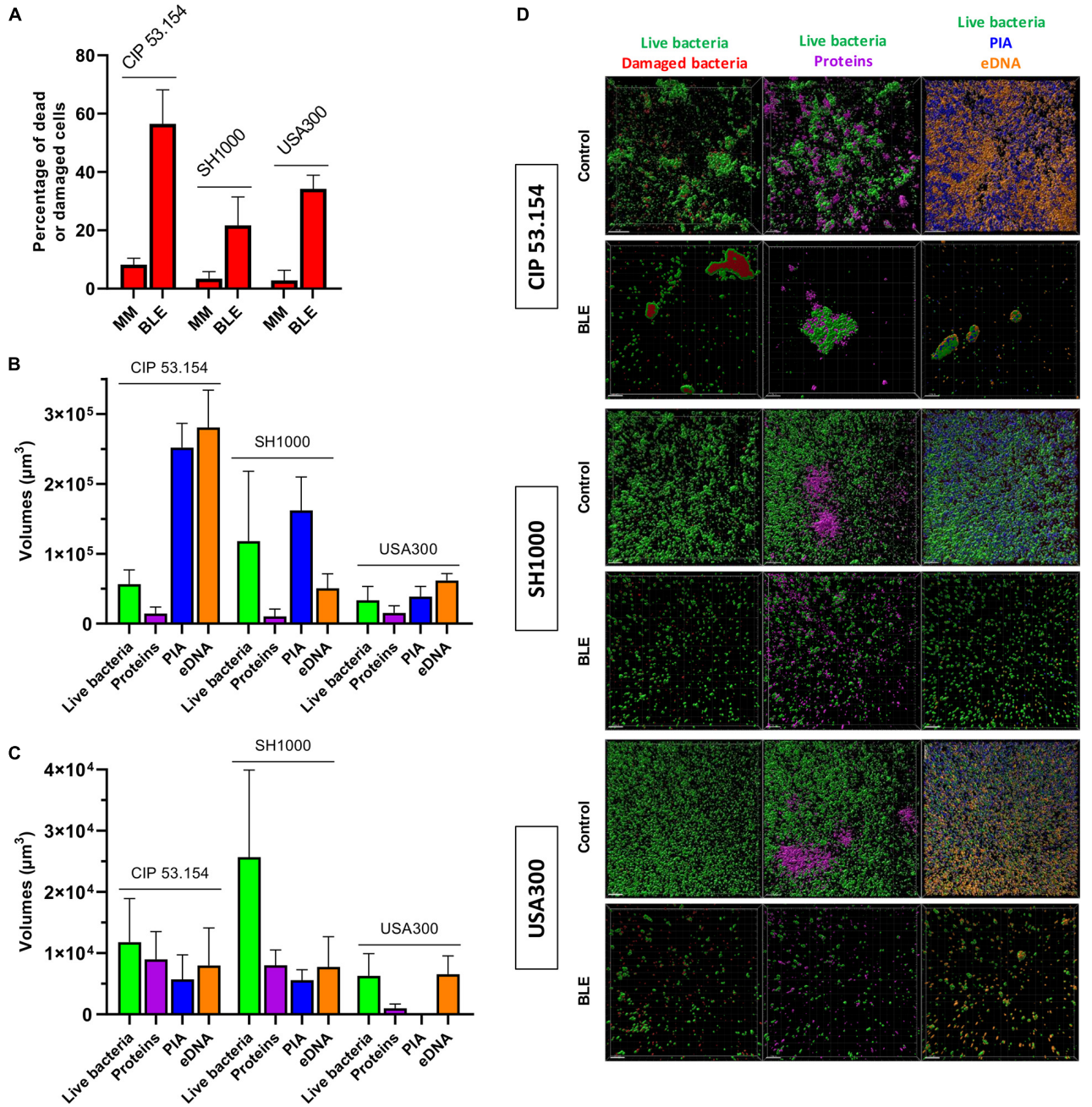

FIGURE 6 | Impact of starvation, magnesium excess, and hypoxia on *S. aureus* biofilm matrix components. Biofilms were grown in minimal medium (MM) or modified minimal medium (BLE: no CAA, without casamino acids; 10 × Mg, 10 × minimal medium concentration; no Gluc, without glucose) without oxygen for 24 h before confocal scanning electron microscopy imaging. **(A)** Results represent the percentage of dead or damaged bacteria (stained by PI) among live bacteria (stained by SYTO™ 9). **(B)** Results represent the volume measurement of SYTO™ 9 (green histograms; live bacteria), SYPRO® Ruby (magenta: protein), WGA (blue: PIA) and TOTO™-3 (orange: extracellular DNA) of bacteria grown in MM without oxygen. **(C)** Results represent the volume measurement as previously described in BLE without oxygen. **(D)** Representative images are shown. Experiments were performed two independent times with three representative acquisitions for each coverslip. Experiments were performed two independent times with three representative acquisitions for each coverslip. Error bars represent standard errors for each average value. Scale bar = 20 µm.

even both MSSA exhibited two different biofilm patterns. CIP 53.154 developed a low amount of biofilm but important aggregates, whereas SH1000, a strong biofilm former, conceived microcolonies with an additive adherent monolayer. MRSA strain showed a third response: biofilm grown in monolayer without any cluster.

While *S. aureus* strains are natural biofilm formers, the host microenvironment strongly modulates their biofilm production

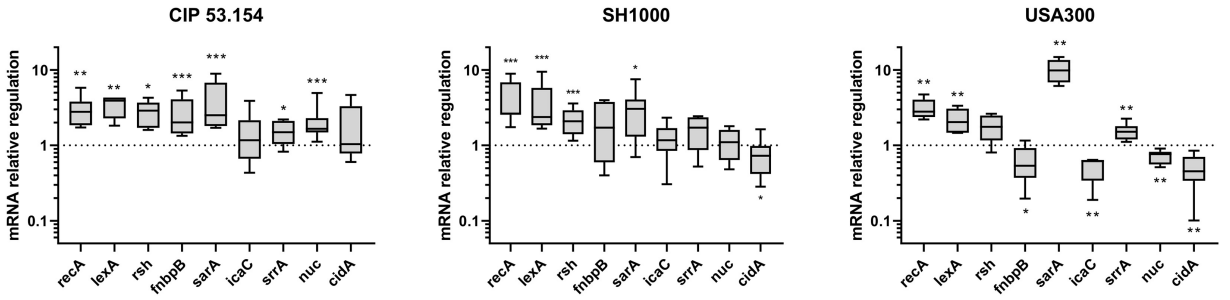

FIGURE 7 | Impact of starvation, magnesium excess, and hypoxia on *S. aureus* gene regulation. Biofilms were grown in minimal medium (MM) or in modified minimal medium (BLE: no CAA, without casamino acids; 10 × Mg, 10 × minimal medium concentration; no Gluc, without glucose) without oxygen for 24 h before RT-qPCR analysis. Results represent the ratio of relative mRNA expressions of bacteria within biofilms grown in BLE vs. those grown in minimal medium. Experiments were performed eight independent times with two technical replicates for each. Results are presented as box and whiskers: whiskers represent minimum and maximum, the bottom and top of the box are the 15th and 85th percentiles, and the black band inside the box stands for the median. Statistical analyses were performed using the exact non-parametric Wilcoxon–Mann–Whitney test for independent samples: *, **, ***Statistically different from minimal medium without oxygen ($p < 0.05$; $p < 0.01$; $p < 0.001$).

and, therefore, influences infection establishment with impact on metabolic changes and antimicrobial tolerance of bacteria (Crabbé et al., 2019). Indeed, bone environment factors influence a MSSA biofilm formation (Reffuveille et al., 2018). In the bone microenvironment, the influence of severe oxygen limitation on bacteria was evidenced in *in vivo* models by the enhanced expression of genes involved in fermentation such as *plfB* and *aldA*, supported by high concentration of lactate and presence of ethanol (Xu et al., 2016). In our hands, hypoxic conditions in MM led to a slight decrease in adherent bacteria proportion and a loss in matrix production for SH1000. USA300 also lost its ability to produce biofilm matrix, and the adherent bacteria proportion was slightly increased. However, biofilm biomass proportion formed by SH1000 and USA300 strains was not increased under hypoxic stress contrary to results reported in another study (Mashruwala et al., 2017). We suggested that the way to generate hypoxia, the growth media used and the culture duration could explain such differences, highlighting the importance of biofilm growth model. Only CIP 53.154 strain seemed to significantly produce more biofilm under lack of oxygen, with high production of matrix, mainly composed of PIA and eDNA. PIA is known to be produced by *S. aureus* under oxygen deprivation (Cramton et al., 2001). The eDNA release could be caused by cell wall embrittlement leading to cell lysis (Mashruwala et al., 2017). Interestingly, the CIP 53.154 proportion of dead bacteria included within the biofilm decreased in MM without oxygen. We speculated that 24-h biofilms were in maturation process and are currently under a reorganization phase: lysed cells were evacuated, and eDNA was used for matrix construction, whereas biofilm-embedded bacteria increased their survival rate. The production of accumulated matrix polysaccharides for this strain needs to be investigated.

Focusing on CIP 53.154 biofilm matrix under hypoxic stress, bacterial response was investigated though RT-qPCR study. Due to bacterial phenotype heterogeneity within biofilms and owing to the fact that only a global response of both active and dormant bacteria within biofilm is evaluated, all significant changes were considered. Two genes were significantly downregulated under hypoxic stress compared to aerobic condition: *lexA* and *nuc*. The SOS response (inducer encoded by *recA* and repressor encoded by *lexA*) is triggered by various endogenous factors including starvation through the activation of the stringent response (*rsh* gene) (Podlesek and Žgur Bertok, 2020). SOS response is involved in biofilm formation and FnbpB production, which is responsible for fibronectin attachment (Podlesek and Žgur Bertok, 2020). Under hypoxic condition, a slight increase in *rsh* was noticed. Surprisingly, no *recA* or *fnbpB* induction was observed. On the contrary, we noticed a non-significant decrease in *fnbpB*. We deduced that hypoxic stress induced a global stress response for the establishment of the biofilm in this particular condition. This could explain the non-significant increase in *icaC* expression. This gene codes for PIA, which allow bacteria to adhere and build biofilm matrix (O'Neill et al., 2007; Archer et al., 2011; Nourbakhsh and Namvar, 2016). The *nuc* downregulation could be expected in the early stage of biofilm construction. Indeed, *nuc* is involved in eDNA cleavage and consequently in the inhibition of biofilm initiation (Mann et al., 2009; Berends et al., 2010; Kiedrowski et al., 2011). Its marked dysregulation in the absence of oxygen showed the importance of the biofilm activation under this stress. *cidA*, a gene involved in cell lysis leading to DNA release to build biofilm matrix, was also downregulated (Rice et al., 2007). We speculated that the high eDNA concentration in CIP 53.154 matrix biofilm after 24 h led to a negative feedback control on *cidA* expression or *lgr* genes, marking the end of initiation and structuration of biofilm (Archer et al., 2011). The reinforcement of biofilm in this hypoxic environment underlined the hypothesis that biofilm is a survival strategy.

In conclusion, hypoxic environment differently affected various *S. aureus* strains. While its importance is obvious, this one factor alone could not explain the ability of *S. aureus* biofilm establishment in bone context. These differential results underline the complexity of biofilm and the impossibility to draw universal conclusion on the influence of one environmental factor on biofilm formation even among the same species. In this study, CIP 53.154 strain demonstrated altered quantity of biofilm matrix in response to hypoxia by greatly increasing

polysaccharides and eDNA concentration. This modification is probably an accentuated stress response, managed by global systems, due to lack of oxygen.

To go further in the study of bone context impact, we modified MM to create a "bone-like environment" under hypoxic condition (Reffuveille et al., 2018). Bone site and, more particularly, the low bone vascularization after surgery lead to nutrient starvation. We found that the lack of amino acid increased biofilm proportion (biomass and adherent cells) for all strains, even without oxygen. This nutritional deficiency is known to be linked with pp(G)pp-mediated stress responses leading to increased biofilm formation (Nguyen et al., 2011; de la Fuente-Núñez et al., 2014). Then, bone tissue is the main reservoir of magnesium of the human body, and the infection causes the bone matrix resorption, which releases a local amount of this cation (Kratz et al., 2004; González et al., 2009; Wright and Nair, 2010). Combined with amino acids depletion, a high concentration of magnesium increased the biofilm biomass proportion, which suggested that bacteria adapted their matrix production. Nevertheless, without glucose, biofilm biomass revealed by crystal violet assay were reduced, with increased or similar proportion of adherent bacteria. This difference between biofilm biomass and adherent bacteria proportion could suggested that matrix formation was impacted. However, SEM acquisitions highlighted that CAA, not only glucose, was important for matrix production of CIP 53.154 strain under hypoxia. Indeed, both MSSA strains under CAA starvation with or without magnesium excess showed a similar aspect of a fibrous matrix but different from control. However, the bone-like environment condition enhanced a similar matrix production for all the studied strains. This particular condition was the only one to enhance matrix production for USA300 MRSA strain. MRSA strains are known to adopt biofilm lifestyle in response to stress such as antibiotic pressure (Mirani et al., 2015). We suggested that USA300 strain only produce matrix under stressful condition such as BLE.

Biofilm matrix in MM without oxygen was mainly composed of PIA and eDNA for CIP 53.154 strain, PIA for SH1000 strain, and eDNA for USA300. These results were sustained by another study comparing MSSA and MRSA biofilm matrix (McCarthy et al., 2015). Grown in a bone-like environment, the three-studied strains harbored the same phenotype regarding the matrix component proportions: less bacteria were quantified, and a drastic decrease in each component was noticed. MSSA strains produce equal amount of matrix components, but SH1000 strain showed a higher proportion of bacteria. USA300 strain built a matrix, which seemed to be mainly composed of eDNA and only few proteins. However, these results are contrasting with observation of biofilms through SEM. Indeed, SH1000 and USA300 strains did not seem to produce matrix under MM and hypoxic condition using SEM, whereas matrix components were detected by CLSM. We suggested that such differences could be explain by the fact that CLSM revealed matrix over and under bacteria, whereas SEM only revealed biofilm surface. Furthermore, preparations steps were not the same and could alter biofilm matrix. Thus, it is important to analyze the experiments altogether to better decipher our results, as crystal violet staining, counting method, and MEB acquisitions tend to lead to similar conclusions. Moreover, MEB images showed structures, which could be dying or dead bacteria providing matrix structures non-labeled by fluorochromes.

To investigate the impact of a bone-like environment on metabolic pathways and stress responses involved in biofilm formed by each strain, several gene expressions were monitored through RT-qPCR, comparing BLE to MM conditions. The matrix produced by biofilm-embedded bacteria in MM without oxygen was different for the three strains, and we expected to get different gene deregulations. Focusing on biofilm initiation by studying global stress response genes, the expression of *recA* and *lexA* was significantly increased for all strains, and the *rsh* gene expression was upregulated. Both enhancement of *recA*, inducer, and of l*exA*, repressor, was surprising regarding the fact that these proteins had an opposite regulator role on the SOS pathway. However, we speculated that the existence of a feedback loop could explain this phenomenon; stringent response encoded by *rsh* gene induced the expression of *recA*, and the overexpression of *recA* led to an overexpression of its regulator l*exA* (Podlesek and Žgur Bertok, 2020). In this same condition, *sarA* was overexpressed for all the three strains. *sarA* is required for several virulence factors transcription and is needed for biofilm formation (Yu et al., 2020). Taking together, these results suggested involvement of common stress responses for *S. aureus* biofilm establishment in a bone-like environment. This environmental stress was confirmed by increased proportion of damaged and dead bacteria for the three strains.

Adhesion is an essential step of biofilm formation for which FnbpB facilitates fibronectin binding (McCourt et al., 2014). Fibronectin rapidly recovers foreign material and lead to initial attachment of bacteria in prosthetic device infection (Buck et al., 2010). Only MSSA strains cultured in BLE displayed an enhanced *fnbpB* expression, which was probably linked to SOS induction (Bisognano et al., 2004). However, its expression was downregulated for MRSA, underlining another involved mechanism for this strain. These results are in accordance with the matrix protein proportion of MSSA strains, which is higher than for USA300 strain.

Then, maturation of biofilm through matrix production (among eDNA and exopolysaccharides components) is a key for biofilm formation. Contrary to CIP 53.154 biofilm under aerobic condition, *icaC* expression was not modified in bone-like environment for MSSA strains and even deregulated for MRSA. However, under hypoxic condition, a study has shown that *srrA* induces PIA production (Kinkel et al., 2013). Unfortunately, even if *srrA* was upregulated for the three strains, PIA quantification through confocal microscopy revealed that this polysaccharide level was reduced into a bone-like condition for MSSA, and MRSA did not seem to produce any PIA. This is consistent with the fact that glucose supply was limited by MM modification (no Gluc), limiting saccharide source to produce PIA. Further investigations are needed to explain these results.

The proportion of eDNA in the matrix could be linked to *cidA* and *nuc* expressions. Interestingly, the expression of these two genes was variable among the three strains. We suggested that 24-h-old biofilms grown in a static assay were composed of

bacteria in different states, and dispersal mechanisms could be engaged. However, the downregulation of *cidA* in SH1000 and USA300 corresponded to a decrease in eDNA level under confocal microscopy. It is interesting to notice that CIP 53.154 matrix decrease in bone-like environment could be linked to an upregulation of *nuc*.

Altogether, our results showed that both MSSA and MRSA responded to bone-like environment, increasing their biofilm biomass and number of adherent cells proportion but with heterogeneous matrix components and production. Moreover, we speculated about a universal response to bone-like environment through stringent and SOS response but also a preferential expression of *sarA* and *srrA* biofilm inducers. Moreover, all strains presented high dead or damaged bacteria level, with eDNA as the main matrix component. The description of this matrix and embedded bacteria will allow the selection of antibiofilm molecules against the biofilm tolerance and persistence in the specific bone context.

To develop future strategies for the prevention of biofilm formation in the bone environment, matrix eDNA seems to be a valid target to weaken the biofilm structure and disturb its formation and maturation. Furthermore, targeting stress response such as SOS-mediated response or global regulatory protein such as SarA could be an interesting approach, but further investigations are needed, by using knockout or suppression mutants for example. Finally, the model developed here will allow the study of clinical strains. In addition, it is important to remember that in this study, we used extreme conditions to be closer to the bone environment but which remained far from the reality of what is occurring *in vivo*. However, our results underlined the need to change the classical laboratory media used (like nutritive medium or brain heart infusion) for more realistic conditions to understand the "real-life" phenomena.

CONCLUSION

In conclusion, we have studied three strains whose *in vitro* biofilms were very different from each other, involving several molecular mechanisms. However, factors mimicking bone microenvironment triggered common responses in these bacteria and lead them to develop more similar biofilms. The identification of host factors that induce biofilm formation will be essential. Targeting these mechanisms is the key in the battle against infection-related biofilms. This study underlined the strain-specific response to the same conditions and the urgent need to develop adapted *in vitro* models to properly screen antibiofilm molecules.

DATA AVAILABILITY STATEMENT

The raw data supporting the conclusions of this article will be made available by the authors, without undue reservation.

AUTHOR CONTRIBUTIONS

FL, FR, and SG designed the research. FL and JV-S performed the experiments. FV performed SEM images. CT provided methodologies to analyze CLSM acquisitions. FL, FR, FV, CM, and CT analyzed the data. FL, SG, FR, and MC wrote the manuscript. All authors reviewed the manuscript.

FUNDING

FL's Ph.D. was supported by the Region Grand-Est and Fondation URCA.

ACKNOWLEDGMENTS

We thank the PICT platform for access to microscopes and specific software.

SUPPLEMENTARY MATERIAL

The Supplementary Material for this article can be found online at: https://www.frontiersin.org/articles/10.3389/fmicb.2021.714994/full#supplementary-material

REFERENCES

Ahmed, W., Zhai, Z., and Gao, C. (2019). Adaptive antibacterial biomaterial surfaces and their applications. *Mater. Today Bio.* 2:100017. doi: 10.1016/j.mtbio.2019.100017

Archer, N. K., Mazaitis, M. J., Costerton, J. W., Leid, J. G., Powers, M. E., and Shirtliff, M. E. (2011). *Staphylococcus aureus* biofilms: properties, regulation, and roles in human disease. *Virulence* 2, 445–459. doi: 10.4161/viru.2.5.17724

Ayciriex, S., Djelti, F., Alves, S., Regazzetti, A., Gaudin, M., Varin, J., et al. (2017). Neuronal cholesterol accumulation induced by Cyp46a1 down-regulation in mouse hippocampus disrupts brain lipid homeostasis. *Front. Mol. Neurosci.* 10:211. doi: 10.3389/fnmol.2017.00211

Berends, E. T. M., Horswill, A. R., Haste, N. M., Monestier, M., Nizet, V., and von Köckritz-Blickwede, M. (2010). Nuclease expression by *Staphylococcus aureus* facilitates escape from neutrophil extracellular traps. *J. Innate Immun.* 2, 576–586. doi: 10.1159/000319909

Bisognano, C., Kelley, W. L., Estoppey, T., Francois, P., Schrenzel, J., Li, D., et al. (2004). A recA-LexA-dependent pathway mediates ciprofloxacin-induced fibronectin binding in *Staphylococcus aureus*. *J. Biol. Chem.* 279, 9064–9071. doi: 10.1074/jbc.M309836200

Bjarnsholt, T. (2013). The role of bacterial biofilms in chronic infections. *APMIS Suppl.* 121, 1–51. doi: 10.1111/apm.12099

Bjarnsholt, T., Alhede, M., Alhede, M., Eickhardt-Sørensen, S. R., Moser, C., Kühl, M., et al. (2013). The in vivo biofilm. *Trends Microbiol.* 21, 466–474. doi: 10.1016/j.tim.2013.06.002

Buck, A. W., Fowler, V. G., Yongsunthon, R., Liu, J., DiBartola, A. C., Que, Y.-A., et al. (2010). Bonds between fibronectin and fibronectin-binding proteins on *Staphylococcus aureus* and *Lactococcus lactis*. *Langmuir* 26, 10764–10770. doi: 10.1021/la100549u

Coenye, T., Kjellerup, B., Stoodley, P., and Bjarnsholt, T. (2020). The future of biofilm research – Report on the '2019 Biofilm Bash'. *Biofilm* 2:100012. doi: 10.1016/j.bioflm.2019.100012

Crabbé, A., Jensen, P. Ø, Bjarnsholt, T., and Coenye, T. (2019). Antimicrobial tolerance and metabolic adaptations in microbial biofilms. *Trends Microbiol.* 27, 850–863. doi: 10.1016/j.tim.2019.05.003

Cramton, S. E., Ulrich, M., Götz, F., and Döring, G. (2001). Anaerobic conditions induce expression of polysaccharide intercellular adhesin in *Staphylococcus aureus* and *Staphylococcus epidermidis*. *Infect. Immun.* 69, 4079–4085. doi: 10.1128/IAI.69.6.4079-4085.2001

de la Fuente-Núñez, C., Reffuveille, F., Haney, E. F., Straus, S. K., and Hancock, R. E. W. (2014). Broad-spectrum anti-biofilm peptide that targets a cellular stress response. *PLoS Pathog.* 10:e1004152. doi: 10.1371/journal.ppat.1004152

DeFrancesco, A. S., Masloboeva, N., Syed, A. K., DeLoughery, A., Bradshaw, N., Li, G.-W., et al. (2017). Genome-wide screen for genes involved in eDNA release during biofilm formation by *Staphylococcus aureus*. *Proc. Natl. Acad. Sci. U.S.A.* 114, E5969–E5978. doi: 10.1073/pnas.1704544114

Diep, B. A., Chambers, H. F., Graber, C. J., Szumowski, J. D., Miller, L. G., Han, L. L., et al. (2008). Emergence of multidrug-resistant, community-associated, methicillin-resistant *Staphylococcus aureus* clone USA300 in men who have sex with men. *Ann. Intern. Med.* 148, 249–257. doi: 10.7326/0003-4819-148-4-200802190-00204

Donlan, R. M. (2001). Biofilms and device-associated infections. *Emerg. Infect. Dis.* 7, 277–281.

Feng, G., Cheng, Y., Wang, S.-Y., Borca-Tasciuc, D. A., Worobo, R. W., and Moraru, C. I. (2015). Bacterial attachment and biofilm formation on surfaces are reduced by small-diameter nanoscale pores: how small is small enough? *npj Biofilms Microbiomes* 1:15022. doi: 10.1038/npjbiofilms.2015.22

Fischer, B., Vaudaux, P., Magnin, M., el Mestikawy, Y., Proctor, R. A., Lew, D. P., et al. (1996). Novel animal model for studying the molecular mechanisms of bacterial adhesion to bone-implanted metallic devices: role of fibronectin in *Staphylococcus aureus* adhesion. *J. Orthop Res.* 14, 914–920. doi: 10.1002/jor.1100140611

Flemming, H.-C., and Wingender, J. (2010). The biofilm matrix. *Nat. Rev. Microbiol.* 8, 623–633. doi: 10.1038/nrmicro2415

Forson, A. M., van der Mei, H. C., and Sjollema, J. (2020). Impact of solid surface hydrophobicity and micrococcal nuclease production on *Staphylococcus aureus* Newman biofilms. *Sci. Rep*. 10:12093. doi: 10.1038/s41598-020-69084-x

Fuller, E., Elmer, C., Nattress, F., Ellis, R., Horne, G., Cook, P., et al. (2005). β-Lactam resistance in *Staphylococcus aureus* cells that do not require a cell wall for integrity. *Antimicrob. Agents Chemother* 49, 5075–5080. doi: 10.1128/AAC.49.12.5075-5080.2005

Geiger, T., Kästle, B., Gratani, F. L., Goerke, C., and Wolz, C. (2014). Two small (p)ppGpp synthases in *Staphylococcus aureus* mediate tolerance against cell envelope stress conditions. *J. Bacteriol.* 196, 894–902. doi: 10.1128/JB.01201-13

Gibon, E., Amanatullah, D. F., Loi, F., Pajarinen, J., Nabeshima, A., Yao, Z., et al. (2017a). The biological response to orthopaedic implants for joint replacement: Part I: metals. *J. Biomed. Mater. Res. B Appl. Biomater.* 105, 2162–2173. doi: 10.1002/jbm.b.33734

Gibon, E., Córdova, L. A., Lu, L., Lin, T.-H., Yao, Z., Hamadouche, M., et al. (2017b).). The biological response to orthopedic implants for joint replacement. II: polyethylene, ceramics, PMMA, and the foreign body reaction. *J. Biomed. Mate.r Res. B Appl. Biomater.* 105, 1685–1691. doi: 10.1002/jbm.b.33676

González, E. P., Santos, F., and Coto, E. (2009). [Magnesium homeostasis. Etiopathogeny, clinical diagnosis and treatment of hypomagnesaemia. A case study]. *Nefrologia* 29, 518–524. doi: 10.3265/Nefrologia.2009.29.6.5534.en.full

Grammatico-Guillon, L., Baron, S., Gettner, S., Lecuyer, A.-I., Gaborit, C., Rosset, P., et al. (2012). Bone and joint infections in hospitalized patients in France, 2008: clinical and economic outcomes. *J. Hosp. Infect.* 82, 40–48. doi: 10.1016/j.jhin.2012.04.025

Hall-Stoodley, L., Costerton, J. W., and Stoodley, P. (2004). Bacterial biofilms: from the natural environment to infectious diseases. *Nat. Rev. Microbiol.* 2, 95–108. doi: 10.1038/nrmicro821

Haney, E. F., Trimble, M. J., Cheng, J. T., Vallé, Q., and Hancock, R. E. W. (2018). Critical assessment of methods to quantify biofilm growth and evaluate antibiofilm activity of host defence peptides. *Biomolecules* 8:29. doi: 10.3390/biom8020029

Heatley, N. G. (1944). A method for the assay of penicillin. *Biochem. J.* 38, 61–65.

Horsburgh, M. J., Aish, J. L., White, I. J., Shaw, L., Lithgow, J. K., and Foster, S. J. (2002). sigmaB modulates virulence determinant expression and stress resistance: characterization of a functional rsbU strain derived from *Staphylococcus aureus* 8325-4. *J. Bacteriol.* 184, 5457–5467. doi: 10.1128/jb.184.19.5457-5467.2002

Josse, J., Laurent, F., and Diot, A. (2017). Staphylococcal adhesion and host cell invasion: fibronectin-binding and other mechanisms. *Front. Microbiol.* 8:2433. doi: 10.3389/fmicb.2017.02433

Karygianni, L., Ren, Z., Koo, H., and Thurnheer, T. (2020). Biofilm matrixome: extracellular components in structured microbial communities. *Trends Microbiol.* 28, 668–681. doi: 10.1016/j.tim.2020.03.016

Kiedrowski, M. R., Kavanaugh, J. S., Malone, C. L., Mootz, J. M., Voyich, J. M., Smeltzer, M. S., et al. (2011). Nuclease modulates biofilm formation in community-associated methicillin-resistant *Staphylococcus aureus*. *PLoS One* 6:e26714. doi: 10.1371/journal.pone.0026714

Kinkel, T. L., Roux, C. M., Dunman, P. M., and Fang, F. C. (2013). The *Staphylococcus aureus* SrrAB two-component system promotes resistance to nitrosative stress and hypoxia. *mBio* 4, e00696–13. doi: 10.1128/mBio.00696-13

Kratz, A., Ferraro, M., Sluss, P. M., and Lewandrowski, K. B. (2004). Normal reference laboratory values. *N. Engl. J. Med.* 351, 1548–1563. doi: 10.1056/NEJMcpc049016

Levack, A. E., Cyphert, E. L., Bostrom, M. P., Hernandez, C. J., von Recum, H. A., and Carli, A. V. (2018). Current options and emerging biomaterials for periprosthetic joint infection. *Curr. Rheumatol. Rep.* 20:33. doi: 10.1007/s11926-018-0742-4

Li, C., Renz, N., and Trampuz, A. (2018). Management of periprosthetic joint infection. *Hip. Pelvis* 30, 138–146. doi: 10.5371/hp.2018.30.3.138

Lister, J. L., and Horswill, A. R. (2014). *Staphylococcus aureus* biofilms: recent developments in biofilm dispersal. *Front. Cell. Infect. Microbiol.* 4:178. doi: 10.3389/fcimb.2014.00178

Liu, Y., Zhang, J., and Ji, Y. (2020). Environmental factors modulate biofilm formation by *Staphylococcus aureus*. *Sci. Prog.* 103:0036850419898659. doi: 10.1177/0036850419898659

Mann, E. E., Rice, K. C., Boles, B. R., Endres, J. L., Ranjit, D., Chandramohan, L., et al. (2009). Modulation of eDNA release and degradation affects *Staphylococcus aureus* biofilm maturation. *PLoS One* 4:e5822. doi: 10.1371/journal.pone.0005822

Mashruwala, A. A., Guchte, A. V., and Boyd, J. M. (2017). Impaired respiration elicits SrrAB-dependent programmed cell lysis and biofilm formation in *Staphylococcus aureus*. *Elife* 6:e23845. doi: 10.7554/eLife.23845

Masters, E. A., Trombetta, R. P., de Mesy Bentley, K. L., Boyce, B. F., Gill, A. L., Gill, S. R., et al. (2019). Evolving concepts in bone infection: redefining "biofilm", "acute vs. chronic osteomyelitis", "the immune proteome" and "local antibiotic therapy.". *Bone Res.* 7:20. doi: 10.1038/s41413-019-0061-z

McCarthy, H., Rudkin, J. K., Black, N. S., Gallagher, L., O'Neill, E., and O'Gara, J. P. (2015). Methicillin resistance and the biofilm phenotype in *Staphylococcus aureus*. *Front. Cell Infect. Microbiol.* 5:1. doi: 10.3389/fcimb.2015.00001

McCourt, J., O'Halloran, D. P., McCarthy, H., O'Gara, J. P., and Geoghegan, J. A. (2014). Fibronectin-binding proteins are required for biofilm formation by community-associated methicillin-resistant *Staphylococcus aureus* strain LAC. *FEMS Microbiol. Lett.* 353, 157–164. doi: 10.1111/1574-6968.12424

Mirani, Z. A., Aziz, M., and Khan, S. I. (2015). Small colony variants have a major role in stability and persistence of *Staphylococcus aureus* biofilms. *J. Antibiotics* 68, 98–105. doi: 10.1038/ja.2014.115

Muthukrishnan, G., Masters, E. A., Daiss, J. L., and Schwarz, E. M. (2019). Mechanisms of immune evasion and bone tissue colonization that make *Staphylococcus aureus* the primary pathogen in osteomyelitis. *Curr. Osteoporos Rep.* 17, 395–404. doi: 10.1007/s11914-019-00548-4

Nandakumar, V., Chittaranjan, S., Kurian, V. M., and Doble, M. (2013). Characteristics of bacterial biofilm associated with implant material in clinical practice. *Polym. J.* 45, 137–152. doi: 10.1038/pj.2012.130

Nguyen, D., Joshi-Datar, A., Lepine, F., Bauerle, E., Olakanmi, O., Beer, K., et al. (2011). Active starvation responses mediate antibiotic tolerance in biofilms and nutrient-limited bacteria. *Science* 334, 982–986. doi: 10.1126/science.1211037

Nourbakhsh, F., and Namvar, A. E. (2016). Detection of genes involved in biofilm formation in *Staphylococcus aureus* isolates. *GMS Hyg. Infect. Control* 11:Doc07. doi: 10.3205/dgkh000267

O'Neill, E., Pozzi, C., Houston, P., Smyth, D., Humphreys, H., Robinson, D. A., et al. (2007). Association between methicillin susceptibility and biofilm

regulation in *Staphylococcus aureus* isolates from device-related infections. *J. Clin. Microbiol.* 45, 1379–1388. doi: 10.1128/JCM.02280-06

O'Toole, G., Kaplan, H. B., and Kolter, R. (2000). Biofilm formation as microbial development. *Annu. Rev. Microbiol.* 54, 49–79. doi: 10.1146/annurev.micro.54.1.49

Podlesek, Z., and Žgur Bertok, D. (2020). The DNA damage inducible SOS response is a key player in the generation of bacterial persister cells and population wide tolerance. *Front. Microbiol.* 11:1785. doi: 10.3389/fmicb.2020.01785

Reffuveille, F., de la Fuente-Núñez, C., Mansour, S., and Hancock, R. E. W. (2014). A broad-spectrum antibiofilm peptide enhances antibiotic action against bacterial biofilms. *Antimicrob. Agents Chemother.* 58, 5363–5371. doi: 10.1128/AAC.03163-14

Reffuveille, F., Josse, J., Velard, F., Lamret, F., Varin-Simon, J., Dubus, M., et al. (2018). Bone environment influences irreversible adhesion of a methicillin-susceptible *Staphylococcus aureus* strain. *Front. Microbiol.* 9:2865. doi: 10.3389/fmicb.2018.02865

Rice, K. C., Mann, E. E., Endres, J. L., Weiss, E. C., Cassat, J. E., Smeltzer, M. S., et al. (2007). The cidA murein hydrolase regulator contributes to DNA release and biofilm development in *Staphylococcus aureus*. *Proc. Natl. Acad. Sci. U.S.A.* 104, 8113–8118. doi: 10.1073/pnas.0610226104

Sadovskaya, I., Chaignon, P., Kogan, G., Chokr, A., Vinogradov, E., and Jabbouri, S. (2006). Carbohydrate-containing components of biofilms produced in vitro by some staphylococcal strains related to orthopaedic prosthesis infections. *FEMS Immunol. Med. Microbiol.* 47, 75–82. doi: 10.1111/j.1574-695X.2006.00068.x

Shoji, M. M., and Chen, A. F. (2020). Biofilms in periprosthetic joint infections: a review of diagnostic modalities, current treatments, and future directions. *J. Knee Surg.* 33, 119–131. doi: 10.1055/s-0040-1701214

Springer, B. D., Cahue, S., Etkin, C. D., Lewallen, D. G., and McGrory, B. J. (2017). Infection burden in total hip and knee arthroplasties: an international registry-based perspective. *Arthroplast Today* 3, 137–140. doi: 10.1016/j.artd.2017.05.003

Stewart, P. S. (2015). Antimicrobial tolerance in biofilms. *Microbiol. Spectr.* 3, 1–30. doi: 10.1128/microbiolspec.MB-0010-2014

Tasse, J., Trouillet-Assant, S., Josse, J., Martins-Simões, P., Valour, F., Langlois-Jacques, C., et al. (2018). Association between biofilm formation phenotype and clonal lineage in *Staphylococcus aureus* strains from bone and joint infections. *PLoS One* 13:e0200064. doi: 10.1371/journal.pone.0200064

Tenover, F. C., and Goering, R. V. (2009). Methicillin-resistant *Staphylococcus aureus* strain USA300: origin and epidemiology. *J. Antimicrob. Chemother.* 64, 441–446. doi: 10.1093/jac/dkp241

Tetz, V. V., and Tetz, G. V. (2010). Effect of extracellular DNA destruction by DNase I on characteristics of forming biofilms. *DNA Cell Biol.* 29, 399–405. doi: 10.1089/dna.2009.1011

Wright, J. A., and Nair, S. P. (2010). Interaction of staphylococci with bone. *Int. J. Med. Microbiol.* 300, 193–204. doi: 10.1016/j.ijmm.2009.10.003

Xu, Y., Maltesen, R. G., Larsen, L. H., Schønheyder, H. C., Le, V. Q., Nielsen, J. L., et al. (2016). In vivo gene expression in a *Staphylococcus aureus* prosthetic joint infection characterized by RNA sequencing and metabolomics: a pilot study. *BMC Microbiol.* 16:80. doi: 10.1186/s12866-016-0695-6

Yu, J., Jiang, F., Zhang, F., Pan, Y., Wang, J., Han, P., et al. (2020). Virtual screening for novel sara inhibitors to prevent biofilm formation of *Staphylococcus aureus* in prosthetic joint infections. *Front. Microbiol.* 11:587175. doi: 10.3389/fmicb.2020.587175

Zapotoczna, M., McCarthy, H., Rudkin, J. K., O'Gara, J. P., and O'Neill, E. (2015). An essential role for coagulase in *Staphylococcus aureus* biofilm development reveals new therapeutic possibilities for device-related infections. *J. Infect. Dis.* 212, 1883–1893. doi: 10.1093/infdis/jiv319

Conflict of Interest: The authors declare that the research was conducted in the absence of any commercial or financial relationships that could be construed as a potential conflict of interest.

Publisher's Note: All claims expressed in this article are solely those of the authors and do not necessarily represent those of their affiliated organizations, or those of the publisher, the editors and the reviewers. Any product that may be evaluated in this article, or claim that may be made by its manufacturer, is not guaranteed or endorsed by the publisher.

frontiers in Microbiology

REVIEW
published: 05 October 2021
doi: 10.3389/fmicb.2021.747618

Alternative Approaches for the Management of Diabetic Foot Ulcers

Cassandra Pouget[1], Catherine Dunyach-Remy[2], Alix Pantel[2], Adeline Boutet-Dubois[2], Sophie Schuldiner[3], Albert Sotto[4], Jean-Philippe Lavigne[2] and Paul Loubet[4]*

[1] Virulence Bactérienne et Infections Chroniques, INSERM U1047, Université de Montpellier, Nîmes, France, [2] Virulence Bactérienne et Infections Chroniques, INSERM U1047, Université de Montpellier, Service de Microbiologie et Hygiène Hospitalière, Clinique du Pied Gard Occitanie, CHU Nîmes, Nîmes, France, [3] Virulence Bactérienne et Infections Chroniques, INSERM U1047, Université de Montpellier, Service des Maladies Métaboliques et Endocriniennes, Clinique du Pied Gard Occitanie, CHU Nîmes, Le Grau-du-Roi, France, [4] Virulence Bactérienne et Infections Chroniques, INSERM U1047, Université de Montpellier, Service des Maladies Infectieuses et Tropicales, Clinique du Pied Gard Occitanie, CHU Nîmes, Nîmes, France

Diabetic foot ulcers (DFU) represent a growing public health problem. The emergence of multidrug-resistant (MDR) bacteria is a complication due to the difficulties in distinguishing between infection and colonization in DFU. Another problem lies in biofilm formation on the skin surface of DFU. Biofilm is an important pathophysiology step in DFU and may contribute to healing delays. Both MDR bacteria and biofilm producing microorganism create hostile conditions to antibiotic action that lead to chronicity of the wound, followed by infection and, in the worst scenario, lower limb amputation. In this context, alternative approaches to antibiotics for the management of DFU would be very welcome. In this review, we discuss current knowledge on biofilm in DFU and we focus on some new alternative solutions for the management of these wounds, such as antibiofilm approaches that could prevent the establishment of microbial biofilms and wound chronicity. These innovative therapeutic strategies could replace or complement the classical strategy for the management of DFU to improve the healing process.

Keywords: alternative therapeutic approaches, biofilm, chronic wound, diabetic foot, antibiofilm

OPEN ACCESS

Edited by:
Giovanna Batoni, University of Pisa, Italy

Reviewed by:
Xingwu Ran, Sichuan University, China
Derek Fleming, Mayo Clinic, United States

****Correspondence:***
Jean-Philippe Lavigne
jean.philippe.lavigne@chu-nimes.fr

Specialty section:
This article was submitted to Infectious Agents and Disease, a section of the journal Frontiers in Microbiology

Received: *26 July 2021*
Accepted: *07 September 2021*
Published: *05 October 2021*

Citation:
Pouget C, Dunyach-Remy C, Pantel A, Boutet-Dubois A, Schuldiner S, Sotto A, Lavigne J-P and Loubet P (2021) Alternative Approaches for the Management of Diabetic Foot Ulcers. Front. Microbiol. 12:747618. doi: 10.3389/fmicb.2021.747618

INTRODUCTION

Diabetic foot ulcers (DFU) have a lifetime prevalence of 15–25% (Armstrong et al., 2017). Infection is the most common, severe and costly (Prompers et al., 2008) DFU complication with high risk of mortality and morbidity associated with lower limb amputation (Bakker et al., 2016). The diagnosis of diabetic foot infection (DFI) is often difficult, leading to the inappropriate use of antibiotics. The bacterial organization in DFU and the involvement of multidrug-resistant (MDR) bacteria require new antimicrobial solutions. This review discusses the role of the biofilm in DFU and alternative approaches to classical treatment that could improve DFU management.

Abbreviations: AMP, antimicrobial peptide; c-di-GMP, cyclic diguanylate; C2DA, *cis*-2-decenoic acid; DFI, diabetic foot infection; DFP, deferiprone; DFU, diabetic foot ulcer; DNA, deoxyribonucleic acid; DMSO, dimethyl sulfoxide; EDTA, ethylene diamine tetra-acetic; EGTA, egtazic acid; EPS, extracellular polymeric substance; FEP, functionally equivalent pathogroups; MDR, multidrug resistance; MRSA, methicillin-resistant *Staphylococcus aureus*; MSC, mesenchymal stem cells; NGAD, next generation antibiofilm carboxymethyl cellulose silver containing wound dressing; QS, quorum sensing.

Clinical and Translational Relevance

Sixty to 80% of chronic wounds harbor bacterial structures in a biofilm (James et al., 2008; Malone et al., 2017a). For the clinician, the main difficulty is to distinguish between infecting and colonizing bacteria. Misclassification can lead to inappropriate antibiotic prescriptions that contribute to promoting the emergence of MDR bacteria, a major DFU health issue (Caravaggi et al., 2013). Better understanding of the bacterial organization of biofilms in chronic wounds would allow development of tailored antimicrobial strategies and improving wound healing. In this context, a large majority of current fundamental studies on DFUs focuses on bacterial cooperation and the impact of local microenvironment on microorganisms. Thus, the host-microorganism interface plays a major role in DFI development. In DFU, bacteria are classically organized in functionally equivalent pathogroups (FEP) where pathogenic and commensal bacteria co-aggregate symbiotically in a pathogenic biofilm to maintain a chronic infection (Dowd et al., 2008). Polymicrobial biofilms have been observed both in pre-clinical studies using animal models and in clinical research on DFU. They represent the main cause of healing delay. Recently, some approaches have targeted biofilm formation with the aim of controlling infections (Snyder et al., 2017). Better understanding of the host-bacterial interactions is essential to develop new therapeutic solutions that take into account the biofilm to limit the diffusion of MDR bacteria.

Diabetic Foot Ulcers and Biofilms

Biofilm formation is a multistep process (see for review Percival et al., 2015) whereby heterogeneous communities of microorganisms (bacteria and/or fungi) are embedded into an extracellular polymeric substance (EPS) matrix that contains proteins, deoxyribonucleic acid (DNA), glycoproteins and polysaccharides, and confers the ability to adhere to biotic or abiotic surfaces (Bjarnsholt, 2013). In DFU, the biofilm architectural structure differs among patients due to the variability of the involved bacterial genera and species. Conversely, the multistep formation process is similar. Biofilm formation is a major mechanism of adaptation that protects bacteria from antibiotics, due to several characteristics (Singh et al., 2017). Biofilm structure provides a protective layer against antimicrobial compounds. Wounds biofilms are polymicrobial, formed by complex and order combinations of microorganisms. Hence, compounds produced by different bacterial strains might impair the contact between the bacterial cell wall and the antibiotic by changing the composition of the EPS. Finally, the production of degradative enzymes by different pathogens can act in synergy against antibiotics. These biofilm aspects are responsible for a reduced diffusion of the antibiotic within the biofilm matrix leading to an inefficient activity of the antibiotic treatment (Sharma et al., 2019). In addition to this feature, the ability to form a biofilm is an effective strategy to enhance survival and persistence of microorganisms by increasing their antimicrobial resistance. The antimicrobial resistance in organisms producing biofilms acts by delayed penetration of the antimicrobial agents through the biofilm matrix, altered growth rate of biofilm organisms, and other physiological changes due to the biofilm mode of growth (Donlan and Costerton, 2002).

CLASSICAL STRATEGIES IN THE MANAGEMENT OF DIABETIC FOOT ULCERS

The management of patients with a DFU is a multidisciplinary approach that includes all relevant specialties (i.e., nursing, orthopedics, plastic surgery, vascular surgery, nutrition, infectious diseases, microbiology, and endocrinology departments) (Cahn et al., 2014). To aid the clinician during the management of DFUs, classification of stage and severity of the wound must be established (Lipsky et al., 2020). The classical care for the control and treatment of DFUs is centered on perfusion, pressure moderation, control of the infection, control of the glycaemic balance, foot discharge and debridement (Wu et al., 2007) (**Table 1**).

Debridement of the Wound

Debridement consists in the removal of necrotic, devitalized and/or infected tissue from a wound, leaving healthy tissue preserved. Surgical debridement is the usual method used. The objective is to control the bacterial load, which, in combination with antimicrobial treatment, allows early closure of the wound (Wolcott et al., 2009). Debridement enables the wound and surrounding tissues to promote normal healing by removing infected tissues, biofilms, and senescent cells. Debridement allows the reepithelialization of soft-tissue by eradication of (early or established) infection and reduction of bioburden, the improvement of local blood flow, and the revitalization of the wound bed. When it was performed correctly, it optimizes the diabetic wound healing.

Negative Pressure Wound Therapy

Associated with debridement, negative pressure wound therapy is an airtight open-pore placed onto the wound and covered by an airtight dressing. Then, the wound is connected to a vacuum source and a negative pressure is generated. The negative pressure at the wound site reduces the size of the wound through contraction; it continuously cleans the wound by removing small debris through suction and reduces levels of proteases through wound fluid removal (Apelqvist et al., 2017). The efficiency of this therapy has been confirmed and it represents an effective measure of promoting wound healing, although the evidence is low (Liu et al., 2018).

Antimicrobial Therapy for Infected Diabetic Foot Ulcers

Antibiotics are not used to manage colonized DFU (Lipsky et al., 2020). Their use concerned the different stages of DFI. Antibiotics are mainly empirical in the first instance, in accordance with the causative pathogen and the severity of the infection. The definitive antibiotic treatment is changed according to the microbiological culture and the response of the

TABLE 1 | *In vitro* and *in vivo* effects of the main alternative approaches studied.

	***In vitro* effects**	***In vivo* effects**	**References**
Debridement			
Negative pressure therapy	–	Enhance wound closure	Apelqvist et al., 2017; Liu et al., 2018
Antimicrobial agents			
Calcium sulfate beads with antibiotics	Decreased viability of MRSA strains	No clinical evaluation	Price et al., 2016
Nanoparticles	Silver nanoparticles affect *P. aeruginosa* biofilm formation	No clinical evaluation	Beyth et al., 2015; Ahmadi and Adibhesami, 2017; Hamdan et al., 2017; Mihai et al., 2018
Oxyclozanide	Enhances aminoglycoside and tetracycline killing in *S. aureus* biofilms	No clinical evaluation	Maiden et al., 2019
Guanylated polymethacrylates	Effective killing of *C. albicans* and *S. aureus* in polymicrobial biofilms	Untested in human DFU	Qu et al., 2016
Guar gum-associated nisin	Reduction of biofilm formation by *S. aureus* isolates from patients	Evaluation with strains isolated from DFI	Cirioni et al., 2006; Dutta and Das, 2016; Santos et al., 2016; Thombare et al., 2016
Acapsil	–	Shorter hospital stay and faster wound healing	Bilyayeva et al., 2017
Antiseptics			
Cadexomer iodine	–	Reduction (1 log10) of microbial load and biofilm in DFU (11/17 patients)	Schwartz et al., 2013; Malone et al., 2017b
Nutraceuticals			
Cranberry	Inhibition of pilus synthesis and prevention of biofilm formation	Decrease of *Escherichia coli, S. aureus* adhesion	LaPlante et al., 2012
Tannic acid	Inhibition of *S. aureus* biofilm formation by peptidoglycan cleavage	Acceleration of cutaneous wound healing in rat model	Payne et al., 2013; Orlowski et al., 2018; Chen et al., 2019
Tea-tree oil and Cinnamon oil	Effect on MRSA biofilm	Reduction of the quantity of colonized MRSA and promotion of healing of chronic wounds in a clinical trial	Kwieciński et al., 2009; Lee et al., 2014; Cui et al., 2016; Seyed Ahmadi et al., 2019
Ellagic acid	Limits *S. aureus* biofilm formation and enhances antibiotic susceptibility	No clinical evaluation	Quave et al., 2012
Propolis and honey	Anti-inflammatory and anti-bacterial properties	Reduction of bacterial load of chronic wounds in combination with antibiotics	Henshaw et al., 2014; Jull et al., 2015; Martinotti and Ranzato, 2015; Minden-Birkenmaier and Bowlin, 2018; McLoone et al., 2020
Probiotics	*Lactobacilli* antibiofilm activity	Acceleration of wound healing in mice	Vuotto et al., 2014; Vågesjö et al., 2018
Phage therapy			
	Reduction of biofilm formation and infection by *P. aeruginosa*, *S. aureus,* and *A. baumannii*	Reduction of bacterial load and wound closure in diabetic mouse wound infections	Mendes et al., 2014; Fish et al., 2018; Hill et al., 2018; Morozova et al., 2018; Taha et al., 2018; Albac et al., 2020; Kifelew et al., 2020
Action on wound healing			
Photodynamic therapy	–	Increase of reepithelization	Tardivo et al., 2014
Hyperbaric oxygen therapy	–	Improvement of short-term healing	Kranke et al., 2015
Non-thermal plasma	–	Acceleration of wound healing in animal models of ulcers	Chatraie et al., 2018; Cooley et al., 2020
Electrostimulation	Enhanced wound closure time	Evaluation with dressings	Barki et al., 2019
Alternatives for inhibition of adhesion and biofilm			
Inhibition of initial bacterial adhesion			
EDTA and citrate	Prevention of biofilm formation and degradation of pre-existing biofilm (via Mg^{2+}, Ca^{2+}, and iron chelators)	Prevention of infection in a rabbit catheter model (with minocycline)	Raad et al., 2008
Aryl rhodanines	Inhibition of biofilm formation by *S. aureus* and other Gram-positive bacteria by targeting early stage of adhesion	No clinical evaluation	Opperman et al., 2009
Interaction with biofilm metabolism by QS stimulus modulation			
Furanone	Inhibition of biofilm formation and expression of *P. aeruginosa* virulence factors	Decrease of *P. aeruginosa* virulence	Kim et al., 2012; García-Contreras et al., 2013
Sodium ascorbate	Modulation of QS signal in *P. aeruginosa*	No clinical evaluation	El-Mowafy et al., 2014

(Continued)

TABLE 1 | (Continued)

	In vitro effects	*In vivo* effects	References
Savarin	Inhibition of *S. aureus* biofilm formation (by targeting *agr*)	No clinical evaluation	Sully et al., 2014
Azithromycin	Inhibition of biofilm formation and expression of *P. aeruginosa* virulence factors	Improvement of clinical signs in patients with CF and *P. aeruginosa* infections	Bala et al., 2011
RNAII inhibiting peptide	Reduction of *S. aureus* virulence	Healing improvement in a chronic wound mouse model	Giacometti et al., 2003
c-di-GMP	Reduction of biofilm formation in *P. aeruginosa* and *A. baumannii*	No clinical evaluation	Romling et al., 2013; Lieberman et al., 2014; Wu et al., 2015
Exo-polysaccharides	Reduction of biofilm formation (*P. aeruginosa*) by targeting virulence factors + PA01 and *S. epidermidis* in co-culture	No clinical evaluation	Pihl et al., 2010; Jiang et al., 2011; Rendueles et al., 2013; Limoli et al., 2015
1,018-peptide and derivates	Disruption of *P. aeruginosa* and *B. cenocepacia* mature biofilms	No clinical evaluation	Willcox et al., 2008; de la Fuente-Núñez et al., 2012, 2014
Deferiprone	Activity against coagulase-negative staphylococci	No clinical evaluation	Coraça-Huber et al., 2018
Enzymes enhancing bacterial dispersion			
α-amylase	Disruption of biofilm formed by *S. aureus*	No clinical evaluation	Kalpana et al., 2012
α-amylase and cellulase	Disruption of biofilm	*In vivo* disruption but the dispersal can cause systemic infection	Fleming et al., 2017
DNase, dispersin B	Eradication of single and multi-species biofilms	No clinical evaluation	Chen and Lee, 2018; Sharma and Pagedar Singh, 2018
2-aminoimidazole	Disruption of biofilms formed by *S. aureus*	No clinical evaluation	Rogers et al., 2010
Lysostaphin	Eradication of *P. aeruginosa* biofilms	Effective treatment for biofilm disruption on jugular vein catheters in mice	Kokai-Kun et al., 2009
C2DA	Dispersion of *S. aureus,* Action on MRSA biofilm	No clinical evaluation	Jennings et al., 2012
Next-generation dressings and grafts			
NGAD NGAD + mesenchymal stem cells	Removal of biofilms by *S. aureus* and antibiotic-resistant *P. aeruginosa*	Evaluation with clinical strains	Parsons et al., 2016; Pérez-Díaz et al., 2018; Tarusha et al., 2018
Electrospun nanofibers	Prevent biofilm formation and enhance fibroblast development	No clinical evaluation	Ramalingam et al., 2019
Surfactant based gel	–	Reduced bacteria development and biofilm infection	Yang et al., 2017; Percival et al., 2018
Dehydrated amniotic membranes	Faster wound healing in patients with severe comorbidities	Lower extremity wounds	Lullove, 2017
Sucrose octasulfate	–	Significant increase of wound closure rate	Edmonds et al., 2018
Skin substitutes	–	Fish skin offers natural anti-inflammatory properties and promotes growth of new skin. Other wounds and patients with burns	See clinicaltrials.gov NCT01348581
Arenicola marina	This new dressing delivers oxygen to the wound bed, enhancing healing and cell proliferation	No evaluation clinical	Le Pape et al., 2018
Epigel®	This new bioactive hydrogel hydrates the wound bed	No clinical evaluation	See www.epinovabiotech.com
Keratinocyte treatment. Skin grafts (epithelial or fetal cells). Stem cells. Collagen I matrix. Human placental tissues.	–	Improve closure time	Kanji and Das, 2017; Lo et al., 2019; Lintzeris et al., 2018; Mao et al., 2018; Momeni et al., 2019; Hassanshahi et al., 2019; Hwang et al., 2019; Oropallo, 2019
3D-printed scaffolds	–	Shorter healing time	Pushparaj and Ranganathan, 2017; Sun et al., 2018

EDTA, ethylene diamine tetra-acetic; EGTA, egtazic acid; MRSA, methicillin-resistant Staphylococcus aureus; QS, quorum sensing; CF, cystic fibrosis; C2DA, cis-2-decenoic acid; DFI, diabetic foot infection; DFU, diabetic foot ulcer; NGAD, next-generation carboxymethylcellulose silver- containing wound dressing.

empirical treatment (Kwon and Armstrong, 2018). Its duration will depend on the severity of the infection. However, Walker et al. (2015) reported that 74% of DFUs did not respond to topical and systemic agents. Recently, Johani et al. (2018) confirmed this observation. Uçkay et al. (2018) could not demonstrate a beneficial effect of topical therapy using gentamicin-sponges in 88 DFUs. Similar conclusions were drawn for vancomycin powder, although infections were more superficial in patients

treated with vancomycin than in controls (untreated) (Wukich et al., 2015). A recent Cochrane review on this topic indicated that randomized controlled data on the effectiveness and safety of topical antimicrobial for DFI are limited (Dumville et al., 2017).

As bacteria in biofilms display 100 to 1,000-fold higher tolerance to antibiotics, new solutions to deliver antibiotics at high concentration into the biofilm have been developed. Delivery systems could be used to administer high concentrations of antibiotics to the wound with limited side effects. Biodegradable vehicles, such as calcium sulfate beads, display a good elution profile and seem to be compatible with many antibiotics. Natural polymers, such as collagen sponges, are another emerging delivery system, although data are still limited for DFU (Markakis et al., 2018). For instance, calcium sulfate beads are mineral elements that are naturally absorbed into biofilms and then slowly dissolve to release antibiotics. Price et al. (2016) showed *in vitro* that calcium sulfate beads loaded with gentamicin or tobramycin eradicated *Pseudomonas aeruginosa* biofilms in DFU, and also reduced the viability of MRSA strains. The main problem of this approach is the potential risk of bacterial resistance selection. Randomized trials are required to confirm the efficacy of these approaches.

Recently, Maiden et al. (2019) showed that the ionophore oxyclozanide can enhance aminoglycoside and tetracycline killing activity in *P. aeruginosa* biofilms by reducing the bacterial cell membrane potential and increasing antibiotic accumulation within the biofilm. Currently, this compound is mainly used in veterinary medicine for parasitic infections, but this finding suggests that in combination with aminoglycosides, oxyclozanide could represent a new antibiofilm agent for chronic wound treatment.

ALTERNATIVE APPROACHES IN THE MANAGEMENT OF DIABETIC FOOT ULCERS

In addition to conventional approaches, new alternative solutions have emerged in recent years, targeting the bacterial organization and notably the biofilm formation of DFU (**Table 1**).

Antimicrobial Peptides and Related Drugs

Santos et al. (2016) reported that nisin, a bacteriocin against Gram-positive bacteria, was active against some Gram-negative bacteria. Nisin promotes the disintegration of the bacterial cell membrane lipid bilayer by electrostatic interactions. Its use in DFU requires an effective delivery system. An *in vitro* study showed that guar gum-associated nisin reduced biofilm formation by 23 *S. aureus* strains isolated from DFU, including MDR strains (Thombare et al., 2016). Similarly, citropin is active against *P. aeruginosa* and *S. aureus* without major toxicity in animal models (Cirioni et al., 2006). However, Dutta and Das (2016) highlighted the limitations of antimicrobial peptides (AMPs), especially in terms of production costs, bioavailability, and difficult clinical translation.

Guanylated polymethacrylates are a new class of antimicrobial agents that structurally mimics AMPs and efficiently kills both fungi and bacteria in polymicrobial biofilms (*Candida albicans* and *S. aureus*) (Qu et al., 2016). A study on 266 patients with venous leg ulcers and DFU showed that, compared with gentaxane and iodine/dimethyl sulfoxide (DMSO), Acapsil® (Willingsford Healthcare), a powder based on a micropore particle technology, accelerated wound healing and reduced hospitalization length (Bilyayeva et al., 2017).

Nanotechnologies

Nanotechnology-based therapies open the door to new therapeutic solutions for chronic wounds (Hamdan et al., 2017). Nanoparticles made of iron, silver, zinc, or titanium showed antibacterial activity (disruption of the bacterial membrane) (Beyth et al., 2015), and due to their high bioavailability, they can penetrate into mature biofilms and target sessile bacteria. Therefore, these materials could be used to target both surface bacteria and biofilm-organized bacteria in deeper tissues. A recent study showed that the combination of silver nanoparticles and tetracycline reduced the bacterial load and promoted healing in wounds inoculated with *P. aeruginosa* in mice (Ahmadi and Adibhesami, 2017). A recent review has summarized nanotechnology-based wound healing approaches and their benefits (Mihai et al., 2018).

Antiseptics

Topical antiseptics are antimicrobial agents that inhibit or reduce the number of microorganisms. Unlike antibiotics, antiseptics have multiple targets and a broader spectrum of activity including bacteria, fungi, viruses, or protozoa. They have commonly been used on wounds to prevent or treat infection; however, antiseptic fluid irrigation have received little scientific study and their efficiency remain questioned (Lipsky et al., 2020). Indeed, wound cleansers may affect normal human cells and may be antimitotic affecting normal tissue repair. Repeated and excessive treatment of wounds with antiseptics without proper indications may have negative outcomes or promote a microenvironment similar to those found in chronic wounds. With the discovery of polymicrobial biofilms and the emergence of bacteria tolerant to antiseptics, their effectiveness is even more questionable (Sheldon, 2005; Ortega Morente et al., 2013; Stewart, 2015). Following these observations, international guidelines suggest that antiseptics are not appropriate in the management of DFU (Lipsky et al., 2020).

However, some recent studies present interesting results. Products, such as Octenilin® (Schülke & Mayr GmbH), iodine-based solutions, polyhexamethylene biguanide or silver-impregnated dressings, are good *in vitro* candidates (Kucisec-Tepes, 2016; Pavlik et al., 2019) to reduce biofilms, but their effectiveness against polymicrobial and complex biofilms remains to be demonstrated (Khan and Naqvi, 2006). Similarly, chlorhexidine action is clearly limited on multi-species biofilms (Touzel et al., 2016). Townsend et al. (2016) developed a new *in vitro* inter-kingdom wound biofilm model on hydrogel-based cellulose to test the efficacy of common topical antiseptics. They treated biofilms composed of *C. albicans, P. aeruginosa,* and

S. aureus with chlorhexidine or povidone iodine, and found that the structure of polymicrobial biofilms was only slightly affected compared with that of monomicrobial biofilms. They also showed that topical antiseptics were less efficient against polymicrobial biofilms.

Cadexomer iodine is a topical antimicrobial agent that could be used to deliver iodine into wounds. Iodine can penetrate the pathogen cell wall and disrupt proteins, as well as the nucleic acid structure and synthesis. Cadexomer iodine can be encapsulated within small polysaccharide beads that, in the presence of the wound exudate, start to swell and release iodine into the wound. *In vivo* studies have demonstrated that cadexomer iodine significantly reduced biofilm and microbial load in DFU (Schwartz et al., 2013; Malone et al., 2017b).

Nutraceuticals

Nutraceuticals are pharmaceutical alternatives that include all foods or food products which provide medical benefits and can be delivered under medical form. These products could present health benefits, and several plant-derived natural compounds could prove clinically beneficial.

A study has reported that cranberry extracts inhibited biofilm production of Gram-positive bacteria (LaPlante et al., 2012). Polyphenolic compounds, such as tannic acid (Orlowski et al., 2018; Chen et al., 2019 in a rats model) and tea-tree oil (Lee et al., 2014 in a clinical trial), also inhibited biofilm formation by *S. aureus*, including methicillin-resistant *S. aureus* (MRSA) (Kwieciński et al., 2009), by cleaving peptidoglycan (Payne et al., 2013). An active compound found in cinnamon oil has also been shown to prevent MRSA biofilm formation *in vitro* (Cui et al., 2016), and also in a mice model of wound infection (Seyed Ahmadi et al., 2019). Finally, ellagic acid derivatives also limited *S. aureus* biofilm formation and enhanced its susceptibility to some antibiotics (Quave et al., 2012). All these compounds must be clinically evaluated in chronic wounds.

The natural anti-inflammatory and antimicrobial properties of propolis produced by honeybees are well known. Its regenerative properties and low cost explain the increased interest in propolis for promoting chronic wound healing (Henshaw et al., 2014; Martinotti and Ranzato, 2015). To our knowledge, propolis alone has not been used in DFU, but a recent review summarized the effect of propolis with a combination of several antibiotics in skin problems including wounds (McLoone et al., 2020).

Honey has been used for a long time to treat wounds with no real proof of its efficiency. A study demonstrated that in animals, honey has a clear antibacterial effect, but no anti-inflammatory activity (Jull et al., 2015). Recently, Minden-Birkenmaier and Bowlin (2018) reviewed the effects of different types of honey on wound closure and antibiofilm activity. They also discussed the advantages of honey in the field of tissue engineering and biomaterials (Cryogels, Electrospun templates, and Hydrogels).

Within a biofilm, intra- and inter-species interactions and cooperation can be observed at the different stages of its formation. Another approach could be to harness the bacterial competition to modify the dispersion or modification of the growing matrix. Probiotic bacteria, such as Lactobacilli, could have antibiofilm activities and be good candidates for wound treatment (Vuotto et al., 2014; Vågesjö et al., 2018 in *in vivo* model).

Phage Therapy

There is renewed interest in bacteriophages to fight bacteria. In this treatment, viruses infect a specific bacterium and reproduce inside it. Several areas must be investigated to evaluate the potential of bacteriophages in the therapeutic arsenal (Knezevic et al., 2021). Indeed, the success of phage therapy is highly dependent on the efficiency and safety of phage preparations, which raises manufacturing and formulation challenges. The production of phages must comply with the strict regulations that are usually applied for pharmaceutical products to ensure the high-quality standards appropriate for their intended. This needs a production with a controlled and reproducible process. One of the requirements is to avoid phages encoding for lysogeny, virulence factors or antibiotic resistance. The presence of impurities such as endotoxins in phage preparations should also be avoided or be below a threshold. The presence/absence of neutralizing antibodies binding against phages must be known. The development of "phagogram" (in parallel to antibiogram) could be also an important way for the routine use of phage therapy. However, this could represent another approach for the treatment of infected wounds with minimal effects on the host microbiome (Hill et al., 2018; Morozova et al., 2018). Mendes et al. (2014) tested an *in vitro* cocktail of bacteriophages targeting *S. aureus, P. aeruginosa,* and *Acinetobacter baumannii* on both planktonic cells and biofilm-associated cells, and found that it reduced biofilm formation and infection. Other case reports have described encouraging results in patients with diabetic foot and chronic wounds (Fish et al., 2018; Taha et al., 2018).

To date, one of the main limitations is that the evaluation of phage efficiency has been performed using mainly *in vitro* studies and a single species in a biofilm. However, biofilms in DFU are multi-species, impacting the spatial organization and the interaction with phages. The specific outcome of phage infection in a multi-species biofilm seems to strongly depend on the bacterial species composing the biofilm (e.g., whether they establish synergist or antagonist interactions). The complexity of phage-biofilm interactions is increased by evidence of biofilm formation induced by exposure to certain phages (Lacqua et al., 2006; Tan et al., 2015; Henriksen et al., 2019). Overall, even if the potential of phages to control the complex biofilm observed in DFU is proved, the complexity and diversity of phage-biofilm interactions could limit broad conclusions and need more research to claim that phage therapy becomes a real solution in the DFU situation.

Therapeutic Solutions on Wound Healing

Photodynamic therapy could be an interesting approach to aid wound healing. In this therapeutic procedure, pathogen cell death is induced upon exposure to light to generate oxygen species by activation of a photosensitizing agent. This agent is non-toxic in the dark, but after illumination, it becomes a very efficient antimicrobial agent. This method is used mainly in oncology, but it could also be employed to manage chronic wounds notably by its ability to prevent amputation in diabetic patients with

DFU. Indeed, a clinical study showed that all non-treated patients (n = 16) underwent amputation, compared to only one patient in the group that received photodynamic therapy (n = 18) (Tardivo et al., 2014).

Another technology uses non-thermal plasma. Here, plasma is a partially ionized medium composed of many elements, such as charged particles (electrons and ions), neutral and excited atoms, UV photons and radicals. A recent study in rats showed that this technology could be used on pressure ulcers to accelerate wound healing (Chatraie et al., 2018). Additional investigations are needed to determine its value in humans, but recent results using an *in vivo* mouse model of type 2 diabetes showed promotion of bacterial killing of *P. aeruginosa* and wound disinfection without metabolic complication (Cooley et al., 2020).

Application of electrical stimulation has also been investigated in wound repair and regeneration. Wireless electroceutical dressings were recently tested in a porcine chronic wound polymicrobial biofilm infection model with *P. aeruginosa* (PAO1) and *A. baumannii* (19606) (Barki et al., 2019). The data suggested that the dressing disrupted wound biofilm aggregates and accelerated wound closure by restoring skin barrier function. The dressing changed expression of *P. aeruginosa* quorum sensing *mvfR* (*pqsR*), *rhlR,* and *lasR* genes and silencing of E-cadherin (a protein required for skin barrier function). Finally, this study highlighted the rescue effect against biofilm-induced persistent inflammation by decreased cytokines production.

Finally, hyperbaric oxygen therapy had been used for several years in the management of DFU. It consists in inhalation of pure oxygen after entering a special compression chamber. The treatment aims to increase the oxygen supply to the wound. However, the value of this therapy is controversial and its effect seems more due to the foot discharge than the oxygen itself. In a Cochrane review, the authors concluded that the therapy improved short-term but not long-term healing in patients with DFUs (Kranke et al., 2015).

Alternatives in the Inhibition of Bacterial Adhesion and Biofilm

Inhibition of Initial Bacterial Adhesion

Bacterial growth requires the presence of metals (particularly, calcium, iron, and magnesium). Ionic chelators could be used to limit bacterial growth and initial adhesion. Ethylene diamine tetra-acetic (EDTA) and citrate are the most promising compounds of this class (Raad et al., 2008). However, the efficiency of these chelators is dependent on the bacterial strains. For instance, Abraham et al. (2012) observed that the anti-biofilm effect varied among *S. aureus* isolates. Aryl rhodanines also can inhibit the early stages of biofilm development by preventing the attachment on the surface of *S. aureus* and other Gram-positive bacteria, but not of Gram-negative bacteria (Opperman et al., 2009).

Inhibiting Biofilm Metabolism

Quorum Sensing (QS) is important for the transition from antimicrobial-sensitive planktonic cells to antimicrobial-resistant cell aggregates in a biofilm. In the absence of QS signal, biofilm formation is inhibited. Many researchers have evaluated compounds to modulate QS, such as furanone that inhibited, among others, *P. aeruginosa* biofilms (Kim et al., 2012), sodium ascorbate that modulated the QS signal in *P. aeruginosa* (El-Mowafy et al., 2014), savarin (a *S. aureus* virulence inhibitor) (Sully et al., 2014), and azithromycin in *P. aeruginosa* (Bala et al., 2011). Moreover, RNA III inhibiting peptide reduced *S. aureus* and *Staphylococcus epidermidis* virulence and improved healing in rats (Giacometti et al., 2003). These approaches are efficient only on a restricted number of bacterial species, and due to their potential toxicity, they have a limited use. Moreover, it has been reported that some bacteria isolated from clinical samples have become resistant to some QS modulators (García-Contreras et al., 2013), suggesting the emergence of multi-QS inhibitor resistant bacteria (Koul et al., 2016).

Another approach uses the cyclic diguanylate inhibition. Cyclic diguanylate (c-di-GMP) is a second messenger that controls many cellular functions, including biofilm formation. Various stress factors, such as starvation, reduced c-di-GMP level, leading to biofilm dispersal (Romling et al., 2013). This study also found that dispersed cells were more virulent compared with the first planktonic cells that induced the biofilm and with biofilm sessile cells. Moreover, small molecules, such as LP 3134, LP 3145, LP 4010, and LP 1062, inhibited a key enzyme that mediated c-di-GMP synthesis and consequently also biofilm formation in *P. aeruginosa* and *A. baumannii* (Wu et al., 2015). Unfortunately, these molecules seem to be toxic to eukaryotic cells. Finally, ebselen inhibited c-di-GMP and displayed good results on *P. aeruginosa* biofilms (Lieberman et al., 2014).

The biofilm matrix mainly contains proteins, extracellular DNA and polysaccharides. Polysaccharides are important for the early stage of biofilm formation and can protect cells during biofilm maturation. They also provide the basal biofilm structure that allows the bacterial community stratification. A recent study demonstrated that the exo-polysaccharide EPS273, obtained from a marine bacterium, reduced biofilm formation in *P. aeruginosa* by targeting virulence factors (Jiang et al., 2011). Other antibiofilm polysaccharides have been discovered, for instance Psl and Pel from *P. aeruginosa* PAO1 that decreased *S. epidermidis* biofilm formation in a co-culture biofilm *in vivo* model (Pihl et al., 2010). Other non-bacterial polysaccharides from animals, plants and algae have also shown antibiofilm activity (Rendueles et al., 2013).

In stress conditions, bacteria synthesize alarmones (guanosine tetraphosphate and guanosine pentaphosphate) called (p)ppGpp (Willcox et al., 2008). The antibiofilm peptide 1,018 inhibited their accumulation upon nutritional stress and prevented biofilm formation. Moreover, at low concentration, it eradicated biofilm-associated bacteria and disrupted mature biofilms. This peptide and its derivatives HE4 and HE10 were similarly effective against *P. aeruginosa* and *Burkholderia cenocepacia* biofilms (de la Fuente-Núñez et al., 2014). In addition, peptide 1,037 reduced biofilms formed by other bacteria (the Gram-negative pathogens *P. aeruginosa* and *B. cenocepacia*, and the Gram-positive *Listeria monocytogenes*) (de la Fuente-Núñez et al., 2012).

Finally, a recent study showed that the iron chelator deferiprone (DFP) affected bacterial biofilm formation and had synergistic effects (antibacterial activity) with some antibiotic

compounds against coagulase-negative staphylococci. The potential of DFP is clearly based on its potentiation of the antibiotics action, leading to a significant biofilm reduction (Coraça-Huber et al., 2018).

Promoting Bacterial Dispersion

One promising therapeutic approach consists in targeting the EPS matrix with dispersing agents in combination with antibiotics. For instance, the α-amylase (Kalpana et al., 2012; Fleming et al., 2017) enzyme, which is produced by marine bacteria, can disrupt polysaccharide bonds. It is now used as a dispersing agent to target the polysaccharide bonds of the EPS matrix, leading to biofilm degradation *in vitro*. Other enzymes (deoxyribonuclease I, the hydrolases dispersin B and DNase) also showed EPS matrix-degrading properties (Fleming et al., 2017; Chen and Lee, 2018; Sharma and Pagedar Singh, 2018).

Some synthetic agents have been developed, such as 2-aminoimidazole for *S. aureus* biofilms (Rogers et al., 2010) and synthetic lysostaphin, an effective treatment for established biofilm infections on implanted jugular vein catheters in mice (Kokai-Kun et al., 2009).

In addition, the enzymes proteinase K and trypsin can eradicate biofilms from a variety of staphylococcal strains on inert surfaces. However, their efficacy for the elimination of established biofilms is not well known *in vivo*, thus limiting their therapeutic potential. Moreover, this strategy might lead to the release of bacteria from the biofilm into the blood circulation that could induce a strong inflammatory response or a systemic acute infection.

Cis-2-Decenoic acid (C2DA) is a fatty acid chemical messenger produced by *P. aeruginos*a that induces the dispersion of biofilms with *S. aureus* and other Gram-positive and Gram-negative bacteria (Davies and Marques, 2009). C2DA controls the initiation of biofilm formation and the dispersion of mature biofilms. C2DA can inhibit MRSA biofilm formation/growth, but cannot eradicate them (Jennings et al., 2012).

New Generation of Dressing and Grafts

Parsons et al. (2016) developed a next-generation antibiofilm carboxymethylcellulose silver-containing wound dressing (NGAD). This hydrofiber dressing was designed to disperse the wound biofilm and to enhance ionic silver antimicrobial action. The authors showed that NGAD was more efficient (biofilm disruption and removal) than other commercial dressings in a large panel of clinical isolates, including *S. aureus* and antibiotic-resistant *P. aeruginosa*. Another *in vitro* study conducted on a novel wound-dressing material based on a matrix of the polysaccharides alginate, hyaluronic acid and Chitlac-silver nanoparticles concluded that hyaluronic acid was able to stimulate the wound healing simultaneously to the silver particles allowing efficient antibacterial activity against biofilms (Tarusha et al., 2018). Pérez-Díaz et al. (2018) combined these nanoparticles with mesenchymal stem cells (MSC) that can improve wound healing due to their ability to differentiate and release growth factors. In addition to the MSC and nanoparticles, they used radiosterilized pig skin as a matrix to deliver MSC into wound beds. *In vitro* data suggested a decrease of bacterial growth and biofilm formation. Finally, Ramalingam et al. (2019) conducted a study presenting the utility of electrospun nanofiber containing a natural extract (Gymnema sylvestre) that prevented biofilm formation, inhibited both Gram-positive and Gram-negative bacteria, and enhanced human dermal fibroblasts development in an *in vitro* model.

A surfactant-based wound gel dressing described in a porcine skin explant infected with *P. aeruginosa* (PAO1) biofilm showed encouraging results. Dressing the wound with this gel reduced bacteria development and biofilm infection (Yang et al., 2017). More recently, Percival et al. (2018) highlighted the effects of a non–ionic surfactant, the Pluronic F127 used in combination with melatonin and chitosan in a wound dressing. The microspheres of Pluronic F127 enhanced chitosan properties allowing antimicrobial and antibiofilm activity against *S. aureus* (Percival et al., 2018).

A dehydrated amniotic membrane allograft was used in 22 patients with lower extremity wounds (Lullove, 2017). At week 12 after application of the human amniotic membrane, DFU were completely healed.

A randomized double-blind clinical trial showed that sucrose octasulfate significantly improves wound closure in neuroischemic DFU after 20 weeks of treatment (Edmonds et al., 2018).

Skin substitutes could be another therapeutic solution in wound healing. The Food and Drug Administration recently approved a treatment for wound care involving fish skin after a clinical trial to determine its effectiveness on burns and different wound types. Fish skin contains omega-3 fatty acids that have natural anti-inflammatory properties and can accelerate healing. An ongoing clinical trial is evaluating an extracellular matrix that binds to the cells around the wound and promotes the growth of new skin (see clinicaltrials.gov/NCT01348581).

Arenicola marina is a technology based on the finding that lack of oxygen in chronic wounds hampers healing and cell proliferation (Le Pape et al., 2018). HEMHealing® (Hemarine) provides oxygenation to the wound by including M101 hemoglobin in the dressing matrix. M101 hemoglobin is an oxygen carrier that belongs to the extra-cellular hemoglobin family and is found in the *Arenicola marina* marine worm. This hemoglobin can naturally fix oxygen from the external environment and then gradually release it in the hypoxic medium to restart the healing process. In a wound context, it could restart cell proliferation and decrease wound budding.

Skin works as an extracellular matrix that binds to the cells around the wound and promotes the growth of new skin. Epigel® (Epinova Biotech) is an innovative patch based on a highly hydrophilic, biocompatible and bioactive hydrogel scaffold that supports wound bed hydration, thus reducing healing time. Clinical trials must be done to evaluate the value of Epigel® as wound dressing.

Hwang et al. (2019) evaluated allogeneic keratinocyte grafts (weekly grafts for up to 12 weeks) in 71 patients with intractable DFUs. They reported wound healing in 78.8% of patients: 64.7% with complete healing within an average of 6.1 weeks, and 14.1% with partial healing and an average 35.5% reduction of the initial size at the end of the follow up. This treatment seems effective for

chronic and difficult-to-treat DFUs. In line with other studies [in fetal cells (Momeni et al., 2019) or epithelial cells (Lo et al., 2019)] in other wound types, this study showed the benefit of skin grafts that could represent the future management of chronic wounds. Indeed, progenitor stem cells present in these grafts can accelerate wound repair and tissue regeneration, and consequently decrease the risk of wound infection. A significant number of stem cell therapies for cutaneous wounds are currently under development (Kanji and Das, 2017).

Chronic wounds are inflammatory processes that result in the increase of proteolytic enzymes and degradation of the extracellular matrix. Two studies investigated the impact of providing a biocompatible scaffold to support the healing. They used a purified Type I collagen matrix containing polyhexamethylene biguanide on patients (n = 8 and n = 41) suffering from DFU. Their results suggested that the collagen matrix improved both wound closure and the wound bed condition (Lintzeris et al., 2018; Oropallo, 2019). Finally, a study investigated the effect of human placental tissues against *P. aeruginosa* and *S. aureus* biofilm (Mao et al., 2018). It highlighted the fact that both human cryopreserved viable amniotic membrane and cryopreserved viable umbilical tissue had antibacterial activity against multiple bacterial pathogens and demonstrated that these tissues released factors that inhibited biofilm formation of *P. aeruginosa* and *S. aureus* in an *ex vivo* porcine model. Recently, use of adipose-derived stem cell improved wound healing by promoting angiogenesis and/or vascularization, modulating immune response, and inducing epithelialization in the wound (Hassanshahi et al., 2019).

The effectiveness of 3D-printed scaffolds in chronic wounds has not yet been proven, but this seems to be a promising strategy. Sun et al. (2018) reported that 3D-printed scaffold membrane alone (n = 1 patient), and 3D-printed scaffold powder mixed with platelet-rich fibrinogen (n = 2) reduced healing time in patients with pressure ulcer and/or DFU (Sun et al., 2018). Another group developed a 3D-printed scaffold that included a drug delivery system based on the body temperature (Pushparaj and Ranganathan, 2017). Although this device has not been tested *in vivo* yet, it is the first step toward the use of 3D-printed scaffolds that incorporate the delivery of drugs (antibiotics or antibiofilm molecules) to shorten healing time and decrease the risks of infection and complication.

CONCLUSION

The severity of DFU and the difficulty in treating it has prompted researchers to take a closer look at these infections and the associated issues. Biofilms play a crucial role in DFUs and contribute to delay healing. Research now must take into account the biofilm bacterial organization in these chronic wounds in order to identify novel alternative therapeutic candidates to improve DFU management. As we described above, alternative strategies such as bacteriophages, probiotics, AMPs or antibiofilms are exciting strategies and show promising results. All these compounds could provide solutions against MDR bacteria. However, additional studies are required to understand the biofilm bacterial organization in DFU, and also the mechanisms behind each of the candidates to improve the wound healing management and thus offer new therapeutic solution for the management of DFU.

AUTHOR CONTRIBUTIONS

CP, PL, J-PL, and AS wrote the manuscript. CD-R, AP, AB-D, and SS critically reviewed the manuscript. All authors contributed to the article and approved the submitted version.

ACKNOWLEDGMENTS

AP, CD-R, AS, PL, and J-PL belong to the FHU INCh (Federation Hospitalo Universitaire Infections Chroniques, Aviesan). We thank the Nîmes University Hospital for its structural, human and financial support through the award obtained by our team during the internal call for tenders "Thématiques phares". We thank Sarah Kabani for her editing assistance.

REFERENCES

Abraham, N. M., Lamlertthon, S., Fowler, V. G., and Jefferson, K. K. (2012). Chelating agents exert distinct effects on biofilm formation in *Staphylococcus aureus* depending on strain background: role for clumping factor B. *J. Med. Microbiol.* 61, 1062–1070. doi: 10.1099/jmm.0.040758-0

Ahmadi, M., and Adibhesami, M. (2017). The effect of silver nanoparticles on wounds contaminated with *Pseudomonas aeruginosa* in mice: an experimental study. *Iran. J. Pharm. Res.* 16, 661–669.

Albac, S., Medina, M., Labrousse, D., Hayez, D., Bonnot, D., Anzala, N., et al. (2020). Efficacy of bacteriophages in a *Staphylococcus aureus* nondiabetic or diabetic foot infection murine model. *Antimicrob. Agents Chemother.* 64, e01870–19. doi: 10.1128/AAC.01870-19

Apelqvist, J., Willy, C., Fagerdahl, A. M., Fraccalvieri, M., Malmsjö, M., Piaggesi, A., et al. (2017). Negative pressure wound therapy - overview, challenges and perspectives. *J. Wound Care*. 26:3. doi: 10.12968/jowc.2017.26.Sup3.S1

Armstrong, D. G., Boulton, A. J. M., and Bus, S. A. (2017). Diabetic Foot Ulcers and Their Recurrence. *N. Engl. J. Med.* 376, 2367–2375. doi: 10.1056/NEJMra1615439

Bakker, K., Apelqvist, J., Lipsky, B. A., Van Netten, J. J., and International Working Group on the Diabetic Foot. (2016). The 2015 IWGDF guidance documents on prevention and management of foot problems in diabetes: development of an evidence-based global consensus. *Diabetes Metab. Res. Rev.* 32, 2–6. doi: 10.1002/dmrr.2694

Bala, A., Kumar, R., and Harjai, K. (2011). Inhibition of quorum sensing in *Pseudomonas aeruginosa* by azithromycin and its effectiveness in urinary tract infections. *J. Med. Microbiol.* 60, 300–306. doi: 10.1099/jmm.0.025387-0

Barki, K. G., Das, A., Dixith, S., Ghatak, P. D., Mathew-Steiner, S., Schwab, E., et al. (2019). Electric Field Based Dressing Disrupts Mixed-Species Bacterial Biofilm Infection and Restores Functional Wound Healing. *Ann. Surg.* 269, 756–766. doi: 10.1097/SLA.0000000000002504

Beyth, N., Houri-Haddad, Y., Domb, A., Khan, W., and Hazan, R. (2015). Alternative antimicrobial approach: nano-antimicrobial materials. *Evid. Based Complement. Alternat. Med.* 2015:246012. doi: 10.1155/2015/246012

Bilyayeva, O. O., Neshta, V. V., Golub, A. A., and Sams-Dodd, F. (2017). Comparative clinical study of the wound healing effects of a novel micropore particle technology: effects on wounds, venous leg ulcers, and diabetic foot ulcers. *Wounds* 29, 1–9.

Bjarnsholt, T. (2013). The role of bacterial biofilms in chronic infections. *APMIS* 136, 1–51. doi: 10.1111/apm.12099

Cahn, A., Elishuv, O., and Olshtain-Pops, K. (2014). Establishing a multidisciplinary diabetic foot team in a large tertiary hospital: a workshop. *Diabetes Metab. Res. Rev.* 30, 350–353. doi: 10.1002/dmrr.2527

Caravaggi, C., Sganzaroli, A., Galenda, P., Bassetti, M., Ferraresi, R., and Gabrielli, L. (2013). The management of the infected diabetic foot. *Curr. Diabetes Rev.* 9, 7–24.

Chatraie, M., Torkaman, G., Khani, M., Salehi, H., and Shokri, B. (2018). In vivo study of non-invasive effects of non-thermal plasma in pressure ulcer treatment. *Sci. Rep.* 8:5621. doi: 10.1038/s41598-018-24049-z

Chen, K. J., and Lee, C. K. (2018). Twofold enhanced dispersin B activity by N-terminal fusion to silver-binding peptide for biofilm eradication. *Int. J. Biol. Macromol.* 118, 419–426. doi: 10.1016/j.ijbiomac.2018.06.066

Chen, Y., Tian, L., Yang, F., Tong, W., Jia, R., Zou, Y., et al. (2019). Tannic Acid Accelerates Cutaneous Wound Healing in Rats Via Activation of the *ERK 1/2* Signaling Pathways. *Adv Wound Care* 8, 341–354. doi: 10.1089/wound.2018.0853

Cirioni, O., Giacometti, A., Ghiselli, R., Kamysz, W., Orlando, F., Mocchegiani, F., et al. (2006). Citropin 1.1-treated central venous catheters improve the efficacy of hydrophobic antibiotics in the treatment of experimental staphylococcal catheter-related infection. *Peptides* 27, 1210–1216. doi: 10.1016/j.peptides.2005.10.007

Cooley, C. R., McLain, J. M., Dupuy, S. D., Eder, A. E., Wintenberg, M., Kelly-Wintenberg, K., et al. (2020). Indirect, Non-Thermal Atmospheric Plasma Promotes Bacterial Killing in vitro and Wound Disinfection in vivo Using Monogenic and Polygenic Models of Type 2 Diabetes (Without Adverse Metabolic Complications). *Shock* 54, 681–687. doi: 10.1097/SHK.0000000000001583

Coraça-Huber, D. C., Dichtl, S., Steixner, S., Nogler, M., and Weiss, G. (2018). Iron chelation destabilizes bacterial biofilms and potentiates the antimicrobial activity of antibiotics against coagulase-negative Staphylococci. *Pathog. Dis.* 76. doi: 10.1093/femspd/fty052

Cui, H., Li, W., Li, C., Vittayapadung, S., and Lin, L. (2016). Liposome containing cinnamon oil with antibacterial activity against methicillin-resistant *Staphylococcus aureus* biofilm. *Biofouling* 32, 215–225. doi: 10.1080/08927014.2015.1134516

Davies, D. G., and Marques, C. N. (2009). A fatty acid messenger is responsible for inducing dispersion in microbial biofilms. *J. Bacteriol.* 191, 1393–1403. doi: 10.1128/JB.01214-08

de la Fuente-Núñez, C., Korolik, V., Bains, M., Nguyen, U., Breidenstein, E. B. M., Horsman, S., et al. (2012). Inhibition of bacterial biofilm formation and swarming motility by a small synthetic cationic peptide. *Antimicrob. Agents Chemother.* 56, 2696–2704. doi: 10.1128/AAC.00064-12

de la Fuente-Núñez, C., Mansour, S., Wang, Z., Jiang, L., Breidenstein, E. B. M., Eliott, M., et al. (2014). Anti-biofilm and immunomodulatory activities of peptides that inhibit biofilms formed by pathogens isolated from cystic fibrosis patients. *Antibiotics* 3, 509–526. doi: 10.3390/antibiotics3040509

Donlan, R. M., and Costerton, J. W. (2002). Biofilms: survival mechanisms of clinically relevant microorganisms. *Clin. Microbiol. Rev.* 15, 167–193. doi: 10.1128/cmr.15.2.167-193.2002

Dowd, S. E., Wolcott, R. D., Sun, Y., McKeehan, T., Smith, E., and Rhoads, D. (2008). Polymicrobial nature of chronic diabetic foot ulcer biofilm infections determined using bacterial tag encoded FLX amplicon pyrosequencing (bTEFAP). *PLoS One* 3:e3326. doi: 10.1371/journal.pone.0003326

Dumville, J. C., Lipsky, B. A., Hoey, C., Cruciani, M., Fiscon, M., and Xia, J. (2017). Topical antimicrobial agents for treating foot ulcers in people with diabetes. *Cochrane Database Syst. Rev.* 6:CD011038. doi: 10.1002/14651858.CD011038.pub2

Dutta, P., and Das, S. (2016). Mammalian antimicrobial peptides: promising therapeutic targets against infection and chronic inflammation. *Curr. Top. Med. Chem.* 16, 99–129. doi: 10.2174/1568026615666150703121819

Edmonds, M., Lázaro-Martínez, J. L., Alfayate-García, J. M., Martini, J., Petit, J. M., Rayman, G., et al. (2018). Sucrose octasulfate dressing versus control dressing in patients with neuroischaemic diabetic foot ulcers (Explorer): an international, multicentre, double-blind, randomised, controlled trial. *Lancet Diabetes Endocrinol.* 6, 186–196. doi: 10.1016/S2213-8587(17)30438-2

El-Mowafy, S. A., Shaaban, M. I., and Abd El Galil, K. H. (2014). Sodium ascorbate as a quorum sensing inhibitor of *Pseudomonas aeruginosa*. *J. Appl. Microbiol.* 117, 1388–1399. doi: 10.1111/jam.12631

Fish, R., Kutter, E., Bryan, D., Wheat, G., and Kuhi, S. (2018). Resolving digital staphylococcal osteomyelitis using bacteriophage—A case report. *Antibiotics* 7:87. doi: 10.3390/antibiotics7040087

Fleming, D., Chahin, L., and Rumbaugh, K. (2017). Glycoside hydrolases degrade polymicrobial bacterial biofilms in wounds. *Antimicrob. Agents Chemother.* 61, e01998–16. doi: 10.1128/AAC.01998-16

García-Contreras, R., Martínez-Vázquez, M., Velázquez Guadarrama, N., Villegas Pañeda, A. G., Hashimoto, T., Maeda, T., et al. (2013). Resistance to the quorum-quenching compounds brominated furanone C-30 and 5-fluorouracil in *Pseudomonas aeruginosa* clinical isolates. *Pathog. Dis.* 68, 8–11. doi: 10.1111/2049-632X.12039

Giacometti, A., Cirioni, O., Gov, Y., Ghiselli, R., Del Prete, M. S., Mocchegiani, F., et al. (2003). RNA III inhibiting peptide inhibits in vivo biofilm formation by drug-resistant *Staphylococcus aureus*. *Antimicrob. Agents Chemother.* 47, 1979–1983. doi: 10.1128/AAC.47.6.1979-1983.2003

Hamdan, S., Pastar, I., Drakulich, S., Dikici, E., Tomic-Canic, M., Deo, S., et al. (2017). Nanotechnology-driven therapeutic interventions in wound healing: potential uses and applications. *ACS Cent. Sci.* 3, 163–175. doi: 10.1021/acscentsci.6b00371

Hassanshahi, A., Hassanshahi, M., Khabbazi, S., Hosseini-Khah, Z., Peymanfar, Y., Ghalamkari, S., et al. (2019). Adipose-derived stem cells for wound healing. *J. Cell Physiol.* 234, 7903–7914. doi: 10.1002/jcp.27922

Henriksen, K., Rørbo, N., Rybtke, M. L., Martinet, M. G., Tolker-Nielsen, T., Høiby, N., et al. (2019). *P. aeruginosa* flow-cell biofilms are enhanced by repeated phage treatments but can be eradicated by phage-ciprofloxacin combination. *Pathog. Dis.* 77:ftz011. doi: 10.1093/femspd/ftz011

Henshaw, F. R., Bolton, T., Nube, V., Hood, A., Veidhoen, D., Pfrunder, L., et al. (2014). Topical application of the bee hive protectant propolis is well tolerated and improves human diabetic foot ulcer healing in a prospective feasibility study. *J. Diabetes Complications* 28, 850–857. doi: 10.1016/j.jdiacomp.2014.07.012

Hill, C., Mills, S., and Ross, R. P. (2018). Phages & antibiotic resistance: are the most abundant entities on earth ready for a comeback? *Future Microbiol.* 13, 711–726. doi: 10.2217/fmb-2017-0261

Hwang, Y. G., Lee, J. W., Park, K. H., and Han, S. H. (2019). Allogeneic keratinocyte for intractable chronic diabetic foot ulcers: a prospective observational study. *Int. Wound J.* 16, 486–491. doi: 10.1111/iwj.13061

James, G. A., Swogger, E., Wolcott, R., Pulcini, Secor, P., Sestrich, J., et al. (eds) (2008). Biofilms in chronic wounds. *Wound Repair. Regen.* 16, 37–44. doi: 10.1111/j.1524-475X.2007.00321.x

Jennings, J. A., Courtney, H. S., and Haggard, W. O. (2012). Cis-2-decenoic acid inhibits *S. aureus* growth and biofilm in vitro: a pilot study. *Clin. Orthop. Relat. Res.* 470, 2663–2670. doi: 10.1007/s11999-012-2388-2

Jiang, P., Li, J., Han, F., Duan, G., Lu, X., Gu, Y., et al. (2011). Antibiofilm activity of an exopolysaccharide from marine bacterium *Vibrio* sp. QY101. *PLoS One* 6:e18514. doi: 10.1371/journal.pone.0018514

Johani, K., Malone, M., Jensen, S. O., Dickson, H. G., Gosbell, I. B., Hu, H., et al. (2018). Evaluation of short exposure times of antimicrobial wound solutions against microbial biofilms: from in vitro to in vivo. *J. Antimicrob. Chemother.* 73, 494–502. doi: 10.1093/jac/dkx391

Jull, A. B., Cullum, N., Dumville, J. C., Westby, M. J., Deshpande, S., and Walker, N. (2015). Honey as a topical treatment for wounds. *Cochrane Database Syst. Rev.* 3:CD005083. doi: 10.1002/14651858.CD005083.pub4

Kalpana, B. J., Aarthy, S., and Pandian, S. K. (2012). Antibiofilm activity of α-amylase from *Bacillus subtilis* S8-18 against biofilm forming human bacterial pathogens. *Appl. Biochem. Biotechnol.* 167, 1778–1794. doi: 10.1007/s12010-011-9526-2

Kanji, S., and Das, H. (2017). Advances of stem cell therapeutics in cutaneous wound healing and regeneration. *Mediators Inflamm.* 2017:5217967. doi: 10.1155/2017/5217967

Khan, M. N., and Naqvi, A. H. (2006). Antiseptics, iodine, povidone iodine and traumatic wound cleansing. *J. Tissue Viability* 16, 6–10. doi: 10.1016/s0965-206x(06)64002-3

Kifelew, L. G., Warner, M. S., Morales, S., Vaughan, L., Woodman, R., Fitridge, R., et al. (2020). Efficacy of phage cocktail AB-SA01 therapy in diabetic mouse

wound infections caused by multidrug-resistant *Staphylococcus aureus*. *BMC Microbiol.* 20:204. doi: 10.1186/s12866-020-01891-8

Kim, S. G., Yoon, Y. H., Choi, J. W., Rha, K. S., and Park, Y. H. (2012). Effect of furanone on experimentally induced *Pseudomonas aeruginosa* biofilm formation: in vitro study. *Int. J. Pediatr. Otorhinolaryngol.* 76, 1575–1578. doi: 10.1016/j.ijporl.2012.07.015

Knezevic, P., Hoyle, N. S., Matsuzaki, S., and Gorski, A. (2021). Advances in phage therapy: present challenges and future perspectives. *Front. Microbiol.* 12:701898. doi: 10.3389/fmicb.2021.701898

Kokai-Kun, J. F., Chanturiya, T., and Mond, J. J. (2009). Lysostaphin eradicates established *Staphylococcus aureus* biofilms in jugular vein catheterized mice. *J. Antimicrob. Chemother.* 64, 94–100. doi: 10.1093/jac/dkp145

Koul, S., Prakash, J., Mishra, A., and Kalia, V. C. (2016). Potential Emergence of Multi-quorum Sensing Inhibitor Resistant (MQSIR) Bacteria. *Indian J. Microbiol.* 56, 1–18. doi: 10.1007/s12088-015-0558-0

Kranke, P., Bennett, M. H., Martyn-St James, M., Schnabel, A., Debus, S. E., and Weibel, S. (2015). Hyperbaric oxygen therapy for chronic wounds. *Cochrane Database Syst. Rev.* 2015:CD004123. doi: 10.1002/14651858.CD004123.pub4

Kucisec-Tepes, N. (2016). [The role of antiseptics and strategy of biofilm removal in chronic wound]. *Acta Med. Croat.* 70, 33–42.

Kwieciński, J., Eick, S., and Wójcik, K. (2009). Effects of tea tree (*Melaleuca alternifolia*) oil on *Staphylococcus aureus* in biofilms and stationary growth phase. *Int. J. Antimicrob. Agents* 33, 343–347. doi: 10.1016/j.ijantimicag.2008.08.028

Kwon, K. T., and Armstrong, D. G. (2018). Microbiology and Antimicrobial Therapy for Diabetic Foot Infections. *Infect. Chemother.* 50, 11–20. doi: 10.3947/ic.2018.50.1.11

Lacqua, A., Wanner, O., Colangelo, T., Martinotti, M. G., and Landini, P. (2006). Emergence of biofilm-forming subpopulations upon exposure of ***Escherichia coli*** to environmental bacteriophages. *Appl. **Environ**. Microbiol.* 72, 956–959. doi: 10.1128/AEM.72.1.956-959.2006

LaPlante, K. L., Sarkisian, S. A., Woodmansee, S., Rowley, D. C., and Seeram, N. P. (2012). Effects of cranberry extracts on growth and biofilm production of *Escherichia coli* and *Staphylococcus* species. *Phyther. Res.* 26, 1371–1374. doi: 10.1002/ptr.4592

Le Pape, F., Richard, G., Porchet, E., Sourice, S., Dubrana, F., Férec, C., et al. (2018). Adhesion, proliferation and osteogenic differentiation of human MSCs cultured under perfusion with a marine oxygen carrier on an allogenic bone substitute. *Artif. Cells Nanomed. Biotechnol.* 46, 95–107. doi: 10.1080/21691401.2017.1365724

Lee, R. L. P., Leung, P. H. M., and Wong, T. K. S. (2014). A randomized controlled trial of topical tea tree preparation for MRSA colonized wounds. *Int. J. Nursing Sci.* 1, 7–14. doi: 10.1016/j.ijnss.2014.01.001

Lieberman, O. J., Orr, M. W., Wang, Y., and Lee, V. T. (2014). High-Throughput screening using the differential radial capillary action of ligand assay identifies Ebselen as an inhibitor of diguanylate cyclases. *ACS Chem. Biol.* 9, 183–192. doi: 10.1021/cb400485k

Limoli, D. H., Jones, C. J., and Wozniak, D. J. (2015). Bacterial extracellular polysaccharides in biofilm formation and function. *Microbiol. Spectr.* 3, 10.1128/microbiolspec.MB-0011-2014.doi: 10.1128/microbiolspec.MB-0011-2014

Lintzeris, D., Vernon, K., Percise, H., Strickland, A., Yarrow, K., White, A., et al. (2018). Effect of a New Purified Collagen Matrix With Polyhexamethylene Biguanide on Recalcitrant Wounds of Various Etiologies: a Case Series. *Wounds* 30, 72–78.

Lipsky, B. A., Senneville, E., Abbas, Z. G., Aragón-Sánchez, J., Diggle, M., Embil, J. M., et al. (2020). Guidelines on the diagnosis and treatment of foot infection in persons with diabetes (IWGDF 2019 update). *Diabetes Metab. Res. Rev.* 36:e3280. doi: 10.1002/dmrr.3280

Liu, Z., Dumville, J. C., Hinchliffe, R. J., Cullum, N., Game, F., Stubbs, N., et al. (2018). Negative pressure wound therapy for treating foot wounds in people with diabetes mellitus. *Cochrane Database Syst. Rev.* 10:CD010318. doi: 10.1002/14651858.CD010318.pub3

Lo, C. H., Akbarzadeh, S., McLean, C., Ives, A., Paul, E., Brown, W. A., et al. (2019). Wound healing after cultured epithelial autografting in patients with massive burn injury: a cohort study. *J. Plast. Reconstr. Aesthet. Surg.* 72, 427–437. doi: 10.1016/j.bjps.2018.11.003

Lullove, E. J. (2017). Use of a dehydrated amniotic membrane allograft in the treatment of lower extremity wounds: a retrospective cohort study. *Wounds* 29, 346–351.

Maiden, M. M., Zachos, M. P., and Waters, C. M. (2019). The ionophore oxyclozanide enhances tobramycin killing of *Pseudomonas aeruginosa* biofilms by permeabilizing cells and depolarizing the membrane potential. *J. Antimicrob. Chemother.* 74, 894–906. doi: 10.1093/jac/dky545

Malone, M., Bjarnsholt, T., McBain, A. J., James, G. A., Stoodley, P., Leaper, D., et al. (2017a). The prevalence of biofilms in chronic wounds: a systematic review and meta-analysis of published data. *J. Wound Care* 26, 20–25. doi: 10.12968/jowc.2017.26.1.20

Malone, M., Johani, K., Jensen, S. O., Gosbell, I. B., Dickson, H. G., McLennan, S., et al. (2017b). Effect of cadexomer iodine on the microbial load and diversity of chronic non-healing diabetic foot ulcers complicated by biofilm in vivo. *J. Antimicrob. Chemother.* 72, 2093–2101. doi: 10.1093/jac/dkx099

Mao, Y., Sharma-Varma, A., Hoffman, T., Dhall, S., Danikovitch, A., Kohn, J., et al. (2018). The Effect of Cryopreserved Human Placental Tissues on Biofilm Formation of Wound-Associated Pathogens. *J. Funct. Biomater.* 9:3. doi: 10.3390/jfb9010003

Markakis, K., Faris, A. R., Sharaf, H., Faris, B., Rees, S., and Bowling, F. L. (2018). Local antibiotic delivery systems: current and future applications for diabetic foot infections. *Int. J. Low Extrem. Wounds* 17, 14–21. doi: 10.1177/1534734618757532

Martinotti, S., and Ranzato, E. (2015). Propolis: a new frontier for wound healing? *Burns Trauma* 3, 9. doi: 10.1186/s41038-015-0010-z

McLoone, P., Tabys, D., and Fyfe, L. (2020). Honey Combination Therapies for Skin and Wound Infections: a Systematic Review of the Literature. *Clin. Cosmet. Investig. Dermatol.* 13, 875–888. doi: 10.2147/CCID.S282143

Mendes, J. J., Leandro, C., Mottola, C., Barbosa, R., Silva, F. A., Oliveira, M., et al. (2014). In vitro design of a novel lytic bacteriophage cocktail with therapeutic potential against organisms causing diabetic foot infections. *J. Med. Microbiol.* 63, 1055–1065. doi: 10.1099/jmm.0.071753-0

Mihai, M. M., Preda, M., Lungu, J., Gestal, M. C., Popa, M. I., and Holban, A. M. (2018). Nanocoatings for Chonic wound repair modulation of microbial colonization and biofilm formation. *Int. J. Mol. Sci.* 19:1179. doi: 10.3390/ijms19041179

Minden-Birkenmaier, B., and Bowlin, G. (2018). Honey-based templates in Wound healing and tissue engineering. *Bioengineering* 5:46. doi: 10.3390/bioengineering5020046

Momeni, M., Fallah, N., Bajouri, A., Bagheri, T., Orouji, Z., Pahlevanpour, P., et al. (2019). A randomized, double-blind, phase I clinical trial of fetal cell-based skin substitutes on healing of donor sites in burn patients. *Burns* 45, 914–922. doi: 10.1016/j.burns.2018.10.016

Morozova, V. V., Vlassov, V. V., and Tikunova, N. V. (2018). Applications of bacteriophages in the treatment of localized infections in humans. *Front. Microbiol.* 9:1696. doi: 10.3389/fmicb.2018.01696

Opperman, T. J., Kwasny, S. M., Williams, J. D., Khan, A. R., Peet, N. P., Moir, D. T., et al. (2009). Aryl rhodanines specifically inhibit staphylococcal and enterococcal biofilm formation. *Antimicrob. Agents Chemother.* 53, 4357–4367. doi: 10.1128/AAC.00077-09

Orlowski, P., Zmigrodzka, M., Tomaszewska, E., Ranoszek-Soliwoda, K., Czupryn, M., Antos-Bielska, M., et al. (2018). Tannic acid-modified silver nanoparticles for wound healing: the importance of size. *Int. J. Nanomed.* 13, 991–1007. doi: 10.2147/IJN.S154797

Oropallo, A. R. (2019). Use of Native Type I Collagen Matrix Plus Polyhexamethylene Biguanide for Chronic Wound Treatment. *Plast. Reconstr. Surg. Glob. Open* 7:e2047. doi: 10.1097/GOX.0000000000002047

Ortega Morente, E., Fernández-Fuentes, M. A., Grande Burgos, M. J., Abriouel, H., Pérez Pulido, R., and Gálvez, A. (2013). Biocide tolerance in bacteria. *Int. J. Food Microbiol.* 162, 13–25. doi: 10.1016/j.ijfoodmicro.2012.12.028

Parsons, D., Meredith, K., Rowlands, V. J., Short, D., Metcalf, D. G., and Bowler, P. G. (2016). Enhanced performance and mode of action of a novel antibiofilm hydrofiber® wound dressing. *Biomed. Res. Int.* 2016:7616471. doi: 10.1155/2016/7616471

Pavlik, V., Sojka, M., Mazúrová, M., and Velebnÿ, V. (2019). Dual role of iodine, silver, chlorhexidine and octenidine as antimicrobial and antiprotease agents. *PLoS One* 14:e0211055. doi: 10.1371/journal.pone.0211055

Payne, D. E., Martin, N. R., Parzych, K. R., Rickard, A. H., Underwood, A., and Boles, B. R. (2013). Tannic acid inhibits *Staphylococcus aureus* surface colonization in an IsaA-dependent manner. *Infect. Immun.* 81, 496–504. doi: 10.1128/IAI.00877-12

Percival, S. L., Chen, R., Mayer, D., and Salisbury, A. M. (2018). Mode of action of poloxamer-based surfactants in wound care and efficacy on biofilms. *Int. Wound J.* 15, 749–755. doi: 10.1111/iwj.12922

Percival, S. L., McCarty, S. M., and Lipsky, B. (2015). Biofilms and Wounds: an Overview of the Evidence. *Adv. Wound Care* 4, 373–381. doi: 10.1089/wound.2014.0557

Pérez-Díaz, M. A., Silva-Bermudez, P., Jiménez-López, B., Martínez-López, V., Melgarejo-Ramire, Y., Brena-Molina, A., et al. (2018). Silver-pig skin nanocomposites and mesenchymal stem cells: suitable antibiofilm cellular dressings for wound healing. *J. Nanobiotechnol.* 16:2. doi: 10.1186/s12951-017-0331-0

Pihl, M., Davies, J. R., Chávez de Paz, L. E., and Svensäter, G. (2010). Differential effects of *Pseudomonas aeruginosa* on biofilm formation by different strains of *Staphylococcus epidermidis*. *FEMS Immunol. Med. Microbiol.* 59, 439–446. doi: 10.1111/j.1574-695X.2010.00697.x

Price, B. L., Lovering, A. M., Bowling, F. L., and Dobson, C. B. (2016). Development of a novel collagen wound model to simulate the activity and distribution of antimicrobials in soft tissue during diabetic foot infection. *Antimicrob. Agents Chemother.* 60, 6880–6889. doi: 10.1128/AAC.01064-16

Prompers, L., Schaper, N., Apelqvist, J., Edmonds, M., Jude, E., Mauricio, D., et al. (2008). Prediction of outcome in individuals with diabetic foot ulcers: focus on the differences between individuals with and without peripheral arterial disease. *Eurodiale Study. Diabetol.* 51, 747–755. doi: 10.1007/s00125-008-0940-0

Pushparaj, M., and Ranganathan, R. (2017). Application of 3D printing in electro-induced drug delivery based on wound temperature. *Int. Res. J. Pharm.* 8, 179–183. doi: 10.7897/2230-8407.0811238

Qu, Y., Locock, K., Verma-Gaur, J., Hay, I. D., Meagher, L., and Traven, A. (2016). Searching for new strategies against polymicrobial biofilm infections: guanylated polymethacrylates kill mixed fungal/bacterial biofilms. *J. Antimicrob. Chemother.* 71, 413–421. doi: 10.1093/jac/dkv334

Quave, C. L., Estévez-Carmona, M., Compadre, C. M., Hobby, G., Hendrickson, H., Beenken, K. E., et al. (2012). Ellagic acid derivatives from *Rubus ulmifolius* inhibit *Staphylococcus aureus* biofilm formation and improve response to antibiotics. *PLoS One* 7:e28737. doi: 10.1371/journal.pone.0028737

Raad, I. I., Fang, X., Keutgen, X. M., Jiang, Y., Sherertz, R., and Hachem, R. (2008). The role of chelators in preventing biofilm formation and catheter-related bloodstream infections. *Curr. Opin. Infect. Dis.* 21, 385–392. doi: 10.1097/QCO.0b013e32830634d8

Ramalingam, R., Dhand, C., Leung, C. M., Ong, S. T., Annamalai, S. K., Kamruddin, M., et al. (2019). Antimicrobial properties and biocompatibility of electrospun poly-ε-caprolactone fibrous mats containing Gymnema sylvestre leaf extract. *Mater. Sci. Eng. C Mater. Biol. Appl.* 98, 503–514. doi: 10.1016/j.msec.2018.12.135

Rendueles, O., Kaplan, J. B., and Ghigo, J. M. (2013). Antibiofilm polysaccharides. *Environ. Microbiol.* 15, 334–346. doi: 10.1111/j.1462-2920.2012.02810.x

Rogers, S. A., Huigens, R. W. III, Cavanagh, J., and Melander, C. (2010). Synergistic effects between conventional antibiotics and 2-aminoimidazole-derived antibiofilm agents. *Antimicrob. Agents Chemother.* 54, 2112–2118. doi: 10.1128/AAC.01418-09

Romling, U., Galperin, M. Y., and Gomelsky, M. (2013). Cyclic di-GMP: the first 25 years of a universal bacterial second messenger. *Microbiol. Mol. Biol. Rev.* 77, 1–52. doi: 10.1128/MMBR.00043-12

Santos, R., Gomes, D., Macedo, H., Barros, D., Tibéro, C., Veiga, A. S., et al. (2016). Guar gum as a new antimicrobial peptide delivery system against diabetic foot ulcers *Staphylococcus aureus* isolates. *J. Med. Microbiol.* 65, 1092–1099. doi: 10.1099/jmm.0.000329

Schwartz, J. A., Lantis, J. C. II, Gendics, C., Fuller, A. M., Payne, W., and Ochs, D. (2013). A prospective, non comparative, multicenter study to investigate the effect of cadexomer iodine on bioburden load and other wound characteristics in diabetic foot ulcers. *Int. Wound J.* 10, 193–199. doi: 10.1111/j.1742-481X.2012.01109.x

Seyed Ahmadi, S. G., Farahpour, M. R., and Hamishehkar, H. (2019). Topical application of Cinnamon verum essential oil accelerates infected wound healing process by increasing tissue antioxidant capacity and keratin biosynthesis. *Kaohsiung J. Med. Sci.* 35, 686–694. doi: 10.1002/kjm2.12120

Sharma, D., Misba, L., and Khan, A. U. (2019). Antibiotics versus biofilm: an emerging battleground in microbial communities. *Antimicrob. Resist. Infect. Control.* 8:76. doi: 10.1186/s13756-019-0533-3

Sharma, K., and Pagedar Singh, A. (2018). Antibiofilm effect of DNase against single and mixed species biofilm. *Foods* 7:E42. doi: 10.3390/foods7030042

Sheldon, A. T. (2005). Antiseptic "Resistance": real or perceived threat? *Clin. Infect. Dis.* 40, 1650–1656. doi: 10.1086/430063

Singh, S., Singh, S. K., Chowdhury, I., and Singh, R. (2017). Understanding the Mechanism of Bacterial Biofilms Resistance to Antimicrobial Agents. *Open Microbiol. J.* 11, 53–62. doi: 10.2174/1874285801711010053

Snyder, R. J., Bohn, G., Hanft, J., Harkless, L., Kim, P., Lavery, L., et al. (2017). Wound Biofilm: current Perspectives and Strategies on Biofilm Disruption and Treatments. *Wounds* 29, S1–S17.

Stewart, P. S. (2015). Antimicrobial tolerance in biofilms. *Microbiol. Spectr.* 3, 10.1128/microbiolspec.MB-0010-2014. doi: 10.1128/microbiolspec.MB-0010-2014

Sully, E. K., Malachowa, N., Elmore, B. O., Alexander, S. M., Femling, J. K., Gray, B. M., et al. (2014). Selective chemical inhibition of *agr* quorum sensing in *Staphylococcus aureus* promotes host defense with minimal impact on resistance. *PLoS Pathog.* 10:e1004174. doi: 10.1371/journal.ppat.1004174

Sun, H., Lv, H., Qiu, F., Sun, D., Gao, Y., Chen, N., et al. (2018). Clinical application of a 3D-printed scaffold in chronic wound treatment: a case series. *J. Wound Care* 27, 262–271. doi: 10.12968/jowc.2018.27.5.262

Taha, O. A., Connerton, P. L., Connerton, I. F., and El-Shibiny, A. (2018). Bacteriophage ZCKP1: a potential treatment for *Klebsiella pneumoniae* isolated from diabetic foot patients. *Front. Microbiol.* 9:2127. doi: 10.3389/fmicb.2018.02127

Tan, D., Dahl, A., and Middelboe, M. (2015). Vibriophages Differentially Influence Biofilm Formation by *Vibrio anguillarum* Strains. *Appl. Environ. Microbiol.* 81, 4489–4497. doi: 10.1128/AEM.00518-15

Tardivo, J. P., Adami, F., Correa, J. A., Pinhal, M. A., and Baptista, M. S. (2014). A clinical trial testing the efficacy of PDT in preventing amputation in diabetic patients. *Photodiagnosis Photodyn. Ther.* 11, 342–350. doi: 10.1016/j.pdpdt.2014.04.007

Tarusha, L., Paoletti, S., Travan, A., and Marsich, E. (2018). Alginate membranes loaded with hyaluronic acid and silver nanoparticles to foster tissue healing and to control bacterial contamination of non-healing wounds. *J. Mater. Sci. Mater. Med.* 29:22. doi: 10.1007/s10856-018-6027-7

Thombare, N., Jha, U., Mishra, S., and Siddiqui, M. Z. (2016). Guar gum as a promising starting material for diverse applications: a review. *Int. J. Biol. Macromol.* 88, 361–372. doi: 10.1016/j.ijbiomac.2016.04.001

Touzel, R. E., Sutton, J. M., and Wand, M. E. (2016). Establishment of a multi-species biofilm model to evaluate chlorhexidine efficacy. *J. Hosp. Infect.* 92, 154–160. doi: 10.1016/j.jhin.2015.09.013

Townsend, E. M., Sherry, L., Rajendran, R., Hansom, D., Butcher, J., MacKay, W. G., et al. (2016). Development and characterisation of a novel three-dimensional inter-kingdom wound biofilm model. *Biofouling* 32, 1259–1270. doi: 10.1080/08927014.2016.1252337

Uçkay, I., Kressmann, B., Malacarne, S., Tournanova, A., Jaafar, J., Lew, D., et al. (2018). A randomized, controlled study to investigate the efficacy and safety of a topical gentamicin-collagen sponge in combination with systemic antibiotic therapy in diabetic patients with a moderate or severe foot ulcer infection. *BMC Infect. Dis.* 18:361. doi: 10.1186/s12879-018-3253-z

Vågesjö, E., Öhnstedt, E., Mortier, A., Lofton, H., Huss, F., Proost, P., et al. (2018). Accelerated wound healing in mice by on-site production and delivery of CXCL12 by transformed lactic acid bacteria. *Proc. Natl. Acad. Sci. U. S. A.* 115, 1895–1900. doi: 10.1073/pnas.1716580115

Vuotto, C., Longo, F., and Donelli, G. (2014). Probiotics to counteract biofilm-associated infections: promising and conflicting data. *Int. J. Oral Sci.* 6, 189–194. doi: 10.1038/ijos.2014.52

Walker, M., Metcalf, D., Parsons, D., and Bowler, P. (2015). A real-life clinical evaluation of a next-generation antimicrobial dressing on acute and chronic wounds. *J. Wound Care* 24, 11–22. doi: 10.12968/jowc.2015.24.1.11

Willcox, M. D. P., Hume, E. B. H., Aliwarga, Y., Kumar, N., and Cole, N. (2008). A novel cationic-peptide coating for the prevention of microbial colonization on contact lenses. *J. Appl. Microbiol.* 105, 1817–1825. doi: 10.1111/j.1365-2672.2008.03942.x

Wolcott, R. D., Kennedy, J. P., and Dowd, S. E. (2009). Regular debridement is the main tool for maintaining a healthy wound bed in most chronic wounds. *J. Wound Care* 18, 54–56.

Wu, H., Moser, C., Wang, H. Z., Høiby, N., and Song, Z. J. (2015). Strategies for combating bacterial biofilm infections. *Int. J. Oral Sci.* 7, 1–7. doi: 10.1038/ijos.2014.65

Wu, S. C., Driver, V. R., Wrobel, J. S., and Armstrong, D. G. (2007). Foot ulcers in the diabetic patient, prevention and treatment. *Vasc. Health Risk Manag.* 3, 65–76.

Wukich, D. K., Dikis, J. W., Monaco, S. J., Strannigan, K., Suder, N. C., and Rosario, B. L. (2015). Topically applied vancomycin powder reduces the rate of surgical site infection in diabetic patients undergoing foot and ankle surgery. *Foot Ankle Int.* 36, 1017–1024. doi: 10.1177/1071100715586567

Yang, Q., Larose, C., Della Porta, A. C., Schultz, G. S., and Gibson, D. J. (2017). A surfactant-based wound dressing can reduce bacterial biofilms in a porcine skin explant model. *Int. Wound J.* 14, 408–413. doi: 10.1111/iwj.12619

Conflict of Interest: CP is the recipient of a grant from Biofilm Control (Bourse CIFRE).

The remaining authors declare that the research was conducted in the absence of any commercial or financial relationships that could be construed as a potential conflict of interest.

frontiers in Microbiology

REVIEW
published: 13 October 2021
doi: 10.3389/fmicb.2021.728585

Metagenomic and Metatranscriptomic Insight Into Oral Biofilms in Periodontitis and Related Systemic Diseases

Yi Huang[1†], Xinyuan Zhao[1†], Li Cui[1,2] and Shaohong Huang[1*]*

[1] Stomatological Hospital, Southern Medical University and Guangdong Provincial Stomatological Hospital, Guangzhou, China, [2] School of Dentistry and Jonsson Comprehensive Cancer Center, University of California, Los Angeles, Los Angeles, CA, United States

OPEN ACCESS

Edited by:
Axel Cloeckaert, Institut National de Recherche pour l'Agriculture, l'Alimentation et l'Environnement (INRAE), France

Reviewed by:
Eija Könönen, University of Turku, Finland
Gajender Aleti, University of California, San Diego, United States
Xuesong He, The Forsyth Institute, United States
Carina Maciel Silva-Boghossian, Federal University of Rio de Janeiro, Brazil

***Correspondence:**
Li Cui
zsucllj@ucla.edu
Shaohong Huang
hsh.china@tom.com

[†] These authors have contributed equally to this work

Specialty section:
This article was submitted to Infectious Agents and Disease, a section of the journal Frontiers in Microbiology

Received: *21 June 2021*
Accepted: *21 September 2021*
Published: *13 October 2021*

Citation:
Huang Y, Zhao X, Cui L and Huang S (2021) Metagenomic and Metatranscriptomic Insight Into Oral Biofilms in Periodontitis and Related Systemic Diseases. Front. Microbiol. 12:728585. doi: 10.3389/fmicb.2021.728585

The oral microbiome is one of the most complex microbial communities in the human body and is closely related to oral and systemic health. Dental plaque biofilms are the primary etiologic factor of periodontitis, which is a common chronic oral infectious disease. The interdependencies that exist among the resident microbiota constituents in dental biofilms and the interaction between pathogenic microorganisms and the host lead to the occurrence and progression of periodontitis. Therefore, accurately and comprehensively detecting periodontal organisms and dissecting their corresponding functional activity characteristics are crucial for revealing periodontitis pathogenesis. With the development of metagenomics and metatranscriptomics, the composition and structure of microbial communities as well as the overall functional characteristics of the flora can be fully profiled and revealed. In this review, we will critically examine the currently available metagenomic and metatranscriptomic evidence to bridge the gap between microbial dysbiosis and periodontitis and related systemic diseases.

Keywords: metagenomics, metatranscriptomics, periodontitis, microbial community, systemic diseases

INTRODUCTION

Periodontitis, triggered by the highly pathogenic biofilm accumulated on teeth, is a chronic inflammatory disease that progressively destroys the supporting periodontal tissues. If left untreated, this oral infectious disease can eventually lead to tooth loss. In addition, accumulating evidence has demonstrated that periodontitis is a potential risk factor for many systemic diseases, such as diabetes, cardiovascular diseases, and rheumatoid arthritis (RA) (Teles et al., 2021). Pathogenic microbes and their products in dental plaque can cause systemic inflammation and immune responses. The prevalence of periodontal diseases is high both in developed and developing countries, ranging from 20 to 50% (Nazir, 2017). In addition, severe periodontitis affects approximately 10% of the global population (Frencken et al., 2017). A survey reported that more than 40% of the U.S. population aged ≥30 years had periodontitis, and 7.8% of these individuals suffered from severe periodontitis (Eke et al., 2020). According to the 4th National Oral Health Epidemiological Survey, periodontitis is highly prevalent in Chinese adults. This issue is especially prevalent in elderly individuals aged 55–74, as 70% of them have detectable periodontal attachment

loss, and approximately 15% of them have detectable deep periodontal pockets (≥6 mm). Even among adults aged 35–44, the detection rate of periodontal attachment loss reaches 33%, which demonstrates that periodontitis has a relatively high prevalence even in young adults (Jiao et al., 2021). According to the Global Burden of Disease Study, periodontal disease is a component of the global burden of chronic diseases and therefore represents a significant public health problem (Vos et al., 2017).

It has been well established that polymicrobial biofilms play an essential role in the initiation and progression of periodontitis. However, a number of questions remain to be addressed. For instance, what are the detailed differences in genomic architecture between microbial biofilms from patients with periodontitis and those from healthy volunteers? How do changes in microbial composition drive the pathogenesis of periodontitis? Are there any special microbial features that link to systemic diseases? In recent years, the development of metagenomics and metatranscriptomics has allowed the high-throughput study of microbial communities, which might shed light on the above questions. In this review, we will critically review the currently available evidence to gain a better understanding of the links between microbial dysbiosis and periodontitis and related systemic diseases.

OVERVIEW OF METAGENOMICS AND METATRANSCRIPTOMICS

Metagenomics, the genomic analysis of all microorganisms in the environment, has utilized sequencing analysis to investigate microbial diversity, population structure, evolutionary relationships, functional activity, mutual collaboration, and the association between microorganisms and the environment (Handelsman, 2004). Via high-throughput sequencing, metagenomics is able to produce a significant quantity of sequence data, with between 120 gigabases and 1.5 terabases per run (Quince et al., 2017). The traditional microbial detection and identification approaches are mainly based on traditional culture methods, including sample preparation, broth culture, plate count, isolation of single bacterial colonies and microbial identification, and are not able to detect uncultivated microbial species. The cultivation-independent property and high sequencing efficiency of metagenomic technology make it possible to analyze the functional diversity of microbial communities, interpret the metabolic pathway compositions, explore the interaction patterns between microbes and the environment, and discover featured genes or species with specific functions (Wang and Jia, 2016).

Metatranscriptomics, emerging after metagenomics, mainly studies the gene expression profile and the *in situ* function of microbial communities (Yu et al., 2019), which also avoids the isolation and cultivation of microorganisms and effectively explores biological diversity at deeper and more intricate levels. Metatranscriptomics provides a broader perspective than metagenomics, as it can reveal details about transcriptionally active populations and contribute to exploring the gene expression pattern and functional characteristics of complex microbial communities (Stavros et al., 2016). Through combining metatranscriptomics and metagenomics, the taxonomy and function of the biological community under particular conditions can be linked together, and sophisticated in-depth related functions of the microbial community can be investigated as a whole (Aguiar-Pulido et al., 2016).

The analysis process of metagenomics and metatranscriptomics can be divided into the following four steps (shown in **Figure 1**): ① Sample collection and extraction: according to the purpose and scheme of the experiment, microbial samples are collected from the oral cavity, and DNA/RNA are extracted. ② Data acquisition: After extracting the DNA/RNA, the data are obtained by constructing a sequencing library and performing high-throughput sequencing. ③ Data processing: Quality control should be carried out on the acquired data to remove artificially added primers and low-quality sequences during the process of library construction and sequencing. Simultaneously, it is necessary to compare with the human genome sequence to filter possible human gene contaminants (Davis et al., 2018). Finally, the clean data are compared with multiple databases to determine the species composition and functional composition (Tsute et al., 2010; Escapa et al., 2018). ④ Statistical analysis: Statistical analysis is conducted based on the sample metadata to explore the potential links between oral microbiota and diseases.

The emergence of next-generation sequencing methods like 454 pyrosequencing, Illumina sequencing technology, ABI SOLiDsequencing technology, and Ion torrent technology as well as third-generation sequencing technology represented by Pacific Biosciences (PacBio) and Oxford Nanopore Technologies (ONT) have put the rapid genome sequencing on the fast track (Slatko et al., 2018). Metagenomics and metatranscriptomics have gradually opened a new chapter in the field of oral microbiology. In 2007, the National Institutes of Health (NIH) launched the Human Microbiome Project (HMP), which sequenced and analyzed microbes in 9 parts of the oral cavity of 242 healthy adults (Huttenhower et al., 2012; Methé et al., 2012). In 2008, the Forsyth Institute and King's College London Dental Institute jointly established the Human Oral Microbiome Database (HOMD), and subsequent studies have continuously enriched the database resources, which offer a significant reference for studying the role of oral microbes in health and diseases (Dewhirst et al., 2010).

The primary goal of oral microbial metagenomics is to reveal the diversity and screen the functional genes of microbial communities. Belda-Ferre et al. (2012) employed metagenomics sequencing to analyze 8 dental plaque samples from a group of individuals with good oral health, a low-activity caries group (less than 4 cavities) and a high-activity caries group (more than 8 cavities). Significant differences were observed in the microbial communities between healthy and diseased individuals at the taxonomic and functional levels. In addition, dominant bacteria such as *Streptococcus oralis*, *Streptococcus mitis,* and *Streptococcus sanguis* isolated from healthy individuals might be used as probiotics to prevent caries. By metagenomic analysis of dental plaques from individuals with periodontitis and healthy individuals, the microbial community structure was

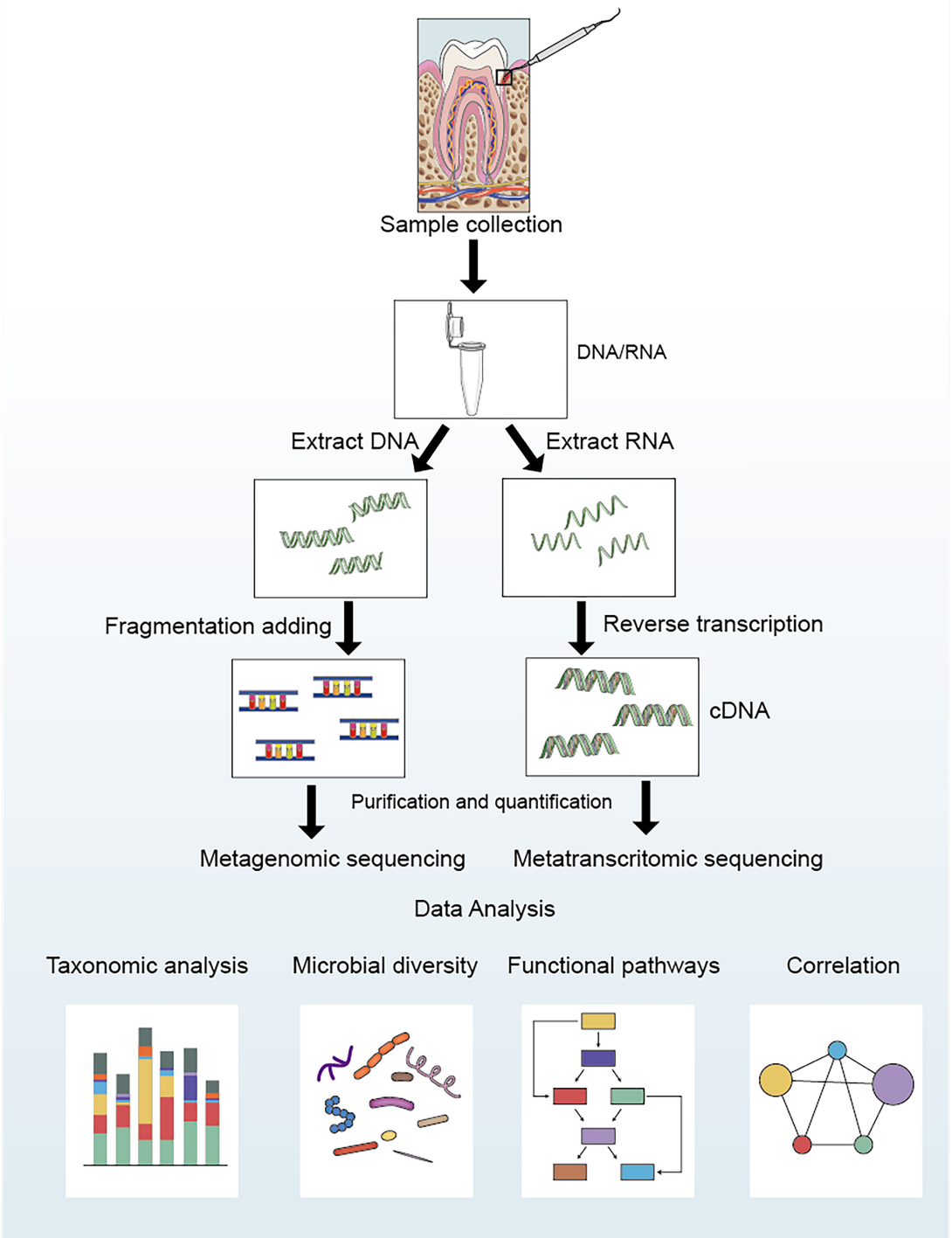

FIGURE 1 | Laboratory flow and bioinformatic analysis for metagenomic and metatranscriptomic studies of oral microbial communities.

found to be closely related to disease manifestations. Moreover, several functional genes and metabolic pathways related to bacterial chemotaxis and biosynthesis of polysaccharides were overexpressed in periodontitis, suggesting that the formation and alteration of the microbial community in the oral cavity significantly affected the pathogenesis of periodontitis (Wang et al., 2013). Similarly, dramatic difference was observed for the functional potential of the subgingival microbiome from the deep sites in generalized aggressive periodontitis, chronic periodontitis and healthy controls (Altabtbaei, 2016). Faust et al.

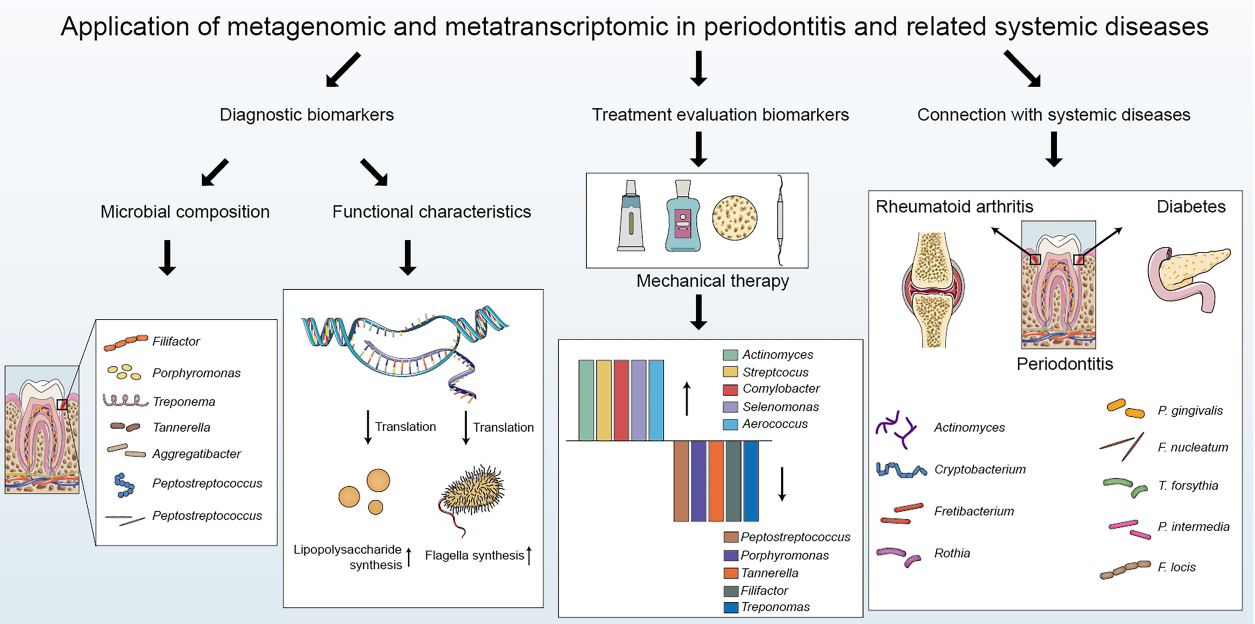

FIGURE 2 | The applications of metagenomics and metatranscriptomics in periodontitis: biomarker detection, treatment evaluation and connection with periodontitis-related systemic diseases.

analyzed the co-occurrence of microbial communities in dental plaque, vagina, gut, and other body site samples from the HMP. The results showed that a small portion of microbes, such as *Firmicutes*, built connections across multiple microbial communities and coordinated microbiota relationships, which verified the potential links between oral diseases and systemic diseases (Faust et al., 2012).

Metatranscriptomics can provide information on the interaction between the functional characteristics of the whole microbial community and diseases, reveal the relevant microbial attributes, and elucidate potential intervention targets. For example, metatranscriptomic analysis of dental caries in children revealed that the alteration of specific enzyme activities might be closely associated with the initiation and progression of caries. The expression level of alcohol dehydrogenase has been found to be increased considerably in a caries-free group, while arginine deiminase and urease levels have been shown to be higher in a dentin caries group (Kressirer et al., 2018). Belstrøm et al. (2017) compared the composition and functional activities of microbial communities in stimulated saliva samples from healthy, periodontitis, and caries individuals with metagenomics and metatranscriptomics. The results showed that the relative abundances of traditional periodontal pathogens such as *Filifactor alocis* and *Porphyromonas gingivalis* and caries-related bacteria such as *Streptococcus mutans* and *Lactobacillus fermentum* were higher in the saliva samples from the periodontitis and caries groups, respectively. In addition, lipid metabolism was found to be suppressed in the caries group, and abnormal carbohydrate metabolism was found in both the periodontitis and caries groups. In brief, the integration of multiomics might be a powerful tool to unravel the complex network of connections between microbial communities and host responses (Manoil et al., 2020).

METAGENOMICS AND METATRANSCRIPTOMICS STUDIES IN PERIODONTITIS

Relationship Between Periodontitis and Oral Microorganisms

Saliva and dental plaque can be easily obtained, and thus, they are optimal for investigating the initiation and development of periodontitis (Lasserre et al., 2018). The dynamic balance between the flora and the host is vital for maintaining oral health. Qualitative or quantitative shifts of the oral microbiome lead to microecological dysbiosis, an imbalance responsible for the development of periodontitis (Dewhirst et al., 2010). Under periodontal health circumstances, gram-positive bacteria such as *Actinomyces* and *Streptococcus* dominate the plaque biofilm, while poor oral hygiene results in a shift toward gram-negative bacteria and motile microorganisms (Ezzo and Cutler, 2003). When the microenvironment fluctuates, dysbiosis occurs in the microbial community, resulting in a reduction in species richness and loss of biodiversity (Kumar P. S., 2017). A more dysbiotic microbial community has been observed in well-maintained patients with chronic periodontitis than in healthy individuals (Lu et al., 2020). There is a bilateral impact between the microbial community and the host. An imbalanced microbial community affects the host response, resulting in an inappropriate and uncontrolled level of inflammation, which

further damages periodontal tissues (Kilian et al., 2016). The inflammatory response leads to changes in the microbiome and the expression of bacterial virulence factors (Curtis et al., 2020). Metagenomics and metatranscriptomics have provided novel insights into the oral microbiome in periodontitis and related systemic diseases (**Figure 2**).

Profiling Periodontitis-Related Pathogens With Metagenomics and Metatranscriptomics

Metagenomic and metatranscriptomic approaches enable the identification of dynamic changes in the composition and structure of the periodontal microflora (**Table 1**). Detecting the specific and robust bacterial species that cause periodontal microbiota dysbiosis is important not only for understanding the molecular mechanisms of periodontitis initiation and progression but also for providing novel targeted therapy for periodontitis. With the metagenomic method, new microbial species related to periodontitis can be discovered, and the periodontal microbial community can be comprehensively classified. Moreover, metagenomics can clarify the differences in the microbiota between healthy and diseased periodontal tissues, helping confirm dominant periodontal bacteria. By using the 16S rRNA metagenomic approach, six genera, *Filifactor*, *Porphyromonas*, *Treponema*, *Tannerella*, *Aggregatibacter*, and *Peptostreptococcus*, have been found to be significantly enriched in the subgingival plaque samples from severe chronic periodontitis patients compared to those from healthy subjects, indicating that microbial transition might play a crucial role in periodontitis pathogenesis. The metagenomic sequencing targets the entirety of the microbial genetic information, which might help gain a better understanding of the complex microbial communities in periodontal diseases (Tsai et al., 2018). A novel periodontal disease-associated bacterium named *Candidatus Bacteroides Periocalifornicus* (CPB) has been mainly detected in the deep periodontal pockets through metagenomics. It might become a candidate member of the red complex, as its relative abundance has been shown to be significantly associated with that of red complex bacteria and was involved in periodontitis-associated virulence (Torres et al., 2019). Subgingival plaque samples from healthy controls, patients with stable periodontitis and patients with progressing periodontitis have been analyzed by a shotgun metagenomic approach. The study revealed a strong correlation between the loss of oral microbial diversity and periodontitis. In addition, the abundances of *Lactobacillus gasseri* and *Olsenella uli* were increased, while *Campylobacter* was decreased in progressing periodontitis compared to those in stable periodontitis, which indicated that the altered microbial profile might be a potential marker for distinguishing the different periodontitis states (Ai et al., 2017). Shotgun metagenomic analysis of subgingival plaque from chronic periodontitis (CP), localized aggressive periodontitis (LAP) and generalized aggressive periodontitis (GAP) has revealed that genes that regulate acetate-scavenging lifestyle, utilization of alternative nutritional sources, oxidative and nitrosative stress responses, and siderophore production were unique to LAP. In addition, the virulence-associated functionalities and stress response were gradually increased from CP to GAP to LAP (Altabtbaei et al., 2021). Using the whole genome shotgun sequencing method, several overrepresented genes encoding proteins involved in fermentation, antibiotic resistance, adhesion, invasion and intracellular resistance were observed, suggesting a more effective gene-centric methodology to identify biomarkers and periodontitis predictors (Dabdoub et al., 2016). Striking differences in the composition of the subgingival microbiome have also been observed during peri-implantitis development. A total of seven discriminative predominant bacteria, *Porphyromonas gingivalis*, *Tannerella forsythia*, *Porphyromonas endodontalis*, *Fretibacterium fastidiosum*, *Prevotella intermedia*, *Fusobacterium nucleatum*, and *Treponema denticola*, have been identified in peri-implantitis by metagenomic sequencing (Ghensi et al., 2020).

Metatranscriptomics is important for determining the ecosystem function of microbial communities. In addition to clarifying the active microbial community in the disease state, metatranscriptomics also provides information on the functional characteristics of the overall microbial community to explore different functional activities in health or disease conditions. Metatranscriptomic analysis of subgingival plaque samples from patients with aggressive periodontitis has demonstrated that the composition of disease-associated communities varied considerably among patients, whereas the metabolic profiles and virulence gene expression were conserved. For example, the expression levels of genes controlling butyrate production, which promoted the development of periodontitis, increased in microbial communities from different patients, providing more profound insights into the relationship between microbe functional activities and periodontitis (Jorth et al., 2014). Through metatranscriptomic methodology, metabolic activities such as iron acquisition, lipopolysaccharide synthesis, and flagella synthesis have been found to be increased in periodontitis. Surprisingly, most virulence factors whose expression was upregulated in patients with periodontitis were from non-dominant periodontitis pathogens. These findings indicate that metatranscriptomics contributes to enhance the understanding of the core activities that represent the characteristics of periodontitis and the role of individual subgingival organisms in periodontitis (Duran-Pinedo et al., 2014). Cobalamin biosynthesis, proteolysis, and potassium transport have been found to be different in subgingival plaque samples from progressing and stable sites of periodontitis, indicating that changes in microbiome function were closely associated with periodontitis development (Yost et al., 2015).

Most of the studies described above are cross-sectional studies that focused on detecting changes in the composition of microbial communities under different conditions and revealed that microbial dysbiosis is directly related to periodontitis occurrence and development. However, additional longitudinal studies are needed to better understand the correlation between the structural composition/metabolic activities of the periodontitis-associated microbiome and disease progression. In addition, it is necessary to combine the expression profile of the host

TABLE 1 | Profiling periodontitis related pathogens with metagenomics and metatranscriptomics.

Microorganism	Sample type	Number of microbial species	Identification method	References
Filifactor; Porphyromonas; Treponema; Tannerella; Aggregatibacter; Peptostreptococcus	Subgingival plaque	6 genera	16S rRNA metagenomic approach	Tsai et al., 2018
Candidatus Bacteroides periocalifornicus	Subgingival plaque	1 new species	Metagenomic read-classification approach	Torres et al., 2019
Lactobacillus gasseri; Osenella uli; Campylobacter showae; Atopobium parvulum, etc.	Subgingival plaque	31 species in stable periodontitis and 34 species in progressing periodontitis	Shotgun metagenomic sequencing approach	Ai et al., 2017
Aggregatibacter actinomycetemcomitans; Fusobacterium nucleatum; Treponema socranskii; Porphyromonas gingivalis	Subgingival plaque	65 species in GAP 63 species in LAP	Shotgun metagenomic sequencing approach	Altabtbaei et al., 2021
Porphyromonas gingivalis; Porphyromonas endodontalis; Tannerella forsythia; Fusobacterium nucleatum; Fretibacterium fastidiosum; Treponema denticola; Prevotella intermedia, etc.	Subgingival plaque	71 species in the peri-implant microbiome	Shotgun metagenomic sequencing approach	Ghensi et al., 2020
Porphyromonas gingivalis; Filifactor alocis; Tannerella forsythia; Parvimonas micra, etc.	Subgingival plaque and saliva	32 species	Metagenomic and metatranscriptomic	Belstrøm et al., 2017
Porphyromonas; Fusobacterium; Fretibacterium; Filifactor; Parvimonas; Selenomonas; Treponema; Kingella, etc.	Subgingival plaque	NA	Whole-genome shotgun sequencing approach	Dabdoub et al., 2016
Fusobacterium nucleatum; Tannerella forsythia; Prevotella tannerae; Porphyromonas gingivalis; Prevotella intermedia	Subgingival plaque	NA	Metatranscriptomic sequencing approach	Jorth et al., 2014
Porphyromonas gingivalis; Tannerella forsythia; Treponema denticola	Subgingival plaque	NA	Metatranscriptomic sequencing approach	Duran-Pinedo et al., 2014
Tannerella forsythia; Porphyromonas gingivalis	Subgingival plaque	NA	Metatranscriptomic sequencing approach	Yost et al., 2015

with microbial community structure, which might contribute to an in-depth understanding of the interaction between the host and microbiome (Solbiati and Frias-Lopez, 2018). Furthermore, proteomics and metabolomics are promising tools for clearly reflecting the functional proteins and final metabolites produced by the microbiome under different conditions, which can accurately reveal the host responses and aid the discovery of potential robust markers at the initial stage of periodontitis.

Detecting the Alteration of Periodontitis-Related Pathogens With Metagenomics Before and After Treatment

The purpose of initial periodontal therapy is to eliminate pathogenic factors, control inflammation, and curb disease development. Multiomic analysis comparing the changes in periodontal microorganisms before and after initial periodontal therapy is conducive to evaluating therapeutic efficacy (**Table 2**). Through the metagenomic shotgun sequencing approach, Shi et al. (2015) compared the dynamic changes in the subgingival microbiota in patients with periodontitis pre- and post-periodontal treatment at the same tooth sites. The relative abundance of periodontitis pathogens and disease-associated pathways involving flagella assembly and bacterial chemotaxis were notably changed after periodontal treatment, indicating that the subgingival microbiome composition and functional activities might be potential indicators for disease diagnosis and prognosis prediction. 16S rRNA metagenomic research has been conducted for comparative analysis of subgingival plaque samples from periodontitis patients using antiadhesive hydroxyapatite toothpaste or antimicrobial and antiadhesive fluoride toothpaste following mechanical periodontal therapy. Interestingly, different kinds of toothpaste did not cause significant changes in the microbial composition, suggesting that the toothpaste ingredients had similar effects on the oral microbiota (Hagenfeld et al., 2019). Pyrosequencing of subgingival plaque samples from patients with mandibular class II buccal furcation defects following furcation therapy with enamel matrix derivative (EMD) showed that EMD treatment selectively changed the subgingival microbial composition by reducing the abundance of pathogens and increasing symbiotic flora richness (Queiroz et al., 2017). Califf et al. (2017) simultaneously used 16S rRNA sequencing and shotgun metagenomic sequencing methodologies to perform multiomic analysis on subgingival and supragingival plaque samples from participants who were requested to rinse their mouths with 0.25% sodium hypochlorite or water as controls to compare the differences in the microbial communities in the periodontal pockets. Significant changes in bacterial genera, species, and metabolites were observed before and after treatment, and metabolite richness might be a more sensitive marker for reflecting the changed periodontitis status. Multiomic approaches, including 16S rRNA sequencing, shotgun metagenomics, and metabolomics,

TABLE 2 | Detecting the alteration of periodontitis related pathogens before and after treatment with metagenomics and metatranscriptomics.

Microorganism that decreased after treatment	Microorganism that increased after treatment	Sample type	Intervention method	Identification method	References
Peptostreptococcus *Porphyromonas* *Treponema* *Tannerella* *Filifactor* *Olsenella*	*Actinomyces* *Streptococcus* *Rothia* *Bergeyella*	Subgingival plaque	Scaling and root planning (SRP) and oral hygiene instructions	Metagenomic shotgun sequencing approach	Shi et al., 2020
No noticeably different change of alpha and beta diversity before and after periodontal therapy		Buccal/lingual, interproximal, and subgingival plaque	Zinc-substituted carbonated hydroxyapatite toothpaste or amine fluoride/stannous fluoride toothpaste	16S rRNA metagenomic approach	Hagenfeld et al., 2019
Filifactor alocis *Fusobacterium nucleatum* *Actinomyces* *Porphyromonas gingivalis*	*Campylobacter* *Parvimonas* *Pseudomonas* *Selenomonas*	Furcation defects plaque	BONE group, EMD group and BONE + EMD group	Pyrosequencing approach	Queiroz et al., 2017
Porphyromonas *Treponema* *Tannerella* *Desulfovibrio*	*Streptococcus* *Aerococcus* *Slackia* *Prevotella* *Selenomonas*	Subgingingival and supragingival plaque	0.25% sodium hypochlorite rinse or water	16S rRNA amplicon sequencing and shotgun metagenomic sequencing approach	Califf et al., 2017

have shown that the relative abundance of *Porphyromonas*, *Treponema*, and *Tannerella*, as well as the levels of many metabolites, were decreased following periodontal therapy. Periodontal intervention not only affected the taxonomic composition of subgingival microbial communities but also allowed species benefiting periodontal health to recolonize the oral cavity (Zhang et al., 2020). To the best of our knowledge, very little information is currently available for the metatranscriptomic changes in the oral microbiome following periodontal treatment.

EVALUATION OF PERIODONTITIS-RELATED SYSTEMIC DISEASES WITH METAGENOMICS

In recent years, a growing number of studies have suggested that periodontal pathogens are closely related to the occurrence and development of various systemic diseases, including cardiovascular diseases, diabetes, RA, Alzheimer's disease, respiratory tract infection, and cancer (Bui et al., 2019). The association between periodontal microbial communities and periodontitis-related systemic diseases detected with metagenomics and metatranscriptomics is summarized in **Table 3**. The whole metagenomic shotgun sequencing approach has been used to analyze subgingival plaque samples from 4 groups based on the presence/absence of type 2 diabetes and moderate-to-severe periodontitis. The existence of diabetes and/or periodontitis markedly reduced the abundance and diversity of subgingival microorganisms, and an increase in *Anaerolineaceae bacterium* abundance was observed in the patients with both type 2 diabetes and periodontitis (Farina et al., 2019). Saeb et al. (2019) compared the microbial diversity and composition in normoglycemic, impaired glucose tolerance, and diabetes conditions by an ion 16S^{TM} metagenomic sequencing approach. The biological and phylogenetic diversity of oral microbial communities in patients with diabetes and prediabetes was significantly reduced compared with those in patients with normoglycemia. In addition, there was a rise in pathogenic components in the hyperglycemic microbiota. The application of the metagenomic sequencing approach to gingival sulcus biofilms from patients affected by periodontitis and type 2 diabetes revealed that the amount of *Sphingobacteriaceae* bacteria in the biofilm was significantly reduced during periodontitis, and *Sphingobacteriaceae* plays an important role in regulating the sensitivity of cells to insulin, suggesting that periodontitis might significantly affect type 2 diabetes development (Babaev et al., 2017). The metagenomic shotgun sequencing approach was performed for a longitudinal analysis of the subgingival microbiome from patients with periodontitis with/without type 2 diabetes. The results showed that patients with type 2 diabetes were more susceptible to a transformation of the subgingival microbiota to a state of dysbiosis, which might be caused by impaired host metabolism and immune regulation. In addition, a set of microbial genes were found to be enriched in the pathways associated with periodontitis and in the pathways that might connect T2DM and periodontitis. These findings might contribute to a better understanding of the two-way relationship between periodontitis and diabetes (Shi et al., 2020). Metagenomics has also revealed a specific correlation between periodontitis and RA. Significant differences have been found in the subgingival microbial structure in periodontally healthy individuals with or without RA. The relative abundance of gram-negative anaerobes in the subgingival microbial community

TABLE 3 | Evaluation of periodontitis related systemic diseases with metagenomics and metatranscriptomics.

Microorganism	Systemic diseases	Sample type	Identification method	References
Higher abundance of *Filifactor alocis* and *Treponema* sp. *OMZ 838*	Periodontitis without type 2 diabetics	Subgingival plaque	Whole metagenomic shotgun sequencing approach	Farina et al., 2019
Higher abundance of *Dialister pneumosintes*	Periodontitis with type 2 diabetics			
Rothia mucilaginosa *Prevotella melaninogenica* *Haemophilus parainfluenzae* *Streptococcus salivarius*	Diabetes	Subgingival plaque	Ion 16S^{TM} metagenomic sequencing approach	Saeb et al., 2019
Haemophilus parainfluenzae *Rothia mucilaginosa* *Prevotella melaninogenica*	Impaired glucose tolerance (IGT)			
Porphyromonas gingivalis *Tannerella forsythia* *Treponema denticola* *Fusobacterium nucleatum* *Porphyromonas endodontalis*	Periodontitis with type 2 diabetes	Gingival sulcus	16S metagenomic sequencing approach	Babaev et al., 2017
Porphyromonas gingivalis *Tannerella forsythia* *Treponema denticola*	Periodontitis without type 2 diabetes	Subgingival plaque	Metagenomic shotgun sequencing approach	Shi et al., 2020
Fusobacterium nucleatum *Campylobacter rectus* *Prevotella intermedia* *Filifactor alocis*	Periodontitis with type 2 diabetes			
Actinomyces *Cryptobacterium* *Fretibacterium* *Desulfovibrio* *Leptotrichia*	Rheumatoid arthritis (RA)	Subgingival plaque	16S rDNA sequencing approach	Lopez-Oliva et al., 2018
Rothia dentocariosa *Lactobacillus salivarius* *Atopobium* spp. *Cryptobacterium curtum*	Rheumatoid arthritis (RA)	Saliva, tooth and fecal	Metagenomic shotgun sequencing approach	Zhang et al., 2015
Lactobacillales *Streptococcaceae* *Firmicutes/Bacteroidetes*	Alzheimer's disease (AD)	Supragingival plaque	PacBio sequencing approach	Wu et al., 2021
Porphyromonas endodontalis *Eubacterium brachy* *Eubacterium saphenum* *Propionibacterium propionicum* *Parvimonas micra*	Cardiovascular disease (CVD)	Subgingival plaque	Metagenomic shotgun sequencing approach	Plachokova et al., 2021
Porphyromonas gingivalis, Fusobacterium nucleatum, *Tannerella forsythia* *Treponema denticola*	Cardiovascular disease (CVD)	Subgingival plaque	Metagenomic sequencing approach	Kumar P. K. V., 2017
High abundance of *Capnocytophaga ochracea*	HPV infection	Periodontal granulation tissue	Metagenomic sequencing approach	Chowdhry et al., 2019

has been found to be increased in RA, manifesting a state of biological disorder. Arachidonic acid and ester lipid metabolism pathways were enriched in the dental plaque biofilm of RA patients. In addition, the periodontal pathogen *Cryptobacterium curtum* identified in RA generates large amounts of citrulline and subsequently promotes the generation of citrullinated RA autoantigens, which confirms a link between periodontitis and RA (Lopez-Oliva et al., 2018). A longitudinal study investigated fecal, tooth, and salivary samples from individuals with RA and healthy controls by using metagenomic shotgun sequencing. The results revealed that the intestinal and oral microbiomes were consistent, which indicated an overlap of species abundance and function at different body parts. Moreover, the dysbiosis of the oral flora in RA patients was partially reversed after RA treatment. Functionally, the transport and metabolism of iron, sulfur, zinc, and arginine were altered in the microbiota of RA patients. These findings provide novel insights into specific alterations in the intestinal and oral microbiomes of RA patients and suggest a promising method for diagnosis and prognosis prediction based on oral microbiome

composition (Zhang et al., 2015). Metagenomic sequencing of supra-gingival dental plaque from patients with Alzheimer's disease (AD) and healthy controls demonstrated that the microbial diversity was lower in AD. In addition, the numbers of *Lactobacillales*, *Streptococcaceae*, and *Firmicutes/Bacteroidetes* were significantly increased, whereas *Fusobacterium* and Proteobacteria were significantly decreased in patients with AD, indicating that detecting the altered oral microbiota might contribute to the diagnosis of AD in the early stages (Wu et al., 2021). Periodontitis induced-systemic inflammation is a risk factor of cardiovascular disease. Metagenomic shotgun sequencing revealed that the composition of subgingival microbiome varied significantly between severe and mild periodontitis. In addition, the bacteria and metabolic pathways more abundant in severe PD was strongly associated with systemic inflammation, supporting the indirect inflammatory mechanism that the oral microbiome produces inflammatory mediators in the systemic circulation (Plachokova et al., 2021). Metagenomic sequencing of bacterial biofilms revealed that periodontal pathogens *Porphyromonas gingivalis*, *Fusobacterium nucleatum*, *Tannerella forsythia,* and *Treponema denticola* were highly correlated with cytokine IL-1β and vascular flow post sodium nitroprusside treatment, indicating the direct link between the abundance of specific periodontal pathogens and CVD (Kumar P. K. V., 2017). Metagenomic sequencing was performed to compare the microbial communities between HPV+ and HPV− CP granulation-samples. The abundance of *Capnocytophaga ochracea* was increased in HPV + CP samples, while *Porphyromonas endodontalis*, *Macellibacteroides fermentas*, *Treponema phagedenis*, and *Campylo-bacter rectus* species were overexpressed in HPV- CP samples. In addition, the changes in species richness led to activate pathways favoring carcinogenesis, indicating that these species might serve as novel biomarkers for oral cancer (Chowdhry et al., 2019). There is currently little information available on evaluating the connection between oral microbiome and periodontitis related systemic diseases with metatranscriptomics.

THE LIMITATION OF THE METAGENOMICS AND METATRANSCRIPTOMICS

The consensus findings of metagenomic and metatranscriptomic studies in periodontitis and related systemic diseases have been summarized in **Table 4**. One major shortcoming of current studies is that the sample size is small, which might significantly affect the interpretation of the impact of periodontal treatment on the periodontal microbiome composition. In addition, the study design, research object, sampling method, therapeutic strategy, and duration of follow-up are very heterogeneous. Therefore, it is still unclear whether metagenomics and metatranscriptomics are more promising than traditional clinical indicators for evaluating the effectiveness of periodontal treatment (Feres et al., 2021). Additional well-designed randomized clinical trials with longer follow-up times, combined with multiomic analysis, are warranted to confirm whether metagenomic/metatranscriptomic changes can be used as outcome indicators and contribute to personalized periodontal therapy.

TABLE 4 | Consensus findings of metagenomic and metatranscriptomic studies in periodontitis and related systemic diseases.

Identification method	Sample type	Periodontal condition	Systemic condition	Periodontal intervention	Findings	References
Metagenomic	Subgingival plaque and saliva	Periodontitis	Health	NA	Increased abundance of *Porphyromonas, Filifactor, Treponema and Tannerella*	Belstrøm et al., 2016; Dabdoub et al., 2016; Ai et al., 2017; Tsai et al., 2018; Ghensi et al., 2020
Metatranscriptomic	Subgingival plaque	Periodontitis	Health	NA	Increased abundance of *Porphyromonas gingivalis and Tannerella forsythia*	Duran-Pinedo et al., 2014; Jorth et al., 2014; Yost et al., 2015
Metagenomic	Subgingingival/ supragingival plaque	Periodontitis	Health	Non-surgical periodontal treatment	Common decreased abundance of *Porphyromonas, Treponema,* and *Tannerella,* increased abundance of *Selenomonas* after non-surgical periodontal treatment	Shi et al., 2015; Califf et al., 2017; Queiroz et al., 2017; Hagenfeld et al., 2019
Metagenomic	Subgingival and supragingival plaque, gingival sulcus and saliva	Periodontitis	Disease	NA	1) The abundance and diversity of oral microorganisms in individuals with periodontitis and systemic diseases were significantly decreased; 2) The oral microbial community in patients with systemic diseases are more likely to display a state of dysbiosis; 3) Periodontal pathogens and related metabolic pathways are strongly corelated with systemic diseases, serving as potential biomarkers.	Babaev et al., 2017; Kumar P. K. V., 2017; Lopez-Oliva et al., 2018; Chowdhry et al., 2019; Farina et al., 2019; Saeb et al., 2019; Shi et al., 2020; Zhang et al., 2020, Wu et al., 2021; Plachokova et al., 2021

MONITORING THE ONSET AND PROGRESSION OF PERIODONTITIS WITH PROTEOMICS AND METABOLOMICS

Proteomics and metabolomics are powerful tools for discovering novel and robust disease markers. In addition, the disease-specific proteins or metabolites can be effortless detected in gingival crevicular fluid (GCF), saliva and dental plaque due to their easy accessibility and availability. Therefore, proteomics and metabolomics have already shown great promise for monitoring the onset and progression of periodontitis. Proteomics analysis of saliva samples from patients with periodontitis, patients with dental caries and healthy individuals revealed that the levels of complement proteins and inflammatory mediators were increased in periodontitis and dental caries (Belstrøm et al., 2016). Similarly, the proteomics analysis showed that beta-2-glycoprotein I, α-fibrinogen, hemopexin, and plasminogen were abnormally expressed in the saliva samples from patients with periodontitis compared to the healthy controls (Orti et al., 2018). Bostanci et al. (2018) compared the protein profiles from unstimulated saliva samples of periodontitis patients, gingivitis patients and healthy subjects. The results demonstrated that metalloproteinase-9, ras-related protein-1 and actin-related protein 2/3 complex subunit 5 were significantly upregulated, while clusterin and deleted in malignant brain tumors 1 were downregulated in the periodontitis group compared to the control group. Interestingly, by comparing the proteomic profiles of pre- and post-treatment GCF samples, a robust protein signature including azurocidin, lysozyme C, myosin 9, and smooth muscle actin was built up for determining the clinical endpoints for CP (Guzman et al., 2018). Similar to proteomics, metabolomics has also been widely used for the diagnosis and prognosis prediction of periodontitis. Metabolomics analysis of GCF samples of patients with general chronic periodontitis and healthy controls indicated that the levels of citramalic acid and N-carbamylglutamate showed good performance for diagnosis of general chronic periodontitis (Pei et al., 2020). The metabolomic profiles of serum and GCF samples varied significantly between the patients with aggressive periodontitis and healthy subjects. Specifically, the levels of urea and allo-inositol were increased, while glutathione, 2,5-dihydroxybenzaldehyde, adipic acid and 2-deoxyguanosine were decreased in the serum samples from patients with aggressive periodontitis. For the GCF samples, the levels of noradrenaline, uridine, α-tocopherol, dehydroascorbic acid, xanthine, galactose, glucose-1-phosphate, and ribulose-5-phosphate were higher in patients with aggressive periodontitis, while thymidine, glutathione and ribose-5-phosphate were lower in the disease group (Chen et al., 2018). By integrating 16S rRNA metagenomic sequencing and metabolomics, many abnormally expressed metabolites were found to be positively correlated with periodontal pathogens such as *Porphyromonas, Prevotella*, and *Fusobacterium* species (Na et al., 2021). Similarly, a strong correlation was found between lipid mediators and subgingival microbiome profile, suggesting that inflammation induced by lipid mediators significantly affected the microbial composition in periodontitis (Lee et al., 2021). Metabolomics might also be used for evaluating the therapeutic efficacy. The salivary metabolomic profile of patients with generalized periodontitis was markedly altered by non-surgical periodontal therapy. Interestingly, many important metabolites returned to normal levels following treatment (Citterio et al., 2020). Interestingly, a recent multiomics study showed that the levels of hosphatidylcholines, plasmenyl-phosphatidylcholines, ceramides, and host proteins related to actin filament rearrangement were increased in the dental plaques from patients with periodontal diseases compared to the healthy controls (Overmyer et al., 2021). Therefore, efficiently integrating proteomics/metabolomics with metagenomics/metatranscriptomics might provide a more comprehensive understanding of the interaction between oral microbiome and periodontitis.

FUTURE PERSPECTIVE AND CONCLUSION

Collectively, the composition and structure of periodontal microbial communities based on different levels of periodontal microecological bacterial taxonomy as well as the functional activity characteristics can be determined with metagenomics and metatranscriptomics. In addition, exploring the potential correlation between the dynamic changes in the functional behaviors of the periodontal microbiome and the progression and outcome of periodontitis provides valuable information for developing effective prevention and treatment strategies. However, a high degree of host interference, low sensitivity in detecting low-abundance genes, and high detection cost are the limitations of metagenomics. Furthermore, metatranscriptomics is not able to detect the final metabolites of the microbial communities. Therefore, more powerful evidence-based experimental studies are needed. Combining proteomic and metabolomic analyses is vital to reflect the functional proteins and metabolites produced by the microbiome under different conditions. The integration of various microbial detection methodologies will contribute significantly to our understanding of the complex subgingival microbial community and periodontitis pathogenesis.

AUTHOR CONTRIBUTIONS

SH and LC: conceptualization and funding acquisition. YH, XZ, SH, and LC: writing–original draft and editing. All authors contributed to the article and approved the submitted version.

FUNDING

This work was supported by the National Natural Science Foundation of China (No. 81901006).

REFERENCES

Aguiar-Pulido, V., Huang, W., Suarez-Ulloa, V., Cickovski, T., Mathee, K., and Narasimhan, G. (2016). Metagenomics, Metatranscriptomics, and Metabolomics Approaches for Microbiome Analysis. *Evol Bioinform.* 12, 5–16. doi: 10.4137/EBO.S36436

Ai, D., Huang, R., Wen, J., Li, C., Zhu, J., and Xia, L. C. (2017). Integrated metagenomic data analysis demonstrates that a loss of diversity in oral microbiota is associated with periodontitis. *BMC Genomics* 18:32545. doi: 10.1186/s12864-016-3254-5

Altabtbaei, K. (2016). *Metagenomic Analysis of Periodontal Bacteria Associated With Generalized Aggressive Periodontitis*. dissertation/master's thesis. Ohio, IL: The Ohio State University.

Altabtbaei, K., Maney, P., Ganesan, S. M., Dabdoub, S. M., and Kumar, P. S. (2021). Anna Karenina and the subgingival microbiome associated with periodontitis. *Microbiome* 9:97. doi: 10.1186/s40168-021-01056-3

Babaev, E., Balmasova, I., Mkrtumyan, A., Kostryukova, S., Vakhitova, E., Ilina, E., et al. (2017). Metagenomic analysis of gingival sulcus microbiota and pathogenesis of periodontitis associated with Type 2 diabetes mellitus. *Bull. Exp. Biol. Med.* 163, 718–721. doi: 10.1007/s10517-017-3888-6

Belda-Ferre, P., Alcaraz, L. D., Cabrera-Rubio, R., Romero, H., Simon-Soro, A., Pignatelli, M., et al. (2012). The oral metagenome in health and disease. *ISME J.* 6, 46–56. doi: 10.1038/ismej.2011.85

Belstrøm, D., Constancias, F., Liu, Y., Yang, L., Drautz-Moses, D. I., Schuster, S. C., et al. (2017). Metagenomic and metatranscriptomic analysis of saliva reveals disease-associated microbiota in patients with periodontitis and dental caries. *NPJ Biofilms Microbiom.* 3, 1–8. doi: 10.1038/s41522-017-0031-4

Belstrøm, D., Jersie-Christensen, R. R., Lyon, D., Damgaard, C., Jensen, L. J., Holmstrup, P., et al. (2016). Metaproteomics of saliva identifies human protein markers specific for individuals with periodontitis and dental caries compared to orally healthy controls. *PeerJ* 4:e2433. doi: 10.7717/peerj.2433

Bostanci, N., Selevsek, N., Wolski, W., Grossmann, J., Bao, K., Wahlander, A., et al. (2018). Targeted proteomics guided by label-free quantitative proteome analysis in saliva reveal transition signatures from health to periodontal disease. *Mol. Cell Proteomics* 17, 1392–1409. doi: 10.1074/mcp.RA118.000718

Bui, F. Q., Almeida-Da-Silva, C. L. C., Huynh, B., Trinh, A., and Ojcius, D. M. (2019). Association between periodontal pathogens and systemic disease. *Biomed. J.* 42, 27–35. doi: 10.1016/j.bj.2018.12.001

Califf, K. J., Schwarzberg-Lipson, K., Garg, N., Gibbons, S. M., Caporaso, J. G., Slots, J. R., et al. (2017). Multi-omics Analysis of Periodontal Pocket Microbial Communities Pre- and Posttreatment. *mSystems* 2, 00016–00017.

Chen, H., Zhou, W., Liao, Y., Hu, S., Chen, T., and Song, Z. (2018). Analysis of metabolic profiles of generalized aggressive periodontitis. *J. Periodontal Res.* 53, 894–901. doi: 10.1111/jre.12579

Chowdhry, R., Singh, N., Sahu, D. K., Tripathi, R. K., and Kant, R. (2019). Dysbiosis and variation in predicted functions of the granulation tissue microbiome in hpv positive and negative severe chronic Periodontitis. *Biomed. Res. Int.* 2019, 1–12. doi: 10.1155/2019/8163591

Citterio, F., Romano, F., Meoni, G., Iaderosa, G., Grossi, S., Sobrero, A., et al. (2020). Changes in the salivary metabolic profile of generalized periodontitis patients after non-surgical periodontal therapy: a metabolomic analysis using nuclear magnetic resonance spectroscopy. *J. Clin. Med.* 9:3977.

Curtis, M. A., Diaz, P. I., and Van Dyke, T. E. (2020). The role of the microbiota in periodontal disease. *Periodontol* 2000, 14–25. doi: 10.1111/prd.12296

Dabdoub, S. M., Ganesan, S. M., and Kumar, P. S. (2016). Comparative metagenomics reveals taxonomically idiosyncratic yet functionally congruent communities in periodontitis. *Sci. Rep.* 6:38993. doi: 10.1038/srep38993

Davis, N. M., Proctor, D. M., Holmes, S. P., Relman, D. A., and Callahan, B. J. (2018). Simple statistical identification and removal of contaminant sequences in marker-gene and metagenomics data. *Microbiome* 6, 1–14. doi: 10.1186/s40168-018-0605-2

Dewhirst, F. E., Chen, T., Izard, J., Paster, B. J., Tanner, A. C. R., Yu, W. H., et al. (2010). The Human Oral Microbiome. *J. Bact.* 192, 5002–5017.

Duran-Pinedo, A. E., Chen, T., Teles, R., Starr, J. R., Wang, X., Krishnan, K., et al. (2014). Community-wide transcriptome of the oral microbiome in subjects with and without periodontitis. *ISME J.* 8:1659. doi: 10.1038/ismej.2014.23

Eke, P. I., Borgnakke, W. S., and Genco, R. J. (2020). Recent epidemiologic trends in periodontitis in the USA. *Periodontol* 82, 257–267.

Escapa, I. F., Chen, T., Huang, Y., Gajare, P., Dewhirst, F. E., Lemon, K. P., et al. (2018). New Insights into Human Nostril Microbiome from the Expanded Human Oral Microbiome Database (eHOMD): a Resource for the Microbiome of the Human Aerodigestive Tract. *mSystems* 3, e118–e187. doi: 10.1128/mSystems.00187-18

Ezzo, P. J., and Cutler, C. W. (2003). Microorganisms as risk indicators for periodontal disease. *Periodontol* 2000, 24–35. doi: 10.1046/j.0906-6713.2003.03203.x

Farina, R., Severi, M., Carrieri, A., Miotto, E., and Scapoli, C. (2019). Whole metagenomic shotgun sequencing of the subgingival microbiome of diabetics and non-diabetics with different periodontal conditions. *Arch. Oral Biol.* 104, 13–23. doi: 10.1016/j.archoralbio.2019.05.025

Faust, K., Sathirapongsasuti, J. F., Izard, J., Segata, N., and Huttenhower, C. (2012). Microbial Co-occurrence Relationships in the Human Microbiome. *PLoS Comput. Biol.* 8:e1002606. doi: 10.1371/journal.pcbi.1002606

Feres, M., Retamal Valdes, B., Goncalves, C., Cristina Figueiredo, L., and Teles, F. (2021). Did Omics change periodontal therapy? *Periodontol* 85, 182–209. doi: 10.1111/prd.12358

Frencken, J. E., Sharma, P., Stenhouse, L., Green, D., Laverty, D., and Dietrich, T. (2017). Global epidemiology of dental caries and severe periodontitis - a comprehensive review. *J. Clin. Periodontol* 44, S94–S105.

Ghensi, P., Manghi, P., Zolfo, M., Armanini, F., Pasolli, E., Bolzan, M., et al. (2020). Strong oral plaque microbiome signatures for dental implant diseases identified by strain-resolution metagenomics. *NPJ Biofilm Microbio.* 6, 1–12. doi: 10.1038/s41522-020-00155-7

Guzman, Y. A., Sakellari, D., Papadimitriou, K., and Floudas, C. A. (2018). High-throughput proteomic analysis of candidate biomarker changes in gingival crevicular fluid after treatment of chronic periodontitis. *J. Clin. Period.* 53, 853–860. doi: 10.1111/jre.12575

Hagenfeld, D., Prior, K., Harks, I., JockelSchneider, Y., May, T. W., Harmsen, D., et al. (2019). No differences in microbiome changes between anti-adhesive and antibacterial ingredients in toothpastes during periodontal therapy. *J. Periodon. Res.* 54, 435–443. doi: 10.1111/jre.12645

Handelsman, J. (2004). Metagenomics: Application of Genomics to Uncultured Microorganisms. *Microbiol. Mol. Biol. Rev.* 68, 669–685.

Huttenhower, C., Gevers, D., Knight, R., Abubucker, S., Badger, J. H., Chinwalla, A. T., et al. (2012). Structure, function and diversity of the healthy human microbiome. *Nature* 486:207. doi: 10.1038/nature11234

Jiao, J., Jing, W., Si, Y., Feng, X., Tai, B., Hu, D., et al. (2021). The prevalence and severity of periodontal disease in mainland china: data from the fourth national oral health survey (2015–2016). *J. Clin. Periodontol* 48, 168–179. doi: 10.1111/jcpe.13396

Jorth, P., Turner, K. H., Gumus, P., Nizam, N., Buduneli, N., and Whiteley, M. (2014). Metatranscriptomics of the human oral microbiome during health and disease. *mBio* 5:e01012. doi: 10.1128/mBio.01012-14

Kilian, M., Chapple, I., Hannig, M., Marsh, P., Meuric, V., Pedersen, A., et al. (2016). The oral microbiome–an update for oral healthcare professionals. *Br. Dent. J.* 221, 657–666. doi: 10.1038/sj.bdj.2016.865

Kressirer, C. A., Tsute, C., Kristie, L. H., Jorge, F. L., Dewhirst, F. E., Tavares, M. A., et al. (2018). Functional profiles of coronal and dentin caries in children. *J. Oral Microbiol.* 10:1495976. doi: 10.1080/20002297.2018.1495976

Kumar, P. S. (2017). From focal sepsis to periodontal medicine: a century of exploring the role of the oral microbiome in systemic disease. *J. Physiol.* 595, 465–476. doi: 10.1113/JP272427

Kumar, P. K. V. (2017). *Metagenomic Analysis Uncovers Strong Relationship between Periodontal Pathogens and Vascular Dysfunction in American Indian Population*. dissertation/master's thesis. San Diego, IL: San Diego State University.

Lasserre, J. F., Brecx, M. C., and Toma, S. (2018). Oral microbes, biofilms and their role in periodontal and peri-implant diseases. *Materials* 11:1802. doi: 10.3390/ma11101802

Lee, C. T., Li, R., Zhu, L., Tribble, G. D., and Dyke, T. (2021). Subgingival Microbiome and Specialized pro-resolving lipid mediator pathway profiles are correlated in periodontal inflammation. *Front. Immunol.* 12:691216.

Lopez-Oliva, I., Paropkari, A. D., Saraswat, S., Serban, S., Yonel, Z., Sharma, P., et al. (2018). Dysbiotic subgingival microbial communities in periodontally healthy patients with rheumatoid arthritis. *Arthritis Rheumatol.* 70, 1008–1013. doi: 10.1002/art.40485

Lu, H., He, L., Xu, J., Song, W., Feng, X., Zhao, Y., et al. (2020). Well-maintained patients with a history of periodontitis still harbor a more disbiotic microbiome than health. *J. Periodontol* 91, 1584–1594. doi: 10.1002/JPER.19-0498

Manoil, D., Al-Manei, K., and Belibasakis, G. N. (2020). A Systematic review of the root canal microbiota associated with apical periodontitis: lessons from next-generation sequencing. *Proteomics Clin. Appl.* 14, 1–17.

Methé, B. A., Nelson, K. E., Pop, M., Creasy, H. H., Giglio, M. G., Huttenhower, C., et al. (2012). A framework for human microbiome research. *Nature* 486:215. doi: 10.1038/nature11209

Na, H. S., Kim, S., Kim, S., Yu, Y., Kim, S. Y., Kim, H.-J., et al. (2021). Molecular subgroup of periodontitis revealed by integrated analysis of the microbiome and metabolome in a cross-sectional observational study. *J. Oral Microbiol.* 13:1902707. doi: 10.1080/20002297.2021.1902707

Nazir, M. A. (2017). Prevalence of periodontal disease, its association with systemic diseases and prevention. *Int. J. Health Sci.* 11:72.

Orti, V., Mertens, B., Vialaret, J., Gibert, P., Relaño-Ginés, A., Lehmann, S., et al. (2018). Data from a targeted proteomics approach to discover biomarkers in saliva for the clinical diagnosis of periodontitis. *Data Brief* 18, 294–299.

Overmyer, K. A., Rhoads, T. W., Merrill, A. E., Ye, Z., Westphall, M. S., Acharya, A., et al. (2021). Proteomics, lipidomics, metabolomics and 16S DNA sequencing of dental plaque from patients with diabetes and periodontal disease. *Mol. Cell Proteomics* 2021:100126. doi: 10.1016/j.mcpro.2021.100126

Pei, J., Li, F., Xie, Y., Liu, J., Yu, T., and Feng, X. (2020). Microbial and metabolomic analysis of gingival crevicular fluid in general chronic periodontitis patients: lessons for a predictive, preventive, and personalized medical approach. *EPMA J.* 11, 197–215. doi: 10.1007/s13167-020-00202-5

Plachokova, A. S., Andreu-Sánchez, S., Noz, M. P., Fu, J., and Riksen, N. P. (2021). Oral Microbiome in Relation to Periodontitis Severity and Systemic Inflammation. *Int. J. Mol. Sci.* 22:5876. doi: 10.3390/ijms22115876

Queiroz, L. A., Casarin, R. C., Dabdoub, S. M., Tatakis, D. N., Sallum, E. A., and Kumar, P. S. (2017). Furcation therapy with enamel matrix derivative: Effects on the subgingival microbiome. *J. Periodontol* 88, 617–625.

Quince, C., Walker, A. W., Simpson, J. T., Loman, N. J., and Segata, N. (2017). Shotgun metagenomics, from sampling to analysis. *Nat. Biotechnol.* 35, 833–844. doi: 10.1038/nbt.3935

Saeb, A. T., Al-Rubeaan, K. A., Aldosary, K., Raja, G. U., Mani, B., Abouelhoda, M., et al. (2019). Relative reduction of biological and phylogenetic diversity of the oral microbiota of diabetes and pre-diabetes patients. *Microb. Pathog.* 128, 215–229. doi: 10.1016/j.micpath.2019.01.009

Shi, B., Chang, M., Martin, J., Mitreva, M., Lux, R., Klokkevold, P., et al. (2015). Dynamic Changes in the subgingival microbiome and their potential for diagnosis and prognosis of periodontitis. *mBio* 6:e01926.

Shi, B., Lux, R., Klokkevold, P., Chang, M., Barnard, E., Haake, S., et al. (2020). The subgingival microbiome associated with periodontitis in type 2 diabetes mellitus. *ISME J.* 14, 519–530. doi: 10.1038/s41396-019-0544-3

Slatko, B. E., Gardner, A. F., and Ausubel, F. M. (2018). Overview of Next-Generation Sequencing Technologies. *Curr. Protoc. Mol. Biol.* 122:e59. doi: 10.1002/cpmb.59

Solbiati, J., and Frias-Lopez, J. (2018). Metatranscriptome of the oral microbiome in health and disease. *J. Dent. Res.* 97, 492–500. doi: 10.1177/0022034518761644

Stavros, B., Gili, Z.-S., and Eran, E. (2016). Use of Metatranscriptomics in Microbiome Research. *Bioinform. Biol. Insights* 10, 19–25. doi: 10.4137/BBI.S34610

Teles, F., Wang, Y., Hajishengallis, G., Hasturk, H., and Marchesan, J. T. (2021). Impact of systemic factors in shaping the periodontal microbiome. *Periodontol* 2021, 126–160. doi: 10.1111/prd.12356

Torres, P. J., Thompson, J., McLean, J. S., Kelley, S. T., and Edlund, A. (2019). Discovery of a novel periodontal disease-associated bacterium. *Microb. Ecol.* 77, 267–276. doi: 10.1007/s00248-018-1200-6

Tsai, C.-Y., Tang, C. Y., Tan, T.-S., Chen, K.-H., Liao, K.-H., and Liou, M.-L. (2018). Subgingival microbiota in individuals with severe chronic periodontitis. *J. Microbiol. Immunol. Infect.* 51, 226–234. doi: 10.1016/j.jmii.2016.04.007

Tsute, C., WenHan, Y., Jacques, I., V, B. O., Abirami, L., and E, D. F. (2010). The Human Oral Microbiome Database: a web accessible resource for investigating oral microbe taxonomic and genomic information. *Database* 2010, 1–10. doi: 10.1093/database/baq013

Vos, T., Abajobir, A. A., Abate, K. H., Abbafati, C., Abbas, K. M., Abd-Allah, F., et al. (2017). Global, regional, and national incidence, prevalence, and years lived with disability for 328 diseases and injuries for 195 countries, 1990–2016: a systematic analysis for the Global Burden of Disease Study 2016. *Lancet* 390, 1211–1259. doi: 10.1016/S0140-6736(17)32154-2

Wang, J., and Jia, H. (2016). Metagenome-wide association studies: fine-mining the microbiome. *Nat. Rev. Microbiol.* 14, 508–522. doi: 10.1038/nrmicro.2016.83

Wang, J., Qi, J., Zhao, H., He, S., Zhang, Y., Wei, S., et al. (2013). Metagenomic sequencing reveals microbiota and its functional potential associated with periodontal disease. *Sci. Rep.* 3:1843.

Wu, Y.-F., Lee, W.-F., Salamanca, E., Yao, W.-L., Su, J.-N., Wang, S.-Y., et al. (2021). Oral microbiota changes in elderly patients, an indicator of alzheimer's disease. *Int. J. Environ. Res. Public Health* 18:4211. doi: 10.3390/ijerph18084211

Yost, S., Duran-Pinedo, A. E., Teles, R., Krishnan, K., and Frias-Lopez, J. (2015). Functional signatures of oral dysbiosis during periodontitis progression revealed by microbial metatranscriptome analysis. *Genome Med.* 7, 1–19.

Yu, K., Yi, S., Li, B., Guo, F., Peng, X., Wang, Z., et al. (2019). An integrated meta-omics approach reveals substrates involved in synergistic interactions in a bisphenol A (BPA)-degrading microbial community. *Microbiome* 7, 1–13. doi: 10.1186/s40168-019-0634-5

Zhang, X., Zhang, D., Jia, H., Feng, Q., Wang, D., Liang, D., et al. (2015). The oral and gut microbiomes are perturbed in rheumatoid arthritis and partly normalized after treatment. *Nat. Med.* 21, 895–905. doi: 10.1038/nm.3914

Zhang, Y., Qi, Y., Lo, E. C., McGrath, C., Mei, M. L., and Dai, R. (2020). Using next-generation sequencing to detect oral microbiome change following periodontal interventions: A systematic review. *Oral Dis.* 27, 1073–1089.

Conflict of Interest: The authors declare that the research was conducted in the absence of any commercial or financial relationships that could be construed as a potential conflict of interest.

Publisher's Note: All claims expressed in this article are solely those of the authors and do not necessarily represent those of their affiliated organizations, or those of the publisher, the editors and the reviewers. Any product that may be evaluated in this article, or claim that may be made by its manufacturer, is not guaranteed or endorsed by the publisher.

frontiers in Microbiology

ORIGINAL RESEARCH
published: 15 October 2021
doi: 10.3389/fmicb.2021.750489

Biofilm Formation in Methicillin-Resistant *Staphylococcus aureus* Isolated in Cystic Fibrosis Patients Is Strain-Dependent and Differentially Influenced by Antibiotics

Agathe Boudet[1†], Pauline Sorlin[2†], Cassandra Pouget[3], Raphaël Chiron[4], Jean-Philippe Lavigne[1], Catherine Dunyach-Remy[1] and Hélène Marchandin[2]*

[1]VBIC, INSERM U1047, Université de Montpellier, Service de Microbiologie et Hygiène Hospitalière, CHU Nîmes, Nîmes, France, [2]HydroSciences Montpellier, Université de Montpellier, CNRS, IRD, Département de Microbiologie, CHU de Nîmes, Montpellier, France, [3]VBIC, INSERM U1047, Université de Montpellier, Nîmes, France, [4]HydroSciences Montpellier, Université de Montpellier, CNRS, IRD, Centre de Ressources et de Compétences de la Mucoviscidose, CHU de Montpellier, Montpellier, France

OPEN ACCESS

Edited by:
Giovanni Di Bonaventura, University of Studies G. d'Annunzio Chieti and Pescara, Italy

Reviewed by:
Barbara C. Kahl, University of Münster, Germany
Rosa Del Campo, Ramón y Cajal Institute for Health Research, Spain
Louise Frances Roddam, University of Tasmania, Australia

***Correspondence:**
Hélène Marchandin
helene.marchandin@umontpellier.fr

[†]These authors have contributed equally to this work

Specialty section:
This article was submitted to Infectious Agents and Disease, a section of the journal Frontiers in Microbiology

Received: 30 July 2021
Accepted: 22 September 2021
Published: 15 October 2021

Citation:
Boudet A, Sorlin P, Pouget C, Chiron R, Lavigne J-P, Dunyach-Remy C and Marchandin H (2021) Biofilm Formation in Methicillin-Resistant Staphylococcus aureus Isolated in Cystic Fibrosis Patients Is Strain-Dependent and Differentially Influenced by Antibiotics. Front. Microbiol. 12:750489. doi: 10.3389/fmicb.2021.750489

Cystic fibrosis (CF) is a genetic disease with lung abnormalities making patients particularly predisposed to pulmonary infections. *Staphylococcus aureus* is the most frequently identified pathogen, and multidrug-resistant strains (MRSA, methicillin-resistant *S. aureus*) have been associated with more severe lung dysfunction leading to eradication recommendations. Diverse bacterial traits and adaptive skills, including biofilm formation, may, however, make antimicrobial therapy challenging. In this context, we compared the ability of a collection of genotyped MRSA isolates from CF patients to form biofilm with and without antibiotics (ceftaroline, ceftobiprole, linezolid, trimethoprim, and rifampicin). Our study used standardized approaches not previously applied to CF MRSA, the BioFilm Ring test® (BRT®), the Antibiofilmogram®, and the BioFlux™ 200 system which were adapted for use with the artificial sputum medium (ASM) mimicking conditions more relevant to the CF lung. We included 63 strains of 10 multilocus sequence types (STs) isolated from 35 CF patients, 16 of whom had chronic colonization. The BRT® showed that 27% of the strains isolated in 37% of the patients were strong biofilm producers. The Antibiofilmogram® performed on these strains showed that broad-spectrum cephalosporins had the lowest minimum biofilm inhibitory concentrations (bMIC) on a majority of strains. A focus on four chronically colonized patients with inclusion of successively isolated strains showed that ceftaroline, ceftobiprole, and/or linezolid bMICs may remain below the resistance thresholds over time. Studying the dynamics of biofilm formation by strains isolated 3 years apart in one of these patients using BioFlux™ 200 showed that inhibition of biofilm formation was observed for up to 36 h of exposure to bMIC and ceftaroline and ceftobiprole had a significantly greater effect than linezolid. This study has brought new insights into the behavior of CF MRSA which has been little studied for its ability to form biofilm. Biofilm formation is a common characteristic of prevalent MRSA clones in CF.

Early biofilm formation was strain-dependent, even within a sample, and not only observed during chronic colonization. Ceftaroline and ceftobiprole showed a remarkable activity with a long-lasting inhibitory effect on biofilm formation and a conserved activity on certain strains adapted to the CF lung environment after years of colonization.

Keywords: cystic fibrosis, methicillin-resistance *Staphylococcus aureus* (MRSA), biofilm, antibiofilm activity, ceftaroline, ceftobiprole, linezolid

INTRODUCTION

Cystic fibrosis (CF) is a recessive genetic disease linked to a mutation in the cystic fibrosis transmembrane conductance regulator (*cftr*) gene encoding for an ion channel whose dysfunction causes thickening of the respiratory mucus in CF patients (Rowe et al., 2005). The resulting dehydrated, sticky mucus provides an ideal environment for bacterial colonization, and CF patients are therefore particularly exposed to pulmonary infections from an early age. Among the prevalent opportunistic pathogens in CF worldwide, *Staphylococcus aureus* is generally the most commonly identified microorganism (Registre français de la mucoviscidose - Bilan des données, 2019; The Cystic Fibrosis Foundation Patient Registry, 2019; Zolin et al., 2020). *S. aureus* is acquired early on in the life of CF patients, and from the age of 5 years, *S. aureus* will colonize or infect approximately 70% of children. Infections may be persistent in certain patients, and in 2018 in Europe, the prevalence of chronic *S. aureus* in CF patients was 35.68% (34.34% in children; 37.12% in adults; Zolin et al., 2020). Multidrug-resistant *S. aureus* strains, known as methicillin-resistant *S. aureus* (MRSA), are of particular concern. A degree of variation in MRSA prevalence is observed between countries for the CF population with a lower prevalence observed in Europe (e.g., 5.9% in France in 2019; Registre français de la mucoviscidose - Bilan des données, 2019) compared with the United States where the widespread distribution of community-acquired MRSA clones like the USA300 clone (Glikman et al., 2008; Goss and Muhlebach, 2011) is associated with a 25% rate of CF patients with at least one MRSA isolate in 2019 (The Cystic Fibrosis Foundation Patient Registry, 2019). In Europe, the epidemiology of circulating MRSA clones in the CF population remains largely unexplored. MRSA eradication in CF patients is currently recommended as compared with methicillin-susceptible *S. aureus* (MSSA), MRSA persists longer in the airways of these patients, resulting in more serious pulmonary dysfunction and lung damage with a greater decline in mean forced expiratory volume in 1 s (FEV1) and in greater use of antibiotics (Ren et al., 2007; Dasenbrook et al., 2008; Vanderhelst et al., 2012). However, MRSA eradication is challenging, not only due to the antimicrobial multidrug resistance patterns of the strains but also to the diverse bacterial adaptation pathways developed in the CF lung environment, including biofilm formation which represents an important barrier to eradication treatment and host defenses, thus contributing to bacterial persistence in the CF lung (Goerke and Wolz, 2010; Hirschhausen et al., 2013). Identifying antimicrobial treatments that may limit biofilm formation has become a matter of concern in the management of numerous infections, particularly those involving *S. aureus* which is a well-known pathogen causing diverse biofilm-associated infections other than those encountered in CF, such as medical device-associated and catheter-related infections, and bone infections (Miquel et al., 2016), and over the years, studies have aimed to evaluate the antibiofilm activity of various antimicrobial agents (antibiotics as well as antimicrobial peptides and natural substances). These studies underline the limitations of *in vitro* studies of bacterial biofilms, particularly the poor reproducibility of certain methods and the influence of cultivation conditions. Considering these limitations, a variety of protocols and methods for *in vitro* drug activity testing against staphylococcal biofilms has been successively introduced with the aim of standardizing protocols and improving inter-laboratory reproducibility, including microfluidics systems which more closely approximate natural biofilms (Benoit et al., 2010; Guzmán-Soto et al., 2021).

In this context, the main objective of our study was to evaluate the effects of antibiotics on the biofilm formation of MRSA isolates from CF patients. Our study focused on trimethoprim, rifampicin, and linezolid which are some of the drugs that may be used to deal with MRSA infections in CF patients (Fusco et al., 2015; Zobell et al., 2015; Akil and Muhlebach, 2018). Two broad-spectrum cephalosporins (more recently approved for the treatment of bacterial pneumonia due to MRSA), ceftaroline and ceftobiprole, were also evaluated. Our study was based on standardized approaches not previously applied to CF MRSA isolates, that is, the BioFilm Ring test® (Chavant et al., 2007; Ren et al., 2007) and the microfluidics system BioFlux™ 200 (Benoit et al., 2010) which were adapted for use with the artificial sputum medium (ASM), a mucin-containing synthetic growth medium (Sriramulu et al., 2005; Dinesh, 2010) to test MRSA biofilm formation, and antibiotic efficacy against biofilm formation in conditions more relevant to the CF lung. The BRT® is used to quickly evaluate bacterial adhesion and early biofilm formation. The BRT® has also been proposed as a tool for evaluating the capacity of antibiotics to inhibit biofilm formation through an approach called the Antibiofilmogram® (Tasse et al., 2016), also used in our study. Finally, we used the BioFlux™ 200 continuous flow system to study biofilm formation in dynamic conditions. Strains studied were clinical isolates genotyped by multi locus sequence typing (MLST)

and, for selected strains, by whole-genome sequencing (WGS). Due to the highly complex patterns of bacterial colonization in CF patients' airways, we also included strains that were co-isolated from within a sample or successively isolated from chronically colonized patients with the aim of bringing new insights into the behavior of strains adapted to the CF lung during persistent colonization.

To the best of our knowledge, studies like this have never been performed before and our study therefore provides original results on comparative biofilm formation with and without antibiotics for a collection of clinically and genetically documented MRSA from CF patients.

MATERIALS AND METHODS

Patients, Strains, and Study Design

Methicillin-resistant *S. aureus* strains included in this study were isolated from routinely sampled sputum specimens in patients attending the CF center at Montpellier University Hospital, France, and analyzed as part of their standard follow-up. Strains were recovered in 35 patients representing all patients with MRSA isolation in our center over a 9-year period. Strains had been stored at −80°C. These strains were studied for their ability to form biofilm in the presence or absence of antibiotics according to the steps presented in the flow diagram in **Figure 1**. Briefly, we first identified strains that were strong biofilm producers among a collection of clinically documented and genetically characterized CF MRSA using the BRT® and the ASM. Strong biofilm producers were then included in the evaluation of antibiotic efficacy against biofilm formation using the Antibiofilmogram® method. Selected isolates were then used to conduct: (i) a longitudinal analysis of the evolution of antibiotic efficacy on biofilm formation over time in chronically colonized patients (selection of clonal strains successively isolated in four patients) and (ii) a study of the dynamics of biofilm formation under flow in the absence and presence of antibiotics (selection of two paired strains successively isolated in a chronically colonized patient).

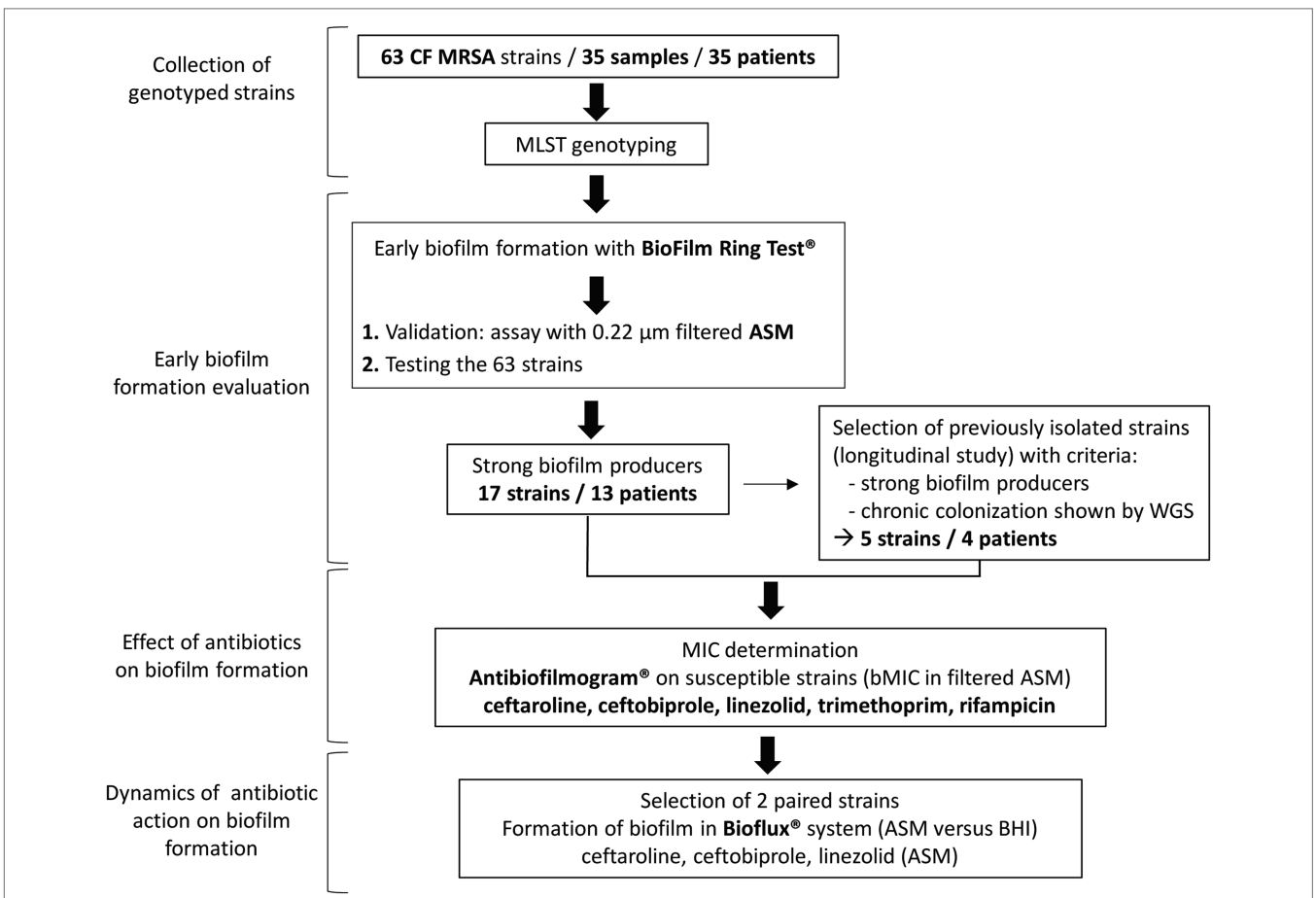

FIGURE 1 | Flowchart showing the main steps of the study. CF, cystic fibrosis; MRSA, methicillin-resistant *Staphylococcus aureus*; MLST, multilocus sequence typing; ASM, artificial sputum medium; WGS, whole-genome sequencing; MIC, minimum inhibitory concentration; bMIC, biofilm MIC; and BHI, brain heart infusion medium.

Multilocus Sequence Typing

All strains were cultured on Trypticase Soy Agar with 5% Sheep Blood (bioMérieux, Marcy l'Étoile, France), and one colony was subcultured on the same agar medium for further analysis. DNA extraction was performed as previously described (Predari et al., 1991). The amplification of the seven housekeeping genes included in the MLST scheme for *S. aureus* was performed as previously described (Enright et al., 2000; Crisóstomo et al., 2001). Sequencing was done on a 3500xL Genetic Analyser (Thermo Fisher Scientific Waltham, Massachusetts, United States), and sequence analysis was performed using SeqScape Software v3.0™ from the same company. The sequence type (ST) was determined for each strain *via* the PubMLST database (Jolley et al., 2018)[1] or after whole-genome sequencing (wgMLST).

Whole-Genome Sequence Analysis

Whole-genome sequencing analysis was performed for the 11 CF MRSA isolates (five "early" isolated strains and six "late" isolated strains in four chronically colonized patients) selected for the longitudinal analysis of the evolution of antibiotic efficacy on biofilm formation over time to prove that the MRSA persistence in these patients was truly a chronic colonization by a clonal strain. For six of these strains, WGSs were available from previous work (Boudet et al., 2021); for the five remaining strains, WGSs were obtained by an Illumina MiSeq platform (Illumina Inc., San Diego, CA, United States) and analyzed as previously described (Boudet et al., 2021). Regarding analysis of single nucleotide polymorphisms (SNPs), SNPs were called using Snippy (Seemann, 2015) and SNPs numbers were interpreted according to the criteria of Ankrum and Hall (2017) which define strains with ≤71 SNPs as the "same" strains, strains with 72–123 SNPs as "very closely related" strains, strains with 124–156 SNPs as "closely related" strains, and strains with ≥157 SNPs as "distantly related" strains.

DDBJ/ENA/GenBank accession numbers for the 11 WGS are JAGPWS000000000, JAGPWY000000000 and JAGPWZ000000000 (strains 5.1, 5.2, and 5.3 in Patient 5); JAGPWI000000000, JAGPWQ000000000 and JAGPWR000000000 (strains 6.1, 6.3, and 6.4 in Patient 6); JAHXBM000000000, JAHXBL000000000, and JAHXBK000000000 (strains 17.2, 17.3, and 17.6 in Patient 17); JAHXBJ000000000 and JAHXBI000000000 (strains 18.1 and 18.2 in Patient 18).

Culture Media and Growth Rates

After initial culture of frozen strains on Trypticase Soy Agar with 5% Sheep Blood (bioMérieux, Marcy l'Étoile, France), we used different media according to the test performed. Mueller-Hinton broth was used as the broth microdilution reference method to determine minimum inhibitory concentrations (MIC) of antibiotics. The ASM, a medium mimicking the sputum found in the respiratory tract of CF patients (Sriramulu et al., 2005; Dinesh, 2010), was used to evaluate biofilm formation and antibiotic efficacy against biofilm formation in conditions more relevant to the CF lung using the different approaches of this study and developed below: the Biofilm ring Test® (BRT®), the Antibiofilmogram®, and the continuous flow system BioFlux™ 200. However, the brain heart infusion (BHI) medium is recommended by the BRT® manufacturer and was therefore used with ASM for comparative purposes. As the opacity of the ASM did not provide a compatible image with the BRT® reading software, 0.22 µm-filtered ASM was compared to BHI medium on selected isolates with the BRT®. BHI medium was also compared with ASM in the assays conducted on the BioFlux™ system. According to the medium used for the assay, strains were pre-cultured for 24 h in the same medium, BHI broth, or ASM. Due to the use of these three culture conditions, growth properties of selected strains in BHI broth, ASM, and 0.22 µm-filtered ASM were compared. Overnight cultures at 37°C were inoculated into the same fresh medium [identical dilution factor for all three conditions to obtain a suspension of optical density (OD) at 600 nm (OD_{600}) of 0.1], and incubation was carried out at 37°C with agitation for 24 h. Cell growth was monitored over 24 h through colony-forming unit (CFU) counts with eight data points: 0, 0.5, 1, 2, 3, 4, 6, and 24 h. For CFU counts, cultures were diluted serially in the medium and plated on Trypticase Soy Agar with 5% Sheep Blood plates which were incubated for 24 h at 37°C. All assays were performed in duplicate.

Bacterial Adhesion and Biofilm Formation Assessment Using Biofilm Ring Test®

The BRT® based on the measurement of the mobility of superparamagnetic microbeads subjected to a magnetic field was used to study the early stages of biofilm formation according to the manufacturer's recommendations (Chavant et al., 2007). Briefly, standardized bacterial cultures were incubated at 37°C in 96-well microtiter plates in the presence of magnetic beads. At set time-points, the plates were placed on a magnetic block and put in the reader. The images of each well before and after magnetic attraction were analyzed with the BioFilm Control software (BFC Elements® 3), which gives a biofilm formation index (BFI). The adhesion ability of each strain was expressed as this BFI that is inversely proportional to the attached cell number. A high BFI value indicates high bead mobility under magnetic action that corresponds to the absence of biofilm formation (a spot is visible due to bead accumulation above the mini-magnet), while lower values reflect partial to complete immobilization of beads due to the bacteria embedded in a biofilm (no visible spot for complete bead immobilization). Two incubation times were defined: 1.5 and 4 h. Three replicate wells were performed per strain and per incubation time in three (BHI/filtered ASM comparison) or two independent experiments (tests in filtered ASM only). A negative control was systematically included in each experiment corresponding to the medium and beads without bacterial suspension. BFI values were calculated for each well, ranging from 0 (total bead

[1]https://pubmlst.org/saureus/

immobilization, i.e., strongly adherent cells/strong biofilm formation) to 20 (no bead aggregation, i.e., non-adherent cells/no biofilm formation in the experiment conditions).

Susceptibility Testing

Minimum inhibitory concentrations of ceftaroline, ceftobiprole, linezolid, rifampicin, and trimethoprim were determined for all CF MRSA strains using the microdilution method in Mueller-Hinton broth. According to the interpretative criteria of the European Committee on Antimicrobial Susceptibility Testing (EUCAST), strains were classified as susceptible (including "susceptible" and "susceptible, increased exposure" categories) or resistant (European Committee on Antimicrobial Susceptibility Testing, 2021). Serial 2-fold dilutions of antibiotics were as follows: 0.125–16 mg/L for ceftaroline, 0.25–32 for ceftobiprole, 0.5–64 mg/L for linezolid, 0.015–2 mg/L for rifampicin, and 0.25–32 for trimethoprim. The reference strain *S. aureus* ATCC 29213 was used to monitor test performance.

The minimum biofilm inhibitory concentrations (bMIC) were determined using the Antibiofilmogram® test (BioFilm Control; Tasse et al., 2016). A schematic representation of the Antibiofilmogram® principle is available in Olivares et al. (2020). The test was performed using 0.22 µm-filtered ASM for initial bacterial growth and suspension preparation. The microplates containing bacteria, magnetic beads, and antibiotics (20 µl of antibiotic solutions) were incubated at 37°C for 4 h before visual reading. The bMIC was determined for each antibiotic as the lowest concentration at which a spot corresponding to free beads attracted to the center of each well during magnetization, similar to negative control (0.22 µm-filtered ASM and magnetic beads), was visible. A well without antibiotics filled with the bacterial suspension in 0.22 µm-filtered ASM and magnetic beads was used as the positive control (absence of spot due to bead immobilization in biofilm). All assays were performed in duplicate.

Biofilm Formation Assessment Using the BioFlux™ 200 System

The kinetics of biofilm formation and quantification in the absence and presence of antibiotics (ceftaroline, ceftobiprole, and linezolid) were assessed with the BioFlux™ 200 microfluid system as previously described (Naudin et al., 2019) with two different media, BHI medium and ASM. In this system, biofilm formation is studied under dynamic and controlled flow conditions and is followed by light microscopy in microfluidic wells (Benoit et al., 2010). The system consists of a 48-well plate with a microchannel connection between 24 pairs of two types of wells, an input well and an output well. Bacteria were grown overnight in each media. Bacterial suspensions with an OD_{600} of 0.1 +/− 0.05 after two 200th serial dilutions from the overnight culture were prepared in both media. To quantify biofilm formation, we prepared BioFlux system by adding 500 µl of medium into the input well with a pressure of 1 dyne/cm^2 for 10 min. At the end of the 10 min, the medium remaining in the input well was removed. Bacterial suspensions were then added in the input well for 36 h of incubation at 37°C in BHI medium and ASM with a pressure of 0.2 dyne/cm^2. The bacterial suspension was either added alone or in the antibiotic solution, i.e., last dilution performed in the antibiotic solution to give final concentrations of bacteria of 10^3 CFU/ml and antibiotic corresponding to the bMIC determined by the Antibiofilmogram® either in BHI broth or in filtered ASM. Biofilms were grown in monoculture, and the quantification of biofilm formation was done at 5, 12, 24, and 36 h post-inoculation in the absence of antibiotics and at 5, 12, and 36 h post-inoculation in the presence of antibiotics. Experiments were performed in duplicate. Biofilms were visualized with a Leica DM IRB inverted fluorescence microscope coupled with a CoolSNAP FX black and white camera (Roper Scientific, Trenton NJ, United States). ImageJ® software was utilized to calculate biofilm percentage. The 16-bit grayscale images were adjusted with the threshold function to fit the bacterial structure and were analyzed using the "Analyze Particles" function to calculate biofilm percentage in the microfluidic channel.

Statistics

Results are presented as the mean ± standard deviation. Statistical analyses were made using a t test in version 7 of GraphPad Prism (comparison of biofilm formed according to the condition, either medium or incubation time, in the BioFlux™ analyses) or using a Mann-Whitney U test in version 3.5.2 of R software (comparison of BFI values in BHI medium and filtered ASM). A value of $p \leq 0.05$ was considered to reflect significance.

RESULTS

Patients and MRSA Collection Characteristics

The 35 CF patients (54.3% of female) had a mean age of 22.1 years at inclusion in the study (range: 2–52 years). Sixteen of them fulfilled the criteria for chronic colonization (>50% of respiratory samples collected during the last 12 months positive for MRSA with at least four samples collected during that period; Zolin et al., 2020). The 63 strains had been isolated between 2007 and 2016 from 35 sputum samples in these patients (2–4 colonial morphotypes visually distinct observed during the routine bacteriological analysis of sputum samples recovered from 18 samples in 18 patients were included; **Supplementary Table**). MLST genotyping showed that the 63 strains belonged to 10 STs (**Figure 2A**). MRSA of ST5 (50.8% of strains and 48.6% of patients) and ST8 (30.2% of strains and 31.4% of patients) were the most frequent representing 81% of the strains (51 strains/63) and being identified in 80% of the patients (28 patients/35). Two patients had co-colonizations with strains from different STs within the same clonal complex (CC) identified in one sample [ST5 and ST4782 (CC5) in Patient 14, ST8 and ST5829 (CC8) in Patient 33]. In these cases, both genotypes identified differed by one (strains in Patient 14) or five mutations (strains in Patient 33) in one of the seven genes of the MLST scheme (*aroE* gene and *gmk* gene, respectively).

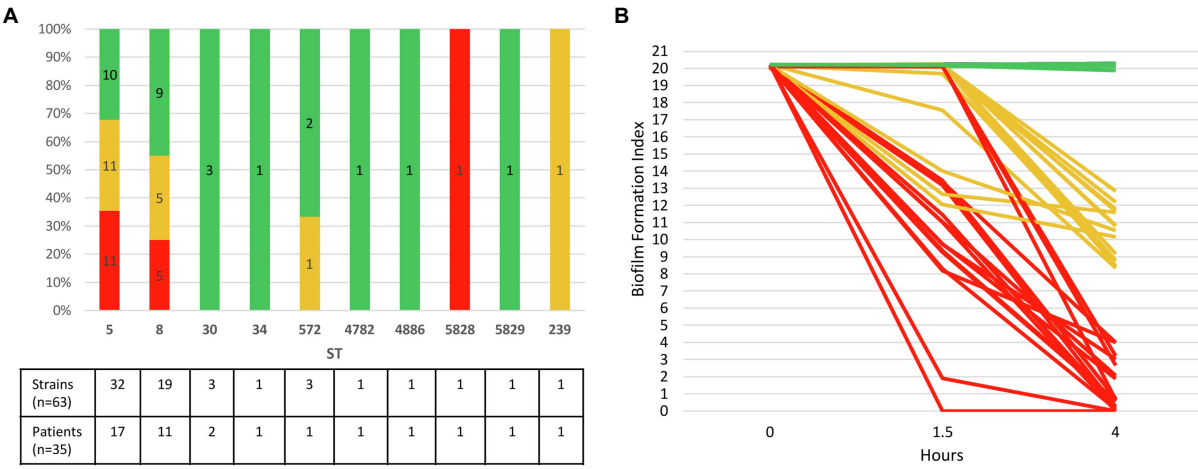

FIGURE 2 | Ability of 63 CF MRSA strains to form early biofilm according to MLST genotype. **(A)** Relative distribution of strains according to their genotype MLST (ST, sequence type) and their ability to form early biofilm as shown in **(B)**. The number of strains and patients are indicated at the bottom of the figure for each ST. **(B)** Dynamics of early biofilm formation determined using BRT® and filtered ASM after 1.5 and 4 h of incubation. Red, strains with low biofilm index (BFI) values (≤4) associated with full immobilization of the magnetic beads due to complete biofilm formation; green, non-adherent strains (BFI values: 19.9–20.3); orange, strains with intermediate BFI values (8.4–13.5).

Use of Artificial Sputum Medium to Test Bacterial Adhesion Using the Biofilm Ring Test®

Brain heart infusion medium is recommended by the BRT® manufacturer. However, the ASM containing mucin, amino acids, and free DNA was formulated to mimic the sputum of CF patients and its use is thought to be more representative of the lung conditions during CF. We therefore aimed to evaluate the use of ASM in the Biofilm Ring Test®, either to characterize the adhesion pattern and ability to form biofilm of clinical CF MRSA (BFI determination) or to perform an Antibiofilmogram® (bMIC determination). ASM is a turbid medium which yields invalid results in the BRT® but using ASM filtered through a 0.22 µM filter system made it possible for the system to calculate the BFI. To go further with the use of filtered ASM, we compared the growth ability in BHI, ASM, and filtered ASM of three selected strains that were further categorized as strong biofilm producers: strains 5.3 and 6.4 that were also used for the comparison of the BRT® use in BHI medium and ASM, and strain 17.6 that was later studied using the BioFlux™ 200 system. Similar growth rates were observed in the three media for these three strains (**Supplementary Figure 1**). We then compared both media for BRT® use by comparing BFI values measured after 4 h of incubation in BHI medium and filtered ASM for strains 5.3 and 6.4 (**Supplementary Figure 2**). Differences in adhesion patterns were observed depending on the medium used, with lower BFI values observed in filtered ASM compared with BHI medium and a significantly more pronounced adherence behavior in ASM compared with BHI medium for strain 5.3 (value of $p < 0.001$ by Mann-Whitney U test). On the whole, these observations led us to consider the use of filtered ASM for further experiments using the BRT®.

Evaluation of Early Biofilm Formation Using Biofilm Ring Test® in Filtered ASM

Biofilm formation index values evaluating the CF MRSA adhesion ability were distributed in three clearly separated groups after an incubation time of 4 h: BFI values ≤ 4, BFI values comprised between 8.37 and 13.52, and BFI values ranging from 19.87 to 20.31 (**Supplementary Table**; **Supplementary Figure 3**). We found that 27% of strains (17/63) isolated in samples from 37.1% of the patients (13/35) formed a strong biofilm after 4 h of incubation in filtered ASM (BFI < 4), including two strains of ST5 (strains 17.6 and 30.1) which were strongly adherent after 1.5 h of incubation (**Figure 2B**). Nearly all the strains (94.1%, 16/17) that were early biofilm producers belonged to ST5 and ST8. It is worth noting that intra-sample heterogeneity in the ability to form biofilm was observed, strong biofilm-producing strains being co-isolated with strains displaying distinct ability to form biofilm in samples from five patients (38.5%, 5/13). A striking example was observed for Patient 25 for whom strong biofilm producers and non-adherent strains coexisted in a sample (**Supplementary Table**). Half of chronically colonized patients (8/16) were colonized by such strains with a strong capacity for biofilm production (**Supplementary Table**). Non-adherent strains represented 44.4% of the strains and were isolated in 18 patients (BFI: 19.87–20.31, as observed for the negative control that contained filtered ASM and beads only). Finally, 28.6% of the strains, isolated from 13 patients, with intermediate BFI values (8.37–13.52), were likely slower biofilm formers, and characterization of their adhesion kinetics would have required a longer incubation time (**Supplementary Table**; **Supplementary Figure 3**).

No obvious relation was observed between the ability to form early biofilm of the MRSA strains and the co-colonizers, particularly *Pseudomonas aeruginosa*. Out of the 63 strains/35

patients of the study, 40 MRSA strains were isolated in 21 patients with chronic colonization by *P. aeruginosa*. These strains were distributed in the three groups of strains defined according to their ability to form early biofilm (13 strains showed BFI ≤ 4, 17 strains were non-adherent and 10 had intermediate BFI values).

Antimicrobial Susceptibility of the 17 Strongly Adherent Strains

Determination of the MICs of the five antibiotics under consideration in this study showed that 11 strains (64.7%) were resistant to rifampicin, and three strains (17.6%) were resistant to linezolid, while the 17 strains were susceptible to trimethoprim, ceftobiprole, and ceftaroline (**Table 1**). bMICs were then determined using the Antibiofilmogram® approach in filtered ASM. Highly distinct patterns of bMICs were observed according to the antimicrobial agent (**Table 1**). No strains displayed bMIC for trimethoprim below the EUCAST threshold for resistance at 4 mg/L (bMIC range: 8– > 32 mg/L) showing that this antibiotic was totally inefficient on biofilm formation initiation. The lowest bMICs were observed for ceftaroline and ceftobiprole with efficacy in preventing biofilm formation observed for 76.5 and 70.6% of strains, respectively (bMICs below the respective resistance breakpoint of 1 and 2 mg/L) compared with linezolid (64.7% of strains with bMICs ≤ 4 mg/L) and rifampicin (17.6% of strains with bMICs ≤ 0.5 mg/L). Individual results for each of the 17 strains under evaluation are presented in **Table 2**. The capacity of rifampicin and linezolid to prevent biofilm installation was also evaluated for the sole strains that were susceptible in planktonic cultures; linezolid was able to inhibit biofilm formation of 78.6% of the susceptible strains (three out of 14) and rifampicin prevented biofilm installation of 50% of the susceptible strains (three out of six; **Table 2**).

For three strains (strains 1.1, 5.3, and 20.1), bMICs of all the five antibiotics were above the corresponding resistance breakpoint and these strains were excluded from further analysis conducted to compare the efficacy of the various antimicrobial agents on biofilm formation by CF MRSA. Analysis was, thus, restricted to susceptible strains (planktonic cultures) that displayed at least one bMIC below the threshold for resistance ($n = 14$; **Table 2**). Under these conditions, bMICs for ceftaroline were below the resistance threshold for 13 strains, bMICs for ceftobiprole were below the resistance threshold for 12 strains, and bMICs for linezolid were below the resistance threshold for 11 strains. A limited effect was observed for rifampicin with three strains out of 14, isolated from three patients, showing low bMIC values < 0.015 mg/L. However for two patients, these strains were associated either with a resistant strain (Patient 28) or with a strain for which the formation of biofilm was not inhibited by rifampicin (Patient 25) thereby making the drug of low interest considering its global effect on biofilm formation inhibition. More generally, intra-sample heterogeneity with coexistence of adaptive variants displaying distinct bMICs was observed for three out of the four patients for whom the analysis of multiple strains from a sample was performed (Patients 5, 25, and 28; **Table 2**).

Study of Clonally-Related, Longitudinally-Isolated Strains in Four Patients

For chronically colonized patients, we searched for strains that had been isolated before the strains studied above, which met the following criteria: (i) strongly adherent strains/strains forming early biofilm as determined by the BRT® in filtered ASM (BFI ≤ 4), and (ii) WGS-based analysis confirming the chronic colonization based on the identification of less than 123 SNPs between the sequences of the "early" and the "late" isolated strains (signing either a "same" strain or "very closely related" strains according to the criteria of Ankrum and Hall, 2017). A total of five earlier-isolated strains from four patients matching these criteria were selected and compared with six strains isolated during patient follow-up. The characteristics of patients and selected strains are presented in **Figure 3A**. MICs were determined, and an Antibiofilmogram® was performed on these strains (as described above), and bMICs are presented in **Figure 3B**. MIC and bMIC values for the five antibiotics were all below the EUCAST threshold for susceptibility for the five strains isolated earlier. For later-isolated strains that remained susceptible to antimicrobial agents in planktonic culture, we showed that ceftaroline and ceftobiprole (Patients 5 and 6) or linezolid (Patients 17 and 18)

TABLE 1 | Overall susceptibility results for the 17 CF MRSA strains that were classified as strongly adherent/strong biofilm producers according to the Biofilm Ring Test® assay.

Antimicrobial agent	Minimal inhibitory concentration (MIC in mg/L)				Minimal biofilm inhibitory concentration (bMIC in mg/L)			
	Range	MIC_{50}	MIC_{90}	Resistant (%, *n*)	Range	$bMIC_{50}$	$bMIC_{90}$	Above the threshold for resistance (%, *n*)
Ceftaroline	<0.125–0.25	0.125	0.25	0	<0.125–4	0.25	4	23.5 (*4*)
Ceftobiprole	<0.25	<0.25	<0.25	0	<0.25–16	2	8	29.4 (*5*)
Linezolid	<0.5–32	1	16	17.6 (*3*)	<0.5–>64	2	>64	35.3 (*6*)
Rifampicin	<0.015–2	2	2	64.7 (*11*)	<0.015–>2	>2	>2	82.4 (*14*)
Trimethoprim	<0.25–2	0.5	2	0	8–>32	>32	>32	100 (*17*)

European Committee on Antimicrobial Susceptibility Testing (EUCAST) breakpoints for resistance were as follows: ceftaroline, 1 mg/L; ceftobiprole, 2 mg/L; linezolid, 4 mg/L; trimethoprim, 4 mg/L, and rifampicin, 0.5 mg/L.

TABLE 2 | Detailed susceptibility results for the 17 CF MRSA strains that were classified as strongly adherent/strong biofilm producers according to the Biofilm Ring Test® assay.

Patient	Strain	ST	BFI	Ceftaroline		Ceftobiprole		Linezolid		Rifampicin		Trimethoprim	
				MIC	bMIC	MIC	bMIC	MIC	bMIC	MIC	bMIC	MIC	bMIC
1	1.1	8	4	<0.125	2	<0.25	16	<0.5	16	2	>2	1	>32
5	5.2	5	0.12	<0.125	<0.125	<0.25	<0.25	32	>64	2	>2	0.5	>32
	5.3	5	0.75	<0.125	4	<0.25	8	16	32	2	>2	1	>32
6	6.3	5	0.58	<0.125	0.25	<0.25	2	1	16	2	>2	1	>32
	6.4	5	0.25	0.25	0.25	<0.25	<0.25	16	>64	2	1	1	>32
7	7.2	5	0.71	0.25	0.25	<0.25	2	<0.5	2	0.5	>2	0.5	8
17	17.6	5	0	<0.125	4	<0.25	4	<0.5	2	2	>2	0.5	>32
18	18.2	8	3.03	<0.125	0.5	<0.25	2	1	1	2	>2	1	8
20	20.1	5828	0.66	<0.125	4	<0.25	4	1	64	2	>2	2	>32
25	25.5	5	4	0.25	0.25	<0.25	<0.25	2	2	<0.015	<0.015	2	32
	25.6	5	3.22	<0.125	0.25	<0.25	8	4	4	<0.015	>2	0.5	>32
26	26.1	8	2.08	<0.125	<0.125	<0.25	2	<0.5	2	<0.015	0.015	<0.25	>32
28	28.3	5	0	<0.125	1	<0.25	2	<0.5	<0.5	2	>2	<0.25	>32
	28.4	5	0.25	<0.125	<0.125	<0.25	<0.25	<0.5	1	<0.015	<0.015	<0.25	8
30	30.1	5	0	<0.125	<0.125	<0.25	<0.25	<0.5	1	<0.015	>2	1	32
31	31.2	8	2.68	<0.125	<0.125	<0.25	0.5	<0.5	1	2	>2	0.5	>32
32	32.1	8	1.89	<0.125	<0.125	<0.25	<0.25	1	1	2	>2	0.5	>32

*Minimum inhibitory concentrations (MIC) and biofilm MIC (bMIC) in mg/L. MICs were determined according to the reference dilution method. bMICs were determined in filtered ASM. Gray cells indicate MIC and bMIC values above the EUCAST breakpoints for resistance (indicated in footnotes of **Table 1**). ST, sequence type. BFI, biofilm formation index.*

retained their ability to prevent biofilm formation (bMICs below the corresponding EUCAST thresholds for resistance) over time. We related these observations to the antimicrobial courses received by the patients (**Figure 3**). The more important antibiotic selective pressure was noted for linezolid and Patients 5 and 6. Three out of the four strains isolated in these patients were resistant to linezolid in planktonic cultures (resistance, investigated in a previous study; Boudet et al., 2021) was related to a G2576T substitution present in a variable number of 23S rRNA gene copies, while susceptible strain 6.3 displayed a high bMIC of 16 mg/L. For strains isolated in Patients 17 and 18 (who had received fewer linezolid courses during their follow-up), increased bMICs were observed over time, but bMICs were still below the resistance threshold (**Figure 3**). Although a low number of rifampicin and trimethoprim courses (possibly associated) were noted in the four patients, both antibiotics were no more active on later-collected strains, showing MICs or bMICs above the corresponding resistance thresholds. None of the patients had received ceftaroline or ceftobiprole.

Dynamics of Biofilm Formation Under Flow in the Presence and Absence of Antibiotics

To complete the characterization of biofilm formation of CF MRSA in the presence or absence of antibiotics, a study was performed in dynamic conditions using the BioFlux™ 200 microfluidic system. We selected strain 17.6, one of the two strains that were strongly adherent after 1.5 h of incubation in the BRT® and the paired 17.2 strain isolated 3 years before in Patient 17. For these paired strains, we first compared their dynamics of biofilm formation over time according to the medium used (BHI or ASM). The formation of biofilm increased regularly over time for each condition of the assay ("early" strain in BHI medium, "late" strain in ASM, "late" strain in BHI medium, "late" strain in ASM) with a systematically higher percentage of biofilm formed in ASM compared with BHI medium and for "late" strain compared with "early" strain (**Figure 4**). Although both strains were shown to have high adhesion ability using the BRT®, these results revealed that strains 17.2 and 17.6 each had distinct dynamics of biofilm formation, with a slower biofilm formation for the earlier-isolated strain 17.2 (**Figure 4**).

Further testing with antibiotics was limited to three times of measure (5, 12, and 36 h) and to the three antimicrobial agents with the lowest bMICs, that is, ceftaroline, ceftobiprole, and linezolid. With the BioFlux™ device, the percentage of biofilm formed in the presence of one of the three drugs tested was drastically lower than that observed for the control without antibiotics showing that all three antibiotics had the ability to limit biofilm formation and that this effect was long-lasting as it was observed up to 36 h of exposure to the bMIC of the corresponding antimicrobial agent in both media (**Figure 5**). Differences in biofilm formation in ASM were compared for statistical significance by a t test. A significantly higher inhibition of biofilm formed by the earlier isolated strain 17.2 was observed from 12 h of incubation and up to 36 h of incubation for ceftaroline and ceftobiprole compared with linezolid (values of $p < 0.05$ at 12 h; values of $p < 0.01$ at 36 h). Differences observed between ceftaroline and ceftobiprole were also statistically significant (value of $p < 0.05$ at 36 h), ceftaroline being more active in biofilm formation inhibition than ceftobiprole after 12 h, whereas ceftobiprole was more active in biofilm formation inhibition than ceftaroline after 36 h. Inhibition of the biofilm formation by the "late" strain 17.6 in ASM was more pronounced with ceftobiprole than with linezolid (values of $p < 0.01$ at 12 and 36 h) or ceftaroline (values of $p < 0.01$ at 36 h). Ceftaroline was also more active than linezolid after 36 h (value of $p < 0.01$).

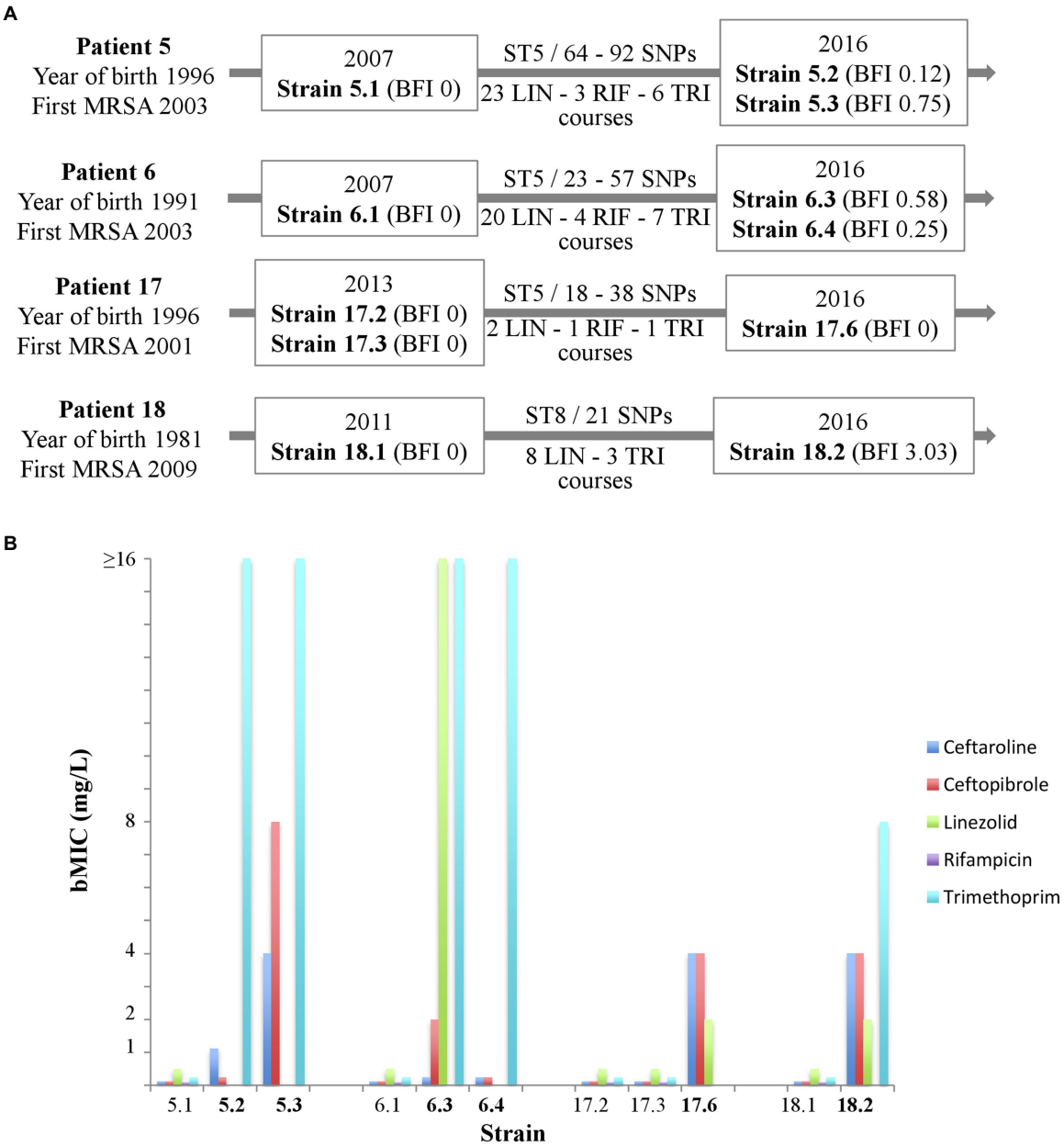

FIGURE 3 | Antibiofilmogram® results for successively isolated MRSA strains in four cystic fibrosis patients (5 « early » strains; 6 « late » strains). **(A)** Schematic presentation of patients (designation, year of birth, and year of first colonization by MRSA), strains [year of isolation, strain designation, biofilm formation index (BFI) value, ST, single nucleotide polymorphism (SNP) number between successively isolated strains], and number of antimicrobial courses (LIN, linezolid; RIF, rifampicin; and TRI, trimethoprim). **(B)** Biofilm minimal inhibitory concentration (bMIC, mg/L) in 0.22 µm-filtered artificial sputum medium of five antibiotics for the 11 strains included (data are presented for strains categorized as susceptible to the antibiotic considered only). European Committee on Antimicrobial Susceptibility Testing (EUCAST) thresholds for susceptibility (at standard or high doses) are as follows: ceftaroline: 1 mg/L (threshold for pneumonia); ceftobiprole: 2 mg/L; linezolid: 4 mg/L; rifampicin: 0.5 mg/L; and trimethoprim: 4 mg/L.

DISCUSSION

Cystic fibrosis is a chronic disease in which bacterial colonizations/infections of the airways are usual. Due to local specific conditions in the CF lung, diverse selective pressure is applied to colonizing microorganisms (interactions with the host immune response, high levels of antibiotic use, oxygen deprivation in mucus, altered antimicrobial peptide production, etc.) which, in turn, develop several traits to adapt to the surrounding environment and survive in the CF lung (Hauser et al., 2011). Among these traits, biofilm growth has been observed with several opportunistic pathogens in certain human diseases including CF, conferring protection against antimicrobial treatments and therefore contributing to bacterial persistence

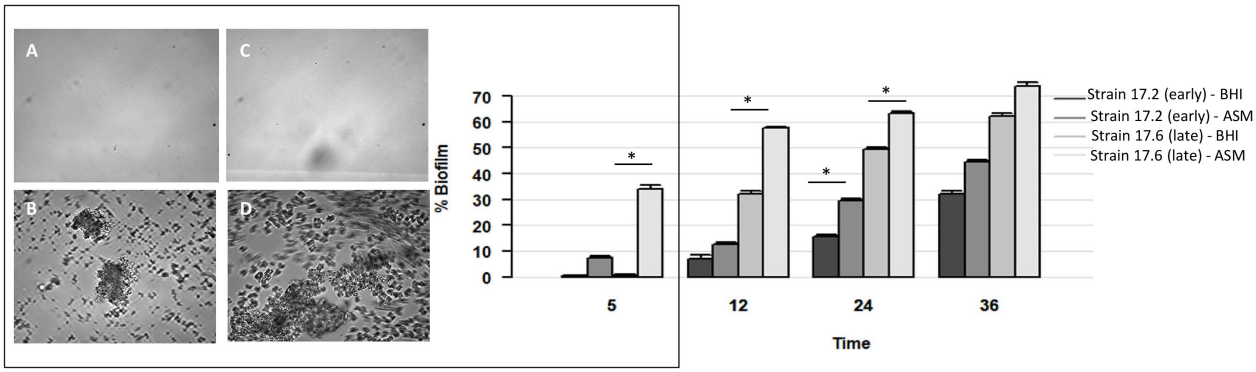

FIGURE 4 | Dynamics of biofilm formation in BHI medium and ASM in the absence of antibiotics for two strains isolated 3 years apart in Patient 17 (strain 17.2: "early" strain and 17.6: "late" strain). Left: Biofilm formation after 5 h of incubation: **(A,B)** early strain 17.2 in BHI medium **(A)** and ASM **(B)**; **(C,D)** late strain 17.6 in BHI medium **(C)** and ASM **(D)**. Right. Percentage of biofilm formed over time (in hours). *p*-values are indicated for comparisons of biofilm formed by a strain depending on the culture medium at each time of the assay. *Value of $p < 0.05$ using *t* test.

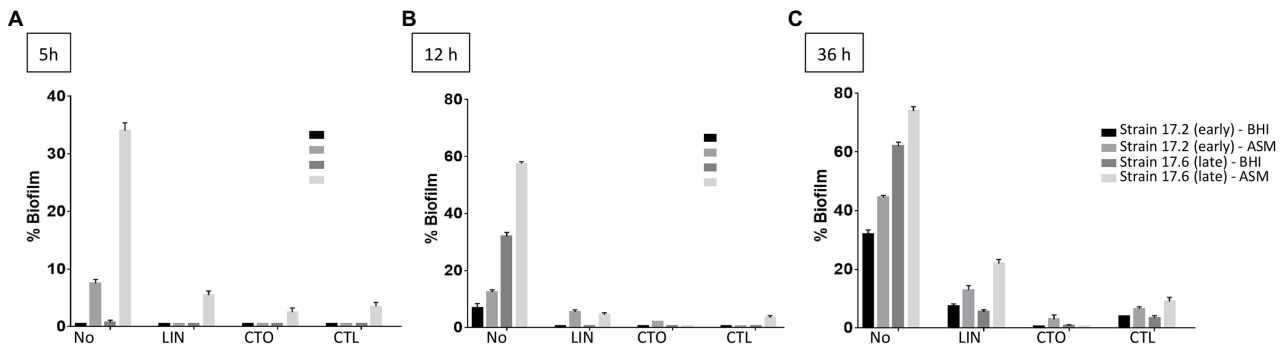

FIGURE 5 | Dynamics of biofilm formation (% of biofilm formed) in BHI medium and ASM in the presence of antibiotics for two strains isolated 3 years apart in Patient 17 (strain 17.2: "early" strain and 17.6: "late" strain). Results are presented comparatively to those observed in the absence of antibiotic previously presented in **Figure 4**. **(A)** After 5 h of incubation; **(B)** after 12 h of incubation; **(C)** after 36 h of incubation. No, no antibiotic; LIN, linezolid; CTO, ceftobiprole; and CTL, ceftaroline. Antibiotics were added to a final concentration equivalent to the minimum biofilm inhibitory concentration (bMIC) in the corresponding medium as follows: strain 17.2, bMICs in BHI medium and in ASM: CTL: 0.125 mg/L, CTO: 0.25 mg/L, LIN: 0.5 mg/L; strain 17.6, bMICs in BHI medium: CTL: 0.25 mg/L, CTO: 0.5 mg/L, LIN: 2 mg/L; bMICs in ASM: CTL: 4 mg/L, CTO: 4 mg/L, and LIN: 2 mg/L. Data are commented for statistical significance in the text.

(Donlan and Costerton, 2002). While the role of biofilm and the dynamics of its formation have been extensively studied for *P. aeruginosa* (Høiby et al., 2010), there have been few studies on MRSA in CF patients. However, biofilm formation is an important virulence trait of *S. aureus* which has been frequently observed (67% of the strains) in a recent study on CF pediatric patients (Kodori et al., 2021). Biofilm formation was also significantly more often observed for strains isolated from CF patients compared with those recovered from non-CF patients (Aktas et al., 2013). In MRSA, biofilm represents an additional obstacle to eradication in addition to multidrug resistance making these strains the most problematic ones and a great matter of concern due to their involvement in negative clinical evolution (Ren et al., 2007; Dasenbrook et al., 2008; Vanderhelst et al., 2012). One recent study found that 85.6% of MRSA isolates were biofilm producers compared with 54.2% of MSSA, suggesting that MRSA isolates are better able to form biofilm during CF (Kadkhoda et al., 2020). Biofilm formation was also observed in 14 of 15 CF MRSA pulsotypes in the study by Molina et al. (2008), supporting the fact that biofilm formation is a common characteristic of CF MRSA. In the specific and distinct conditions of our study – BRT® used with a 4-h incubation for selection of strong producers of early biofilm rather than the microtiter test used in previous studies, we found a rate of strong biofilm-forming MRSA of 27% of the strains and these strains had been isolated in samples from 37% of the studied patients.

Previous studies have related the propensity of specific clones of *S. aureus* for forming biofilm (Vanhommerig et al., 2014; Tasse et al., 2018) as well as *Escherichia coli* (Flament-Simon et al., 2019). For CF MRSA, due to the lack of studies including genetically characterized strains, it remains to be explored whether some lineages are more prone to forming biofilm. More generally, there is a lack of knowledge of MRSA clones circulating in the CF population in Europe (Vu-Thien et al., 2010; Cocchi et al., 2011) although no comparisons can be drawn with non-European data, particularly American data, due to the highly distinct epidemiology between these continents

(Glikman et al., 2008). Congruent with the studies of Vu-Thien et al. (2010) in France and Cocchi et al. (2011) in Italy, we observed that ST5 and ST8 were the most frequent STs identified in our study with 81% of the strains isolated in 80% of the patients belonging to these MLST genotypes. We observed that clonal lineages differed in terms of their biofilm-forming capacities as the majority of strong biofilm-producing strains belonged to ST5 and ST8, a trait that may contribute to the large representation of both genotypes in CF. However, due to the important representation of both STs in the overall population, ST5 and ST8 were major MLST genotypes observed in the three groups of BFI values in our study. They are also major MRSA lineages in the global population. Previous studies showed that some MRSA lineages like the predominant clone of community-acquired (CA)-MRSA in the United States, the USA300 clone in the clonal complex 8, have enhanced biofilm-forming capacity (Vanhommerig et al., 2014). Strains included in our study did not harbor the Panton-Valentine leukocidin-encoding gene characteristic of some CA-MRSA clones (unpublished) but were not characterized further in our study, thus preventing any conclusions about the implication of specific biofilm-forming lineages of ST5 or ST8 in CF.

Although antimicrobial treatments are considered as effective according to the results of *in vitro* assays, microorganisms may still persist in the CF airways for years, partly due to their ability to be protected within the polymer matrix produced during biofilm formation. In this context, the efficacy of antimicrobial therapy is reduced within the biofilm and approaches targeting bacterial biofilms in cystic fibrosis airways are required (Martin et al., 2021). However, as recently stated by Guzmán-Soto et al. (2021), "for the successful development of antibiofilm treatments and therapies, understanding biofilm development and being able to mimic such processes is vital." Several natural or synthetic compounds have shown to be active on biofilm formed by *S. aureus* (Miquel et al., 2016). However, most studies on *S. aureus* focused on the effects of antibiotics on established biofilm in the context of biofilm-associated infections other than CF, mainly medical device-associated infections. The antibiofilm activity of antibiotics on *S. aureus* isolated from CF patients has been scarcely investigated. Considering the 5 antibiotics included in this work, a PubMed search conducted on July 19, 2021, with « ceftaroline » or « ceftobiprole » or « linezolid » or « rifampicin » or « trimethoprim » and « *Staphylococcus aureus* » and « cystic fibrosis » and « biofilm » found five non-redundant publications supporting the need for data acquisition on the subject of antibiotics' antibiofilm activity against CF *S. aureus* isolates (Molina et al., 2008; Aktas et al., 2013; Iglesias et al., 2019; Gilpin et al., 2021; Harrington et al., 2021). This is reinforced by the observations that most of these antimicrobial agents have been found to display an antibiofilm activity on *S. aureus* isolated in other settings. For example, ceftaroline was effective against biofilm established by MRSA *in vitro* and *in vivo* models of catheter-associated biofilm formation suggesting that ceftaroline could be considered for the treatment of biofilm-associated MRSA infections (Meeker et al., 2016). In CF, ceftaroline was recently shown to represent an effective antimicrobial option for the management of acute pulmonary exacerbations involving MRSA in pediatric CF patients (Branstetter et al., 2020) and, on the other hand, has been shown to have an antibiofilm effect on biofilm-producing MRSA in other chronic infections (Mottola et al., 2016). Ceftobiprole has also previously demonstrated promising activity against biofilm from methicillin-resistant staphylococci (Abbanat et al., 2014). However, previous studies mainly included limited numbers of strains, either reference strains that may not reflect the behavior of CF strains or strains with no associated clinical data. In our study, we report the first data on the effect of antibiotics, including fifth-generation cephalosporins, on biofilm formation *via* a collection of clinically documented and genotypically characterized CF MRSA and seek to mimic CF sputum by using ASM in the different *in vitro* assays.

Due to the strong influence of environmental conditions on bacterial biofilm formation, the use of ASM formulated to mimic the sputum of CF patients appears promising for *in vitro* studies on CF isolates (Sriramulu et al., 2005; Dinesh, 2010). However, this technique remains little used in published studies and has mostly been used in studies on *P. aeruginosa* (Sriramulu et al., 2005; Kirchner et al., 2012; Rozenbaum et al., 2019; Iglesias and Van Bambeke, 2020). For *S. aureus*, it was previously used in a single study to determine the influence of the medium on the antibiofilm activity of antibiotics including two of those under consideration in this study (linezolid and rifampicin). ASM, containing amino acids, mucin, and free DNA, was shown to provide the most protective matrix (Rozenbaum et al., 2019) and all the antibiotics previously tested were drastically less potent and less effective in ASM than in comparators with respect to viability, metabolic activity, and biomass (Iglesias and Van Bambeke, 2020; Frisch et al., 2021). Here, through the comparative study of biofilm formation dynamics in ASM and BHI medium, we show that the use of ASM should be encouraged for further studies on biofilm formation by CF MRSA clinical isolates as an enhanced and accelerated biofilm formation was observed in ASM. However, we also found that ASM was not adaptable to all devices probably due to some of its characteristics like turbidity and viscoelasticity (Iglesias et al., 2019) and we had to consider filtered ASM for use in the BRT® despite the impact of the ASM filtration and the components which may be affected by this step remain unknown. Of note, ASM did not contain glucose despite glucose is present, at various levels according to the studies, in the sputum of CF patients (Van Sambeek et al., 2015; Nielsen et al., 2020) and glucose was shown to promote *S. aureus* biofilm formation (Lade et al., 2019). The supplementation of ASM with glucose may thus represent an interesting perspective for future work unless the best glucose concentration to be used can be defined considering the inter-individual (but also intra-individual) variability highlighted in previous studies of sputum samples from CF patients (Van Sambeek et al., 2015; Nielsen et al., 2020).

The inhibition of early biofilm formation observed in ASM in this study for linezolid and, more markedly, for ceftobiprole and ceftaroline represents an important finding because the first

two stages of biofilm development, that is, adsorption and adhesion, are key determinants in the next stages leading to biofilm development during initial colonization by MRSA and also during the biofilm life cycle at the dispersal stage. These observations warrant complementary studies on established biofilm and on antibiotic combinations as previously studied in other settings such as endocarditis, diabetic foot infections, and medical device-associated infections for associations including ceftaroline (Barber et al., 2015; Mottola et al., 2016; Thieme et al., 2018), as they may contribute to the required optimization of antibiotic regimens against biofilm (Lebeaux et al., 2014).

Bacterial populations colonizing CF patients are known to be highly complex and dynamic, encompassing a variety of variants whose equilibrium varies according to the changing conditions of the surrounding environment. This population diversification is an increasingly well-known host adaptation strategy which has been widely studied in Gram-negative bacilli during chronic colonization of CF patients' lungs (Winstanley et al., 2016; Menetrey et al., 2021). For *S. aureus*, diversified populations have been more rarely documented in CF (Goerke et al., 2007; Vu-Thien et al., 2010; Hirschhausen et al., 2013; Ankrum and Hall, 2017; Boudet et al., 2021; Wieneke et al., 2021). Regarding biofilm formation, we observed that patients may be colonized by clonally related strains corresponding to adaptive variants displaying distinct abilities to form biofilm, as previously described (Savage et al., 2013; Wieneke et al., 2021). Such diversification of MRSA populations and intra-sample heterogeneity of biofilm formation ability may contribute to compromising the antibiotic management of CF airway infections. Other adaptive phenotypic modifications observed for CF *S. aureus* have included the increase in antimicrobial resistance and the biofilm development observed in certain studies (Hirschhausen et al., 2013). In our study, strains adapted to the CF lung environment after years of colonization may still display low bMICs for ceftaroline, an observation that requires further investigation on a larger panel of MRSA strains isolated in chronically colonized patients. Adaptive modifications like mucoidy and nuclease activity were recently shown to be more frequently observed in case of *P. aeruginosa* co-colonization highlighting the importance of cross-talk and interactions between bacterial pathogens in shaping the adaptation of *S. aureus* to the CF lung environment (Wieneke et al., 2021). In our study, no obvious association was observed between chronic colonization by *P. aeruginosa* and the ability of MRSA to form early biofilm. Finally, future studies are still needed to investigate the behavior of CF MRSA within multispecies biofilm as well as the effect of exposure of these multispecies biofilms to different antibiotics (Vandeplassche et al., 2020).

CONCLUSION

We hereby report the first data on early biofilm formation by MRSA clinical isolates from CF patients using original and standardized approaches which had never been previously applied to such isolates and whose use should be encouraged. Indeed, the BRT® is well-designed to investigate the early and capital stages of biofilm formation contrarily to the most frequently used microtiter plate dye-staining (crystal violet) assays and presents the other advantages of being a rapid, high-throughput, easy-to-handle, and highly reproducible method. The BioFlux is meanwhile a fully integrated and easy-to-use system allowing the study of the dynamic formation of the biofilm and the small volumes required make this system highly applicable for screening of biofilm inhibitory agents (for a critical review of methods usable to study biofilm formation, see Azeredo et al., 2017).

As previously observed for other CF pathogens like *P. aeruginosa* or in other settings like medical device-associated infections, antibiotic susceptibility was reduced in biofilm, thereby complicating anti-MRSA treatments and representing a risk of treatment failure in CF patients. The Antibiofilmogram® is a promising tool for guiding the choice of the most effective drugs against biofilm formation by MRSA in CF airways. In our study, the two broad-spectrum anti-MRSA cephalosporins ceftaroline and ceftobiprole displayed a notable ability to limit biofilm formation of CF MRSA. Hitherto little used for CF patients, the characteristics of both antimicrobial agents, together with recent studies showing that ceftaroline represents an additional treatment option for treating MRSA-associated acute pulmonary exacerbations (Branstetter et al., 2020), should promote their larger use in the management of CF patients infected by MRSA.

DATA AVAILABILITY STATEMENT

The datasets presented in this study can be found in online repositories. The names of the repository/repositories and accession number(s) can be found in the article/**Supplementary Material**.

ETHICS STATEMENT

The studies involving human participants were reviewed and approved by the Institutional Review Board at Nîmes University hospital (Interface Recherche Bioéthique IRB n 21.03.01, March 04, 2021). Written informed consent from the participants' legal guardian/next of kin was not required to participate in this study in accordance with the national legislation and the institutional requirements.

AUTHOR'S NOTE

This work was partly presented at the 44th European Cystic Fibrosis Conference (digital), 9–12 June 2021.

AUTHOR CONTRIBUTIONS

HM: conceptualization. AB, PS, and CP: methodology. AB, PS, CP, CD-R, and HM: formal analysis. AB, PS, and RC: investigation. AB, PS, CP, and RC: data curation. AB, PS, and HM: writing – original draft preparation. CP, CD-R, RC, and J-PL: writing – review and editing. AB, CD-R, and HM: supervision. CD-R, J-PL,

and HM: funding acquisition. All authors contributed to the article and approved the submitted version.

FUNDING

This research was funded by the University Hospital of Nîmes (NîmAO 2018.02 grant).

ACKNOWLEDGMENTS

The authors gratefully acknowledge Teresa Sawyers, English medical writer at Nîmes University Hospital, for editing this paper, and Bastien Baud and Vincenette Lopez for their help with clinical and therapeutic data collection. We thank Nîmes University Hospital for its structural, human, and financial support through the award obtained by our team during the internal call for tenders "Thématiques phares." All authors belong to the FHU InCh (Fédération Hospitalo-Universitaire Infections Chroniques, Aviesan).

SUPPLEMENTARY MATERIAL

The Supplementary Material for this article can be found online at: https://www.frontiersin.org/articles/10.3389/fmicb.2021.750489/full#supplementary-material

REFERENCES

Abbanat, D., Shang, W., Amsler, K., Santoro, C., Baum, E., Crespo-Carbone, S., et al. (2014). Evaluation of the in vitro activities of ceftobiprole and comparators in staphylococcal colony or microtitre plate biofilm assays. *Int. J. Antimicrob. Agents* 43, 32–39. doi: 10.1016/j.ijantimicag.2013.09.013

Akil, N., and Muhlebach, M. S. (2018). Biology and management of methicillin resistant *Staphylococcus aureus* in cystic fibrosis. *Pediatr. Pulmonol.* 53, S64–S74. doi: 10.1002/ppul.24139

Aktas, N. C., Erturan, Z., Karatuna, O., and Yagci, A. K. (2013). Panton-valentine leukocidin and biofilm production of *Staphylococcus aureus* isolated from respiratory tract. *J. Infect. Dev. Ctries.* 7, 888–891. doi: 10.3855/jidc.4135

Ankrum, A., and Hall, B. G. (2017). Population dynamics of *Staphylococcus aureus* in cystic fibrosis patients to determine transmission events by use of whole-genome sequencing. *J. Clin. Microbiol.* 55, 2143–2152. doi: 10.1128/JCM.00164-17

Azeredo, J., Azevedo, N. F., Briandet, R., Cerca, N., Coenye, T., Costa, A. R., et al. (2017). Critical review on biofilm methods. *Crit. Rev. Microbiol.* 43, 313–351. doi: 10.1080/1040841X.2016.1208146

Barber, K. E., Smith, J. R., Ireland, C. E., Boles, B. R., Rose, W. E., and Rybak, M. J. (2015). Evaluation of ceftaroline alone and in combination against biofilm-producing methicillin-resistant *Staphylococcus aureus* with reduced susceptibility to daptomycin and vancomycin in an in vitro pharmacokinetic/pharmacodynamic model. *Antimicrob. Agents Chemother.* 59, 4497–4503. doi: 10.1128/AAC.00386-15

Benoit, M. R., Conant, C. G., Ionescu-Zanetti, C., Schwartz, M., and Matin, A. (2010). New device forhigh-throughput viability screening of flow biofilms. *Appl. Environ. Microbiol.* 76, 4136–4142. doi: 10.1128/AEM.03065-09

Boudet, A., Jay, A., Dunyach-Remy, C., Chiron, R., Lavigne, J.-P., and Marchandin, H. (2021). In-host emergence of linezolid resistance in a complex pattern of toxic shock syndrome toxin-1-positive methicillin-resistant *Staphylococcus aureus* colonization in siblings with cystic fibrosis. *Toxins* 13:317. doi: 10.3390/toxins13050317

Branstetter, J., Searcy, H., Benner, K., Yarbrough, A., Crowder, C., and Troxler, B. (2020). Ceftaroline vs vancomycin for the treatment of acute pulmonary exacerbations in pediatric patients with cystic fibrosis. *Pediatr. Pulmonol.* 55, 3337–3342. doi: 10.1002/ppul.25029

Chavant, P., Gaillard-Martinie, B., Talon, R., Hebraud, M., and Bernardi, T. (2007). A new device for rapid evaluation of biofilm formation potential by bacteria. *J. Microbiol. Methods* 68, 605–612. doi: 10.1016/j.mimet.2006.11.010

Cocchi, P., Cariani, L., Favari, F., Lambiase, A., Fiscarelli, E., Gioffré, F. V., et al. (2011). Molecular epidemiology of meticillin-resistant *Staphylococcus aureus* in Italian cystic fibrosis patients: a national overview. *J. Cyst. Fibros.* 10, 407–411. doi: 10.1016/j.jcf.2011.06.005

Crisóstomo, M. I., Westh, H., Tomasz, A., Chung, M., Oliveira, D. C., and De Lencastre, H. (2001). The evolution of methicillin resistance in *Staphylococcus aureus*: similarity of genetic backgrounds in historically early methicillin-susceptible and resistant isolates and contemporary epidemic clones. *Proc. Natl. Acad. Sci. U. S. A.* 98, 9865–9870. doi: 10.1073/pnas.161272898

Dasenbrook, E. C., Merlo, C. A., Diener-West, M., Lechtzin, N., and Boyle, M. P. (2008). Persistent methicillin-resistant *Staphylococcus aureus* and rate of FEV_1 decline in cystic fibrosis. *Am. J. Respir. Crit. Care Med.* 178, 814–821. doi: 10.1164/rccm.200802-327OC

Dinesh, S. D. (2010). Artificial sputum medium. *Protoc. Exch.* doi: 10.1038/protex.2010.212

Donlan, R. M., and Costerton, J. W. (2002). Biofilms: survival mechanisms of clinically relevant microorganisms. *Clin. Microbiol. Rev.* 15, 167–193. doi: 10.1128/CMR.15.2.167-193.2002

Enright, M. C., Day, N. P. J., Davies, C. E., Peacock, S. J., and Spratt, B. G. (2000). Multilocus sequence typing for characterization of methicillin-resistant and methicillin-susceptible clones of *Staphylococcus aureus*. *J. Clin. Microbiol.* 38, 1008–1015. doi: 10.1128/JCM.38.3.1008-1015.2000

European Committee on Antimicrobial Susceptibility Testing (2021). Breakpoint tables for interpretation of MICs and zone diameters. Version 11.0. Available at: https://www.eucast.org/fileadmin/src/media/PDFs/EUCAST_files/Breakpoint_tables/v_11.0_Breakpoint_Tables.pdf (Accessed February 8, 2021).

Flament-Simon, S.-K., Duprilot, M., Mayer, N., García, V., Alonso, M. P., Blanco, J., et al. (2019). Association between kinetics of early biofilm formation and clonal lineage in *Escherichia coli*. *Front. Microbiol.* 10:1183. doi: 10.3389/fmicb.2019.01183

Frisch, S., Boese, A., Huck, B., Horstmann, J. C., Ho, D. K., Schwarzkopf, K., et al. (2021). A pulmonary mucus surrogate for investigating antibiotic permeation and activity against *Pseudomonas aeruginosa* biofilms. *J. Antimicrob. Chemother.* 76, 1472–1479. doi: 10.1093/jac/dkab068

Fusco, N. M., Toussaint, K. A., and Prescott, W. A. Jr. (2015). Antibiotic management of methicillin-resistant *Staphylococcus aureus*--associated acute pulmonary exacerbations in cystic fibrosis. *Ann. Pharmacother.* 49, 458–468. doi: 10.1177/1060028014567526

Gilpin, D., Hoffman, L. R., Ceppe, A., and Muhlebach, M. S. (2021). Phenotypic characteristics of incident and chronic MRSA isolates in cystic fibrosis. *J. Cyst. Fibros.* 20, 692–698. doi: 10.1016/j.jcf.2021.05.015

Glikman, D., Siegel, J. D., David, M. Z., Okoro, N. M., Boyle-Vavra, S., Dowell, M. L., et al. (2008). Complex molecular epidemiology of methicillin-resistant *Staphylococcus aureus* isolates from children with cystic fibrosis in the era of epidemic community-associated methicillin-resistant *S aureus*. *Chest* 133, 1381–1387. doi: 10.1378/chest.07-2437

Goerke, C., Gressinger, M., Endler, K., Breitkopf, C., Wardecki, K., Stern, M., et al. (2007). High phenotypic diversity in infecting but not in colonizing *Staphylococcus aureus* populations. *Environ. Microbiol.* 9, 3134–3142. doi: 10.1111/j.1462-2920.2007.01423.x

Goerke, C., and Wolz, C. (2010). Adaptation of *Staphylococcus aureus* to the cystic fibrosis lung. *Int. J. Med. Microbiol.* 300, 520–525. doi: 10.1016/j.ijmm.2010.08.003

Goss, C. H., and Muhlebach, M. S. (2011). Review: *Staphylococcus aureus* and MRSA in cystic fibrosis. *J. Cyst. Fibros.* 10, 298–306. doi: 10.1016/j.jcf.2011.06.002

Guzmán-Soto, I., McTiernan, C., Gonzalez-Gomez, M., Ross, A., Gupta, K., Suuronen, E. J., et al. (2021). Mimicking biofilm formation and development: recent progress in in vitro and in vivo biofilm models. *iScience* 24:102443. doi: 10.1016/j.isci.2021.102443

Harrington, N. E., Sweeney, E., Alav, I., Allen, F., Moat, J., and Harrison, F. (2021). Antibiotic efficacy testing in an ex vivo model of *Pseudomonas aeruginosa* and *Staphylococcus aureus* biofilms in the cystic fibrosis lung. *J. Vis. Exp.* doi: 10.3791/62187

Hauser, A. R., Jain, M., Bar-Meir, M., and McColley, S. A. (2011). Clinical significance of microbial infection and adaptation in cystic fibrosis. *Clin. Microbiol. Rev.* 24, 29–70. doi: 10.1128/CMR.00036-10

Hirschhausen, N., Block, D., Bianconi, I., Bragonzi, A., Birtel, J., Lee, J. C., et al. (2013). Extended *Staphylococcus aureus* persistence in cystic fibrosis is associated with bacterial adaptation. *Int. J. Med. Microbiol.* 303, 685–692. doi: 10.1016/j.ijmm.2013.09.012

Høiby, N., Ciofu, O., and Bjarnsholt, T. (2010). *Pseudomonas aeruginosa* biofilms in cystic fibrosis. *Future Microbiol.* 5, 1663–1674. doi: 10.2217/fmb.10.125

Iglesias, Y. D., and Van Bambeke, F. (2020). Activity of antibiotics against *Pseudomonas aeruginosa* in an in vitro model of biofilms in the context of cystic fibrosis: influence of the culture medium. *Antimicrob. Agents Chemother.* 64, e02204–e02219. doi: 10.1128/AAC.02204-19

Iglesias, Y. D., Wilms, T., Vanbever, R., and Van Bambeke, F. (2019). Activity of antibiotics against *Staphylococcus aureus* in an in vitro model of biofilms in the context of cystic fibrosis: influence of the culture medium. *Antimicrob. Agents Chemother.* 63, e00602–e00619. doi: 10.1128/AAC.00602-19

Jolley, K. A., Bray, J. E., and Maiden, M. C. J. (2018). Open-access bacterial population genomics: BIGSdb software, the PubMLST.org website and their applications. *Wellcome Open Res.* 3:124. doi: 10.12688/wellcomeopenres.14826.1

Kadkhoda, H., Ghalavand, Z., Nikmanesh, B., Kodori, M., Houri, H., Maleki, D. T., et al. (2020). Characterization of biofilm formation and virulence factors of *Staphylococcus aureus* isolates from paediatric patients in Tehran, Iran. *Iran J. Basic Med. Sci.* 23, 691–698. doi: 10.22038/ijbms.2020.36299.8644

Kirchner, S., Fothergill, J. L., Wright, E. A., James, C. E., Mowat, E., and Winstanley, C. (2012). Use of artificial sputum medium to test antibiotic efficacy against *Pseudomonas aeruginosa* in conditions more relevant to the cystic fibrosis lung. *J. Vis. Exp.* 64:e3857. doi: 10.3791/3857

Kodori, M., Nikmanesh, B., Hakimi, H., and Ghalavand, Z. (2021). Antibiotic susceptibility and biofilm formation of bacterial isolates derived from pediatric patients with cystic fibrosis from Tehran, Iran. *Arch. Razi. Inst.* 76, 397–406. doi: 10.22092/ari.2020.128554.1416

Lade, H., Park, J. H., Chung, S. H., Kim, I. H., Kim, J. M., Joo, H. S., et al. (2019). Biofilm formation by *Staphylococcus aureus* clinical isolates is differentially affected by glucose and sodium chloride supplemented culture media. *J. Clin. Med.* 8:1853. doi: 10.3390/jcm8111853

Lebeaux, D., Ghigo, J. M., and Beloin, C. (2014). Biofilm-related infections: bridging the gap between clinical management and fundamental aspects of recalcitrance toward antibiotics. *Microbiol. Mol. Biol. Rev.* 78, 510–543. doi: 10.1128/MMBR.00013-14

Martin, I., Waters, V., and Grasemann, H. (2021). Approaches to targeting bacterial biofilms in cystic fibrosis airways. *Int. J. Mol. Sci.* 22:2155. doi: 10.3390/ijms22042155

Meeker, D. G., Beenken, K. E., Mills, W. B., Loughran, A. J., Spencer, H. J., Lynn, W. B., et al. (2016). Evaluation of antibiotics active against methicillin-resistant *Staphylococcus aureus* based on activity in an established biofilm. *Antimicrob. Agents Chemother.* 60, 5688–5694. doi: 10.1128/AAC.01251-16

Menetrey, Q., Sorlin, P., Jumas-Bilak, E., Chiron, R., Dupont, C., and Marchandin, H. (2021). *Achromobacter xylosoxidans* and *Stenotrophomonas maltophilia*: emerging pathogens well-armed for life in the cystic fibrosis patients' lung. *Gene* 12:610. doi: 10.3390/genes12050610

Miquel, S., Lagrafeuille, R., Souweine, B., and Forestier, C. (2016). Anti-biofilm activity as a health issue. *Front. Microbiol.* 7:592. doi: 10.3389/fmicb.2016.00592

Molina, A., Del Campo, R., Máiz, L., Morosini, M. I., Lamas, A., Baquero, F., et al. (2008). High prevalence in cystic fibrosis patients of multiresistant hospital-acquired methicillin-resistant *Staphylococcus aureus* ST228-SCC*mec*I capable of biofilm formation. *J. Antimicrob. Chemother.* 62, 961–967. doi: 10.1093/jac/dkn302

Mottola, C., Matias, C. S., Mendes, J. J., Melo-Cristino, J., Tavares, L., Cavaco-Silva, P., et al. (2016). Susceptibility patterns of *Staphylococcus aureus* biofilms in diabetic foot infections. *BMC Microbiol.* 16:119. doi: 10.1186/s12866-016-0737-0

Naudin, B., Heins, A., Pinhal, S., Dé, E., and Nicol, M. (2019). BioFlux™ 200 microfluidic system to study *A. baumannii* biofilm formation in a dynamic mode of growth. *Methods Mol. Biol.* 1946, 167–176. doi: 10.1007/978-1-4939-9118-1_16

Nielsen, B. U., Kolpen, M., Jensen, P. Ø., Katzenstein, T., Pressler, T., Ritz, C., et al. (2020). Neutrophil count in sputum is associated with increased sputum glucose and sputum L-lactate in cystic fibrosis. *PLoS One* 15:e0238524. doi: 10.1371/journal.pone.0238524

Olivares, E., Badel-Berchoux, S., Provot, C., Prévost, G., Bernardi, T., and Jehl, F. (2020). Clinical impact of antibiotics for the treatment of *Pseudomonas aeruginosa* biofilm infections. *Front. Microbiol.* 10:2894. doi: 10.3389/fmicb.2019.02894

Predari, S. C., Ligozzi, M., and Fontana, R. (1991). Genotypic identification of methicillin-resistant coagulase-negative staphylococci by polymerase chain reaction. *Antimicrob. Agents Chemother.* 35, 2568–2573. doi: 10.1128/AAC.35.12.2568

Registre français de la mucoviscidose - Bilan des données (2019). Vaincre la Mucoviscidose Paris, 2020. Available at: https://www.vaincrelamuco.org/sites/default/files/registre_2019_vf.pdf (Accessed July 24, 2021).

Ren, C. L., Morgan, W. J., Konstan, M. W., Schechter, M. S., Wagener, J. S., and Fisher, K. A., et al. (2007). Presence of methicillin resistant *Staphylococcus aureus* in respiratory cultures from cystic fibrosis patients is associated with lower lung function. *Pediatr. Pulmonol.* 42, 513–518. doi: 10.1002/ppul.20604

Rowe, S. M., Miller, S., and Sorscher, E. J. (2005). Cystic fibrosis. *N. Engl. J. Med.* 352, 1992–2001. doi: 10.1056/NEJMra043184

Rozenbaum, R. T., van der Mei, H. C., Woudstra, W., de Jong, E. D., Busscher, H. J., and Sharma, P. K. (2019). Role of viscoelasticity in bacterial killing by antimicrobials in differently grown *Pseudomonas aeruginosa* biofilms. *Antimicrob. Agents Chemother.* 63, e01972–e02018. doi: 10.1128/AAC.01972-18

Savage, V. J., Chopra, I., and O'Neill, A. J. (2013). Population diversification in *Staphylococcus aureus* biofilms may promote dissemination and persistence. *PLoS One* 8:e62513. doi: 10.1371/journal.pone.0062513

Seemann, T. (2015). Snippy: Fast bacterial variant calling from NGS reads. Available at: https://github.com/tseemann/snippy (Accessed July 2, 2021).

Sriramulu, D. D., Lünsdorf, H., Lam, J. S., and Römling, U. (2005). Microcolony formation: a novel biofilm model of *Pseudomonas aeruginosa* for the cystic fibrosis lung. *J. Med. Microbiol.* 54, 667–676. doi: 10.1099/jmm.0.45969-0

Tasse, J., Croisier, D., Badel-Berchoux, S., Chavanet, P., Bernardi, T., Provot, C., et al. (2016). Preliminary results of a new antibiotic susceptibility test against biofilm installation in device-associated infections: the Antibiofilmogram®. *Pathog. Dis.* 74:ftw057. doi: 10.1093/femspd/ftw057

Tasse, J., Trouillet-Assant, S., Josse, J., Martins-Simões, P., Valour, F., Langlois-Jacques, C., et al. (2018). Association between biofilm formation phenotype and clonal lineage in *Staphylococcus aureus* strains from bone and joint infections. *PLoS One* 13:e0200064. doi: 10.1371/journal.pone.0200064

The Cystic Fibrosis Foundation Patient Registry (2019). Annual data report 2020. Available at: https://www.cff.org/Research/Researcher-Resources/Patient-Registry/2019-Patient-Registry-Annual-Data-Report.pdf (Accessed July 24, 2021).

Thieme, L., Klinger-Strobel, M., Hartung, A., Stein, C., Makarewicz, O., and Pletz, M. W. (2018). In vitro synergism and anti-biofilm activity of ampicillin, gentamicin, ceftaroline and ceftriaxone against *Enterococcus faecalis*. *J. Antimicrob. Chemother.* 73, 1553–1561. doi: 10.1093/jac/dky051

Vandeplassche, E., Sass, A., Ostyn, L., Burmølle, M., Kragh, K. N., Bjarnsholt, T., et al. (2020). Antibiotic susceptibility of cystic fibrosis lung microbiome members in a multispecies biofilm. *Biofilm* 2:100031. doi: 10.1016/j.bioflm.2020.100031

Vanderhelst, E., De Meirleir, L., Verbanck, S., Piérard, D., Vincken, W., and Malfroot, A. (2012). Prevalence and impact on FEV_1 decline of chronic methicillin-resistant *Staphylococcus aureus* (MRSA) colonization in patients with cystic fibrosis: a single-center, case control study of 165 patients. *J. Cyst. Fibros.* 11, 2–7. doi: 10.1016/j.jcf.2011.08.006

Vanhommerig, E., Moons, P., Pirici, D., Lammens, C., Hernalsteens, J.-P., De Greve, H., et al. (2014). Comparison of biofilm formation between major clonal lineages of methicillin resistant *Staphylococcus aureus*. *PLoS One* 9:e104561. doi: 10.1371/journal.pone.0104561

Van Sambeek, L., Cowley, E. S., Newman, D. K., and Kato, R. (2015). Sputum glucose and glycemic control in cystic fibrosis-related diabetes: a cross-sectional study. *PLoS One* 10:e0119938. doi: 10.1371/journal.pone.0119938

Vu-Thien, H., Hormigos, K., Corbineau, G., Fauroux, B., Corvol, H., Moissenet, D., et al. (2010). Longitudinal survey of *Staphylococcus aureus* in cystic fibrosis

patients using a multiple-locus variable number of tandem-repeats analysis method. *BMC Microbiol.* 10:24. doi: 10.1186/1471-2180-10-24

Wieneke, M. K., Dach, F., Neumann, C., Görlich, D., Kaese, L., Thißen, T., et al. (2021). Association of diverse *Staphylococcus aureus* populations with *Pseudomonas aeruginosa* coinfection and inflammation in cystic fibrosis airway infection. *mSphere* 6:e0035821. doi: 10.1128/mSphere.00358-21

Winstanley, C., O'Brien, S., and Brockhurst, M. A. (2016). *Pseudomonas aeruginosa* evolutionary adaptation and diversification in cystic fibrosis chronic lung infections. *Trends Microbiol.* 24, 327–337. doi: 10.1016/j.tim.2016.01.008

Zobell, J. T., Epps, K. L., Young, D. C., Montague, M., Olson, J., Ampofo, K., et al. (2015). Utilization of antibiotics for methicillin-resistant *Staphylococcus aureus* infection in cystic fibrosis. *Pediatr. Pulmonol.* 50, 552–559. doi: 10.1002/ppul.23132

Zolin, A., Orenti, A., Naehrlich, L., Jung, A., and van Rens, J. (2020). ECFSPR annual report 2018. Available online: https://www.ecfs.eu/sites/default/files/general-content-files/working-groups/ecfs-patient-registry/ECFSPR_Report_2018_v1.4.pdf (Accessed July 24, 2021).

Conflict of Interest: The authors declare that this research was conducted in the absence of any commercial or financial relationships that could be construed as potential conflicts of interest.

Publisher's Note: All claims expressed in this article are solely those of the authors and do not necessarily represent those of their affiliated organizations, or those of the publisher, the editors and the reviewers. Any product that may be evaluated in this article, or claim that may be made by its manufacturer, is not guaranteed or endorsed by the publisher.

frontiers in Microbiology

ORIGINAL RESEARCH
published: 18 October 2021
doi: 10.3389/fmicb.2021.761583

A New pH-Responsive Nano Micelle for Enhancing the Effect of a Hydrophobic Bactericidal Agent on Mature *Streptococcus mutans* Biofilm

*Meng Zhang[1], Zhiyi Yu[2] and Edward Chin Man Lo[1]**

[1] Faculty of Dentistry, The University of Hong Kong, Pok Fu Lam, Hong Kong, SAR China, [2] Department of Medicinal Chemistry, School of Pharmaceutical Sciences, Cheeloo College of Medicine, Shandong University, Jinan, China

The bactericidal effect on biofilm is the main challenge currently faced by antibacterial agents. Nanoscale drug-delivery materials can enhance biofilm penetrability and drug bioavailability, and have significant applications in the biomedical field. Dental caries is a typical biofilm-related disease, and the acidification of biofilm pH is closely related to the development of dental caries. In this study, a pH-responsive core-shell nano micelle (mPEG-b-PDPA) capable of loading hydrophobic antibacterial agents was synthesized and characterized, including its ability to deliver antibacterial agents within an acidic biofilm. The molecular structure of this diblock copolymer was determined by hydrogen-1 nuclear magnetic resonance (^{1}H-NMR) and gel permeation chromatography (GPC). The characters of the micelles were studied by dynamic light scattering (DLS), TEM, pH titration, and drug release detection. It was found that the hydrophilic micelles could deliver bedaquiline, a hydrophobic antibacterial agent on *S. mutans*, in acidic environments and in mature biofilm. No cytotoxic effect on the periodontal cells was detected within 48 h. This pH-responsive micelle, being able to load hydrophobic antibacterial agent, has good clinical application potential in preventing dental caries.

Keywords: pH-responsive micelle, drug delivery systems, hydrophobic antibacterial agent, dental caries, *Streptococcus mutans*

OPEN ACCESS

Edited by:
Enea Gino Di Domenico, Istituti Fisioterapici Ospitalieri, Scientific Institute for Research, Hospitalization and Healthcare (IRCCS), Italy

Reviewed by:
Yan Xiao, Qingdao Institute of Bioenergy and Bioprocess Technology, Chinese Academy of Sciences (CAS), China
Laura Chronopoulou, Sapienza University of Rome, Italy

****Correspondence:***
Edward Chin Man Lo
edward_lo@hku.hk

Specialty section:
This article was submitted to Infectious Agents and Disease, a section of the journal Frontiers in Microbiology

Received: *20 August 2021*
Accepted: *23 September 2021*
Published: *18 October 2021*

Citation:
Zhang M, Yu Z and Lo ECM (2021) A New pH-Responsive Nano Micelle for Enhancing the Effect of a Hydrophobic Bactericidal Agent on Mature Streptococcus mutans Biofilm. Front. Microbiol. 12:761583. doi: 10.3389/fmicb.2021.761583

INTRODUCTION

The oral cavity harbors an extremely sophisticated microbial environment in nature. As many as 700 strains live on hard and soft tissue surfaces. Maturation of biofilm and the imbalance of microecology contribute to the development of oral diseases (Gao et al., 2018). Dental plaque biofilm is closely related to the occurrence and development of dental caries (Pitts et al., 2017). Different bacteria colonize the tooth surface in a well-programmed way and form a biofilm (Kolenbrander et al., 2006). This microecology not only provides a great haven for the reproduction of caries pathogens and the fermentation of an acidic environment (Filoche et al., 2010) but also resists attack from foreign substances, including antibiotics and antibacterial agents (Pizzolato-Cezar et al., 2019). Many agents have an antibacterial effect on cariogenic pathogens in suspension (Jiang et al., 2020; Zhang et al., 2021), but it is extremely difficult for these agents to penetrate into biofilm and attack the pathogens in the biofilm. This is a major challenge for the clinical applications of these agents for dental caries management.

Nanoscale drug carriers have been shown to be able to release its cargo in a controlled manner, increase the penetration to biofilms, improve drug stability, and enhance drug bioavailability (Mura et al., 2013; Liu et al., 2016; Mishra et al., 2019). Nanoparticles, as a biofilm-targeting approach, have become increasingly popular due to their versatility and biological activity (Koo et al., 2017). Multidrug-resistant bacterial infection is also expected to be overcome by effective antibacterial agents with the assistance of nanoscale drug carriers (Qing et al., 2019). Based on the properties and advantages of nanoscale materials, they have good potential to be selected as an adjuvant to tackle the abovementioned challenges in dental caries management by optimizing the clinical application of antibacterial agents (Hannig and Hannig, 2010). Some nanomaterial studies have achieved good results on dental surface coating and biofilm penetration. Liu et al. (2016) designed and confirmed a mixed-shell-polymeric-micelle [PEG-poly(β-amino ester)] which enhanced the penetration capability and bactericidal effectiveness of triclosan to *Staphylococcal* biofilms. Another group of researchers (Horev et al., 2015) found that nanomicelles [p(DMAEMA-co-BMA-co-PAA)] loaded with antibacterial agent displayed multi-targeted binding on tooth surfaces, pH-responsive drug release, and more powerful destruction to biofilm than the antibacterial agent alone.

pH is a critical risk factor to keep the balance of dental biofilm micro-ecological environment (Pitts et al., 2017; Bowen et al., 2018). In neutral pH, various bacteria colonize the tooth surface together and maintain a biofilm environment that is compatible with health. On exposure to an abundant supply of carbohydrates, large amounts of acidic bacterial metabolites will be produced and a low pH environment in biofilm (pH 4.5–5.5) will be formed (Vroom et al., 1999; Takahashi, 2005). This acidic environment will suppress bacteria that have a low acid resistance and allow bacteria with high acid resistance to flourish and produce more acids, thereby causing tooth demineralization and development of dental caries (Hwang et al., 2016; Bowen et al., 2018). Hence, delivering effective antibacterial agents into mature biofilm, which has an acidic environment, to act on the cariogenic bacteria will be a good caries prevention strategy. Currently, many pH-responsive drug delivery nano-materials have been explored in acidic pathological environments, such as cancer microenvironment, bone infections, and *Pseudomonas aeruginosa* infections (Cicuéndez et al., 2018; Naha et al., 2019; Chen et al., 2021). However, relatively limited research has been conducted on their application in the prevention of dental caries (Horev et al., 2015; Zhao et al., 2019; Liang et al., 2020).

Bedaquiline is an inhibitor that targets an acid-resistant protein H^+-ATPase (Preiss et al., 2015). Results of our previous study show that bedaquiline can potently inhibit the growth of *Streptococcus mutans* (*S. mutans*) suspension and biofilm generation in acidic environment (pH 5) but has no effect in neutral environment (Zhang et al., 2021). Besides, this hydrophobic agent cannot exert bactericidal effect on the bacteria within biofilm. Subsequently, in order to enhance the bactericidal effect of bedaquiline in mature biofilms, and to promote the clinical application of hydrophobic antibacterial agents in caries prevention, an effective carrier such as pH-responsive drug delivery nano micelle needs to be exploited to tackle this challenge.

Therefore, in the present study, a pH-responsive nano micelle [methoxypolyethylene glycol-b-poly-2-(diisopropylamino) ethyl methacrylate (mPEG-b-PDPA)] with and without bedaquiline loading was synthesized using ATRP (atom transfer radical polymerization). Its physical characterization was carried out by Hydrogen-1 nuclear magnetic resonance (^{1}H-NMR), gel permeation chromatography (GPC), critical micelles concentrations (CMC), dynamic light scattering (DLS), and transmission electron microscopy (TEM). The cytotoxic effect on the periodontal cells and the antibacterial effect of micelles on *S. mutans* and the bactericidal effect on mature *S. mutans* biofilm were determined.

MATERIALS AND METHODS

Materials

Methoxypolyethylene glycol-OH (mPEG, MW2000); α-bromoisobutyryl bromide (EBiB, 98%, 195.05 g mol^{-1}); 2,2-dipyridyl (bPy, 99%, 156.19 g mol^{-1}); cuprous bromide (CuBr, 99%, 143.15 g mol^{-1}); N,N,N′,N′,N′-pentamethyldiethylenetriamine (PMDETA, 173.3 g mol^{-1}); dichloromethane (DCM); triethylamine; tetrahydrofuran (THF); and phosphotungstic acid were purchased from Macklin (Shanghai, China). 2-(Diisopropylamino) ethyl methacrylate (DPA) was purchased from Sigma-Aldrich (Merck KGaA, German). Bedaquiline was purchased from MedChemExpress (United States).

Synthesis of Methoxypolyethylene Glycol-Br Macroinitiator

The preparation of mPEG-Br macroinitiator followed the method in a previous study with some modifications as described below (Yu et al., 2011). mPEG (2 g, 1 mmol) was dissolved in 10 ml of DCM in a Schlenk flask followed by the addition of triethylamine (416 μl, 3 mmol). α-Bromoisobutyryl bromide (371 μl, 3 mmol) was quickly dropped into the mPEG DCM solution and immediately sealed for 2 h in ice bath. The reaction continued overnight at room temperature. The product was purified by filtration, rotary evaporation, dialyzing (MWCO 1000 Da) against Milli-Q water, and dried by lyophilizing.

Synthesis of Methoxypolyethylene-b-Poly-2-(Diisopropylamino) Ethyl Methacrylate Diblock Copolymer *via* Atom Transfer Radical Polymerization

The synthesis of mPEG-b-PDPA diblock copolymer essentially followed the method in previous studies (Du and Armes, 2005). Macroinitiator mPEG-Br (430 mg, 0.2 mmol) and 2,2-dipyridyl (62.5 mg, 0.4 mmol) were dissolved in 35 ml of DMF/DI water mixture (v/v 4:1, Schlenk flask), stirring 15 min in an ice bath. DPA (4.74 ml, 20 mmol) was added and immediately degassed by three nitrogen cycles. Anhydrous CuBr (290 mg, 2 mmol) was immediately added and degassed by three nitrogen cycles. The

polymerization was carried out at 40°C for 12 h. The product was purified by dialyzing against Milli-Q water (MWCO 3500 Da). Two milligrams of PMDETA was added to the first few dialysis cycles to replace the Cu ions in the product and the Cu ions were removed until no blue product precipitated. Then the product was dialyzed for another 3–5 cycles and dried by lyophilizing.

Preparation of Methoxypolyethylene Glycol-b-Poly-2-(Diisopropylamino) Ethyl Methacrylate Micelles

Typically, 10 mg of mPEG-b-PDPA diblock copolymer was dissolved in 1 ml of THF. The mPEG-b-PDPA micelles were formed by adding the solution into 4 ml PBS (pH 7.4, 1 mmol L^{-1}) dropwise, while stirring it for 12 h to volatilize the THF. The micelles were further purified by dialyzing against Milli-Q water (MWCO 3500 Da) and the precipitate was collected by centrifugation (14,000 rpm, 10 min, repeat 4 times). The storage micelle dispersion solution was prepared by adding 400 μl Milli-Q water (free micelles: 25 mg ml^{-1} mPEG-b-PDPA). The bedaquiline-loading micelles (10 mg ml^{-1} bedaquiline if it was completely encapsulation) were prepared as follows. In brief, 4 mg of bedaquiline was dissolved in 1 ml THF solution containing 10 mg of mPEG-b-PDPA diblock copolymer, followed by adding this solution dropwise into 4 ml PBS. The following protocol was exactly the same as those of mPEG-b-PDPA micelles' synthesis.

Structural Characterizations of Polymers and Micelles

The ^{1}H-NMR spectra of mPEG-Br and mPEG-b-PDPA dissolving in D_2O and CD_2Cl_2 were recorded with Bruker AVANCE III HD 400 MHz. The molecular weight and polydispersity index (PDI) of mPEG-b-PDPA polymer were acquired from GPC, THF was selected as the eluent. The hydrodynamic size diameter and zeta-potential of free micelles and bedaquiline-loading micelles at different pH values (5–7.4) were measured by dynamic light scattering (DLS, Zetasizer μV, Malvern).

pH Titration of Methoxypolyethylene Glycol-b-Poly-2-(Diisopropylamino) Ethyl Methacrylate Copolymers

The mPEG-b-PDPA copolymer was first dissolved in 0.1 N (0.1 mol L^{-1}) HCl to prepare a stock solution at a concentration of 5 mg ml^{-1}. pH titration was carried out by adding 20 μl increments of 0.1 N (0.1 mol L^{-1}) NaOH solution under stirring. The increase in pH in the range of 3–8 was monitored as a function of the total added volume of NaOH (V_{NaOH}). The pH values were measured using pH meter.

Measurement of Critical Micelles Concentrations

The CMC of the free micelles was determined by surface tension (platinum Wilhelmy plate). A set of solutions (1 ml) with different copolymer concentrations were dropped into 20 ml PBS under stirring to prepare the micelles solutions. The surface tension of micelles solutions was measured using Force Tensiometer (Sigma 700/701, Biolin Scientific, Sweden) and the CMC were calculated using the software OneAttension.

Bedaquiline-Loading Ratio and Encapsulation Efficiency

Ten microliters of the bedaquiline-loading micelles and free micelles were dissolved in 1 ml of THF solution. The absorption (309_{nm}) of these two solutions was determined by UV-Vis spectra. Based on the standard curve of UV-Vis absorption of a set of bedaquiline THF solutions with defined concentrations, the bedaquiline-loading weight (m3) was determined. The bedaquiline-loading ratio and encapsulation efficiency were calculated as follows:

$$\text{Loading ratio} = m3/m1 \times 100\%$$

$$\text{Encapsulation efficiency} = m3/m2 \times 100\%$$

where m1 is the weight of the nanoparticles, and m2 is the total weight of bedaquiline fed.

Transmission Electron Microscopy Imaging of Free Micelles

The storage micelles diluted 10^6 times were negatively stained using 1% freshly prepared phosphotungstic acid (w/v%, PBS, pH 7), and then dropped on the copper grid and dried. The images of micelles were captured under TEM.

The Cumulative Release of Bedaquiline in Different pH Buffer

The 0.1 M PBS buffers of pH 5, 6, and 7.4 were prepared. Ten microliters of the bedaquiline-loading micelles and free micelles were separately mixed in 1 ml of PBS buffers with different pH. The release of bedaquiline was determined by UV-Vis spectra ($\lambda = 309_{nm}$) until the cumulative release reached close to 100%.

The Antibacterial Activity of Micelles

Both the bacterial killing and the antibiofilm formation efficacy of micelles and bedaquiline-loaded micelles in pH 5 and 7 condition were assessed. The fourfold dilution of the storage micelle solution was prepared as working solution [if there was no loss (ideal situation): free micelles, 6 mg ml^{-1} mPEG-b-PDPA; bedaquiline-loaded micelles, 2.5 mg ml^{-1} bedaquiline]. In brief, study solutions containing 1, 0.5, or 0.1% working solution were mixed with BHI medium at pH 5 or 7 in a sterile 96-well plate and incubated with *Streptococcus mutans* UA159 (ATCC10449; mid-logarithmic stage, 10^6 CFU ml^{-1}) under anaerobic condition at 37°C for 24 h. For the BHI medium for biofilm formation, 1% (w/v%) of sucrose solution was added at a ratio of 1:100. Then the absorption value at 600_{nm} was measured to assess bacterial growth.

Live/Dead Bacteria Staining

Streptococcus mutans UA159 was incubated in BHI containing 1% sucrose at 37°C for 24 h in sterile 96-well microplates to

form a mature biofilm on cover glass. Then different ratios of micelle solutions were mixed with fresh BHI (pH 7.4) and applied onto the biofilms. The different solutions contained were sterile Milli-Q water, 1, 0.5, and 0.1% working solutions, including free micelles and bedaquiline-loading micelles (corresponding bedaquiline-loading concentrations: 25, 12.5, and 2.5 $\mu g\ ml^{-1}$). After 2 h, the cover glasses with biofilm were gently washed with PBS to remove the unattached bacteria and stained with SYTO9 and propidium iodide for 30 min (Invitrogen^{TM}, United States). The stained samples were imaged with Olympus Fluoview FV1000.

Cytotoxicity Assay

The *in vitro* cytotoxicity of micelles was evaluated by CCK-8 assay using periodontal ligament stem cells (PDLSCs, P5). In brief, PDLSCs (5,000 cells/well) were seeded in 96-well microplates and incubated at 37°C for 24 h. Subsequently, the medium was replaced by fresh culture media containing 1, 0.5, and 0.1% working micelles solutions for further cultivation of 24 and 48 h. Then cell counting kit-8 (CCK8, DOJINDO, Japan) solution was added into each well and incubated in the dark at 37°C for 2 h. Finally, the absorption values were measured by a microplate reader at 450_{nm}. Five parallel groups were used for each group.

Statistical Analysis

Each of the above-described tests was repeated three times to generate data for analysis. All data were statistically analyzed using SPSS Statistics v17 and the figures were drawn using GraphPad. *T*-test and one-way analysis of variance (ANOVA) were performed to assess the statistical significance of the differences in means among groups, with the significance level set at 0.05.

RESULTS AND DISCUSSION

Synthesis and Characterization of Polymers

In this study, well-defined poly (ethylene glycol)-block-poly [2-(diisopropylamino) ethyl methacrylate] (mPEG-b-PDPA) diblock copolymers were obtained *via* atom transfer radical polymerization (ATRP, see **Figure 1A**). The copolymer had polymer molecular weights Mw: 20,941 and Mn: 16,271 as measured by GPC, and polydispersity indices (PDI) of 1.28 (**Table 1**). The ^{1}H-NMR spectra of PEG-Br and mPEG-b-PDPA are shown in **Figures 1B,C**. The methyl protons of the α-bromoisobutyryl bromide group of PEG-Br showed the characteristic chemical shift at 3.562 ppm, which indicates the successful synthesis of PEG-Br macroinitiator (**Figure 1B**). The chemical shift at 1.120 and 3.060 ppm was the unreacted triethylamine. It has been removed by the repeat dialysis. For the spectra of mPEG-b-PDPA (**Figure 1C**), the newly appeared chemical shifts located at 0.75, 0.92, 1.65, 2.52, 2.90, and 3.73 ppm were due to the resonance of PDPA. The integrals ratio of PEG block and PDPA block was similar to the added molar ratio (0.2:20 mmol), and the estimate was 44:(102–112). These test results verified the successful synthesis of mPEG-b-PDPA copolymer with low polydispersity. Compared with the synthesis of other pH-responsive nanopolymers, the synthesis of mPEG-b-PDPA is simple (Horev et al., 2015; Deirram et al., 2019; Naha et al., 2019; Zhao et al., 2019; Liang et al., 2020).

In addition, pH titration results of mPEG-b-PDPA copolymers (**Figure 2A**) showed that when NaOH was continuously added dropwise, a sharp turn of pH curve occurred at pH 6 and remained at this level. This phenomenon is probably because of the deprotonation of DPA tertiary ammonium groups (Zhou et al., 2011), and is in agreement with the acid dissociation constant of PDPA segment (pKa = 6.3) (Yu et al., 2011).

The UV-Vis spectra results showed that the bedaquiline-loading weight (m3) was 3.7 mg. It was calculated that 1 ml of storage micelles contained *ca.* 9.25 mg bedaquiline. The bedaquiline-loading ratio and encapsulation efficiency of mPEG-b-PDPA were calculated as 37 and 92.5%, respectively (m1 = 10 mg, m2 = 4 mg). This micelle displays a good hydrophobic agent encapsulation capacity (Horev et al., 2015; Qing et al., 2019).

Physical Characterization of Micelles

mPEG-b-PDPA micelles were prepared with and without bedaquiline-loading. First, we measured the diameter of micelles in different pH aqueous solution using DLS (**Table 2**). All micelles showed relatively narrow size distribution (polydispersity < 0.3). At pH 7.4, free micelles had a diameter of around 322.4 ± 2.69, while the diameter of bedaquiline-loaded micelles slightly decreased (260.2 ± 2.02, $p < 0.05$). At pH 6, the diameter of micelles with and without bedaquiline-loading increased significantly (1,133.0 ± 40.43 and 905.8 ± 35.73), and the diameter could not be measured at pH 5.

In this study, the changes of nanometer size in different pH solutions are consistent with the pH-responsive property of PDPA and the pH titration results. When the environmental pH drops below the pK_a (pH < 6), the protonation of PDPA segment shifts the hydrophobic in the core to hydrophilic, the drug is released, and the spherical nano structure of micelle swells and even disassembles (Deirram et al., 2019). This property of regulating drug release through protonation and deprotonation is shared by pH-responsive materials (Belkova et al., 2005; Horev et al., 2015; Bazban-Shotorbani et al., 2017), which makes them regulate drug release in a more precise environment. The PDPA segment selected in this study can start to release the drug in an environment below pH 6, which enables the drug to enter the local cariogenic environment at a good opportune moment and to exert its bactericidal effect. This property is important for clinical application because the initiation of dental decay occurs in the acidic environment between pH 4.5–5.5 caused by acid-resistant pathogens (Bowen et al., 2018).

The spherical core-shell morphology of the free micelles is shown in the TEM images, especially in **Figure 2Bii**. However, the diameter of nano micelles in the TEM images is larger than the result of DLS, which may be related to the treatment of phosphotungstic acid. During the sample preparation process, the prepared neutral phosphotungstic acid solution may have been slightly acidified, resulting in swelling of the nanomicelles.

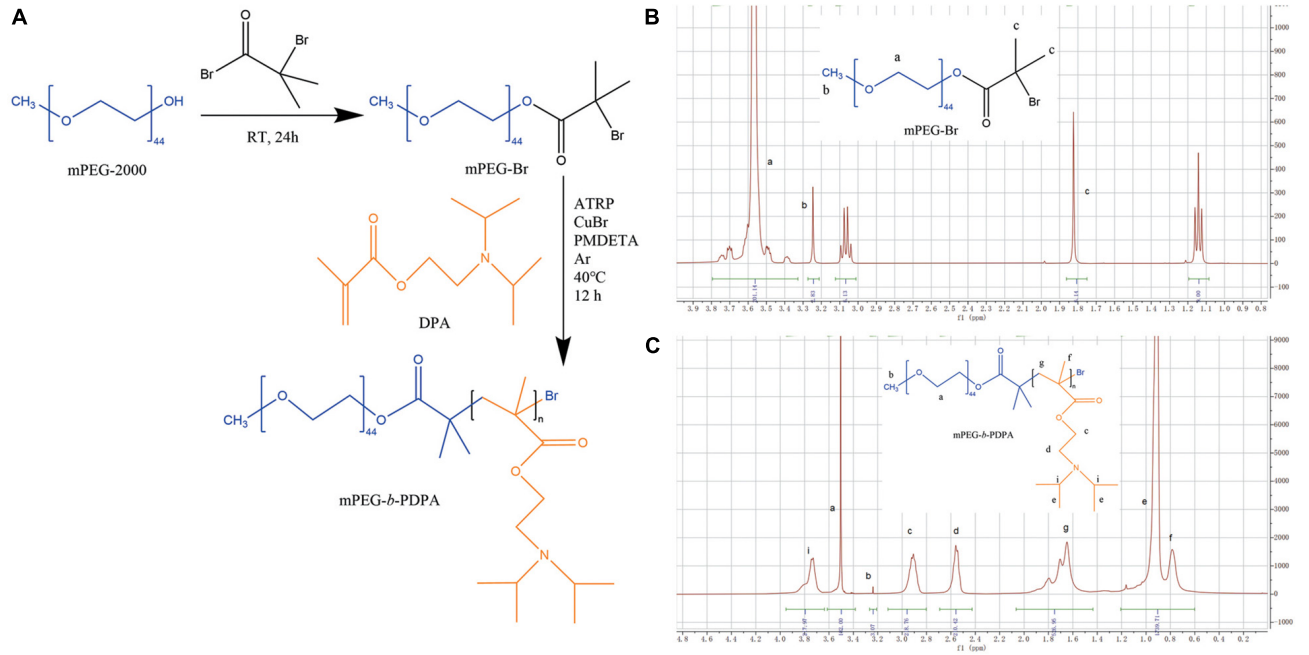

FIGURE 1 | Synthetic routes of methoxypolyethylene glycol-b-poly-2-(Diisopropylamino) ethyl methacrylate (mPEG-b-PDPA) **(A)** and hydrogen-1 nuclear magnetic resonance (^{1}H-NMR) spectra of mPEG-Br in D_2O **(B)** and PEG-b-PDPA in CD_2Cl_2 **(C)**.

The size of the micelles in this study is 300_{nm}, which is larger than that of the micelles synthesized by other researches (Horev et al., 2015; Zhao et al., 2019). The micelle itself usually has no antibacterial effect (Natan and Banin, 2017; Qing et al., 2019; Zhao et al., 2019), but its size may affect its ability to penetrate into biofilm, its drug loading, and its encapsulation ability. So far, no articles report on the influence of micelle size on its antibacterial ability. This is different from the metal nano materials (Natan and Banin, 2017; Paula and Koo, 2017), for example, the size of silver nanoparticles significantly affects its antibacterial capability, and nanoparticles with smaller sizes generally show greater antibacterial effects (Choi et al., 2008; Sotiriou and Pratsinis, 2010). So, it is necessary to explore the influence of micelle size on its properties in future studies.

In addition, zeta potentials results showed that the micelles in aqueous solution were positively charged under neutral and acidic environments (**Table 2**). At pH 7.4, the zeta potential of both the free micelle group ($\zeta = 39.8 \pm 0.45$ mV) and the bedaquiline-loaded micelle group ($\zeta = 47.1 \pm 0.74$ mV) exceeded 30 mV. This indicates that the synthesized micelles were colloidally stable at pH 7.4 (Pate and Safier, 2016), which is a vital property of micelles. The free micelles group at pH 5 was also stable, with a zeta potential at 47.8 ± 2.84 mV. However, the zeta potentials (absolute value) of the free micelles at pH 6 and the bedaquiline-loading micelles at pH 5–6 were lower than 5 mV, indicating these micelles were unstable. These findings are consistent with the results of size detection and pH-response characterization. The incomplete protonation of PDPA segment in acidic milieus (pH 6) triggered the swelling of micelles and turned the micelles into an unstable state. With the complete protonation of PDPA segment at pH 5 the micelles dissembled, i.e., not existing as a core-shell structure, but became stable. In addition, the loaded hydrophobic agent had a negative effect on the stability of micelles in a pH 5 environment.

It should be noted that the micelles in neutral environment are positively charged, which may contribute to the capability of micelles to coat tooth surface and promote bacterial adhesion by electrostatic adsorption. Previous studies found many factors, including energy, charge, composition, stiffness, and hydrophobicity of tooth surface (Belas, 2014; Song et al., 2015, 2017; Teschler et al., 2015), as well as size, charge, and ionic strength of micelles (Paula and Koo, 2017; Narayanan et al., 2020; Li and Liu, 2021), can affect the binding between micelles and tooth surfaces. These binding-promoting properties of micelles should be further studied to improve their clinical application potential.

TABLE 1 | Molecular weight results of mPEG-b-PDPA polymer based on GPC.

Composition	Mw	Mn	PDI	CMC (mg L^{-1})
mPEG-b-PDPA	20,941	16,271	1.28	3.8

mPEG-b-PDPA, methoxypolyethylene glycol-b-poly-2-(diisopropylamino)ethyl methacrylate; GPC, gel permeation chromatography; PDI, polydispersity index; CMC, critical micelles concentrations.

Bedaquiline Release of Micelles

Bedaquiline release from the micelles is displayed in **Figure 2C**. At pH 7, the rate of release of bedaquiline was very gentle, not exceeding 35% in the first 12 h, and the cumulative release

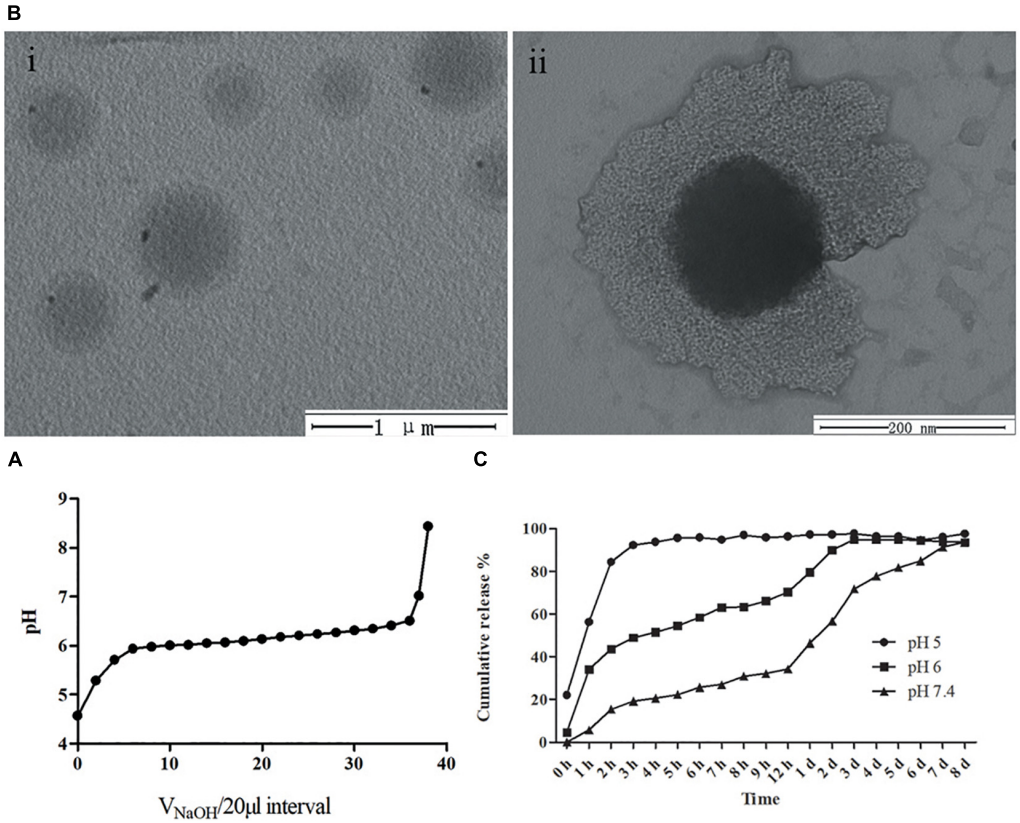

FIGURE 2 | (A) pH titration curve of mPEG-b-PDPA polymer; **(B)** transmission electron microscopy (TEM) image of free micelles at pH 7 **(i)**, and typical core-shell structure image of micelle **(ii)**. **(C)** Cumulative drug release curves of bedaquiline-loading micelles at pH 5, 6, and 7.4 PBS buffer.

reached over 90% only after 8 days. At pH 6, the amount released within 12 h reached 70.3%, and this reached 94.8% on the third day. At pH 5, the amount released reached 92.2% in 3 h. These findings show the bedaquiline-release of mPEG-b-PDPA mainly relay on the pH-sensitive properties of PDPA block (Yu et al., 2011, 2013). Under neutral pH conditions, the PDPA block is hydrophobic, and the hydrophilic PEG surrounds the PDPA to form a core-shell structure. Hydrophobic agents such as bedaquiline can be encapsulated by the micelle. When the micelle is put in acidic environments (pH < 6), protonation of the PDPA block converts it into hydrophilic. Then, the micelle will gradually swell and the core-shell structure will dissemble, releasing the bedaquiline in the core (see the **Scheme 1**). This is the most common mechanism of pH-responsive nanocarrier materials. This kind of pH-responsive property allows the encapsulated drug to be released rapidly and massively in a local acidic environment (Yu et al., 2011; Liu et al., 2016; Bazban-Shotorbani et al., 2017; Deirram et al., 2019), which greatly improves the local working concentration and efficiency.

TABLE 2 | Particle size and zeta potential of free micelles and bedaquiline-loading micelles based on DLS.

		Free micelles	Bedaquiline-loading micelles
pH 7.4	Size	322.4 ± 2.69	260.2 ± 2.02
	PDI	0.146 ± 0.03	0.145 ± 0.02
	ζ	39.8 ± 0.45	47.1 ± 0.74
pH 6	Size	905.8 ± 35.73	1133.0 ± 40.43
	PDI	0.248 ± 0.03	0.071 ± 0.01
	ζ	4.97 ± 1.03	–0.09 ± 0.15
pH 5	Size	–	–
	PDI	–	–
	ζ	47.8 ± 2.84	–0.36 ± 0.57

mPEG-b-PDPA, methoxypolyethylene glycol-b-poly-2-(diisopropylamino)ethyl methacrylate; GPC, gel permeation chromatography; PDI, polydispersity index; CMC, critical micelles concentrations; DLS, dynamic light scattering.

Antibacterial and Anti-biofilm Formation Effect of the Study Micelles

The antibacterial effect of the study micelles with and without bedaquiline loading on *S. mutans* in pH 5 and 7 are summarized in **Figure 3**. Compared with the control group, at pH 7, the growth of *S. mutans* suspension in all the free micelles groups and the bedaquiline-loaded micelles groups were not inhibited (**Figure 3A**). In the *S. mutans* biofilm model, free micelles had no inhibitory effect on biofilm formation at pH 7 (**Figure 3B**), while the inhibitory effect of the bedaquiline-loaded micelles increased with the concentration of bedaquiline-loaded micelles

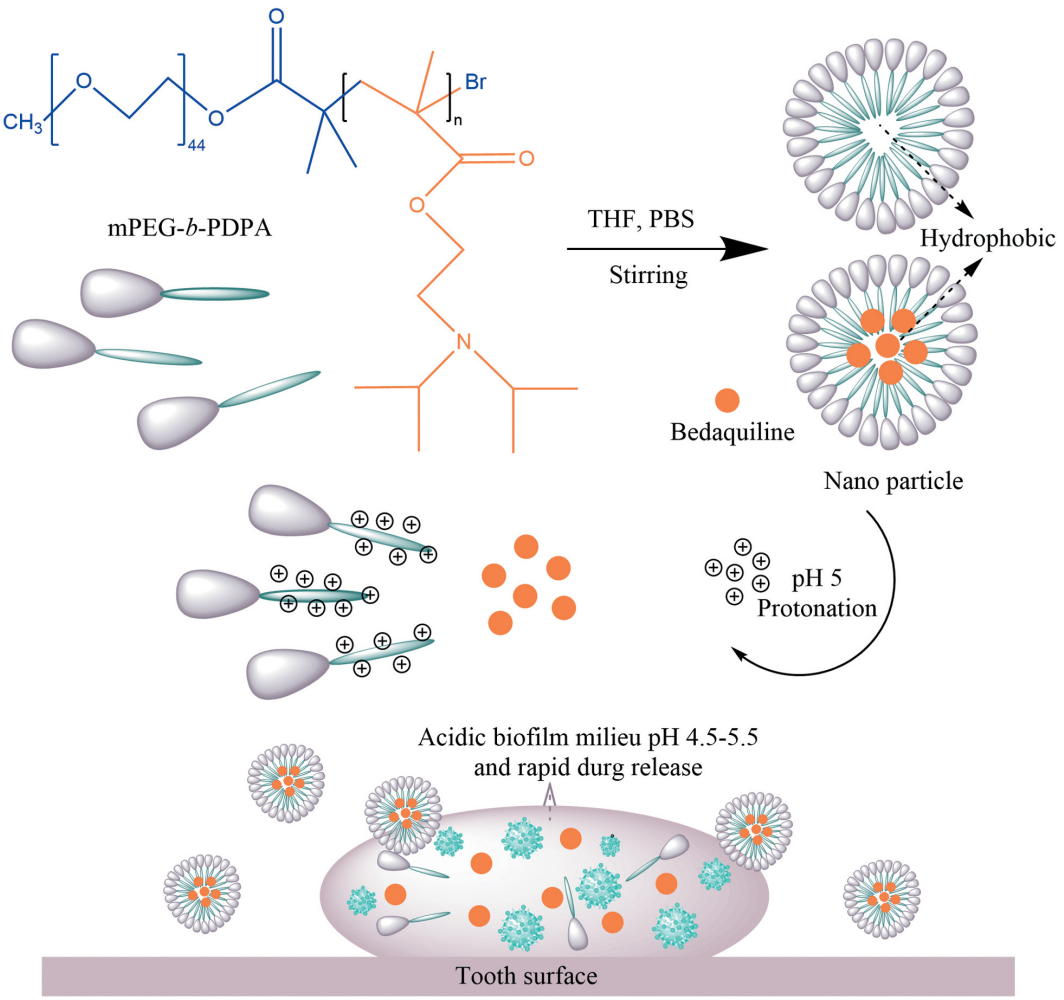

SCHEME 1 | Scheme Chemical formulas of diblock copolymer (mPEG-b-PDPA); Schematic representation for the formation and pH-responsive property of micelles; and the proposed mode of pH-responsive of micelles for biofilm penetration property.

($p < 0.05$). Among them, the 1% bedaquiline-loaded micelles group (contain *ca.* 25 μg ml^{-1} bedaquiline) reduced the growth rate of the bacteria to half that of the control ($p < 0.001$). Our pervious study had found that at pH 7, bedaquiline cannot inhibit the biofilm formation of *S. mutans* (Zhang et al., 2021). In order to figure out the reasons for these inconsistent results, we had conducted additional study to measure the pH change of medium during bacterial growth. It was found that without any intervention, when *S. mutans* planktonic bacteria were cultured for 24 h at pH 7, the pH of the medium dropped to about 5.8, while in the model where extra 1% sucrose was added to construct the *S. mutans* biofilm, the pH of the medium dropped to about 4.9 (data not shown). Therefore, we speculate that during biofilm development, when the pH of biofilm internal environment dropped to about 5, the nano micelles that had penetrated into the biofilm released the encapsulated bedaquiline and exerted a bactericidal effect. However, the pH of the suspended bacterial medium did not reach the level at which the encapsulated bedaquiline would be released, so no inhibitory effect was detected in the suspension groups. The inhibitory effect of bedaquiline-loaded micelles on *S. mutans* biofilm formation at neutral environment also indicates that the study nano micelles can penetrate into the biofilm and release antibacterial agent in an acidic environment.

When *S. mutans* was incubated in an acidic environment, the acidic environment itself had an inhibitory effect on the bacterial growth (see the control group in **Figures 3A–D**). At pH 5, bedaquiline-loaded micelles further significantly inhibited the growth of planktonic bacteria and also the formation of biofilms (**Figures 3C,D**). In the model of *S. mutans* suspension at pH 5 (**Figure 3C**), the free micelles groups did not show a significant antibacterial effect. While in the 0.1% bedaquiline-loaded micelles group [contain *ca.* 2.5 μg ml^{-1} bedaquiline (IC_{50})] the growth of *S. mutans* in suspension was significantly reduced to half ($p = 0.015$). The growth of *S. mutans* in the 0.5% and the 1% bedaquiline-loaded micelles groups was even lower ($p = 0.003$ and $p < 0.001$). In the *S. mutans* biofilm model at pH 5 (**Figure 3D**), compared with the control, the free

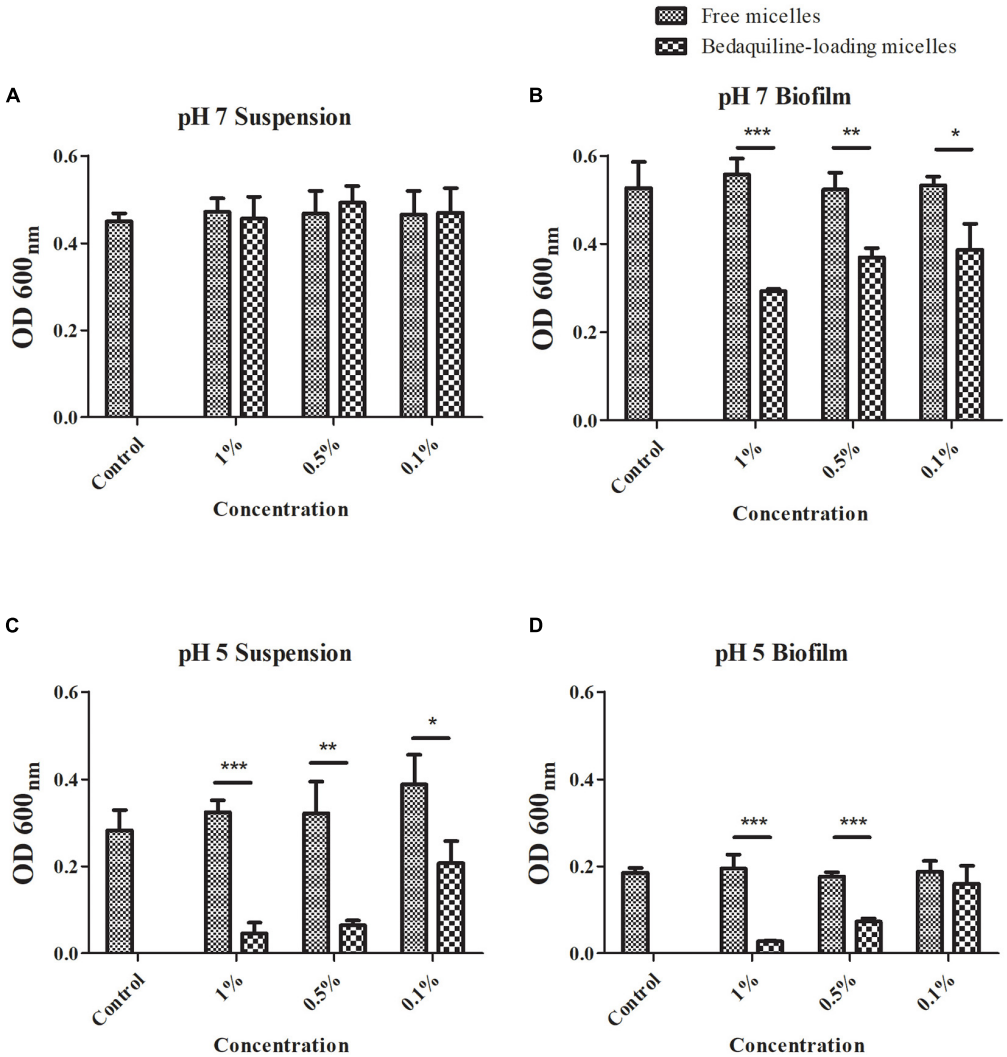

FIGURE 3 | Antibacterial effect of free micelles and bedaquiline-loading micelles at pH 7 and 5 BHI broth. At pH 7, antibacterial effect of free micelles and bedaquiline-loading micelles at 0.1, 0.5, and 1% ratio (v/v%) against **(A)** *Streptococcus mutans* suspension and **(B)** biofilm formation. At pH 5, antibacterial effect of free micelles and bedaquiline-loading micelles against **(C)** *S. mutans* suspension and **(D)** biofilm formation. $^{*}P < 0.05$, $^{**}P < 0.005$, and $^{***}P < 0.001$.

micelles groups and the 0.1% bedaquiline-loaded micelles group had no antibacterial effect ($p > 0.05$) while the 0.5% and the 1% bedaquiline-loaded micelles groups significantly inhibited the development of biofilm ($p < 0.001$).

Bacterial-Killing Effects of Bedaquiline-Loading Micelles Against Mature *Streptococcus mutans* Biofilm

The live/dead bacteria staining imaging of mature biofilms treated with micelles are shown in **Figure 4**. The images in the control and the free micelle groups, presence of dead bacteria (red staining) was not obvious. In contrast, the bedaquiline-loaded micelles had bactericidal effects which increased with the micelle concentration. In the 0.5% and the 1% groups, most of the bacteria in the biofilm were dead.

The stable and cohesive biofilm formed by *S. mutans* (Cross et al., 2006; Koo et al., 2013) can block the penetration of antibacterial agents, including bedaquiline (Zhang et al., 2021). This is a key self-protection property of biofilms. Dental biofilm mainly relies on exopolysaccharides to strengthen the interconnection between bacterial cells (Koo et al., 2013; Lin et al., 2021). Bedaquiline has no influence on the carbohydrate metabolism of *S. mutans*, while it can bind to H^{+}-ATPase and destroy the cell membrane, exerting a bactericidal effect (Zhang et al., 2021). The bactericide effect on mature biofilm found in the present study shows that the study nanomicelle drug delivery system facilitates the penetration of bedaquiline into bacterial biofilm, making the contact between bedaquiline and bacteria available, and then killing the bacteria inside the biofilm. Theoretically, any hydrophobic agents can be loaded by this nanocarrier system (mPEG-b-PDPA).

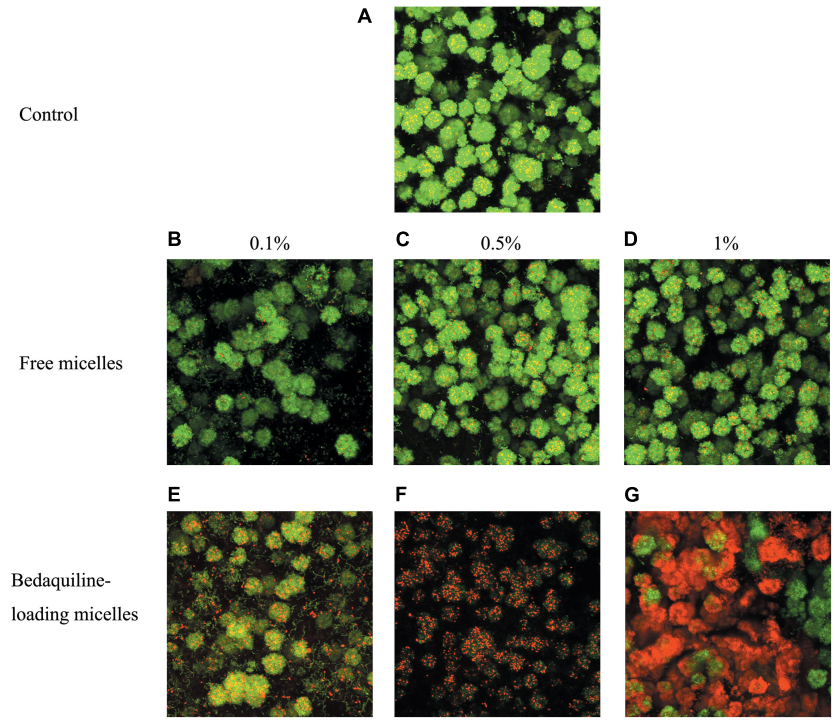

FIGURE 4 | Live/dead bacterial staining of *S. mutans* biofilm. Mature biofilm was shocked for 2 h by BHI broth (positive control **A**), free micelles at 0.1% **(B)**, 0.5% **(C)**, 1% **(D)** ratio (v/v%), and bedaquiline-loading micelles at 0.1% **(E)**, 0.5% **(F)**, 1% **(G)** (v/v%). Green, live bacteria; red, dead bacteria; yellow, merged image of live and dead bacteria.

Cytotoxicity Assay

To study the safety of this pH-responsive nanocarrier system, 48-h cytotoxicity assay of micelles on PDLSCs cells was evaluated. As shown in **Figure 5**, both micellar nanocarrier groups (unloaded and bedaquiline-loaded) did not exhibit significant cytotoxicity against PDLSCs cells at 24 and 48 h. Therefore, this pH-responsive nanomicelle is biocompatible and can be used safely for hydrophobic antibacterial drug delivery (Zhao et al., 2019).

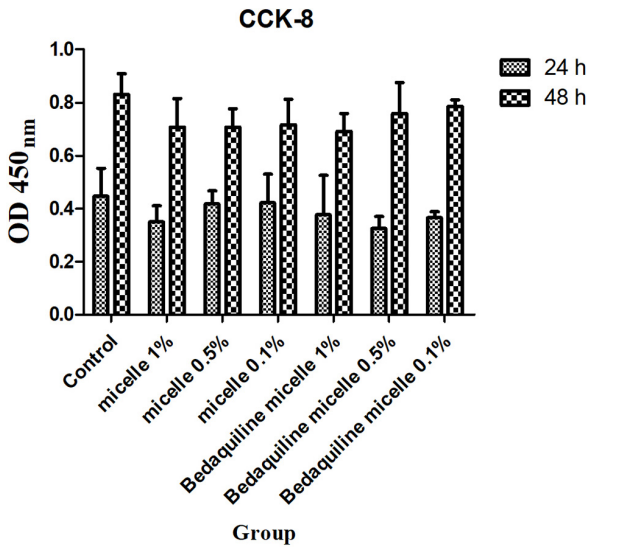

FIGURE 5 | Cytotoxicity assay of free micelles and bedaquiline-loading micelles at different concentrations.

Limitation of the pH-Responsive Nanocarrier Micelles

The study pH-responsive nanocarrier micelle, mPEG-b-PDPA, is simple to synthesize and can encapsulate hydrophobic antibacterial agents. Its good performance on antibacterial and bactericidal effects against *S. mutans* suspension and biofilm shows its clinical application potential. However, there are some limitations. First, the solvent used to prepare the micelles needs to be applicable for the hydrophobic antibacterial agents and be easy to remove. Second, due to the agent-loading to micelles weight ratio has not been optimized, this limits its application for hydrophobic antibacterial agents with high MIC values (over than 100 μg/ml). Third, this micelle-loading agent is a one-time release system, it is difficult to re-encapsulate agents and form micelles when the pH returns to neutral. Hence, a reversible micellar system capable of loading antibacterial agent needs further exploration.

CONCLUSION

To sum up, in this study a two-block micellar nanocarrier, mPEG-b-PDPA, was synthesized using a simple ATRP method.

The micelle surface is positively charge and can be loaded with hydrophobic drugs. The bedaquiline-loaded nano-micelles inhibit the growth of *S. mutans* in neutral and acidic environments, and have a good bactericidal effect on mature biofilm. Furthermore, it does not have any cytotoxic effect on periodontal cells. The study findings show that it has a good potential for clinical application in dental caries prevention.

DATA AVAILABILITY STATEMENT

The original contributions presented in the study are included in the article/supplementary material, further inquiries can be directed to the corresponding author.

AUTHOR CONTRIBUTIONS

MZ, ZY, and EL conceived this study and analyzed the data. MZ conducted the experiments and wrote the manuscript. All authors contributed to the article and approved the submitted version.

FUNDING

This work was financially supported by the grants from four sources, namely, the Tam Wah-Ching Endowed Professorship of the University of Hong Kong, the National Natural Science Foundation of China (No. 81903445), the Taishan Scholars Program of Shandong Province, and the Interdisciplinary Innovative Project of the Shandong University (No. 2020QNQT002).

ACKNOWLEDGMENTS

We would like to acknowledge Xuebo Dou from the Shandong University for his technical support.

REFERENCES

Bazban-Shotorbani, S., Hasani-Sadrabadi, M., Karkhaneh, A., Serpooshan, V., Jacob, K., Moshaverinia, A., et al. (2017). Revisiting structure-property relationship of pH-responsive polymers for drug delivery applications. *J. Control. Release* 253, 46–63. doi: 10.1016/j.jconrel.2017.02.021

Belas, R. (2014). Biofilms, flagella, and mechanosensing of surfaces by bacteria. *Trends Microbiol.* 22, 517–527. doi: 10.1016/j.tim.2014.05.002

Belkova, N., Shubina, E., and Epstein, L. (2005). Diverse world of unconventional hydrogen bonds. *Acc. Chem. Res.* 38, 624–631. doi: 10.1021/ar040006j

Bowen, W., Burne, R., Wu, H., and Koo, H. (2018). Oral biofilms: pathogens, matrix, and polymicrobial interactions in microenvironments. *Trends Microbiol.* 26, 229–242. doi: 10.1016/j.tim.2017.09.008

Chen, X., Guo, R., Wang, C., Li, K., Jiang, X., He, H., et al. (2021). On-demand pH-sensitive surface charge-switchable polymeric micelles for targeting *Pseudomonas aeruginosa* biofilms development. *J.Nanobiotechnol.* 19:99. doi: 10.1186/s12951-021-00845-0

Choi, O., Deng, K., Kim, N., Ross, L., Surampalli, R., and Hu, Z. (2008). The inhibitory effects of silver nanoparticles, silver ions, and silver chloride colloids on microbial growth. *Water Res.* 42, 3066–3074. doi: 10.1016/j.watres.2008.02.021

Cicuéndez, M., Doadrio, J., Hernández, A., Portolés, M., Izquierdo-Barba, I., and Vallet-Regí, M. (2018). Multifunctional pH sensitive 3D scaffolds for treatment and prevention of bone infection. *Acta Biomater.* 65, 450–461. doi: 10.1016/j.actbio.2017.11.009

Cross, S., Kreth, J., Zhu, L., Qi, F., Pelling, A., Shi, W., et al. (2006). Atomic force microscopy study of the structure-function relationships of the biofilm-forming bacterium *Streptococcus mutans*. *Nanotechnology* 17, S1–S7. doi: 10.1088/0957-4484/17/4/001

Deirram, N., Zhang, C., Kermaniyan, S., Johnston, A., and Such, G. (2019). pH-responsive polymer nanoparticles for drug delivery. *Macromol. Rapid Commun.* 40:e1800917. doi: 10.1002/marc.201800917

Du, J., and Armes, S. (2005). pH-responsive vesicles based on a hydrolytically self-cross-linkable copolymer. *J. Am. Chem. Soc.* 127, 12800–12801. doi: 10.1021/ja054755n

Filoche, S., Wong, L., and Sissons, C. (2010). Oral biofilms: emerging concepts in microbial ecology. *J. Dent. Res.* 89, 8–18. doi: 10.1177/0022034509351812

Gao, L., Xu, T., Huang, G., Jiang, S., Gu, Y., and Chen, F. (2018). Oral microbiomes: more and more importance in oral cavity and whole body. *Protein cell* 9, 488–500. doi: 10.1007/s13238-018-0548-1

Hannig, M., and Hannig, C. (2010). Nanomaterials in preventive dentistry. *Nat. Nanotechnol.* 5, 565–569. doi: 10.1038/nnano.2010.83

Horev, B., Klein, M. I., Hwang, G., Li, Y., Kim, D., Koo, H., et al. (2015). pH-activated nanoparticles for controlled topical delivery of farnesol to disrupt oral biofilm virulence. *ACS Nano* 9, 2390–2404. doi: 10.1021/nn507170s

Hwang, G., Liu, Y., Kim, D., Sun, V., Aviles-Reyes, A., Kajfasz, J., et al. (2016). Simultaneous spatiotemporal mapping of in situ pH and bacterial activity within an intact 3D microcolony structure. *Sci. Rep.* 6:32841. doi: 10.1038/srep32841

Jiang, W., Wang, Y., Luo, J., Chen, X., Zeng, Y., Li, X., et al. (2020). Antimicrobial peptide GH12 prevents dental caries by regulating dental plaque microbiota. *Appl. Environ. Microbiol.* 86:e00527-20. doi: 10.1128/aem.00527-20

Kolenbrander, P., Palmer, R., Rickard, A., Jakubovics, N., Chalmers, N., and Diaz, P. (2006). Bacterial interactions and successions during plaque development. *Periodontology* 42, 47–79. doi: 10.1111/j.1600-0757.2006.00187.x

Koo, H., Allan, R., Howlin, R., Stoodley, P., and Hall-Stoodley, L. (2017). Targeting microbial biofilms: current and prospective therapeutic strategies. *Nat. Rev. Microbiol.* 15, 740–755. doi: 10.1038/nrmicro.2017.99

Koo, H., Falsetta, M., and Klein, M. (2013). The exopolysaccharide matrix: a virulence determinant of cariogenic biofilm. *J. Dent. Res.* 92, 1065–1073. doi: 10.1177/0022034513504218

Li, P., and Liu, T. (2021). The size effect in adhesive contact on gradient nanostructured coating. *Nanotechnology* 32:235704. doi: 10.1088/1361-6528/abe9e6

Liang, J., Liu, F., Zou, J., Xu, H., Han, Q., Wang, Z., et al. (2020). pH-responsive antibacterial resin adhesives for secondary caries inhibition. *J. Dent. Res.* 99, 1368–1376. doi: 10.1177/0022034520936639

Lin, Y., Chen, J., Zhou, X., and Li, Y. (2021). Inhibition *Streptococcus mutans* of biofilm formation by strategies targeting the metabolism of exopolysaccharides. *Crit. Rev. Microbiol.* 47, 667–677. doi: 10.1080/1040841x.2021.1915959

Liu, Y., Busscher, H., Zhao, B., Li, Y., Zhang, Z., van der Mei, H., et al. (2016). Surface-adaptive, antimicrobially loaded, micellar nanocarriers with enhanced penetration and killing efficiency in staphylococcal biofilms. *ACS Nano* 10, 4779–4789. doi: 10.1021/acsnano.6b01370

Mishra, R. K., Tiwari, S. K., Mohapatra, S., and Thomas, S. (2019). "Chapter 1-efficient nanocarriers for drug-delivery systems: types and fabrication," in *Nanocarriers for Drug Delivery*, eds S. S. Mohapatra, S. Ranjan, N. Dasgupta, R. K. Mishra, and S. Thomas (Amsterdam: Elsevier), 1–41.

Mura, S., Nicolas, J., and Couvreur, P. (2013). Stimuli-responsive nanocarriers for drug delivery. *Nat. Mater.* 12, 991–1003. doi: 10.1038/nmat3776

Naha, P., Liu, Y., Hwang, G., Huang, Y., Gubara, S., Jonnakuti, V., et al. (2019). Dextran-coated iron oxide nanoparticles as biomimetic catalysts for localized and pH-activated biofilm disruption. *ACS Nano* 13, 4960–4971. doi: 10.1021/acsnano.8b08702

Narayanan, A., Menefee, J., Liu, Q., Dhinojwala, A., and Joy, A. (2020). Lower critical solution temperature-driven self-coacervation of nonionic polyester underwater adhesives. *ACS Nano* 14, 8359–8367. doi: 10.1021/acsnano.0c02396

Natan, M., and Banin, E. (2017). From Nano to Micro: using nanotechnology to combat microorganisms and their multidrug resistance. *FEMS Microbiol. Rev.* 41, 302–322. doi: 10.1093/femsre/fux003

Pate, K., and Safier, P. (2016). "12-Chemical metrology methods for CMP quality," in *Advances in Chemical Mechanical Planarization (CMP)*, ed. S. Babu (Sawston: Woodhead Publishing), 299–325.

Paula, A., and Koo, H. (2017). Nanosized building blocks for customizing novel antibiofilm approaches. *J. Dent. Res.* 96, 128–136. doi: 10.1177/0022034516679397

Pitts, N. B., Zero, D. T., Marsh, P. D., Ekstrand, K., Weintraub, J. A., Ramos-Gomez, F., et al. (2017). Dental caries. *Nat. Rev. Dis. Prim.* 3:17030. doi: 10.1038/nrdp.2017.30

Pizzolato-Cezar, L., Okuda-Shinagawa, N., and Machini, M. (2019). Combinatory therapy antimicrobial peptide-antibiotic to minimize the ongoing rise of resistance. *Front. Microbiol.* 10:1703. doi: 10.3389/fmicb.2019.01703

Preiss, L., Langer, J., Yildiz, Ö, Eckhardt-Strelau, L., Guillemont, J., Koul, A., et al. (2015). Structure of the mycobacterial ATP synthase Fo rotor ring in complex with the anti-TB drug bedaquiline. *Sci. Adv.* 1:e1500106. doi: 10.1126/sciadv.1500106

Qing, G., Zhao, X., Gong, N., Chen, J., Li, X., Gan, Y., et al. (2019). Thermo-responsive triple-function nanotransporter for efficient chemo-photothermal therapy of multidrug-resistant bacterial infection. *Nat. Commun.* 10:4336. doi: 10.1038/s41467-019-12313-3

Song, F., Brasch, M., Wang, H., Henderson, J., Sauer, K., and Ren, D. (2017). How bacteria respond to material stiffness during attachment: a role of *Escherichia coli* flagellar motility. *ACS Appl. Mater. Interfaces* 9, 22176–22184. doi: 10.1021/acsami.7b04757

Song, F., Koo, H., and Ren, D. (2015). Effects of material properties on bacterial adhesion and biofilm formation. *J. Dent. Res.* 94, 1027–1034. doi: 10.1177/0022034515587690

Sotiriou, G., and Pratsinis, S. (2010). Antibacterial activity of nanosilver ions and particles. *Environ. Sci. Technol.* 44, 5649–5654. doi: 10.1021/es101072s

Takahashi, N. (2005). Microbial ecosystem in the oral cavity: metabolic diversity in an ecological niche and its relationship with oral diseases. *Int. Congr. Ser.* 1284, 103–112. doi: 10.1016/j.ics.2005.06.071

Teschler, J., Zamorano-Sánchez, D., Utada, A., Warner, C., Wong, G., Linington, R., et al. (2015). Living in the matrix: assembly and control of *Vibrio cholerae* biofilms. *Nat. Rev. Microbiol.* 13, 255–268. doi: 10.1038/nrmicro3433

Vroom, J., De Grauw, K., Gerritsen, H., Bradshaw, D., Marsh, P., Watson, G., et al. (1999). Depth penetration and detection of pH gradients in biofilms by two-photon excitation microscopy. *Appl. Environ. Microbiol.* 65, 3502–3511. doi: 10.1128/aem.65.8.3502-3511.1999

Yu, H., Xu, Z., Wang, D., Chen, X., Zhang, Z., Yin, Q., et al. (2013). Intracellular pH-activated PEG-b-PDPA wormlike micelles for hydrophobic drug delivery. *Polym. Chem.* 4, 5052–5055. doi: 10.1039/C3PY00849E

Yu, H., Zou, Y., Wang, Y., Huang, X., Huang, G., Sumer, B., et al. (2011). Overcoming endosomal barrier by amphotericin B-loaded dual pH-responsive PDMA-b-PDPA micelleplexes for siRNA delivery. *ACS Nano* 5, 9246–9255. doi: 10.1021/nn203503h

Zhang, M., Yu, W., Zhou, S., Zhang, B., Lo, E. C. M., Xu, X., et al. (2021). In vitro antibacterial activity of an FDA-approved H+-ATPase inhibitor, bedaquiline, against *Streptococcus mutans* in acidic milieus. *Front. Microbiol.* 12:647611. doi: 10.3389/fmicb.2021.647611

Zhao, Z., Ding, C., Wang, Y., Tan, H., and Li, J. (2019). pH-Responsive polymeric nanocarriers for efficient killing of cariogenic bacteria in biofilms. *Biomat. Sci.* 7, 1643–1651. doi: 10.1039/c8bm01640b

Zhou, K., Wang, Y., Huang, X., Luby-Phelps, K., Sumer, B. D., and Gao, J. (2011). Tunable, ultrasensitive pH-responsive nanoparticles targeting specific endocytic organelles in living cells. *Angew. Chem.* 50, 6109–6114. doi: 10.1002/anie.201100884

Conflict of Interest: The authors declare that the research was conducted in the absence of any commercial or financial relationships that could be construed as a potential conflict of interest.

Publisher's Note: All claims expressed in this article are solely those of the authors and do not necessarily represent those of their affiliated organizations, or those of the publisher, the editors and the reviewers. Any product that may be evaluated in this article, or claim that may be made by its manufacturer, is not guaranteed or endorsed by the publisher.

frontiers in Microbiology

REVIEW
published: 22 October 2021
doi: 10.3389/fmicb.2021.749685

Biofilm-Related Infections in Gram-Positive Bacteria and the Potential Role of the Long-Acting Agent Dalbavancin

*Alessandra Oliva[1], Stefania Stefani[2], Mario Venditti[1] and Enea Gino Di Domenico[3]**

[1] Department of Public Health and Infectious Diseases, "La Sapienza" University of Rome, Rome, Italy, [2] Laboratory of Molecular Medical Microbiology and Antimicrobial Resistance Research (Mmarl), Department of Biomedical and Biotechnological Sciences (Biometec), University of Catania, Catania, Italy, [3] Microbiology and Virology, IRCCS San Gallicano Institute, Rome, Italy

Infections caused by Gram-positive bacteria are a major public health problem due to their increasing resistance to antibiotics. *Staphylococcus* and *Enterococcus* species' resistance and pathogenicity are enhanced by their ability to form biofilm. The biofilm lifestyle represents a significant obstacle to treatment because bacterial cells become highly tolerant to a wide range of antimicrobial compounds normally effective against their planktonic forms. Thus, novel therapeutic strategies targeting biofilms are urgently needed. The lipoglycopeptide dalbavancin is a long-acting agent for treating acute bacterial skin and skin structure infections caused by a broad range of Gram-positive pathogens. Recent studies have shown promising activity of dalbavancin against Gram-positive biofilms, including methicillin-resistant *S. aureus* (MRSA), methicillin-resistant *S. epidermidis* (MRSE), and vancomycin-susceptible enterococci. This review outlines the mechanisms regulating biofilm development in *Staphylococcus* and *Enterococcus* species and the clinical impact of biofilm-related infections. In addition, it discusses the clinical implications and potential therapeutic perspectives of the long-acting drug dalbavancin against biofilm-forming Gram-positive pathogens.

Keywords: biofilm, dalbavancin, *Staphylococcus aureus*, Gram-positive, skin, soft tissue infections

OPEN ACCESS

Edited by:
Daniel Pletzer,
University of Otago, New Zealand

Reviewed by:
Kristi L. Frank,
Uniformed Services University of the Health Sciences, United States
Durg Vijai Singh,
Central University of South Bihar, India
Rosalia Cavaliere,
University of Technology Sydney, Australia
Oana Ciofu,
University of Copenhagen, Denmark

****Correspondence:***
Enea Gino Di Domenico
enea.didomenico@ifo.gov.it

Specialty section:
This article was submitted to Infectious Agents and Disease, a section of the journal Frontiers in Microbiology

Received: *29 July 2021*
Accepted: *04 October 2021*
Published: *22 October 2021*

Citation:
Oliva A, Stefani S, Venditti M and Di Domenico EG (2021) Biofilm-Related Infections in Gram-Positive Bacteria and the Potential Role of the Long-Acting Agent Dalbavancin. Front. Microbiol. 12:749685. doi: 10.3389/fmicb.2021.749685

INTRODUCTION

Gram-positive bacteria are the most common human pathogens associated with medical device-related infections and skin and soft tissue infections (SSTI) (Del Pozo and Patel, 2009; Kaye et al., 2019). *Staphylococcus aureus* is the leading pathogen of catheters and prosthetic related infections or in chronic ulcers, while *Enterococcus faecalis* and *Enterococcus faecium* have become prominent etiological agents of nosocomial infections worldwide (Tong et al., 2015; Guzman Prieto et al., 2016). The global prevalence of drug-resistant strains of Gram-positive bacteria is increasing. Specifically, community- and hospital-acquired infections caused by Methicillin-resistant *S. aureus* (MRSA) and vancomycin-resistant *E. faecium* (VRE) have become a serious concern (Huang et al., 2019).

The increasing prevalence of drug-resistant pathogens is further worsened by observing that pathogenic Gram-positive bacteria are particularly predisposed to form biofilms (Lebeaux et al., 2014). In hospital settings, biofilms are implicated in the pathogenesis of approximately 80% of chronic microbial infections or medical device-associated infections (MDI)

(Römling and Balsalobre, 2012; Lebeaux et al., 2014). Furthermore, the biofilm lifestyle provides a broad and intrinsic multidrug tolerance allowing bacterial cells to survive a transient exposure to antibiotics without developing resistance (Di Domenico et al., 2019; Nguyen et al., 2020). Indeed, antibiotic resistance is genetically acquired by horizontal gene transfer or mutations, while the biofilm-related tolerance constitutes a multi-layered defense mechanism requiring slow-growing or non-dividing persister cells, poor antibiotic penetration, and adaptive stress responses (Lebeaux et al., 2014; Nguyen et al., 2020). Thus, the development of antibiotics with anti-biofilm activity represents a recognized need.

Dalbavancin is a semisynthetic lipoglycopeptide antibiotic structurally related to teicoplanin, with a long half-life and a unique dosage regimen, allowing for a single 1,500 mg dose or a two-dose (1,000 mg at day 1 and 500 mg at day 8) regimen (Boucher et al., 2014; Dunne et al., 2016). This antibiotic has a broad spectrum of action against Gram-positive cocci, including MRSA, and is approved for the treatment of SSTI (Arrieta-Loitegui et al., 2020). There is a growing amount of evidence that dalbavancin could be useful in other invasive Gram-positive infections that need prolonged intravenous treatments, including osteomyelitis, prosthetic joint infections (PJI), infective endocarditis, and catheter-related bacteremia (David et al., 2017). In addition, recent studies conducted *in vitro* and on human and animal models demonstrated that dalbavancin might also be effective against bacterial biofilms produced by staphylococci and enterococci (Knafl et al., 2017; Neudorfer et al., 2018; Silva et al., 2020; Žiemytė et al., 2020).

This review highlights the basic mechanisms regulating biofilm development in Gram-positive bacteria in the most clinically relevant infections along with the general principles of antimicrobial treatment of biofilm-associated infections. In addition, this review summarizes the current understanding and potential therapeutic activity of dalbavancin against *in vitro* and *in vivo* models of biofilm-related infections caused by Gram-positive bacteria.

Role of Biofilms in Gram-Positive Infections

Immediately after placing a medical device into the patient's body, biomaterials are rapidly coated with a conditioning film, a layer of the host organic elements absorbed onto the substratum. This conditioning layer generally provides a favorable substrate for bacteria to attach to the implant (Neoh et al., 2017). The adhesion of planktonic cells to the implant surface is the first step toward biofilm formation (Berne et al., 2018). In staphylococci, the adhesion to human tissue or indwelling medical devices is regulated by a large variety of surface-anchored proteins that bind to host tissues and cells, referred to as microbial surface components recognizing adhesive matrix molecules (MSCRAMMs) (Foster, 2019). These proteins are also present on *Enterococcus faecalis* and *Enterococcus faecium* and are required in the first step of human tissues colonization (Sava et al., 2010). There are two families of MSCRAMM molecules related to clumping factor A (ClfA) of *S. aureus* and serine-aspartate repeat protein G (SdrG) of *S. epidermidis* and another group referred to as the collagen-binding protein of *S. aureus* (the Cna family) (Foster, 2019). A single MSCRAMM protein performs several functions as binding to a diverse array of host ligands. Those molecules allow for unspecific attachment mediated by hydrophobic, electrostatic hydrogen-bonding, and van der Waals interactions with complementary receptors present in the conditioning film (Katsikogianni and Missirlis, 2004). In the early stages of biofilm growth, adherent cells are loosely associated with a surface. This is called the reversible attachment stage (Berne et al., 2018). During this phase complete eradication of the MDI can be achieved by the careful surgical debridement of tissue and bone marrow, and local antimicrobial therapy to eliminate planktonic bacteria (Høiby et al., 2015; Masters et al., 2019; da Silva et al., 2021). Indeed, in the early onset of a MDI, a major role is played by the potent virulence response of the infectious pathogen, which causes tissue destruction that may sometimes culminate in fulminant infections (Zimmerli et al., 2004; Masters et al., 2019; Seebach and Kubatzky, 2019). After the initial bacterial attachment to a surface, intracellular accumulation and biofilm maturation occur (Nguyen et al., 2020). The presence of a mature biofilm in either the local tissue or the implant requires more radical procedures (i.e., the complete removal of the implant) and prolonged therapies, often by the intravenous route, to remove the infection (Masters et al., 2019). During biofilm maturation, individual cells enter the irreversible attachment stage, and the bacterial cells produce the biofilm matrix. The irreversible attachment can be modulated by environmental factors such as pH, hydrodynamics, nutrient availability, temperature, osmolarity, oxygen, or other host factors (Palmer et al., 2007; Lister and Horswill, 2014; Berne et al., 2018). At this stage, mature biofilms are highly tolerant to host immune defenses, stresses, starvation, dehydration and cannot be eradicated by antibiotic treatments alone (Masters et al., 2019). In staphylococci and enterococci, similar factors contribute to the biofilm matrix composition including polysaccharides, proteins, teichoic and lipoteichoic acids, and extracellular DNA (eDNA) (Ch'ng et al., 2019; Karygianni et al., 2020). In staphylococci, the polysaccharide intercellular adhesin (PIA), also known as poly-N-acetyl glucosamine (PNAG), according to the chemical composition (Nguyen et al., 2020) is an important adhesive molecule during biofilm formation. The biosynthesis and accumulation of PIA on the bacterial surface are regulated by the intercellular adhesion (*ica*) gene locus products, including the *ica*A, *ica*D, *ica*B, and *ica*C genes. Although PIA plays a central role in staphylococcal biofilm, several studies have demonstrated that biofilm formation can be accomplished by *S. epidermidis* and *S. aureus* isolates in the absence of the *ica* operon by a PIA-independent mechanism (Otto, 2018; Nguyen et al., 2020). This process is particularly relevant to methicillin-resistant *S. aureus* (MRSA) strains where biofilm formation depends mainly on proteins rather than polysaccharides (McCarthy et al., 2015). In *E. faecalis*, the *dlt*ABCD operon is required to obtain d-alanine esters of lipoteichoic acids, which is an essential constituent of the Gram-positive bacterial cell wall (Ch'ng et al., 2019). A deletion mutant of the *dlt*A gene in *E. faecalis* produces significantly less biofilm *in vitro*, reduced

adherence to epithelial cells, and increased susceptibility to cationic antimicrobial peptides. These results suggest a potential contribution of d-alanine of lipoteichoic acids in the pathogenesis of *E. faecalis* (Fabretti et al., 2006).

A mature biofilm is typically associated with chronic infections, which persist despite apparently adequate antibiotic treatment. Indeed, chronic infections may have a silent course for several months, perhaps years before the clinical symptoms appear. Chronic infections are mainly characterized by a local and persistent inflammatory response surrounding the biofilm. The infection's signs and symptoms may vary depending on the organ's function or implanted device (Høiby et al., 2015). An infection frequently characterized by less dramatic outcomes and persistent pain as the only manifestation (together with elevated C-reactive protein levels, although not always present) is a PJI (Masters et al., 2019). The majority of PJIs are thought to occur during surgery, due to the incidental introduction of skin commensals into the surgical site or onto the newly implanted device (Zimmerli et al., 2004). In a late PJI, biofilm cells remain quiescent and localized in the implant surface and the surrounding tissues. However, bacterial cells may continuously release from the biofilm by a dispersal process which may contribute to bacteremia and sepsis or disseminate to other implants within the body (Lister and Horswill, 2014). Dispersion of *S. aureus* from the biofilm into the environment is an active mechanism mediated by the production of extracellular enzymes or surfactants controlled by the activity of the accessory gene regulator (*agr*) system (Otto, 2018). As a quorum-sensing (QS) communication system, the *agr* locus regulates more than 70 genes in *S. aureus*, 23 of which are directly involved in its virulence (Otto, 2018). Specifically, the *agr* locus controls the expression of surface binding proteins, toxins, proteases, lipases, nucleases. The QS response also regulates matrix modification and dispersion in *E. faecalis* (Ch'ng et al., 2019). The Fsr (*Enterococcus faecalis* sensor regulator) QS system is a signal transduction system that controls the extracellular metalloprotease, gelatinase (GelE) (Ch'ng et al., 2019). Mutations in the *fsr* system or *gelE* revealed that gelatinase has an important role in *E. faecalis* biofilm formation and increased virulence in different animal infection models (Hancock and Perego, 2004; Sava et al., 2010). The released cell subpopulation, spreading from the original colony, is typically more virulent, with altered metabolic activity and antimicrobial susceptibilities than their biofilm and planktonic counterparts. Thus, the dispersed cell may result in more severe and persistent infections (Rumbaugh and Sauer, 2020).

Clinical-Therapeutic Approach to Biofilm-Related Infections

General Principles

As a general concept, the clinical management of biofilm-related infections requires the complete removal of the infected device with surgical debridement followed by implant replacement along with targeted antibiotics against biofilms and planktonic cells (Høiby et al., 2015; Agarwal et al., 2020). Indeed, using antimicrobials with activity against biofilm positively influences the outcome, irrespective of the type of surgery performed (Gellert et al., 2020; Köder et al., 2020).

The purpose of surgery is to remove (i) the foreign body along with the surrounding patchy distributed biofilm, (ii) the infecting sessile germs, and (iii) the devitalized tissue, if any (Høiby et al., 2015; Izakovicova et al., 2019; Agarwal et al., 2020). At this stage, it is essential to put in place a targeted therapy (**Table 1**) to minimize the bacterial adhesion ability and prevent new biofilm formation by the residual microbial burden. One exception to the complete removal of a foreign body is the presence of early biofilm (i.e., implant infection within 3 weeks from implant placement or during concomitant bacteremia with further involvement of the implant). In this case, surgical debridement and the possibility of keeping the essential parts of the foreign body are recommended.

The so-called Debridement, Antibiotics, and Implant Retention (DAIR) approach is considered the optimal choice, showing a high clinical cure rate, especially in PJIs. During this procedure, radical debridement of all necrotic tissues, synovectomy, excision of sinus tracts and thorough irrigation with copious volumes of sterile saline is performed, combined with replacement of mobile, easily exchangeable prosthetic parts and targeted therapy for 6–12 weeks with the antibiotics listed in **Table 1** (Høiby et al., 2015; Izakovicova et al., 2019; Agarwal et al., 2020). However, individual patients may not be candidates for any device removal, i.e., subjects with an unacceptably high risk for mortality due to surgery, subjects with a limited life expectancy, or those refusing device explanation (Peacock et al., 2018).

In these cases, alternative options such as conservative management with device retention and long-term suppressive antimicrobial therapy may be considered (Segreti et al., 1998; Pavoni et al., 2002, 2004; Peacock et al., 2018; Izakovicova et al., 2019).

Antimicrobial Treatment

Biofilm-embedded bacteria are up to 100–1,000 times less susceptible to antibiotics than their planktonic counterpart (Sharma et al., 2019). In this context, conventional *in vitro* susceptibility testing methods are unsuitable; therefore, when choosing antimicrobials, the key step is to consider their anti-biofilm activity. **Table 1** attempts to list the characteristics of the most common antibiotics with efficacy against biofilm and summarizes the current knowledge on the two main steps of antimicrobial activity in this setting, i.e., diffusion through the biofilm matrix and activity against sessile bacterial cells (Ciofu et al., 2017; Izakovicova et al., 2019; Abad et al., 2020). There is also a third, preliminary stage, which has been described for rifampicin, minocycline, linezolid, macrolides, colistin, and dalbavancin: the ability to prevent/impair bacterial adhesion on inert surfaces and subsequent biofilm deposition (Parra-Ruiz et al., 2012; Ciofu et al., 2017; Albano et al., 2019; Izakovicova et al., 2019; Di Pilato et al., 2020). The anti-staphylococcal biofilm agent *par excellence* is rifampicin, followed by two drugs with similar potentials, the long-acting agents rifabutin and rifapentine. Nevertheless, rifampicin should not be used as monotherapy due to the risk of rapid development

TABLE 1 | Activity of different antibiotics against biofilm-growing Gram-positive bacteria.

Author, year	Antimicrobial agent	Penetration into the biofilm matrix	Activity against sessile cells
Landini et al. (2015) and Lázaro-Díez et al. (2016)	Beta-lactams	Reduced to a varying degree	None
Jo and Ahn (2016) and Di Domenico et al. (2019)	Quinolones	Yes	Active
Henry-Stanley et al. (2014) and Di Domenico et al. (2019)	Aminoglycosides	Reduced	Reduced
Darouiche et al. (1999)	Minocycline	Yes	Active
Tang et al. (2013) and Di Domenico et al. (2019)	Rifampicin	Yes	Active
Darouiche et al. (1994) and Doroshenko et al. (2014)	Vancomycin	Severely reduced	Not known
Leite et al. (2011) and Parra-Ruiz et al. (2012)	Daptomycin	Yes	Not known
Parra-Ruiz et al. (2012)	Linezolid	Yes	Reduced
Tang et al. (2012)	Fosfomycin	Yes	Active
Silva et al. (2020) and Žiemytė et al. (2020)	Dalbavancin	Reduced	Not known
Landini et al. (2015) and Lázaro-Díez et al. (2016)	Beta-lactams	Reduced to a varying degree	None
Jo and Ahn (2016) and Di Domenico et al. (2019)	Quinolones	Yes	Active
Henry-Stanley et al. (2014) and Di Domenico et al. (2019)	Aminoglycosides	Reduced	Reduced
Darouiche et al. (1999)	Minocycline	Yes	Active
Tang et al. (2013) and Di Domenico et al. (2019)	Rifampicin	Yes	Active
Darouiche et al. (1994) and Doroshenko et al. (2014)	Vancomycin	Severely reduced	Reduced
Leite et al. (2011) and Parra-Ruiz et al. (2012)	Daptomycin	Yes	Not known
Parra-Ruiz et al. (2012)	Linezolid	Yes	Reduced
Tang et al. (2012); Mihailescu et al. (2014), and Oliva et al. (2014)	Fosfomycin	Yes	Active
Silva et al. (2020) and Žiemytė et al. (2020)	Dalbavancin	Reduced	Not known

of *in vivo* resistance (Høiby et al., 2015; Ciofu et al., 2017; Izakovicova et al., 2019). Therefore, the association with other anti-staphylococcal drugs is recommended not only on account of their frequent synergistic activity but also to minimize the development of resistance. To this end, since the emergence of rifampicin resistance is proportional to the bacterial burden, there is also a recommendation to initiate the antimicrobial therapy with partner antibiotics such as oxacillin, daptomycin, or dalbavancin, to reduce the bacterial load, and then after 3–5 days add rifampicin in association (Høiby et al., 2015; Izakovicova et al., 2019). In *in vitro* and animal models, rifampicin showed activity also against biofilm formed by *Cutibacterium acnes* (Furustrand Tafin et al., 2012). However, in a recent study on PJI caused by *C. acnes*, rifampicin therapy did not seem to improve outcomes, suggesting the need for additional studies on humans (Vilchez et al., 2021).

The choice of antibiotics against enterococcal biofilms is limited, and, with this regard, no activity of rifampicin has been shown (Oliva et al., 2014). On the other hand, the "old" antibiotic fosfomycin, which has been recently rediscovered mostly to treat multidrug-resistant bacteria, showed high activity against both staphylococcal and enterococcal biofilms (Mihailescu et al., 2014; Oliva et al., 2014; Zheng et al., 2019). Nevertheless, similarly to rifampicin, fosfomycin monotherapy allows the rapid selection of resistant variants, and therefore it should always be used in combination. As an alternative to the traditional approach combining surgery plus antibiotics, chronic suppressive therapy is selected when a patient's general conditions or the technical difficulties connected with the surgery are such as to preclude both removal and replacement of the foreign body and debridement. After initial targeted therapy with antibiotics by the intravenous route, the subsequent step is to keep the infection "silent" by administering a prolonged oral therapy for an indefinite duration, including, amongst others, the use of minocycline and/or trimethoprim/sulfamethoxazole and/or fluoroquinolones, according to the causative agent and the patient's characteristics (Pavoni et al., 2004; Izakovicova et al., 2019; Qu et al., 2019). This approach is mainly described in orthopedic implant infections and more rarely in the management of cardiac implant or vascular graft infections (Segreti et al., 1998; Pavoni et al., 2002, 2004; Peacock et al., 2018; Izakovicova et al., 2019; Blomström-Lundqvist et al., 2020). However, some patients do not even tolerate this approach, mainly due to side effects during suppressive therapy (Segreti et al., 1998; Spaziante et al., 2019). In such cases, an alternative option, currently under study, is the use of dalbavancin for a prolonged period with intravenous administrations at intervals of up to 12 weeks apart, driven by the determination of the serum bactericidal assay, as recently described (Spaziante et al., 2019). Another alternative strategy aimed to retain in place the foreign body is represented by intra-lock therapy, which refers to the treatment of catheter-related bloodstream infections and may be considered only if there are absolute contraindications to catheter removal. Antibiotics for the lock therapy are at high concentrations (up to 100–1,000 times higher than the MIC). They may include aminoglycosides, beta-lactams, fluoroquinolones, glycopeptides, daptomycin, linezolid, minocycline, and tigecycline, with the largest evidence for gentamicin and vancomycin (Justo and Bookstaver, 2014). However, when selecting antimicrobials for the intra-lock therapy, additional characteristics such as stability, compatibility with anticoagulants, selection of resistance, rate of systemic

TABLE 2 | Dalbavancin in the treatment of bone and joint infections: an analysis of the literature.

Author, year	Study design, cases	Dose° and duration of dalbavancin therapy	Clinical success	Adverse events
Almangour et al. (2017)	Case report, spondylodiscitis caused by MRSA	1 × 1,000 mg loading dose, then 500 mg/week × 6 times	Yes, at the end of therapy (follow up: no)	None
Bouza et al. (2018)	Retrospective: 12 OM, 5 PJI	Varying: mean of 4 doses (range 1–9), 3-week duration (range 1–24)	92% for OM, 80% for PJI (follow up: 1 month)	13%, mild
Rappo et al. (2018)	Prospective randomized; Dal: 70 vs. ST: 10; 80 OM	1 gr IV on days 1 and 8	96% dal vs. 88% ST	None for dal
Tobudic et al. (2018)	Retrospective: 20 OM, 8 PJI; 14 SPD, 4 SAR	Varying: median duration of 8 weeks (range 4–32)	60% for OM, 38% for PJI; 50% for SPD; 100% for SAR (follow up: 6 months)	2.8%, mild
Wunsch et al. (2019)	Retrospective: 30 OM, 32 PJI	Varying: mean of 3 doses (range 1–32)	89% for OM, 91% for PJI (at the end of therapy, no follow up)	3%, mild
Bryson-Cahn et al. (2019)	Retrospective: 7 OM	Varying: median of 1 dose (range 1–5)	71% (follow up: 1 year)	None
Morata et al. (2019)	Retrospective: 19 OM/SPD, 26 PJI	Varying: median of 5 doses (IQR 3–8)	90% for OM/SPD; 65% for PJI (follow up: 6 months)	11%, mild
Almangour et al. (2019)	Retrospective: 29 OM/SPD, 2 PJI	Varying: median of 3 doses (range 1–14)	93% for OM/SPD, 100% for PJI (follow up: 3 months)	None
Bartoletti et al. (2019)	Retrospective: 15 sternal OM post-cardiac surgery	Varying: median of 4 doses	93% (follow up: 6 months) (follow up: 1 month)	None
Bork et al. (2019)	Retrospective: 11 OM, 1 PJI	Varying: median of 3 doses (IQR 4.5)	55% for OM; 100% for IPA	13%, mild
Streifel et al. (2019)	Retrospective: 11 OM	Varying: mean of 2.7 weeks	76% (follow up: 1 month)	8%, mild
Almangour and Alhifany (2020)	Retrospective case-control Dal: 11 OM vs. ST 11 OM	Varying: mean of 2 doses	100% in both arms	None
Loupa et al. (2020)	Case report, diabetic foot OM caused by multi-drug resistant *Enterococcus faecium*	2 × 1,500 mg in combination with oral lin and intravenous tig	Yes, at the end of the therapy	None
Veve et al. (2020)	Retrospective: osteoarticular infection (OM, PJI, septic arthritis), infective endocarditis or other bloodstream infection 70 dal and 145 ST	Varying: the most frequent (34%) was 1,500 mg for two doses 1 week apart	Lower rate of 90-day infection-related readmission in dal treated (17%) vs. ST (28%)	3% dal vs. 14% ST
Matt et al. (2021)	Retrospective: 17 PJI	Varying: the most frequent (8 patients) was 1,500 mg at Day 1 and 1,500 mg at Day 7	47% after a median follow-up of 299 days	Not specified
Navarro-Jiménez et al. (2021)	Retrospective, descriptive study: 23 OM (diabetic foot infection)	Varying: the most frequent (8 patients) was 1,000 mg followed by 500 mg weekly for 5 weeks	87% at 90 days after completion of dal	13%, mild

Clinical success is defined as the disappearance of any clinical, laboratory, and microbiological evidence of persistent or relapsing infection at the last clinical assessment after dalbavancin discontinuation;° intravenous administration; OM, osteomyelitis; PJI, prosthetic joint infection; SPD, spondylodiscitis; SAR, septic arthritis; lin, linezolid; dal, dalbavancin; tig, tigecycline; ST, standard therapy.

absorption with possible consequent side effects, and cost-effectiveness should be considered (Justo and Bookstaver, 2014).

Overall, foreign body infections are associated with increasingly complex implications as the number and variety of implantable devices grow, especially in subjects with critical conditions or peculiar psychological profiles (i.e., refusal of surgery). Therefore, clinicians are often called upon to "invent" new therapeutic strategies (Pavoni et al., 2002).

It should also be taken into account that the traditional antimicrobial strategy toward implant-associated infections requires prolonged antimicrobial administration, largely by intravenous route. Consequently, multiple or prolonged hospitalizations may be required, therefore exposing patients, especially those with several comorbidities or immune suppression, to the risk of acquiring nosocomial and multidrug-resistant microorganisms (Buke et al., 2007). This is especially true if elderly patients are considered and if additional invasive procedures are necessary (i.e., central venous access placement for antibiotic administration). Therefore, alternative strategies such as the Outpatient Parenteral Antibiotic Therapy (OPAT) and the long-acting dalbavancin are increasingly adopted to overcome these drawbacks.

Potential Role of Dalbavancin in the Treatment of Gram-Positive Biofilms

Dalbavancin currently represents the ultralong acting agent with the most extensive experience of use (Baldoni et al., 2013). Specifically, dalbavancin is a novel semisynthetic antimicrobial agent belonging to the second-generation lipoglycopeptides family approved by the FDA and the EMA for the treatment of acute bacterial skin and skin structure infections (ABSSSI). Dalbavancin inhibits the late stages of peptidoglycan synthesis, interrupting bacterial

TABLE 3 | Dalbavancin in the treatment of infective endocarditis: an analysis of the literature.

Author, year	Study design, cases	Prior therapy	Dose° and duration of dalbavancin therapy	Clinical response*	Adverse events
Steele et al. (2018)	1 NVE-rt in pregnancy, MRSA	Van 5 dd, dap 27 dd	1 × 1,000 mg loading dose, then 500 mg/week × 3 times	Failure; success with cef + dap	The emergence of van-intermediate/tel non-susceptible MRSA during therapy with dal
Tobudic et al. (2018)	Retrospective: 27 cases of endocarditis: 59% NVE, 22% PVE, 19% PME; surgical therapy: 80% in PVE/PME.	89% prior therapies, with dal initiated after bacteremia clearance	33%: 1,000 mg load, then 500 mg/week; 66% 1,500 mg load, then 1,000 mg/week. Mean duration: 42 dd	92% clinical success	1 nausea; 1 increased serum creatinine
Kussmann et al. (2018)	1 PME, MSSA (PM not removable?)	5 prior therapies for over 1 year	Doses and dosing intervals not specified; duration of about 30 weeks	Not reported; isolation of strains not sensitive to dal from blood culture and explanted PM	Resistance to dal, case of PM not explanted
Dinh et al. (2019)	Retrospective: 9 NVE, 10 PVE	99% prior therapies with a median duration (IQR) of 23 dd; dal initiated after 2.5 lines of therapy (mean)	53%: 1 or 2 doses of 1,500 mg weekly	73% clinical success	Stop dal: = 0%; 2 hypersensitivity reactions°°
Morrisette et al. (2019)	Retrospective: 5 NVE	91% prior therapies with a mean duration of 27 dd; 30% combo∧	60% dal 1 × 1,500 mg dose at end of therapy	100% clinical success	Infusion reactions, phlebitis at the infusion site
Bryson-Cahn et al. (2019)	Retrospective: 9 NVE-rt, 0MSSA, 7 MRSA	100% prior therapies; bacteremia clearance before initiating dal	6 cases of 1 × 1,000 mg dose; 3 cases of two doses (1,000 mg then 500 mg after 7 dd)	5/9 clinical success; 4/9 discharged patients improved but were lost at follow-up	None
Wunsch et al. (2019)	Retrospective: 15 NVE, 6 PVE, 4 PME; 3 cases of associated spondylodiscitis	100 prior therapies; 60% combo	9 cases of 1 × 1,500 mg dose; 8 cases of multiple weekly doses of 500 mg, preceded by a loading dose of 1,000 mg	89% clinical success; 1 death during therapy	1 hypertension during infusion; 1 muscle weakness; 1 vertigo
Hidalgo-Tenorio et al., 2019	Retrospective: 83 (59.04% bloodstream infection, 49.04% infective endocarditis (44.04% PVE, 32.4% NVE, 23.5% pacemaker lead)	Dap (68.6%), cex (28.6%), van (22.9%), lin (8.6%)	Varying: the most frequent (12 patients) was 1,500 mg (1 day)	In hospital clinical cure in all patients; at 12 months, 2.9% therapeutic failure	4.8%, mild
Spaziante et al. (2019)	1 PVE MRSE + *S. mitis*, considered to be inoperable	Pip/taz + dap, then cef + dap. Dal initiated after bacteremia clearance	1,500 mg on days 1, 7, 42, 112, 189, 255″, 315″, 370″ (the frequency of infusions was guided by *SBP*-values ≤ 1:8)	Net clinical and PET/CT improvement, no relapse after more than 1 year from dal discontinuation§	None
Veve et al. (2020)	Retrospective: osteoarticular infection (OM, PJI, septic arthritis), infective endocarditis or other bloodstream infection 70 dal and 145 ST	Not specified for the infective endocarditis group (all patients in the dal group received prior antibiotics during the hospitalization preceding definite dal therapy)	Varying: the most frequent (34%) was 1,500 mg for two doses 1 week apart	Lower rate of 90-day infection-related readmission in dalbavancin treated (17%) vs. ST (28%)	3% dal vs. 14% ST

**Clinical success is defined as the disappearance of any clinical, laboratory and microbiological evidence of persistent or relapsing infection at the last clinical assessment after dalbavancin discontinuation;° intravenous administration; NVE, native valve endocarditis; NVE-rt, right-sided native valve endocarditis (unless specified, NVEs should be considered to be left-sided); PVE, prosthetic valve endocarditis; dd, days; cef, ceftaroline; cex, ceftriaxone; dal, dalbavancin; dap, daptomycin; lin, linezolid; tel, telavancin; van, vancomycin; stop dal, discontinuation of dalbavancin due to an adverse event; ° °fever, rash, chills and/or fever during the first infusion; ∧ = dalbavancin in combination with other antibiotic(s); PME, pacemaker endocarditis; MSSA, methicillin-sensitive S. aureus; MRSA, methicillin-resistant S. aureus; MRSE, methicillin-resistant S. epidermidis; S. mitis, Streptococcus mitis. ", infusions performed after the article was written; SBP, serum bactericidal power, when the value was ≤ 1:8 dalbavancin infusion was performed. § Reported in the article: note of the author (MV) who followed up the case.*

cell wall synthesis by binding to the terminal D-alanyl–D-alanine terminus of pentapeptide peptidoglycan precursors, resulting in bactericidal activity against most Gram-positive microorganisms. Notably, recent data showed that dalbavancin MIC_{90} values remained unchanged, being ≤ 0.06 μg/mL against different species of Gram-positive germs, with overall

low values: *Staphylococcus aureus* (MIC50/90 0.03 mg/L for both MSSA and MRSA), vancomycin-susceptible *Enterococcus faecalis* (MIC50/90, 0.03/0.06 mg/L), β-hemolytic streptococci (MIC50/90, 0.008/0.015 mg/L), and *Streptococcus anginosus* group (MIC50/90, ≤ 0.004/ ≤ 0.004 mg/L) (Jones et al., 2013). Interestingly, dalbavancin resistance during or immediately after the antibiotic treatment was evidenced in only two cases (Kussmann et al., 2018; Werth et al., 2018), with the hypothesized mechanisms underlying the reduced susceptibility being linked to an increase in cell-wall thickness (Kussmann et al., 2018). From a clinical point of view, dalbavancin has been approved for use as a 2-dose regimen (1,000 mg IV on day 1 and 500 mg IV on day 8) or 1-dose regimen (1,500 mg IV) for the treatment of ABSSSI, with an efficacy equal to and fewer adverse reactions than the standard treatment with vancomycin followed by oral linezolid (Soriano et al., 2020). Besides being a good choice in managing SSTI, dalbavancin may represent a valuable option for other invasive Gram-positive infections requiring prolonged intravenous treatments, including osteomyelitis, PJI, infective endocarditis, and catheter-related bacteremia (David et al., 2017). Retrospective analyses of patients with these types of infections being treated with dalbavancin showed a favorable outcome in most cases and an excellent safety profile (**Tables 2**, **3**). The efficacy of dalbavancin was also proved in vulnerable patients with osteomyelitis or non-complicated bacteremia where the first-line antimicrobial therapy failed (Bork et al., 2019). Subsequent successful use of dalbavancin in patients with infective endocarditis was also reported (Tobudic et al., 2018). Since endocarditis or MDIs are at high risk of biofilm development, it has been speculated that dalbavancin efficacy in such patients may be linked to a direct mechanism on biofilm eradication. Different studies evaluated the *in vitro* activity of dalbavancin against biofilms formed by Gram-positive infections. In *in vitro* biofilm models of Gram-positive cocci, dalbavancin inhibited biofilm formation at low concentrations in a broad number of *S. aureus*, *S. epidermidis*, and enterococci (Fernández et al., 2016; Neudorfer et al., 2018). These values were lower than those observed for other agents such as vancomycin and daptomycin. An exception was represented by vancomycin-resistant strains, which showed very high minimum biofilm bactericidal concentrations for all tested agents, including dalbavancin (Fernández et al., 2016; Neudorfer et al., 2018). A recent study evaluated the time-kill kinetics of dalbavancin against biofilm formed by *S. aureus* and coagulase-negative staphylococci (CoNS) (Di Pilato et al., 2020). Dalbavancin and vancomycin, used at a concentration achievable *in vivo* in bone tissue (1, 4, and 16 μg/mL) for 7 days, showed concentration and time-dependent activities against all tested strains. Besides, dalbavancin showed a greater reduction of biofilm-embedded bacteria in most strains studied, especially at 4 μg/mL and 16 μg/mL. In biofilms formed on titanium and cobalt chrome disks, dalbavancin was more active than vancomycin at medium concentrations (4 μg/mL), which are easily reached in bone tissue (Dunne et al., 2015). The activity of dalbavancin against *S. aureus* and *S. epidermidis* biofilms was compared to other antimicrobials (linezolid, rifampicin, vancomycin, cloxacillin). Notably, the minimal biofilm inhibitory concentration (MBIC) of dalbavancin ranged from 0.5 to 2 μg/mL, and in combination with rifampicin, showed the highest biofilm inhibitory effect. In addition, dalbavancin was able to eradicate 6–9-h old biofilms at concentrations of 8–32 μg/mL. The other antimicrobials showed no activity against biofilms formed by *S. aureus*. Dalbavancin was effective against *S. epidermidis* biofilm; however, cloxacillin plus rifampicin showed lower MBIC values (Žiemytė et al., 2020). A recent study analyzing the effect of different antibiotics on biofilm-producing MRSA strains from patients with SSTI showed that dalbavancin was 16 and 8 times more active than linezolid and vancomycin, respectively, with an $MBIC_{90}$ of 0.5 μg/mL (range 0.12–0.5 mg/L) (Sivori et al., 2021).

A few *in vivo* experimental models evaluated dalbavancin activity in biofilm prevention and treatment. Darouiche and Mansouri evaluated biofilm prevention in a rabbit model inoculated with *S. aureus* and treated with either dalbavancin or vancomycin (Darouiche and Mansouri, 2005). The percentage of colonized devices was comparable in the vancomycin and control group (47%). In contrast, the dalbavancin group showed a lower trend in device colonization (28%), although not statistically significant (Darouiche and Mansouri, 2005). Nevertheless, the rate of foreign body contamination in rabbits receiving placebo was around 50% (lower than other animal models), thus questioning the validity of the model and its discriminatory power for assessing the efficacy of antimicrobials. In 2013, Baldoni et al. tested dalbavancin activity, alone and in combination with rifampicin, on MRSA biofilm in an animal model of tissue-cage infection. Dalbavancin did not show antagonist or synergistic activity with rifampicin; however, when used in combination with rifampicin, it was able to eradicate the biofilm and achieve cure rates of 25–36% compared to monotherapy. In addition, dalbavancin prevented the insurgence of rifampicin resistance (Baldoni et al., 2013). A more recent paper by Silva et al. (2020) evaluated dalbavancin activity in a rat model of implant-associated orthopedic infection by MRSA. Efficacy was assessed at 7 and 14 days after dalbavancin administration, showing a significant reduction in bacterial colonies on bone tissue and implant.

However, some limitations from these pre-clinical reports should be highlighted: the dosages of dalbavancin in some of the *in vivo* models may have provided lower antibiotic exposure compared to human pharmacokinetics; the chosen animal models may not represent the ideal *in vivo* condition for biofilm growth; more data on the combination therapies, especially with rifampicin, would be essential to fully understand the possible role of dalbavancin in hard-to-treat infections.

Furthermore, the clinical evidence available so far derives mostly from retrospective observational studies or case reports (**Tables 2**, **3**). The only prospective randomized study comparing dalbavancin with the standard of care included patients with osteomyelitis, a condition that is associated with biofilm but that does not involve a foreign body (Rappo et al., 2018). Therefore, based on these promising but still preliminary data, additional prospective randomized trials evaluating the role of dalbavancin in patients with implant-associated infections are strongly encouraged.

CONCLUSION

With an aging population and the resulting increase in diseases such as cancer and diabetes, together with the development of new implantable medical devices, there is an increasingly growing incidence of chronic infections typically associated with biofilm formation.

The current management of several biofilm-related Gram-positive infections requires prolonged antibiotic therapy and, in the majority of the cases, the complete removal of the implant.

Amongst the available antimicrobials with different degrees of activity against biofilm, dalbavancin seems to provide effective therapy in a significant proportion of cases due to its ultra-long activity and effectiveness in the setting of MDIs with a relatively low number of adverse effects. Furthermore, its ease of administration allows to accelerate patients' discharge from hospital and increase patients' compliance to the therapy, thus reducing both healthcare costs and the risks of developing multidrug-resistant bacterial infections due to prolonged hospital stay.

AUTHOR CONTRIBUTIONS

All authors designed the study, wrote the manuscript, interpreted the clinical data, contributed to the article, and approved the submitted version.

ACKNOWLEDGMENTS

We sincerely thank Mirella Biava for her expertise and assistance throughout all aspects of our study and for the help in writing the manuscript.

REFERENCES

Abad, L., Josse, J., Tasse, J., Lustig, S., Ferry, T., Diot, A., et al. (2020). Antibiofilm and intraosteoblastic activities of rifamycins against *Staphylococcus aureus*: promising *in vitro* profile of rifabutin. *J. Antimicrob. Chemother.* 75, 1466–1473. doi: 10.1093/jac/dkaa061

Agarwal, A., Kelkar, A., Agarwal, A. G., Jayaswal, D., Schultz, C., Jayaswal, A., et al. (2020). Implant Retention or Removal for Management of Surgical Site Infection After Spinal Surgery. *Global Spine J.* 10, 640–646. doi: 10.1177/2192568219869330

Albano, M., Karau, M. J., Greenwood-Quaintance, K. E., Osmon, D. R., Oravec, C. P., Berry, D. J., et al. (2019). *In Vitro* Activity of Rifampin, Rifabutin, Rifapentine, and Rifaximin against Planktonic and Biofilm States of Staphylococci Isolated from Periprosthetic Joint Infection. *Antimicrob. Agents Chemother.* 63, e00959–19. doi: 10.1128/AAC.00959-19

Almangour, T. A., and Alhifany, A. A. (2020). Dalbavancin for the management of osteomyelitis: a major step forward? *J. Antimicrob. Chemother.* 75, 2717–2722. doi: 10.1093/jac/dkaa188

Almangour, T. A., Fletcher, V., Alessa, M., Alhifany, A. A., and Tabb, D. (2017). Multiple Weekly Dalbavancin Dosing for the Treatment of Native Vertebral Osteomyelitis Caused by Methicillin-Resistant *Staphylococcus Aureus*: a Case Report. *Am. J. Case Rep.* 18, 1315–1319. doi: 10.12659/ajcr.905930

Almangour, T. A., Perry, G. K., Terriff, C. M., Alhifany, A. A., and Kaye, K. S. (2019). Dalbavancin for the management of gram-positive osteomyelitis: effectiveness and potential utility. *Diagn. Microbiol. Infect. Dis.* 93, 213–218. doi: 10.1016/j.diagmicrobio.2018.10.007

Arrieta-Loitegui, M., Caro-Teller, J. M., Ortiz-Pérez, S., López-Medrano, F., San Juan-Garrido, R., and Ferrari-Piquero, J. M. (2020). Effectiveness, safety and cost analysis of dalbavancin in clinical practice. *Eur. J. Hosp. Pharm.* doi: 10.1136/ejhpharm-2020-002315 [Epub Online ahead of print].

Baldoni, D., Furustrand Tafin, U., Aeppli, S., Angevaare, E., Oliva, A., Haschke, M., et al. (2013). Activity of dalbavancin, alone and in combination with rifampicin, against methicillin-resistant *Staphylococcus aureus* in a foreign-body infection model. *Int. J. Antimicrob. Agents* 42, 220–225. doi: 10.1016/j.ijantimicag.2013.05.019

Bartoletti, M., Mikus, E., Pascale, R., Giannella, M., Tedeschi, S., Calvi, S., et al. (2019). Clinical experience with dalbavancin for the treatment of deep sternal wound infection. *J. Glob. Antimicrob. Resist.* 18, 195–198. doi: 10.1016/j.jgar.2019.03.015

Berne, C., Ellison, C. K., Ducret, A., and Brun, Y. V. (2018). Bacterial adhesion at the single-cell level. *Nat. Rev. Microbiol.* 16, 616–627. doi: 10.1038/s41579-018-0057-5

Blomström-Lundqvist, C., Traykov, V., Erba, P. A., Burri, H., Nielsen, J. C., Bongiorni, M. G., et al. (2020). European Heart Rhythm Association (EHRA) international consensus document on how to prevent, diagnose, and treat cardiac implantable electronic device infections-endorsed by the Heart Rhythm Society (HRS), the Asia Pacific Heart Rhythm Society (APHRS), the Latin American Heart Rhythm Society (LAHRS), International Society for Cardiovascular Infectious Diseases (ISCVID) and the European Society of Clinical Microbiology and Infectious Diseases (ESCMID) in collaboration with the European Association for Cardio-Thoracic Surgery (EACTS). *Europace* 22, 515–549. doi: 10.1093/europace/euz246

Bork, J. T., Heil, E. L., Berry, S., Lopes, E., Davé, R., Gilliam, B. L., et al. (2019). Dalbavancin Use in Vulnerable Patients Receiving Outpatient Parenteral Antibiotic Therapy for Invasive Gram-Positive Infections. *Infect. Dis. Ther.* 8, 171–184. doi: 10.1007/s40121-019-0247-0

Boucher, H. W., Wilcox, M., Talbot, G. H., Puttagunta, S., Das, A. F., Dunne, M. W., et al. (2014). Once-weekly dalbavancin versus daily conventional therapy for skin infection. *N. Engl. J. Med.* 370, 2169–2179. doi: 10.1056/NEJMoa1310480

Bouza, E., Valerio, M., Soriano, A., Morata, L., Carus, E. G., Rodríguez-González, C., et al. (2018). Dalbavancin in the treatment of different gram-positive infections: a real-life experience. *Int. J. Antimicrob. Agents* 51, 571–577. doi: 10.1016/j.ijantimicag.2017.11.008

Bryson-Cahn, C., Beieler, A. M., Chan, J. D., Harrington, R. D., and Dhanireddy, S. (2019). Dalbavancin as Secondary Therapy for Serious *Staphylococcus aureus* Infections in a Vulnerable Patient Population. *Open Forum Infect. Dis.* 6:ofz028. doi: 10.1093/ofid/ofz028

Buke, C., Armand-Lefevre, L., Lolom, I., Guerinot, W., Deblangy, C., Ruimy, R., et al. (2007). Epidemiology of multidrug-resistant bacteria in patients with long hospital stays. *Infect. Control Hosp. Epidemiol.* 28, 1255–1260. doi: 10.1086/522678

Ch'ng, J. H., Chong, K. K. L., Lam, L. N., Wong, J. J., and Kline, K. A. (2019). Biofilm-associated infection by enterococci. *Nat. Rev. Microbiol.* 17, 82–94. doi: 10.1038/s41579-018-0107-z

Ciofu, O., Rojo-Molinero, E., Macià, M. D., and Oliver, A. (2017). Antibiotic treatment of biofilm infections. *APMIS* 125, 304–319. doi: 10.1111/apm.12673

da Silva, R. A. G., Afonina, I., and Kline, K. A. (2021). Eradicating biofilm infections: an update on current and prospective approaches. *Curr. Opin. Microbiol.* 63, 117–125. doi: 10.1016/j.mib.2021.07.001

Darouiche, R. O., Dhir, A., Miller, A. J., Landon, G. C., Raad, I. I., and Musher, D. M. (1994). Vancomycin penetration into biofilm covering infected prostheses and effect on bacteria. *J. Infect. Dis.* 170, 720–723. doi: 10.1093/infdis/170.3.720

Darouiche, R. O., and Mansouri, M. D. (2005). Dalbavancin compared with vancomycin for prevention of *Staphylococcus aureus* colonization of devices in vivo. *J. Infect.* 50, 206–209. doi: 10.1016/j.jinf.2004.05.006

Darouiche, R. O., Raad, I. I., Heard, S. O., Thornby, J. I., Wenker, O. C., Gabrielli, A., et al. (1999). A comparison of two antimicrobial-impregnated central venous catheters. Catheter Study Group. *N. Engl. J. Med.* 7, 1–8. doi: 10.1056/NEJM199901073400101

David, M. Z., Dryden, M., Gottlieb, T., Tattevin, P., and Gould, I. M. (2017). Recently approved antibacterials for methicillin-resistant *Staphylococcus aureus* (MRSA) and other Gram-positive pathogens: the shock of the new. *Int. J. Antimicrob. Agents* 50, 303–307. doi: 10.1016/j.ijantimicag.2017.05.006

Del Pozo, J. L., and Patel, R. (2009). Clinical practice. Infection associated with prosthetic joints. *N. Engl. J. Med.* 361, 787–794. doi: 10.1056/NEJMcp0905029

Di Domenico, E. G., Rimoldi, S. G., Cavallo, I., D'Agosto, G., Trento, E., Cagnoni, G., et al. (2019). Microbial biofilm correlates with an increased antibiotic tolerance and poor therapeutic outcome in infective endocarditis. *BMC Microbiol.* 19:228. doi: 10.1186/s12866-019-1596-2

Di Pilato, V., Ceccherini, F., Sennati, S., D'Agostino, F., Arena, F., D'Atanasio, N., et al. (2020). *In vitro* time-kill kinetics of dalbavancin against Staphylococcus spp. biofilms over prolonged exposure times. *Diagn. Microbiol. Infect. Dis.* 96:114901. doi: 10.1016/j.diagmicrobio.2019.114901

Dinh, A., Duran, C., Pavese, P., Khatchatourian, L., Monnin, B., Bleibtreu, A., et al. (2019). French national cohort of first use of dalbavancin: a high proportion of off-label use. *Int. J. Antimicrob. Agents* 54, 668–672. doi: 10.1016/j.ijantimicag.2019.08.006

Doroshenko, N., Tseng, B. S., Howlin, R. P., Deacon, J., Wharton, J. A., Thurner, P. J., et al. (2014). Extracellular DNA impedes the transport of vancomycin in Staphylococcus epidermidis biofilms preexposed to subinhibitory concentrations of vancomycin. *Antimicrob. Agents Chemother.* 58, 7273–7282. doi: 10.1128/AAC.03132-14

Dunne, M. W., Puttagunta, S., Giordano, P., Krievins, D., Zelasky, M., and Baldassarre, J. (2016). A Randomized Clinical Trial of Single-Dose Versus Weekly Dalbavancin for Treatment of Acute Bacterial Skin and Skin Structure Infection. *Clin. Infect. Dis.* 62, 545–551. doi: 10.1093/cid/civ982

Dunne, M. W., Puttagunta, S., Sprenger, C. R., Rubino, C., Van Wart, S., and Baldassarre, J. (2015). Extended-duration dosing and distribution of dalbavancin into bone and articular tissue. *Antimicrob. Agents Chemother.* 59, 1849–1855. doi: 10.1128/AAC.04550-14

Fabretti, F., Theilacker, C., Baldassarri, L., Kaczynski, Z., Kropec, A., Holst, O., et al. (2006). Alanine esters of enterococcal lipoteichoic acid play a role in biofilm formation and resistance to antimicrobial peptides. *Infect Immun.* 74, 4164–4171. doi: 10.1128/IAI.00111-06

Fernández, J., Greenwood-Quaintance, K. E., and Patel, R. (2016). *In vitro* activity of dalbavancin against biofilms of staphylococci isolated from prosthetic joint infections. *Diagn. Microbiol. Infect. Dis.* 85, 449–451. doi: 10.1016/j.diagmicrobio.2016.05.009

Foster, T. J. (2019). The MSCRAMM Family of Cell-Wall-Anchored Surface Proteins of Gram-Positive Cocci. *Trends Microbiol.* 27, 927–941. doi: 10.1016/j.tim.2019.06.007

Furustrand Tafin, U., Corvec, S., Betrisey, B., Zimmerli, W., and Trampuz, A. (2012). Role of rifampin against Propionibacterium acnes biofilm *in vitro* and in an experimental foreign-body infection model. *Antimicrob. Agents Chemother.* 56, 1885–1891. doi: 10.1128/AAC.05552-11

Gellert, M., Hardt, S., Köder, K., Renz, N., Perka, C., and Trampuz, A. (2020). Biofilm-active antibiotic treatment improves the outcome of knee periprosthetic joint infection: results from a 6-year prospective cohort study. *Int. J. Antimicrob. Agents* 55:105904. doi: 10.1016/j.ijantimicag.2020.105904

Guzman Prieto, A. M., van Schaik, W., Rogers, M. R., Coque, T. M., Baquero, F., Corander, J., et al. (2016). Global Emergence and Dissemination of Enterococci as Nosocomial Pathogens: attack of the Clones? *Front. Microbiol.* 7:788. doi: 10.3389/fmicb.2016.00788

Hancock, L. E., and Perego, M. (2004). Systematic inactivation and phenotypic characterization of two-component signal transduction systems of Enterococcus faecalis V583. *J. Bacteriol.* 186, 7951–7958. doi: 10.1128/JB.186.23.7951-7958.2004

Henry-Stanley, M. J., Hess, D. J., and Wells, C. L. (2014). Aminoglycoside inhibition of *Staphylococcus aureus* biofilm formation is nutrient dependent. *J. Med. Microbiol.* 63, 861–869. doi: 10.1099/jmm.0.068130-0

Hidalgo-Tenorio, C., Vinuesa, D., Plata, A., Martin Dávila, P., Iftimie, S., Sequera, S., et al. (2019). DALBACEN cohort: dalbavancin as consolidation therapy in patients with endocarditis and/or bloodstream infection produced by gram-positive cocci. *Ann. Clin. Microbiol. Antimicrob.* 18:30. doi: 10.1186/s12941-019-0329-6

Høiby, N., Bjarnsholt, T., Moser, C., Bassi, G. L., Coenye, T., Donelli, G., et al. (2015). ESCMID guideline for the diagnosis and treatment of biofilm infections 2014. *Clin. Microbiol. Infect.* 21, S1–S25. doi: 10.1016/j.cmi.2014.10.024

Huang, L., Zhang, R., Hu, Y., Zhou, H., Cao, J., Lv, H., et al. (2019). Epidemiology and risk factors of methicillin-resistant *Staphylococcus aureus* and vancomycin-resistant enterococci infections in Zhejiang China from 2015 to 2017. *Antimicrob. Resist. Infect. Control* 8:90. doi: 10.1186/s13756-019-0539-x

Izakovicova, P., Borens, O., and Trampuz, A. (2019). Periprosthetic joint infection: current concepts and outlook. *EFORT Open Rev.* 4, 482–494. doi: 10.1302/2058-5241.4.180092

Jo, A., and Ahn, J. (2016). Phenotypic and genotypic characterisation of multiple antibiotic-resistant *Staphylococcus aureus* exposed to subinhibitory levels of oxacillin and levofloxacin. *BMC Microbiol.* 16:170. doi: 10.1186/s12866-016-0791-7

Jones, R. N., Flamm, R. K., and Sader, H. S. (2013). Surveillance of dalbavancin potency and spectrum in the United States (2012). *Diagn. Microbiol. Infect. Dis.* 76, 122–123. doi: 10.1016/j.diagmicrobio.2013.01.003

Justo, J. A., and Bookstaver, P. B. (2014). Antibiotic lock therapy: review of technique and logistical challenges. *Infect. Drug Resist.* 7, 343–363. doi: 10.2147/IDR.S51388

Karygianni, L., Ren, Z., Koo, H., and Thurnheer, T. (2020). Biofilm Matrixome: extracellular Components in Structured Microbial Communities. *Trends Microbiol.* 28, 668–681. doi: 10.1016/j.tim.2020.03.016

Katsikogianni, M., and Missirlis, Y. F. (2004). Concise review of mechanisms of bacterial adhesion to biomaterials and of techniques used in estimating bacteria-material interactions. *Eur. Cell Mater.* 8, 37–57. doi: 10.22203/ecm.v008a05

Kaye, K. S., Petty, L. A., Shorr, A. F., and Zilberberg, M. D. (2019). Current Epidemiology, Etiology, and Burden of Acute Skin Infections in the United States. *Clin. Infect. Dis.* 68, S193–S199. doi: 10.1093/cid/ciz002

Knafl, D., Tobudic, S., Cheng, S. C., Bellamy, D. R., and Thalhammer, F. (2017). Dalbavancin reduces biofilms of methicillin-resistant *Staphylococcus aureus* (MRSA) and methicillin-resistant Staphylococcus epidermidis (MRSE). *Eur. J. Clin. Microbiol. Infect. Dis.* 36, 677–680. doi: 10.1007/s10096-016-2845-z

Köder, K., Hardt, S., Gellert, M. S., Haupenthal, J., Renz, N., Putzier, M., et al. (2020). Outcome of spinal implant-associated infections treated with or without biofilm-active antibiotics: results from a 10-year cohort study. *Infection* 48, 559–568. doi: 10.1007/s15010-020-01435-2

Kussmann, M., Karer, M., Obermueller, M., Schmidt, K., Barousch, W., Moser, D., et al. (2018). Emergence of a dalbavancin induced glycopeptide/lipoglycopeptide non-susceptible *Staphylococcus aureus* during treatment of a cardiac device-related endocarditis. *Emerg. Microbes Infect.* 7:202. doi: 10.1038/s41426-018-0205-z

Landini, G., Riccobono, E., Giani, T., Arena, F., Rossolini, G. M., and Pallecchi, L. (2015). Bactericidal activity of ceftaroline against mature *Staphylococcus aureus* biofilms. *Int. J. Antimicrob. Agents* 45, 551–553. doi: 10.1016/j.ijantimicag.2015.01.001

Lázaro-Díez, M., Remuzgo-Martínez, S., Rodríguez-Mirones, C., Acosta, F., Icardo, J. M., Martínez-Martínez, L., et al. (2016). Effects of Subinhibitory Concentrations of Ceftaroline on Methicillin-Resistant *Staphylococcus aureus* (MRSA) Biofilms. *PLoS One* 11:e0147569. doi: 10.1371/journal.pone.0147569

Lebeaux, D., Ghigo, J. M., and Beloin, C. (2014). Biofilm-related infections: bridging the gap between clinical management and fundamental aspects of recalcitrance toward antibiotics. *Microbiol. Mol. Biol. Rev.* 78, 510–543.

Leite, B., Gomes, F., Teixeira, P., Souza, C., Pizzolitto, E., and Oliveira, R. (2011). In vitro activity of daptomycin, linezolid and rifampicin on Staphylococcus epidermidis biofilms. *Curr. Microbiol.* 63, 313–317. doi: 10.1007/s00284-011-9980-7

Lister, J. L., and Horswill, A. R. (2014). *Staphylococcus aureus* biofilms: recent developments in biofilm dispersal. *Front. Cell. Infect. Microbiol.* 4:178. doi: 10.3389/fcimb.2014.00178

Loupa, C. V., Lykoudi, E., Meimeti, E., Moisoglou, I., Voyatzoglou, E. D., Kalantzi, S., et al. (2020). Successful Treatment of Diabetic Foot Osteomyelitis with Dalbavancin. *Med. Arch.* 74, 243–245. doi: 10.5455/medarh.2020.74.243-245

Masters, E. A., Trombetta, R. P., de Mesy Bentley, K. L., Boyce, B. F., Gill, A. L., Gill, S. R., et al. (2019). Evolving concepts in bone infection: redefining "biofilm",

"acute vs. chronic osteomyelitis", "the immune proteome" and "local antibiotic therapy". *Bone Res.* 7:20. doi: 10.1038/s41413-019-0061-z

Matt, M., Duran, C., Courjon, J., Lotte, R., Moing, V. L., Monnin, B., et al. (2021). Dalbavancin treatment for prosthetic joint infections in real-life: a national cohort study and literature review. *J. Glob. Antimicrob. Resist.* 25, 341–345. doi: 10.1016/j.jgar.2021.03.026

McCarthy, H., Rudkin, J. K., Black, N. S., Gallagher, L., O'Neill, E., and O'Gara, J. P. (2015). Methicillin resistance and the biofilm phenotype in *Staphylococcus aureus*. *Front. Cell. Infect. Microbiol.* 5:1. doi: 10.3389/fcimb.2015.00001

Mihailescu, R., Furustrand Tafin, U., Corvec, S., Oliva, A., Betrisey, B., Borens, O., et al. (2014). High activity of Fosfomycin and Rifampin against methicillin-resistant *staphylococcus aureus* biofilm *in vitro* and in an experimental foreign-body infection model. *Antimicrob. Agents Chemother.* 58, 2547–2553. doi: 10.1128/AAC.02420-12

Morata, L., Cobo, J., Fernández-Sampedro, M., Guisado Vasco, P., Ruano, E., Lora-Tamayo, J., et al. (2019). Safety and Efficacy of Prolonged Use of Dalbavancin in Bone and Joint Infections. *Antimicrob. Agents Chemother.* 63, e02280–18. doi: 10.1128/AAC.02280-18

Morrisette, T., Miller, M. A., Montague, B. T., Barber, G. R., McQueen, R. B., and Krsak, M. (2019). On- and off-label utilization of dalbavancin and oritavancin for Gram-positive infections. *J. Antimicrob. Chemother.* 74, 2405–2416. doi: 10.1093/jac/dkz162

Navarro-Jiménez, G., Fuentes-Santos, C., Moreno-Núñez, L., Alfayate-García, J., Campelo-Gutierrez, C., and Sanz-Márquez, S. (2021). Experience in the use of dalbavancin in diabetic foot infection. *Enferm. Infecc. Microbiol. Clin.* doi: 10.1016/j.eimc.2020.11.013 [Epub Online ahead of print].

Neoh, K. G., Li, M., Kang, E. T., Chiong, E., and Tambyah, P. A. (2017). Surface modification strategies for combating catheter-related complications: recent advances and challenges. *J. Mater. Chem. B* 5, 2045–2067. doi: 10.1039/c6tb03280j

Neudorfer, K., Schmidt-Malan, S. M., and Patel, R. (2018). Dalbavancin is active in vitro against biofilms formed by dalbavancin-susceptible enterococci. *Diagn. Microbiol. Infect. Dis.* 90, 58–63. doi: 10.1016/j.diagmicrobio.2017.09.015

Nguyen, H. T. T., Nguyen, T. H., and Otto, M. (2020). The staphylococcal exopolysaccharide PIA - Biosynthesis and role in biofilm formation, colonization, and infection. *Comput. Struct. Biotechnol. J.* 18, 3324–3334. doi: 10.1016/j.csbj.2020.10.027

Oliva, A., Furustrand Tafin, U., Maiolo, E. M., Jeddari, S., Bétrisey, B., and Trampuz, A. (2014). Activities of fosfomycin and rifampin on planktonic and adherent Enterococcus faecalis strains in an experimental foreign-body infection model. *Antimicrob. Agents Chemother.* 58, 1284–1293. doi: 10.1128/AAC.02583-12

Otto, M. (2018). Staphylococcal Biofilms. *Microbiol. Spectr.* 6:6.4.27. doi: 10.1128/microbiolspec.GPP3-0023-2018

Palmer, J., Flint, S., and Brooks, J. (2007). Bacterial cell attachment, the beginning of a biofilm. *J. Ind. Microbiol. Biotechnol.* 34, 577–588. doi: 10.1007/s10295-007-0234-4

Parra-Ruiz, J., Bravo-Molina, A., Peña-Monje, A., and Hernández-Quero, J. (2012). Activity of linezolid and high-dose daptomycin, alone or in combination, in an *in vitro* model of *Staphylococcus aureus* biofilm. *J. Antimicrob. Chemother.* 67, 2682–2685. doi: 10.1093/jac/dks272

Pavoni, G. L., Falcone, M., Baiocchi, P., Tarasi, A., Cassone, M., Serra, P., et al. (2002). Conservative medical therapy of infections following osteosynthesis: a retrospective analysis of a six-year experience. *J. Chemother.* 14, 378–383. doi: 10.1179/joc.2002.14.4.378

Pavoni, G. L., Giannella, M., Falcone, M., Scorzolini, L., Liberatore, M., Carlesimo, B., et al. (2004). Conservative medical therapy of prosthetic joint infections: retrospective analysis of an 8-year experience. *Clin. Microbiol. Infect.* 10, 831–837. doi: 10.1111/j.1469-0691.2004.00928.x

Peacock, J. E. Jr., Stafford, J. M., Le, K., Sohail, M. R., Baddour, L. M., Prutkin, J. M., et al. (2018). Attempted salvage of infected cardiovascular implantable electronic devices: are there clinical factors that predict success? *Pacing Clin. Electrophysiol.* 41, 524–531. doi: 10.1111/pace.13319

Qu, G. X., Zhang, C. H., Yan, S. G., and Cai, X. Z. (2019). Debridement, antibiotics, and implant retention for periprosthetic knee infections: a pooling analysis of 1266 cases. *J. Orthop. Surg. Res.* 14:358. doi: 10.1186/s13018-019-1378-4

Rappo, U., Puttagunta, S., Shevchenko, V., Shevchenko, A., Jandourek, A., Gonzalez, P. L., et al. (2018). Dalbavancin for the Treatment of Osteomyelitis in Adult Patients: a Randomized Clinical Trial of Efficacy and Safety. *Open Forum Infect. Dis.* 6:ofy331. doi: 10.1093/ofid/ofy331

Römling, U., and Balsalobre, C. (2012). Biofilm infections, their resilience to therapy and innovative treatment strategies. *J. Intern. Med.* 272, 541–561. doi: 10.1111/joim.12004

Rumbaugh, K. P., and Sauer, K. (2020). Biofilm dispersion. *Nat. Rev. Microbiol.* 18, 571–586. doi: 10.1038/s41579-020-0385-0

Sava, I. G., Heikens, E., and Huebner, J. (2010). Pathogenesis and immunity in enterococcal infections. *Clin. Microbiol. Infect.* 16, 533–540. doi: 10.1111/j.1469-0691.2010.03213.x

Seebach, E., and Kubatzky, K. F. (2019). Chronic Implant-Related Bone Infections-Can Immune Modulation be a Therapeutic Strategy? *Front. Immunol.* 10:1724. doi: 10.3389/fimmu.2019.01724

Segreti, J., Nelson, J. A., and Trenholme, G. M. (1998). Prolonged suppressive antibiotic therapy for infected orthopedic prostheses. *Clin. Infect. Dis.* 27, 711–713. doi: 10.1086/514951

Sharma, D., Misba, L., and Khan, A. U. (2019). Antibiotics versus biofilm: an emerging battleground in microbial communities. *Antimicrob. Resist. Infect. Control* 8:76. doi: 10.1186/s13756-019-0533-3

Silva, V., Antão, H. S., Guimarães, J., Prada, J., Pires, I., Martins, Â, et al. (2020). Efficacy of dalbavancin against MRSA biofilms in a rat model of orthopaedic implant-associated infection. *J. Antimicrob. Chemother.* 75, 2182–2187. doi: 10.1093/jac/dkaa163

Sivori, F., Cavallo, I., Ensoli, F., and Di Domenico, E. G. (2021). Dalbavancin activity against biofilm-growing MRSA isolated from patients with complicated skin and soft tissue infections. *Eur Congr. Clin. Microbiol. Infect. Dis.* 2975:24

Soriano, A., Rossolini, G. M., and Pea, F. (2020). The role of dalbavancin in the treatment of acute bacterial skin and skin structure infections (ABSSSIs). *Expert Rev. Anti Infect. Ther.* 18, 415–422. doi: 10.1080/14787210.2020.1746643

Spaziante, M., Franchi, C., Taliani, G., D'Avolio, A., Pietropaolo, V., Biliotti, E., et al. (2019). Serum Bactericidal Activity Levels Monitor to Guide Intravenous Dalbavancin Chronic Suppressive Therapy of Inoperable Staphylococcal Prosthetic Valve Endocarditis: a Case Report. *Open Forum Infect. Dis.* 6:ofz427. doi: 10.1093/ofid/ofz427

Steele, J. M., Seabury, R. W., Hale, C. M., and Mogle, B. T. (2018). Unsuccessful treatment of methicillin-resistant *Staphylococcus aureus* endocarditis with dalbavancin. *J. Clin. Pharm. Ther.* 43, 101–103. doi: 10.1111/jcpt.12580

Streifel, A. C., Sikka, M. K., Bowen, C. D., and Lewis, J. S. II (2019). Dalbavancin use in an academic medical centre and associated cost savings. *Int. J. Antimicrob. Agents* 54, 652–654. doi: 10.1016/j.ijantimicag.2019.08.007

Tang, H. J., Chen, C. C., Cheng, K. C., Toh, H. S., Su, B. A., Chiang, S. R., et al. (2012). *In vitro* efficacy of fosfomycin-containing regimens against methicillin-resistant *Staphylococcus aureus* in biofilms. *J. Antimicrob. Chemother.* 67, 944–950. doi: 10.1093/jac/dkr535

Tang, H. J., Chen, C. C., Cheng, K. C., Wu, K. Y., Lin, Y. C., Zhang, C. C., et al. (2013). *In vitro* efficacies and resistance profiles of rifampin-based combination regimens for biofilm-embedded methicillin-resistant *Staphylococcus aureus*. *Antimicrob. Agents Chemother.* 57, 5717–5720. doi: 10.1128/AAC.01236-13

Tobudic, S., Forstner, C., Burgmann, H., Lagler, H., Ramharter, M., Steininger, C., et al. (2018). Dalbavancin as Primary and Sequential Treatment for Gram-Positive Infective Endocarditis: 2-Year Experience at the General Hospital of Vienna. *Clin. Infect. Dis.* 67, 795–798. doi: 10.1093/cid/ciy279

Tong, S. Y., Davis, J. S., Eichenberger, E., Holland, T. L., and Fowler, V. G. Jr. (2015). *Staphylococcus aureus* infections: epidemiology, pathophysiology, clinical manifestations, and management. *Clin. Microbiol. Rev.* 28, 603–661. doi: 10.1128/CMR.00134-14

Veve, M. P., Patel, N., Smith, Z. A., Yeager, S. D., Wright, L. R., and Shorman, M. A. (2020). Comparison of dalbavancin to standard-of-care for outpatient treatment of invasive Gram-positive infections. *Int. J. Antimicrob. Agents* 56:106210. doi: 10.1016/j.ijantimicag.2020.106210

Vilchez, H. H., Escudero-Sanchez, R., Fernandez-Sampedro, M., Murillo, O., Auñón, Á, Rodríguez-Pardo, D., et al. (2021). Prosthetic Shoulder Joint Infection by *Cutibacterium* acnes: does Rifampin Improve Prognosis? A Retrospective, Multicenter, Observational Study. *Antibiotics* 10:475. doi: 10.3390/antibiotics10050475

Werth, B. J., Jain, R., Hahn, A., Cummings, L., Weaver, T., Waalkes, A., et al. (2018). Emergence of dalbavancin non-susceptible, vancomycin-intermediate

Staphylococcus aureus (VISA) after treatment of MRSA central line-associated bloodstream infection with a dalbavancin- and vancomycin-containing regimen. *Clin. Microbiol. Infect.* 24, 429.e1–429.e5. doi: 10.1016/j.cmi.2017.07.028

Wunsch, S., Krause, R., Valentin, T., Prattes, J., Janata, O., Lenger, A., et al. (2019). Multicenter clinical experience of real life Dalbavancin use in gram-positive infections. *Int. J. Infect. Dis.* 81, 210–214. doi: 10.1016/j.ijid.2019.02.013

Zheng, J. X., Sun, X., Lin, Z. W., Qi, G. B., Tu, H. P., Wu, Y., et al. (2019). In vitro activities of daptomycin combined with fosfomycin or rifampin on planktonic and adherent linezolid-resistant isolates of Enterococcus faecalis. *J. Med. Microbiol.* 68, 493–502. doi: 10.1099/jmm.0.00094.5

Žiemytė, M., Rodríguez-Díaz, J. C., Ventero, M. P., Mira, A., and Ferrer, M. D. (2020). Effect of dalbavancin on staphylococcal biofilms when administered alone or in combination with biofilm-detaching compounds. *Front. Microbiol.* 11:553. doi: 10.3389/fmicb.2020.00553

Zimmerli, W., Trampuz, A., and Ochsner, P. E. (2004). Prosthetic-joint infections. *N. Engl. J. Med.* 351, 1645–1654. doi: 10.1056/NEJMra040181

Conflict of Interest: The authors declare that the research was conducted in the absence of any commercial or financial relationships that could be construed as a potential conflict of interest.

Publisher's Note: All claims expressed in this article are solely those of the authors and do not necessarily represent those of their affiliated organizations, or those of the publisher, the editors and the reviewers. Any product that may be evaluated in this article, or claim that may be made by its manufacturer, is not guaranteed or endorsed by the publisher.

frontiers in Microbiology

REVIEW
published: 29 October 2021
doi: 10.3389/fmicb.2021.750460

Challenges in the Microbiological Diagnosis of Implant-Associated Infections: A Summary of the Current Knowledge

Alessandra Oliva[1]†, Maria Claudia Miele[1†], Dania Al Ismail[1†], Federica Di Timoteo[1], Massimiliano De Angelis[1], Luigi Rosa[1], Antimo Cutone[2], Mario Venditti[1], Maria Teresa Mascellino[1], Piera Valenti[1] and Claudio Maria Mastroianni[1]*

[1] Department of Public Health and Infectious Diseases, Sapienza University of Rome, Rome, Italy, [2] Department of Biosciences and Territory, University of Molise, Pesche, Italy

Implant-associated infections are characterized by microbial biofilm formation on implant surface, which renders the microbiological diagnosis challenging and requires, in the majority of cases, a complete device removal along with a prolonged antimicrobial therapy. Traditional cultures have shown unsatisfactory sensitivity and a significant advance in the field has been represented by both the application of the sonication technique for the detachment of live bacteria from biofilm and the implementation of metabolic and molecular assays. However, despite the recent progresses in the microbiological diagnosis have considerably reduced the rate of culture-negative infections, still their reported incidence is not negligible. Overall, several culture- and non-culture based methods have been developed for diagnosis optimization, which mostly relies on pre-operative and intra-operative (i.e., removed implants and surrounding tissues) samples. This review outlines the principal culture- and non-culture based methods for the diagnosis of the causative agents of implant-associated infections and gives an overview on their application in the clinical practice. Furthermore, advantages and disadvantages of each method are described.

Keywords: implant-associated infection, biofilm, sonication, culture-based methods, diagnosis, BioTimer Assay, molecular methods, metabolic assays

OPEN ACCESS

Edited by:
María Guembe, Gregorio Marañón Hospital, Spain

Reviewed by:
Werner Zimmerli, Cantonal Hospital Baselland (KSBL), Switzerland
Claus Moser, Rigshospitalet, Denmark

***Correspondence:**
Alessandra Oliva
alessandra.oliva@uniroma1.it

† These authors have contributed equally to this work

Specialty section:
This article was submitted to Infectious Agents and Disease, a section of the journal Frontiers in Microbiology

Received: *30 July 2021*
Accepted: *04 October 2021*
Published: *29 October 2021*

Citation:
Oliva A, Miele MC, Al Ismail D, Di Timoteo F, De Angelis M, Rosa L, Cutone A, Venditti M, Mascellino MT, Valenti P and Mastroianni CM (2021) Challenges in the Microbiological Diagnosis of Implant-Associated Infections: A Summary of the Current Knowledge. Front. Microbiol. 12:750460. doi: 10.3389/fmicb.2021.750460

INTRODUCTION

Implant-associated infections (IAIs) are associated with high morbidity and increased costs for the healthcare systems (Hedrick et al., 2006). IAIs, including, amongst other, those associated with totally intracorporeal devices [Prosthetic Joint Infections (PJIs), Cardiovascular Implantable Electronic Device Infections (CIED-Is), Neurosurgical Infections (NS-Is), Ureteral Stent Infections

Abbreviations: IAIs, Implant-associated infections; PJIs, Prosthetic Joint Infections; CIED-Is, Cardiovascular Implantable Electronic Device Infections; NS-Is, Neurosurgical Infections; US-Is, Ureteral Stent Infections; VG-Is, Vascular Graft Infections; BI-Is, Breast Implant Infections; TC, Tissue Culture; CoNS, Coagulase Negative Staphylococci; SFC, Sonication Fluid Culture; CFU, Colony-Forming Units; EBJIS, European Bone and Joint Infection Society; ICM, International Consensus Meeting; BCB, Blood Cultures Bottles; CSF, cerebrospinal fluid; EVDs, external ventricular drains; VP, ventriculo-peritoneal; MUSC, microbial colonization of the ureteral stent; DTT, Dithiothreitol; XTT, 2,3-bis (2-methoxy-4-nitro-5-sulfophenyl)-5-[(phenylamino) carbonyl]- 2H-tetrazolium hydroxide; BTA, BioTimer Assay (BTA); PCR, Polymerase Chain Reaction; qPCR, quantitative Polymerase Chain Reaction; NGS, next-generation sequencing (NGS); OTUs, Operational taxonomic units; MALDI-TOF, matrix-associated laser desorption/ionization time-of-flight.

(US-Is), Vascular Graft Infections (VG-Is), and Breast Implant Infections (BI-Is)], are characterized by microbial biofilm formation on implant surface, which makes the microbiological diagnosis difficult and requires a complete device removal for their correct management (Deng and Lv, 2016).

In general, implants are made of synthetic abiotic material or devitalized biological structures. Furthermore, medical devices are either crossing the anatomic barriers (i.e., central venous or urologic catheters, dental implants) or are totally intracorporeal (i.e., orthopedic, neurosurgical, cardiac, vascular implants), with the latter group being classified as intravascular and extravascular implants. The pathogenesis of these various devices as well as the interaction with the host are quite different. Indeed, while intravascular implants mainly interact with coagulation factors and circulating blood cells, extravascular implants interact with surrounding tissue, interstitial fluid, and attracted phagocytes, in the absence of direct interaction with the circulating blood (Zimmerli and Sendi, 2011).

Although many progresses have been made, the diagnosis of the causative microorganisms of IAIs still remains challenging. In fact, diagnostic sensitivity might be reduced since not all the techniques are able to completely detach biofilm from removed implants and the antibiogram is generally performed on planktonic form of detached bacteria (Drago, 2017). Furthermore, a previous antimicrobial therapy might influence the diagnostic yield of culture-based methods (Xu et al., 2017).

In the last years, several approaches have been developed to overcome the above-mentioned limitations, including sonication of the implants before culture, molecular assays, methods based on bacterial metabolism in the biofilm or their combinations (Høiby et al., 2015).

In this report, the application of culture- and non-culture based methods for the diagnosis of causative agents of IAIs will be reviewed, with a main focus on infections of totally intracorporeal devices. In fact, although also catheter-related infections are characterized by biofilm formation, the diagnostic methods between infections associated to devices crossing anatomic barriers and those totally implanted are quite different.

LITERATURE SEARCH

The online database PubMed was searched using the following terms: "implant-associated-infections," "biofilm-infections," "microbiological diagnosis," AND "implant-associated-infections" OR "biofilm-infections," "sonication," "molecular analyses," AND "implant-associated-infections" OR "biofilm-infections," "metabolic assays," AND "implant-associated-infections" OR "biofilm-infections," "tissue culture," AND "implant-associated-infections" OR "biofilm-infections," "Resazurin Assay," "BioTimer Assay," "XTT Assay," "Gram stain," "microscopy," "Broad-range 16S rRNA gene PCR" AND "implant-associated-infections" OR "biofilm-infections," "sequencing" AND "implant-associated-infections" OR "biofilm-infections," "Multiplex PCR" AND "implant-associated-infections" OR "biofilm-infections," "IBIS T5000" AND "implant-associated-infections" OR "biofilm-infections," "dithiothreitol." The combination of the abovementioned terms with "Cardiac Device Infections," "CIED infections," "Ureteral Stent infections," "Prosthetic Joint Infections," "Neurosurgical Infections," "Vascular Graft Infections" and "Breast Implant Infections" was also used.

CULTURE-BASED METHODS

Swabs and Tissue Cultures

Tissue swabs are never indicated for the diagnosis of IAIs due to their lower sensitivity compared to tissue culture (Dy Chua et al., 2005; Drago et al., 2019). Furthermore, superficial swabs (i.e., from fistula) can be easily contaminated by normal skin flora, therefore not representing the true pathogen and possibly contributing to an erroneous etiological diagnosis.

On the other hand, cultures from the tissue (TC, tissue culture) adjacent to the device are part of the diagnostic approach toward IAIs (Peel et al., 2017).

Sonication

Method

Sonication is a quantitative method based on the application of long-wave ultrasounds (frequencies above the range of human hearing, 20 kHz) which has been increasingly used in order to enhance bacterial growth by liberating sessile organisms embedded in biofilm (Nguyen et al., 2002; Klug et al., 2003; Carmen et al., 2005; Bjerkan et al., 2009; Rieger et al., 2009; Sampedro et al., 2010; Bonkat et al., 2011). Technically, ultrasound waves radiate through a liquid media and produce high- and low-pressure areas. During the low-pressure phase, microscopic bubbles form and further collapse during the high-pressure phase by releasing a high amount of energy on the surface of the foreign body, which is able to dislodge bacteria from the device (Pitt and Ross, 2003; Trampuz et al., 2003). Sonication is also able to lyse bacterial cells, and whether bacteria are dislodged from foreign bodies or lysed depends on several factors such as acoustic frequency, energy, temperature and time of ultrasound exposure, duration of sonication and the shape of bacteria (Osmon et al., 2013). Among different sonication protocols (Tande and Patel, 2014), the most widely used for dislodging bacteria from foreign bodies are based on 1-min (Trampuz et al., 2007; Hoekstra et al., 2020) or 5-min duration of sonication at power of 0.22 ± 0.04 W/cm^2 (McDowell and Patrick, 2005; Sampedro et al., 2010; Oliva et al., 2013, 2016), with or without the centrifugation as a concentration process. The process of sonication is depicted in **Figure 1**.

As a matter of fact, the use of sonication in the clinical microbiology laboratory has been investigated for the diagnosis of PJIs, CIED-Is, NS-Is, VG-Is, and US-Is and is therefore reviewed in the following paragraphs.

Sonication for Prosthetic Joint Infection

PJIs represent an important complication of prosthetic surgery, occurring in 1–2% after primary hip or shoulder arthroplasty, 2–4% after knee arthroplasty and up to 9% after elbow arthroplasty (Izakovicova et al., 2019). Microbiological diagnosis of PJIs

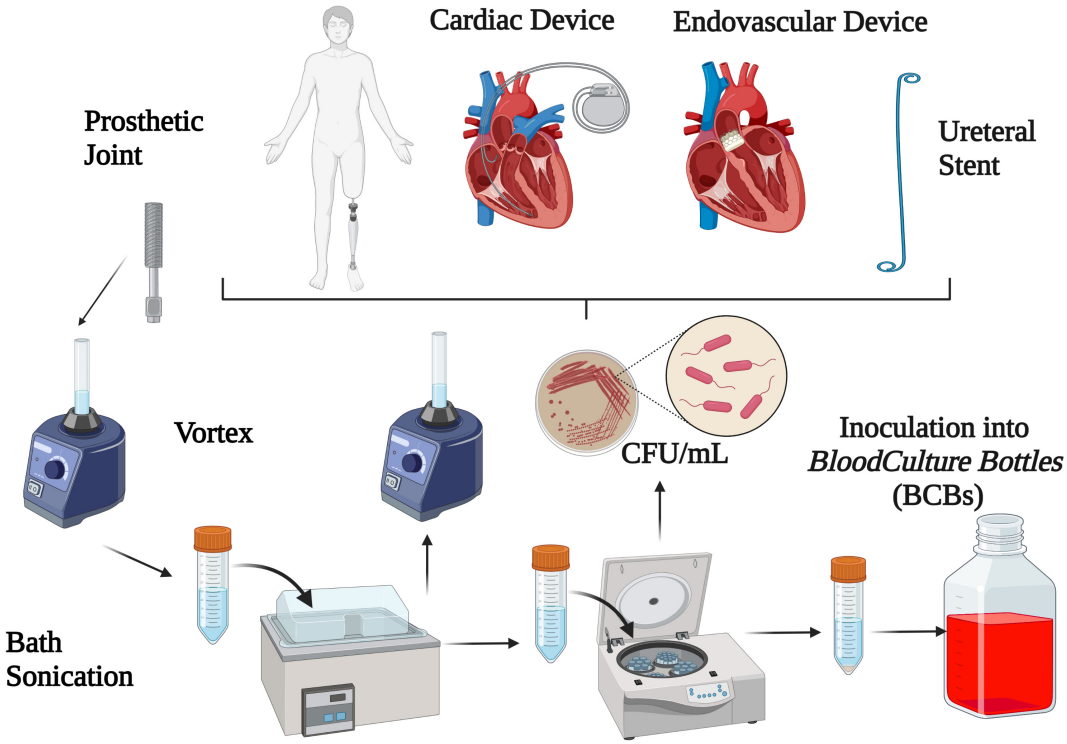

FIGURE 1 | Overview of sonication method for the diagnosis of implant-associated infections.

mostly relies on pre-operative (i.e., synovial fluid cultures) and intra-operative (i.e., tissue culture and implant sonication) samples (Osmon et al., 2013). The sensitivity of synovial fluid culture ranges from 45 to 75%, with a specificity of 95% (Izakovicova et al., 2019); however, up to one-third of intra-operatively culture-positive episodes were negative in pre-operative synovial fluid culture (Schulz et al., 2021).

Sonication was popularized as a diagnostic tool for PJIs by Trampuz et al. (2007), where authors were able to (i) demonstrate higher sensitivity of sonication than TC, (ii) find an optimal cut-off differentiating infection from non-infection, and (iii) demonstrate that the sensitivity of sonication was not hampered by a previous antibiotic therapy (Trampuz et al., 2007). Afterward, several studies have investigated the diagnostic performance of sonication in this setting and, according to the International Consensus Meeting on PJIs in 2018, sonication was recommended as an important element in PJIs diagnostics (Parvizi et al., 2018).

So far, two meta-analyses investigating the sensitivity and specificity of sonication (Zhai et al., 2014; Liu et al., 2017) have been performed. The first was conducted by Zhai et al. (2014) including 12 studies and showing a pooled sensitivity and specificity of 80 and 95%, respectively. Subgroup analyses showed that (i) a 14-day anaerobic culture may improve sensitivity, (ii) the use of centrifugation or vortexing may improve specificity, (iii) using high amount or Ringer's solution for containers may improve sensitivity and specificity, and (iv) the best sonication fluid culture (SFC) cut-off was > 5 Colony-Forming Units (CFUs) (Zhai et al., 2014). These results were further confirmed by Liu et al. including 16 studies with a pooled sensitivity and specificity of sonication for the diagnosis of PJI of 79 and 95%, respectively. High variability in the method amongst included studies was, however, detected, i.e., for different definitions of PJIs, sample size (59–434 subjects), application of vortexing or centrifugation (11 out of 16 studies), cut-off (not applicable in 6 studies, ranging from 1 to 100 CFU in the other studies) and especially duration of incubation (5–30 days) (Liu et al., 2017). Furthermore, among these studies, 6 compared SFC with TC and overall showed higher sensitivity (but not specificity) of SFC than that of TC and, for patients receiving antimicrobials, this better diagnostic performance was confirmed. Subgroup analyses showed that the specificity of the method may be improved by applying vortexing and centrifugation steps.

Nevertheless, while most studies are in accordance with the superiority of sonication over TC (Portillo et al., 2014; Rothenberg et al., 2017; Renz et al., 2018), several studies have also found the contrary (Van Diek et al., 2017; Grosso et al., 2018). As a matter of fact, Dudareva et al. (2018) demonstrated that the sensitivity of TC was higher than sonication (69% vs. 57%). These findings were further confirmed by a recent study showing higher sensitivity of TC than sonication (94.3% vs. 80.5%), although a certain diagnosis of PJIs was only possible throughout SFC in a not-negligible rate of cases (9%) (Hoekstra et al., 2020). Even more recently, Rieber et al. (2021) showed that the overall sensitivity of TC and SFC was similar (91.3% vs. 90.8%, respectively) and, surprisingly, TC showed

significantly better results than SFC in detecting polymicrobial infections (97.0% vs. 67.0%).

In the never-ending debate on whether SFC is better than TC or *viceversa*, it should be noticed that the divergence in results between studies could be attributed to the variability of study conditions, rendering the interpretation of all data even more challenging (Trampuz et al., 2007; Piper et al., 2009; Bjerkan et al., 2012; Borens et al., 2013; Dudareva et al., 2018; Sandbakken et al., 2020). Furthermore, the diagnostic performance of the method also depends on the adopted criteria for defining infection; for instance, Bellova et al. (2019) found different sensitivity and specificity of SFC and TC when using the European Bone and Joint Infection Society (EBJIS) or the International Consensus Meeting (ICM) 2018 definitions, respectively (Bellova et al., 2019).

In light of this, since both sensitivity and specificity of sonication for the diagnosis of PJIs may be influenced by some parameters such as incubation time, previous antibiotic therapy, type of infection (acute or chronic) and the CFU cut-off defined, studies investigating these parameters are following reviewed.

Duration of Incubation

Duration of incubation is an important parameter influencing the diagnostic performance of sonication; in fact, on one side a too short incubation may lower bacterial detection, especially when considering low-virulent ones, on the other side a too long incubation may promote contamination of the medium and, therefore, alter the results (Esteban et al., 2013).

However, there has been debate about the optimal length of incubation of PJI samples and systematic assessment of culture duration has not been defined yet (Virolainen et al., 2002; Neut et al., 2003; Williams et al., 2004; Nelson et al., 2005; Parvizi et al., 2006; Trampuz and Widmer, 2006; Trampuz et al., 2007; Piper et al., 2009; Holinka et al., 2011; Esteban et al., 2013; Portillo et al., 2013, 2014; Shen et al., 2015; Renz et al., 2018). Several authors have recommended incubation for 10–14 days in order to improve the sensitivity (Butler-Wu et al., 2011; Minassian et al., 2014; Portillo et al., 2015; Hoekstra et al., 2020; Rieber et al., 2021) whereas only one study, to our knowledge, proposed 30 days of incubation to detect anaerobic bacteria (Esteban et al., 2008). A 2-week incubation period seems to be optimal since early detected species (mostly Staphylococci) emerge predominantly during the first week, whereas late-detected agents (mostly *Cutibacterium* species, formerly known as *Propionibacterium* spp.) are detected mainly during the second week of incubation (Lutz et al., 2005; Schäfer et al., 2008; Portillo et al., 2014). Interestingly, microorganisms grow faster in SFC than in TC. With this regard, Portillo et al. (2014) showed that a difference in bacterial detection between SFC and TC already emerged after 2 days of incubation (48% vs. 26%) and this difference was even more evident after one and 2 weeks of incubation (77% vs. 59% and 81% vs. 61%), respectively.

Recently, Talsma et al. (2021) found that, despite a similar median time to pathogen detection between acute and chronic PJIs (2 days), in acute PJIs all isolates grew within 5 days and therefore a prolonged incubation time may not be necessary. In contrast, for chronic PJIs the time for bacterial growth was longer (11 days) and therefore prolonged incubation appears crucial. When comparing SFC with TC depending on the time of infection (acute vs. chronic PJIs), the same authors found that in acute infections the time to bacterial growth was similar between the 2 methods whereas SFC exhibited a faster pathogen detection than TC in chronic infections (78% vs. 52% after 2 days) (Talsma et al., 2021). Should these results be confirmed, there is the potential to reduce the workload of handling PJI cultures in the laboratory and, consequently, the diagnostic costs according to the time of infection.

Effect of Antimicrobial Therapy

One of the major challenges in the diagnosis of PJIs is the possibility that a previous antimicrobial therapy may hamper the diagnostic sensitivity of the method. With this regard, several studies investigated the sensitivity of SFC compared with that of TC in patients receiving antimicrobial therapy up to 14 days before specimen collection and authors found that, despite the sensitivity of SFC is overall reduced in subjects receiving antimicrobial therapy, still SFC was more sensitive (Trampuz et al., 2007; Holinka et al., 2011; Portillo et al., 2013, 2014, 2015; Liu et al., 2017). As a matter of fact, in the review from Liu et al. (2017) in patients who received antibiotic therapy within 14 days sonication performed better than traditional TC. Yan et al. (2018) showed a similar sensitivity of SFC in patients who had received antibiotics and those who had not within 4 weeks before surgery (76.3% vs. 71.2%) and in the recent study from Schulz et al. (2021) the administration of antibiotics did not show any effect on the diagnostic microbiological yield. In detail, when microbiological and non-microbiological diagnostic tests were considered together, the positivity rate was 98 and 97% with and without antibiotics, whereas when considering only SFC the pathogen detection rate was 82% in presence of antibiotics compared to 74% of TC (Schulz et al., 2021).

When taking into account the colony count cut-off, Portillo et al. (2013) found that sensitivity of sonication fluid cultures was significantly lower if patients had previously received antibiotics. As a matter of fact, using the cut-off of 50 CFU/mL, SFC showed a high discriminative power for differentiating between infection and non-infection (Izakovicova et al., 2019), whereas in patients who had received antimicrobials previous to surgery this cut-off should not be used and, consequently, any growth in SFC from patients who had taken antibiotics within 2 weeks from sample collection should be considered positive (Portillo et al., 2013; Stylianakis et al., 2018). Another interesting aspect was that a previous antimicrobial treatment reduced the culture sensitivity of sonication fluid more in acute than in chronic PJIs (Portillo et al., 2013). This finding may be easily explained by the fact that antimicrobial therapy mostly acts on planktonic bacteria, which are more present in acute infections, whereas the killing efficacy of antimicrobials is reduced in chronic infections, which are characterized by a more biofilm formation and, consequently, the diagnostic performance of SFC is augmented (Portillo et al., 2014).

Sonication Fluid Inoculated Into Blood Culture Bottles

A promising approach to increase sensitivity is represented by the inoculation of SFC into BCBs. As a matter of fact, a recent meta-analysis including 4 studies (Janz et al., 2013; Portillo et al., 2015; Shen et al., 2015; Stylianakis et al., 2018) showed a pooled sensitivity and specificity of 0.85 and 0.86, respectively (Li et al., 2018), even in patients receiving antibiotics (Portillo et al., 2015). This was especially true considering that growth media in blood culture bottles contain antimicrobial removal systems and therefore allows growth of microorganisms immediately after inoculation.

Inoculating SFC into BCBs was also able to reduce the time of microorganism detection (2.9 vs. 4.2 days) (Janz et al., 2017). Likewise, Portillo et al. (2015) showed that the incubation time was shorter with SFC-BCB than periprosthetic TC and conventional sonication method (72% vs. 18% and 28% after 1 day of incubation, respectively).

However, one of the main limitations of this method is represented by the absence of defining a colony count threshold to define positive culture, therefore influencing the specificity of the method (Jan et al., 2013; Portillo et al., 2015; Stylianakis et al., 2018). Shen et al. (2015) compared SFC in BACTEC bottles with synovial fluid cultures in BACTEC bottles and showed that (i) SFC-BCBs detected a higher number of pathogens than synovial fluid-BCBs, (ii) the sensitivity of SFC-BCBs was higher than that of synovial fluid cultures-BCBs (88% vs. 64%) independently of receiving antimicrobial therapy, and (iii) the specificity of SFC-BCBs was lower than that of synovial fluid cultures-BCBs (87% vs. 98%). Likewise, Janz et al. (2017) found a lower percentage of positive cultures in synovial fluid-BCBs than SFC-BCBs (22% vs. 44%), but the average duration of positive growth in synovial fluid was shortened to 1.8 days, compared with 2.9 days in SF (Janz et al., 2017).

Nevertheless, Rieber et al. (2021) showed that SFC-BCBs is less efficient if anaerobes are the suspected cause of infection and therefore recommended caution when dealing with anaerobes possibly causing PJIs until a gold standard for laboratory handling of anaerobes has been established. Furthermore, the same authors showed that using inoculation into thioglycollate broth was better than into BCBs (Rieber et al., 2021).

Sonication for Implant-Associated Infections Other Than Prosthetic Joint Infections

Cardiac Implantable Electronic Device Infection

CIED-Is are dangerous conditions with an increasingly incidence over the last years and a significant rate of mortality.

Sonication has been investigated as a diagnostic tool for the diagnosis of CIED-Is, showing overall higher sensitivity than traditional cultures (Rohacek et al., 2010, 2015; Mason et al., 2011; Oliva et al., 2013, 2018; Inacio et al., 2015; Nagpal et al., 2015; Tascini et al., 2016) and, according to the recent guidelines (Blomström-Lundqvist et al., 2020) is considered as an useful diagnostic tool for the etiological diagnosis of CIED-Is, although no definite evidence is provided (Viola et al., 2009). A major study conducted by our group showed that in a total of 20 subjects with clinically defined CIED-Is, SFC was positive in 18/20 (90%) patients in contrast to conventional culture and surgical swab (16/20, 80% and 6/20, 30%, respectively) (Oliva et al., 2013), thus confirming the results obtained by Mason et al. (2011). Subsequently, Nagpal et al. (2015) and Rohacek et al. (2015) demonstrated that bacterial growth was more frequent after sonication than with traditional cultures including swabs, TCs and BCs (Nagpal et al., 2015; Rohacek et al., 2015). Interestingly, sonication was the only method that detected bacteria in four patients (Rohacek et al., 2015) and showed a higher pathogen detection rate in patients on antibiotic therapy than TC (Inacio et al., 2015; Oliva et al., 2018).

In addition, sonication can provide information not only on the detection of the causative pathogen of CIED-Is, but also on its pathogenesis, by evaluating the different rate of pathogen detection according to the different samples analyzed (i.e., generators vs. electrodes) (Oliva et al., 2013, 2018; Rosa et al., 2019).

The diagnostic accuracy of SFC in comparison with 16S rRNA PCR/sequencing on sonication fluid for infected (n = 278) and non-infected (n = 44) CIEDs has been recently investigated by Esquer Garrigos et al. (2020). Authors found that the sensitivity of 16S rRNA PCR/sequencing was higher than SFC (64% vs. 57.5%, confirmed when considering only definite infections, 76.4% vs. 69.3%), with a similar high specificity (97.7% vs. 95.4%). Interestingly, 16S rRNA PCR/sequencing detected a potential pathogen in a not-negligible rate of culture-negative samples (23.7%).

Sonication for Infections After Neurosurgery

Microbiological diagnosis of infections after neurosurgery is essential and it is mainly based on the cerebrospinal fluid (CSF) culture, which, however, can be negative in 23–78% of patients, especially those receiving antibiotics (Martin et al., 2018), combined with the analysis of the implants, when removed. Following the favorable experience with sonication in the setting of other IAIs, different studies evaluated the diagnostic performance of this method in the setting of external ventricular drains (EVDs) and ventriculo-peritoneal (VP) shunts infections (Jost et al., 2014; Prinz et al., 2019; Apostolakis, 2020; Conen et al., 2020). Jost et al. (2014) compared sonication with CSF cultures in 27 explanted devices (14 EVDs, 13 VPSs). In the EVD group, culture after sonication grew significantly more bacteria than the aspirated ventricular CSF cultures (64% vs. 14%), whereas in the VPS group the difference was not significant. Interestingly, the development of clinical significant meningitis might be anticipated by the positivity of EVD or VPS sonication culture.

A not recent study investigating the rate of bacterial colonization in cerebral catheters by using roll-plate or sonication method found that both antibiotic impregnated and non-impregnated catheters were colonized whereas CSF cultures were positive only in a minority of patients (Zabramski et al., 2003). In the study authored by Prinz et al. (2019), tissue homogenate, CSF, and deep swabs were collected for microbiological examination and, in a subset of patients, the removed implants were also sonicated (n = 22). Sonication cultures showed a positive microbiological result in the totality of cases (100%), while with the combination of conventional microbiological methods the responsible organism was identified in 60% of the samples

(tissue homogenate 57.7%, deep swabs 71.4%, CSF 19.4% each, respectively). Interestingly, in those patients receiving antimicrobial treatment before device explantation, SFC showed 100% of sensitivity compared to 50% of conventional methods, suggesting its use in the clinical practice of EVD and VP infections. The difference between sonication and conventional methods was more evident in the case of low-virulent pathogens (sensitivity 100% vs. 55% in sonication and conventional cultures, respectively).

In the study authored by Roethlisberger et al. (2018) bacterial growth was observed in 19 ventricular EVDs and 21 subcutaneous EVDs throughout sonication of the subcutaneous portion of the catheter and of its tip, the main pathogens being CoNS and *C. acnes*.

Apostolakis (2020) performed a meta-analysis including 6 studies (4 involving EVDs or VP, 1 cranioplasty, 1 spinal fusion instrumentation) with the aim to assess the efficiency of sonication in the diagnostic work-up of postoperative infections following NS. Potential superiority of sonication over conventional microbiologic methods was found in the detection of gram-positive bacteria and in particular of CoNS, with an overall sensitivity of 0.87 and a specificity of 0.57 (Apostolakis, 2020).

Sonication for Vascular Graft Infections

VG-Is, although rare, are associated with high morbidity and mortality and the success of antibiotic treatments relies on early and accurate diagnosis (Lyons et al., 2016). However, conventional reference microbiological methods have a low sensitivity rate, as up to 45% of VG-Is still remain culture negative (Legout et al., 2012). Tollefson et al. (1987) first evaluated biofilm breakdown by sonication in an animal model of contamination and in 7 graft materials excised from patients undergoing femoral anastomotic pseudoaneurysm repair. Sonication significantly increased the incidence of positive cultures of graft material compared with broth and blood agar plate culture techniques (Tollefson et al., 1987). In the following years, only few studies investigated the potential diagnostic role of sonication in the setting of VGIs, in combination with molecular methods (Puges et al., 2018; Ulcar et al., 2018). A retrospective study in 2017 highlighted the importance of SFC in parallel with broad-PCR, as they contribute to the optimization of antimicrobial treatment. Indeed, in a total of 22 patients with VG-Is, preoperative BCs were positive in 35.3%, intraoperative TCs in 31.8%, SFC in 79.2%, and PCR from sonicated fluid in 66.7% (Ulcar et al., 2018). Similarly, Puges et al. (2018) compared conventional bacterial cultures with and without prior sonication of specimens and a genus-specific PCR analysis targeted to the most frequent bacteria involved in VG-Is. The sensitivity of the graft culture was 85.7%, of the SFC was 89.7%, and of the genus-specific PCR was 79.5%, respectively. The combination of SFC and PCR achieved a microbiological diagnosis for all patients with VGIs, with a sensitivity of 100% and a specificity of 83.3% (Puges et al., 2018).

Sonication for Ureteral Stent Infections

Ureteral stents represent a significant inherent risk of microbial colonization and biofilm formation because they provide an ideal surface for microbial adherence (Joshi et al., 2003; Bonkat et al., 2011; Scotland et al., 2019). Diagnosis of microbial colonization of the ureteral stent (MUSC) is difficult because the cultural methods normally used are not useful in detecting microorganisms embedded in biofilm and consequently a negative urine culture does not rule out biofilm formation. Bonkat et al. (2011) developed a sonication system based on the method described by Trampuz et al. (2007) and showed that SFC detected MUSC in 36% of 408 stents and 93 were positive with sonication alone compared to 8 positive with urine culture alone (Bonkat et al., 2011). The importance of sonication in MUSCs was confirmed by a second study performed by the same group in which the yield of microbial growth using sonication was significantly higher than that observed in urine cultures (Bonkat et al., 2012).

Subsequently, the same research group performed a prospective randomized study comparing the roll-plate technique with sonication in the diagnosis of MUSC. The roll-plate technique showed a higher detection rate of MUSC than sonication and CUC (35% vs. 28 and 8%, respectively). This study demonstrated the superiority of the roll-plate technique, but still confirmed the efficiency of sonication in identifying mixed biofilms (Bonkat et al., 2013).

Sonication for Breast Implant Infections

Breast implants are widely used for cosmetic purposes and after mastectomy. Apart from clinical evident infection, a common complication after breast surgery with prosthesis implantation is capsular contracture (Spear and Baker, 1995), whose etiology remains still unclear, although bacterial colonization and biofilm formation by CoNS, *C. acnes,* and other skin-flora microorganisms with consequent low-grade infection are considered the causative mechanism (Pajkos et al., 2003; Del Pozo et al., 2009). Indeed, a statistically significant correlation between a positive culture and symptomatic capsular contracture was found in several studies (Dobke et al., 1995; Ahn et al., 1996; Virden et al., 2020), especially when using sonication as a diagnostic method (Pajkos et al., 2003; Del Pozo et al., 2009; Rieger et al., 2009, 2013, 2016; Reischies et al., 2017). Pajkos et al. (2003) performed a study including implants and capsules removed from patients with or without capsular contracture and showed that the majority of samples obtained from patients with contracture yielded bacteria, significantly higher than in samples obtained from patients without contracture. Del Pozo et al. (2009) analyzed 45 breast implants removed for reasons other than overt infection including capsular contracture (27/45, 60%) and demonstrated that there was a significant association between capsular contracture and the presence of bacteria on the implant. In the following years, Rieger et al. (2013) published a multicentric study including 121 removed implants and, again, a strong correlation between the degree of capsular contracture and positive sonication culture was shown. Subsequently, Karau et al. (2013) prospectively included 328 breast tissue expanders removed for any reason including infection and, apart from showing that in the infection group (n = 7) sonication showed higher sensitivity than tissue cultures, demonstrated that a not-negligible rate of breast tissue expanders (16%) appeared to

be asymptomatically colonized with normal skin flora. More recently, Reischies et al. (2017) showed a high sensitivity of sonication of implants removed for reasons other than infection and, more interestingly, noticed that the microorganisms isolated (CoNs, *C. acnes*) and suspected to trigger the formation of capsular contracture were not adequately targeted by the common antibiotics used for prophylaxis.

Conclusive Remarks of Sonication Method in the Diagnosis of Implant-Associated Infections

Overall, the use of SFC, alone of combined with molecular or metabolic methods or with inoculation into BCBs, exhibited a high performance for the etiological diagnosis of IAIs. Although the majority of data come from PJIs, increasing interest has been shown also for other types of IAIs including endovascular, neurosurgical and ureteral stent ones. The main reason for the high sensitivity of this method relies on the ability of low-grade ultrasounds to detach, but not kill, bacteria adherent to the surface of an implant and, at the end, to permit bacterial culture. Interestingly, sonication seems to be less influenced by a previous antimicrobial therapy than other culture-based diagnostic methods. Amongst other characteristics, sonication is able to detect polymicrobial infections and permits the enumeration of bacteria in the biofilm with, in some circumstances, the possibility of good discrimination between infective and non-infective conditions. Last but not least, SFC is an easy-to-perform and low-cost diagnostic method, which, therefore, may be implemented in all the microbiology laboratories (**Table 1**).

However, it should be highlighted that, as sonication requires multiple processing steps, especially when combined with vortexing and centrifugation, the risk of contamination may occur, frequently caused by low-virulent organisms such as CoNS and *C. acnes*. This also applies if bag leakage during sample collection occurs (Trampuz and Widmer, 2006) and, with this regard, the use of solid and air-tight containers may further reduce the risk of contamination (Trampuz et al., 2007). Therefore, adequate staff training and use of appropriate containers are crucial. Another disadvantage of sonication is represented by the long-lasting incubation period, which may influence the start of adequate antimicrobial treatment. To overcome these limitations, the combination with metabolic or molecular assays may be of high importance in order to shorten the time to pathogen detection.

TABLE 1 | Overview of the principal advantages and disadvantages of culture- and non-culture based methods for the diagnosis of implant-associated infections.

	Advantages	Disadvantages
Culture-based methods		
Tissue swab	- Permits bacterial identification	- High possibility of contamination; - Not representative of the real pathogen; - Not recommended in the guidelines
Tissue culture	- Permits bacterial identification; - Easy to perform; - Possibility of using tissues for additional analyses	- Prolonged incubation time; - Possibility of contamination
Sonication	- High sensitivity; - Able to detach, and not kill, adherent bacteria; - Permits bacterial identification; - Permits the enumeration of bacteria; - Detects polymicrobial infections; - Easy to perform; - Possibility of using sonication fluid for additional analyses	- Prolonged incubation time; - Possibility of contamination; - Need of appropriate apparatus; - Possibility of bacterial lysis if no appropriate parameters are used
Non-culture-based methods		
Dithiothreitol (DTT) assay	- Easy to perform; - Low cost; - High sensitivity to detach the adherent bacteria	- Toxic effect on bacterial cells creating false negatives
Metabolic assays		
Resazurin assay	- High sensitivity and specificity	- The reliability is influenced by the bacterial respiratory efficiency; - The presence of antibacterial compounds decreases the reliability; - The time of resazurin reduction is species and strain specific
XTT Assay	- Procedure efficient and intuitional	- The different metabolism gradients slow down the reduction of XTT
BioTimer Assay	- Easy to perform; Low cost; - Diagnosis of the infected device in a short time; - Identification of fermenting or non-fermenting bacteria; - Enumeration of the actual number of microorganisms in planktonic, adherent, aggregated or biofilm lifestyle; - No manipulation of the samples; - Application of the antibiogram directly on colonized devices	- Unable to determine microbial genus or species

(Continued)

NON-CULTURE BASED METHODS

Dithiothreitol Assay

DTT is a strong reducing agent that reduces disulfide bonds at the sulfhydryl group in peptides and proteins. Specifically, by cleaving disulfide bonds between cysteine groups, it acts as a protein denaturant (Olofsson et al., 2003). Based on these considerations, Drago et al. (2012) hypothesized that a new treatment with DTT could be able to remove bacterial biofilm from prosthetic implants. Specifically, in their first pilot *in vitro* study, authors compared the detection rate of DTT compared to that of N-Acetyl cysteine (Drago et al., 2012), scraping and

TABLE 1 | (Continued)

	Advantages	Disadvantages
Molecular assays	- Identification of rare, unusual and non-cultivable microorganisms; - Short response time; - Easy combination among assays; - Possible application for patients receiving antibiotic treatment prior to surgery; - Molecular antibiogram	- Contamination by host DNA; - Contamination by dead microorganisms; Purification and enrichment of high quality DNA; - Quality database; Detection limit for NGS; - Arbitrary criteria for the inclusion/exclusion of pathogens for Multiplex PCR
Microscopy methods		
Gram staining	- Easy to perform; - Low cost; - High specificity	- Low sensitivity;
Other microscopy methods (confocal laser scanning microscopy, scanning electron microscopy, fuorescence microscopy)	- High quality images; - Biofilm's structural integrity is maintained; - Species-specific fluorescence probes - Possibility of distinguish between live/dead bacteria	- High cost; - Need of experienced and highly trained users

sonication from polyethylene and titanium discs. Treatment with DTT showed a marked increase in bacterial colony counts detection. Detachment of *Pseudomonas aeruginosa* and *Escherichia coli* showed similar yields for DTT and sonication, but lower than for scraping and N-Acetyl cysteine treatment, whereas detachment of *Staphylococcus aureus* and *Staphylococcus epidermidis* was greater for DTT-treated discs than for those treated with sonication, scraping and N-Acetyl cysteine. Overall, these data suggest that the treatment of prostheses with DTT could be useful for the diagnosis of PJIs (Olofsson et al., 2003). To this end, the same authors conducted a study on joint prostheses and compared DTT treatment with sonication and periprosthetic TC. In terms of sensitivity and specificity, DTT provided values of 85.7% and 94.1%, respectively, which were very close to those for sonication (71.4% and 94.1%, respectively), thus representing a valid alternative to sonication in the microbiological diagnosis of PJI (Drago et al., 2013).

Sambri et al. (2018) proposed DTT treatment as an alternative to sonication in a randomized trial that enrolled 232 patients undergoing knee and hip replacements. The aim was to compare DTT treatment and sonication technique with standard TC for the diagnosis of PJIs. As a matter of fact, sonication fluid culture and DTT showed higher sensitivity (89% and 91%, respectively) than TC (79%). Most important, in the group of patients in whom infection was not suspected before surgical intervention, the sensitivity of DTT showed a higher value (100%) than sonication and TC (70% and 50%, respectively). In contrast, no increase in sensitivity was observed among the 3 techniques for cases in which infection was suspected (Sambri et al., 2018). In contrast to Sambri et al. (2018) and Randau et al. (2020) recently reported that DTT fluid cultures were less sensitive than SFC (65% vs. 75%).

Based on the work done by Drago et al., also De Vecchi et al. (2016) conducted a study on periprosthetic tissue samples treated with DTT for the diagnosis of PJIs compared with simple washing in normal saline. Treatment with DTT showed a sensitivity of 88% and specificity of 97.8%, significantly higher than those obtained for saline (72% and 91.1%, respectively) (Drago and De Vecchi, 2017). The same research group has expanded the DTT treatment by enriching it with specific culture broths for aerobic and anaerobic bacteria suggesting that this approach may be useful to increase the detachment of bacteria from biofilm and optimize bacterial growth and PJIs diagnosis (De Vecchi et al., 2017).

More recently, it was shown that, compared to the conventional culture of periprosthetic tissue samples, a commercial device using DTT, the MicroDTTect system, was able to improve the microbiological diagnosis of low-grade PJIs throughout the identification of additional bacteria. Furthermore, it reduced the time to positivity of cultures, especially in the case of *C. acnes* infection (Kolenda et al., 2021).

The advantages of DTT derive from its simplicity of use, i.e., the lack of special instrumentation, the low costs and the possibility to treat both tissues and devices and therefore it may provide valuable additional support to conventional techniques that are used in the diagnosis of IAIs. However, a disadvantage of DTT is represented by the toxic effect on bacterial cells, possibly misreporting the results of the DTT fluid culture and, thus, creating false negatives (**Table 1**). Additional studies evaluating the role of DTT in IAIs other than PJIs are warranted.

Metabolic Assays

The identification and enumeration of the actual number of bacteria in biofilms has been a challenge for microbiologists due to lack of exploratory methods (Pantanella et al., 2008). In the last decades, three metabolic assays have been discovered and implemented for the diagnosis of IAIs, including the Resazurin Assay (RA), the 2,3-bis (2-methoxy-4-nitro-5-sulfophenyl)-5-[(phenylamino) carbonyl]- 2H-tetrazolium hydroxide (XTT) assay and the BioTimer Assay (BTA). Herein, the pros and cons of these methods are reviewed (**Table 1**).

Resazurin Assay

The resazurin assay, also named Alamar Blue assay is a simple, rapid, and sensitive measurement for the viability of bacteria. Living cells, metabolically active, are able to reduce, in an irreversible process, the blue-non-fluorescent resazurin (7-hydroxy-3H-phenoxazin-3-one-10-oxide) to the pink-fluorescent resorufin up to a completely reduced colorless state (Pantanella et al., 2013). Pink-fluorescent resorufin can be measured through spectrophotometer. For this purpose, resazurin has been used to determine the actual number of viable cells in biofilm and to detect viable microorganisms in many studies on antimicrobial compounds (Guerin et al., 2001; Peeters et al., 2008; Mariscal et al., 2009).

Recently, the resazurin assay was used to detect 92 colistin-resistant and colistin-susceptible *Acinetobacter baumannii* and

Pseudomonas aeruginosa isolates. Sensitivity and specificity were 100 and 95%, respectively, compared with the standard broth microdilution method (Lescat et al., 2019). In addition, this assay was used to develop a microplate assay for the evaluation of the antimicrobial activity of electrospun nano fiber filtration membranes for water treatment technologies against the Gram-negative microorganism *Escherichia coli* and the Gram-positive *Enterococcus faecalis* (Travnickova et al., 2019). Resazurin was used as an indicator of the amount of viable microorganisms. Antimicrobial activities of the membranes were evaluated by either resazurin assay or modified ISO 20743 plate count assay. The comparison between resazurin microplate assay and modified ISO 20743 plate count assay showed comparable results, thus indicating that resazurin microplate assay is efficient, faster and less demanding respect to the traditionally one (Travnickova et al., 2019).

However, some limitations have been reported. In fact, the reliability of this assay is influenced by the bacterial respiratory efficiency that, in turn, is conditioned by the microbial growth phase, the age and thickness of the biofilm. Moreover, as the time of resazurin reduction is species and strain-related and some experimental conditions must be standardized. In addition, the presence of antibacterial compounds decreases the resazurin reduction, thus diminishing the reliability of this method in anti-biofilm researches (O'Brien et al., 2000; Mariscal et al., 2009; Sandberg et al., 2009; Skogman et al., 2012; Pantanella et al., 2013).

2,3-Bis (2-Methoxy-4-Nitro-5-Sulfophenyl)-5-[(Phenylamino) Carbonyl]- 2H-Tetrazolium Hydroxide (XTT) Assay

The 2,3-bis (2-methoxy-4-nitro-5-sulfophenyl)-5-[(phenyl amino) carbonyl]- 2H-tetrazolium hydroxide (XTT) is a kind of tetrazolium salt and it is a substrate of mitochondria dehydrogenase. The XTT assay measured the reduction of water-soluble formazan in viable cells. This method uses a redox indicator to enumerate viable cells in biofilm through spectrophotometry (Pantanella et al., 2013). The number of viable bacteria in biofilm is measured through the absorbance of supernatant after the metabolic reduction of XTT. The results allow direct reading of the absorbance measurement, which makes the procedure efficient and intuitional (Adam et al., 2002; Xu et al., 2016). However, the different metabolism gradients present in the heterogeneity composition of biofilm as well as the formation of mature biofilm slow down the reduction of XTT or partially retain it, and, therefore, represent the main limitations of this method (Honraet et al., 2005; Pantanella et al., 2013).

BioTimer Assay

BioTimer Assay (BTA) is a metabolic method able to determine the actual number of microorganisms in planktonic, aggregated, adherent and biofilm lifestyle using an original reactive containing Phenol Red or Resazurin as indicators. The Phenol Red changes color from red to yellow indicating the presence of fermenting microorganisms, while Resazurin switches from violet to pink detecting non-fermenting ones (Pantanella et al., 2013; Rosa et al., 2017). The time required for indicators' switching is related to the initial number of microorganisms (N0) through a genus-specific correlation line described by the following equation: $t = \log(1 + a/N0)/k$ where "k" indicates the growth rate and "a" is a function of the metabolic product responsible for the indicator switching (Berlutti et al., 2003; **Figure 2**).

Noteworthy, BTA does not require sample manipulation. As a matter of fact, BTA is a low cost, easy to perform method and has been applied: (i) to quantitatively evaluate bacteria adherent to polyelectrolyte HEMA-based hydrogels (Berlutti et al., 2003); (ii) to evaluate antibiotic susceptibility of biofilm (Pantanella et al., 2008), and (iii) to verify microbiological quality of foods (Giusti et al., 2011).

Recently, BTA has been applied to enumerate adherent bacteria to different medical devices (Rosa et al., 2017, 2019). In particular, BTA was used to evaluate Central Venous Catheters colonization in comparison with the vortex method. 125 Central Venous Catheters removed from patients for suspected Catheter-related Bloodstream Infection or at hospital discharge were examined. BTA was reliable, in 100% agreement with vortex method, in assessing the sterility and catheters colonization and in discriminating fermenting from non-fermenting bacteria (97.1% agreement with vortex method) (Rosa et al., 2017). BTA also shortened the analytical time by 2/3-fold compared with standard culture methods (Rosa et al., 2017). Remarkably, the ascertained Catheter-related Bloodstream Infection diagnosis caused the switch of BTA reagent(s) within 8 h in 18 Central Venous Catheters analyzed (100% agreement) and within 12 h in other 11 catheters analyzed (67% of agreement) (Rosa et al., 2017). In this respect, as blood culture requires more time to confirm Catheter-related Bloodstream Infection due to microbial growth, a rapid change of BTA reagents indicates a high number of colonizing bacteria on Central Venous Catheters thus alerting the physician to the possibility of Catheter-related Bloodstream Infection.

However, BTA is unable to determine microbial genus or species. To overcome this intrinsic limit, the use of BTA, in combination with Vortex-Sonication-Vortex Method for the diagnosis of IAIs has been applied (Rosa et al., 2019). The implants analyzed included CIEDs, Peripherally Inserted Central Catheters, port-a-caths, Central Venous Catheters, and ureteral stents. In addition, a new version of BTA, containing both Phenol Red and Resazurin as indicators, was set-up in order to enumerate both fermenting and non-fermenting microorganisms. If fact, this new reagent is able to selectively distinguish fermenting from non-fermenting microorganisms through the indicators' color switch from violet-to-yellow and from violet-to-orange, respectively (Rosa et al., 2019). Over 2016–2018, 46 patients with IAIs were enrolled and their 82 explanted devices were analyzed with Vortex-Sonication-Vortex and BTA. In particular, in order to permit the simultaneous analysis by Vortex-Sonication-Vortex and BTA, each device was covered in the BTA reagent instead of the standard saline solution and, successively, each device was vortexed, sonicated, and vortexed again as previously described (Oliva et al., 2016). After Vortex-Sonication-Vortex treatment, a small amount of the suspension was used for classical microbiological

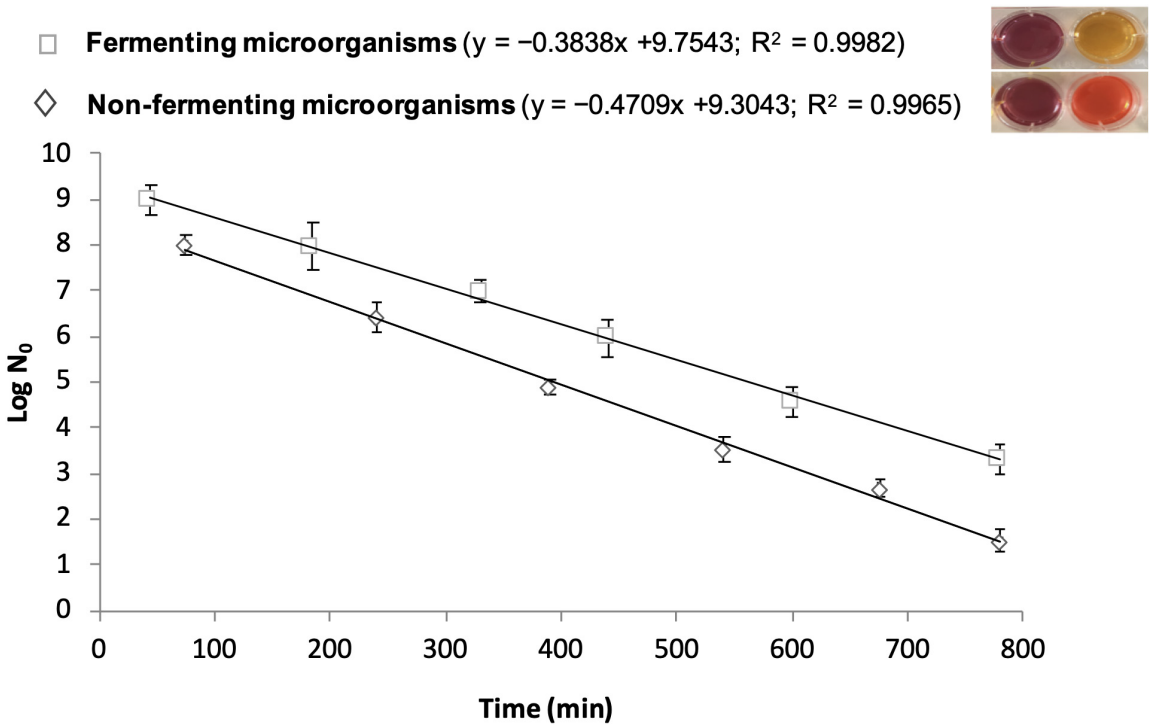

FIGURE 2 | Correlation lines obtained by BioTimer Assay with the reagent containing both Phenol Red and Resazurin as indicators in order to enumerate fermenting (color switch from violet-to-yellow) and non-fermenting (color switch from violet-to-orange) microorganisms. The correlation lines show the relationship between the time (*X*-axis) required for color switch and the initial number of microorganisms (*Y*-axis). The equations and the linear correlation coefficients describing the correlation lines for both fermenting and non-fermenting microorganisms are reported in parenthesis.

analysis and, contemporary, each device immerged in BTA reagent was incubated at 37°C and monitored for the color switch (Rosa et al., 2019). Vortex-Sonication-Vortex plus BTA found microorganisms in 39/46 patients (84.7%) compared with 32/46 (69.5%) and 31/46 (67.3%) by Vortex-Sonication-Vortex and BTA alone, respectively. The combined methods led to microorganism detection in 54/82 devices (65.9%) compared with 43/82 (52.4%) for Vortex-Sonication-Vortex alone and 44/82 (53.6%) for BTA alone (Rosa et al., 2019).

Overall, the combination of both methods permits (i) to diagnose an infected device in a short time; (ii) to identify as fermenting or non-fermenting bacteria and enumerate the actual number of microorganisms directly on the implants without any manipulation of the sample; and (iii) to eliminate false-negative results, thus representing a simple and accurate approach for the identification and enumeration of microorganisms adherent to devices.

Moreover, BTA can be also applied to carry out antibiogram directly on colonized devices without any manipulation (Pantanella et al., 2013).

Molecular Assays

The culture-based methods are fully effective in the identification and characterization of planktonic bacteria causing systemic infections, whereas they show limitations for identifying bacteria in the biofilm. Currently, most of the microbiological fields, with the exception of clinical microbiology, have shifted from culture to molecular methods. These techniques, which can be performed on the majority of medical devices, can allow the identification of microorganisms even in the case of negative-cultures, occurring for either the presence of non-cultivable microorganisms or a prior antibiotic therapy causing the inhibition of microbial growth. Currently, standard molecular approaches include the extraction of microbial DNA, or RNA, from the specimens, the subsequent amplification by universal or specific Polymerase Chain Reaction (PCR), and sequencing. Among critical steps in such procedures, the employment of efficient lysis buffer to ensure the lysis of all bacterial cells as well as the accurate rinse of the medical device before the extraction of bacterial DNA are imperative to ensure that all and only biofilm bacteria are identified. As a matter of fact, a critical limitation of molecular methods relies on the possible contamination of the specimen by host DNA. On the other hand, also bacterial DNA can contaminate sterile surgical grade irrigation fluids and sampling containers (Burmølle et al., 2010; Swearingen et al., 2016), thus rendering difficult to distinguish between bacterial contamination, which can derive from different sources such as the operating room environment or the patient skin, and actual infective clinical bacteria. In addition, free DNA from dead bacteria can represent a source of contamination, which can be avoided by the use of reverse transcriptase for mRNA

amplification, a technique specifically identifying live and active bacteria (Stoodley et al., 2011). To overcome such contamination issue, clinical devices are usually rinsed with large volumes of PBS to remove debris of host tissue as well as planktonic or scarcely adhered bacteria. Indeed, to improve the detection of bacterial DNA in clinical samples, it is pivotal to purify high quality DNA enriched in bacterial source, as a high background of host DNA may hinder the downstream detection of bacterial DNA. Moreover, sequencing process can result in the identification of hundreds of bacterial species in varying amounts, thus requiring a somewhat arbitrary cutoff points to discard false positives. So far, a novel approach for the diagnosis of infections associated to medical devices combines two complementary methods, the sonication of removal implants and subsequent PCR of the resulting sonication fluid (Achermann et al., 2010). Generally, two different amplification-based approaches have been applied to IAIs: (i) broad-range 16S rRNA gene PCR screening followed by sequencing, which allows the identification of any bacterial DNA present in a clinical sample; (ii) multiplex PCR, which targets common causative microorganisms.

Broad-Range 16S Ribosomal RNA Gene Polymerase Chain Reaction and Sequencing

PCR is routinely applied in clinical practice, from genetic testing to the identification of infectious agents (Hamady and Knight, 2009; Moure et al., 2011). In microbiological diagnosis, the most targeted gene is the 16S ribosomal RNA (rRNA), as it includes both highly conserved and hypervariable regions: the first serving as target sites for universal bacteria primers whereas the latter used for the identification of bacterial taxa. Moreover, broad-range 16S rRNA amplification has been reported to be a potential tool for the identification of novel microorganisms (Relman et al., 1992; Drancourt et al., 2004; Meddeb et al., 2016), and the combination with sequencing techniques allows the identification of bacterial strains not identified by conventional phenotypic methods or mass spectrometry (Clarridge, 2004; Petti et al., 2005). Similar to standard or quantitative PCR (qPCR), the broad-range 16S rDNA PCR is able to detect both viable and non-viable bacteria, thus representing a useful tool when microbiological techniques give negative results (Rothman et al., 2010; Meddeb et al., 2016). Indeed, the identified bacteria are often rare, unusual, difficult to culture, or bacteria for which a specific PCR is not available (Rothman et al., 2010). However, the breadth of broad-range 16S rDNA PCR makes it susceptible to contamination. In this regard, the amplification of environmental or PCR mixture contaminants (Corless et al., 2000; Aslanzadeh, 2004; Chang et al., 2011) as well as of eukaryotic DNA from the host (Horz et al., 2008; Handschur et al., 2009) represent a criticism for the sensitivity and specificity of such technique. The incidence of false positive can be limited by performing PCR on independent samples from each patient and/or by employing specific primers for pathogen virulence factor genes beside the 16S rRNA gene primers, increasing specificity. Another pivotal drawback regards the pathogen identification which can result circuitous: the use of universal primers for the amplification of 16S rRNA genes will generate a pool of PCR amplicons of all the bacteria present in the sample, thus requiring the sequencing and comparing to known sequences, a lengthy and costly process that requires quality databases (Tzeng et al., 2015). On the other hand, when taxon-specific 16S rRNA gene primers are employed, bacteria not belonging to the plotted taxa will not be detected. Notably, improvements have been developed for both approaches, and wide-ranging databases of human-associated microbes have become available (Human Microbiome Project Consortium, 2012).

The next-generation sequencing (NGS) technique, and in particular the pyrosequencing, enables the parallel and fast identification of bacteria at a much lower cost than traditional Sanger sequencing.

Interestingly, although NGS technique has been widely used to study human microbiome as well as 16S rRNA amplicons to profile the bacterial diversity in a specimen, few studies have employed such methods for the diagnosis of implant-associated infections, including prosthesis joint infection (PJI) and urinary tract catheter-associated infection (Gomez et al., 2012; Xu et al., 2012; Kotaskova et al., 2019). Indeed, conversely to body sites with abundant bacteria, applying NGS to a normally sterile site (such as for medical devices) for the detection of pathogens, can result in significant issues about specimen contamination. Specimens with a high amount of bacteria present less contamination issues than samples with a lower amount since the target will outcompete contaminants in the initial steps of PCR amplification. Moreover, when working with periprosthetic tissue specimens, another crucial issue is represented by the detection limit of NGS, strongly dependent on the DNA extraction efficiency which, in turn, is influenced by the ratio of host to bacterial DNA (Ryu et al., 2014). In these specimens, the recovered amount of bacterial DNA can be very low, due to either the relative abundance of human DNA or inefficient DNA extraction methods, thus globally leading to false negative results.

Hence, in most cases, culture-based methods may represent a better tool for the diagnosis of IAIs than NGS, concerning detection limit, cost, and handling time. However, DNA amplification-based methods can be valuable in cases where culture results negative despite a clinical suspicion of infection, or where rare, difficult-to-culture (i.e., *C. acnes*) or uncultivable bacteria are supposed to be present. Few studies have compared standard and molecular methods for implanted devices (Xu et al., 2012; Ivy et al., 2018; Puges et al., 2018; Thoendel et al., 2018; Esquer Garrigos et al., 2020). In an explorative investigation, Xu et al. (2012) evaluated, by both culture and non-culture based approaches, the bacterial colonization of 55 specimens from patients clinically suspected of having PJIs. NGS analysis and microbiological cultures were concordant for 15/25 specimen sets (60%; five positive, 10 negative), whereas additional taxa were detected by gene analysis in four sets and discrepant data were obtained for six sets (5/6 negative on culture) (Xu et al., 2012). In another study, 408 sonicate fluid samples, from resected knee and hip arthroplasties, were analyzed by metagenomics and compared to results obtained by vortexing/sonication method (Thoendel et al., 2018). The data showed how metagenomics identified known pathogens in 94.8% (109/115) of culture-positive PJIs and new potential

pathogens in 43.9% (43/98) of culture-negative PJIs, whereas the detection of microbes in samples from cases of uninfected aseptic failure was rare (3.6%, 7/195 cases) (Thoendel et al., 2018). A similar study, carried out by the same group on 168 failed total knee arthroplasties, reported that genus- and species-level metagenomics detected, respectively, known pathogens in 74 (90%) and 68 (83%) out of 82 culture-positive PJIs, as well as 19 (76%) and 21 (84%) out of 25 culture-negative PJIs (Ivy et al., 2018). The authors conclude that metagenomic shotgun sequencing can be a powerful tool for the identification of a wide range of PJI pathogens, including difficult-to-detect ones in culture-negative infections Taken together, the use of NGS in the clinical diagnosis of infections requires the use of appropriate controls as well as knowledge of the limitations of the chosen method for accurate interpretation of the data. More studies are necessary to define their role in the diagnosis of biofilm-related infections, as well as protocols which describe their use, their application and make their use mainstream in clinical laboratories, in the perspective that they should complement it rather than replace it.

Multiplex Polymerase Chain Reaction

Considerable efforts and handling time can be saved by the simultaneous amplification of multiple sequences in a single reaction, a process known as multiplex PCR. Multiplex PCR is based on the combination of different pairs of primer that amplify unique regions of DNA, under a single set of reaction conditions. This requires specific methods for the analysis of each amplification product from the obtained mixture. Such technique is becoming a rapid and convenient tool in both the clinical and the research laboratory. The development of a multiplex PCR requires strategic planning for the optimization of reaction conditions. Multiplex PCRs can present several issues, such as poor specificity, sensitivity or the preferential amplification of specific targets (Zhang et al., 2015; Huang et al., 2018). The use of more than one primer pair makes it prone to spurious amplification products, mainly due to the formation of primer dimers (Brownie et al., 1997). Usually, these unspecific products are more efficiently amplified than the desired target, thus resulting in time- and cost-consuming. In addition, multiplex PCR requires a rational approach for the inclusion/exclusion of specific pathogens in the assay. The choice of the pathogens to be included may depend on the patient's symptoms or the affected tissue/organ, in relation to the epidemiological characteristics of these pathogens. The pairs of primer must cover as many strains as possible of the target pathogens and should produce amplicons easily to be resolved by using gel electrophoresis or hybridized with maximum specificity (Elnifro et al., 2000). The choice of target species for multiplex PCR assays is dependent on knowledge of the spectrum of bacteria previously linked to PJI, and therefore non-typical bacteria will not be detected by this diagnostic approach. However, this method is expedient and may additionally provide same-day diagnosis, possibly making multiplex PCR diagnostics superior to bacteriological culture. Multiplex PCR has been successfully employed for PJIs in several studies (Renz et al., 2017, 2018; Lausmann et al., 2020), resulting critical for patients receiving antibiotic treatment prior to surgery (Portillo et al., 2012; Cazanave et al., 2013; Ryu et al., 2014; Malandain et al., 2018). Cazanave et al. (2013) found advantageous the combination of broad-range and specific primer pairs for the most common PJI bacteria, like Staphylococci. Morgenstern et al. (2018) reported that, whereas the overall performance of synovial fluid PCR was comparable to culture, multiplex PCR was superior for detection of low-virulent bacteria such as *Cutibacterium* spp. and CoNS. In addition, multiplex PCR provided results within 5 h against several days for synovial fluid culture (Morgenstern et al., 2018). Further, the new generation of multiplex-PCR improves microbial detection, offering the option of faster and targeted antimicrobial therapy, particularly in the context of an acute periprosthetic infection (Lausmann et al., 2020). Interestingly, a recent meta-analysis study demonstrated that PCR of fluid after sonication is reliable and of great value in PJI diagnosis, and that multiplex PCR may improve sensitivity and specificity (Liu et al., 2018).

Polymerase Chain Reaction/ESI-MS

A novel alternative to sequencing is represented by electrospray ionization mass spectrometry for the determination of the mass, and therefore base pair compositions and abundances, of PCR amplicons (PCR/ESI-MS). The obtained composition is compared with known bacterial and fungal base compositions to provide the corresponding taxonomic information. Bacteria can then be identified by algorithmic comparison with an extensive database of microbial signature masses (Ecker et al., 2008; Costerton et al., 2011). In addition, a molecular antibiogram can be obtained by including primers for important antibiotic-resistant genes (i.e., mecA for methicillin-resistant *S. aureus*, vanA for vancomycin-resistant Enterococci). The major advantage of using these platforms, of which IBIS T5000 represents the first version, is that all bacterial DNA is amplified by the primer cocktail, rather than just organisms specifically selected, as with cultures and conventional PCR. This makes this technology not only a highly effective diagnostic method, but also an important research tool because new unexpected etiologies will arise from its routine use. So far, this technique has been applied to IAIs in very few studies. Stoodley et al. (2011) were able to identify the presence of *S. aureus*, *S. epidermidis*, and the methicillin-resistant mecA gene in tissue of the removed device from total ankle arthroplasty. Additionally, the Ibis detected that there was close to 10 times more *S. aureus* in comparison to the *S. epidermidis*. Of all the techniques investigated, the authors proposed the IBIS T5000 technology to have the most potential in aiding with clinical detection of PJI with total ankle arthroplasty (Stoodley et al., 2011). Another application was reported for orthopedic surgeons, showing a higher sensitivity than culture-methods in the identification of bacterial pathogens. Of note, it was able to detect bacteria in biofilms when culture was negative, demonstrating its efficacy in case of non-cultivable bacteria from a biofilm (Firoozabadi et al., 2015). Currently, the new version of such technique, the IRIDICA system, has improved the moderate sensitivity showed by IBIS 5000 (around 50–68% vs. culture methods for the identification of bloodstream infections) (Jordana-Lluch et al., 2013), up to

83–91%. Such improvements are due to the optimization of PCR conditions, the increase of blood volume to be tested (5 mL vs. 1.25 mL in the former version) and an ameliorated downstream processing and analysis step to provide high sensitivity (Bacconi et al., 2014).

A correlated technique using matrix-associated laser desorption/ionization time-of-flight (MALDI-TOF) mass spectrometry, in combination with the Biotyper database to detect microbes by their distinct native protein peaks, has been used for the identification of bacterial clinical isolates (Seng et al., 2009; Harris et al., 2010). Further, pyrosequencing and mass spectrometry approaches have been also applied for characterizing microbial antibiotic sensitivity (Seng et al., 2009; Kristiansson et al., 2011).

Microscopy Methods

Gram Staining

Microscopic analysis can be done by means of light microscopy and Gram stain, which may be performed on peri-prosthetic tissues or sonicate fluid. Gram staining is a widely used test for the diagnosis of IAIs, although it is not routinely recommended due to its low sensitivity (Tande and Patel, 2014). Indeed, a meta-analysis conducted by Ouyang et al. (2015) including 18 studies and 4.647 patients found that Gram staining had a very low sensitivity and high specificity (0.19 and 1.00, respectively). Interestingly, the authors suggested that, in the setting of PJIs, Gram stain at revision arthroplasty may guide early antibiotic treatment in case of re-implantation with a preoperative diagnosis of Gram−positive bacterial infection or evidence of purulence (Ouyang et al., 2015). Accordingly, Gram staining alone is not adequate for the microbiological diagnosis of IAIs but it may be used as an adjuvant tool in combination with other diagnostic methods (Ouyang et al., 2015).

Recently, Wouthuyzen-Bakker et al. (2019) evaluated the sensitivity of Gram staining on synovial fluid in late acute *S. aureus* PJIs. Overall, Gram staining was positive for Gram-positive cocci in 59.6% of cases, but the most interesting finding was that Gram staining's sensitivity was significantly higher when C-reactive protein value at clinical presentation was > 150 mg/L, compared to patients with a lower value (77% vs. 40%, $p = 0.02$), probably due to a higher bacterial inocolum. Accordingly, authors concluded that Gram staining may be a reliable diagnostic tool in late acute PJI to identify *S. aureus* PJI (Wouthuyzen-Bakker et al., 2019).

Other Microscopy Methods

Analysis of biofilms on the surface of implants is traditionally performed through culture methods, as described above, or, alternatively, by using crystal violet stain along with spectrophotometry (Wilson et al., 2017). Nevertheless, additional microscopy techniques allowing the visualization of the microbial biofilm may also be considered in the diagnostic approach of IAIs (Høiby et al., 2015). Indeed, methods such as confocal laser scanning microscopy and scanning electron microscopy appear to be very appropriate in revealing biofilms, since they provide images while maintaining biofilm's structural integrity (Høiby et al., 2015; Grossman et al., 2021). Furthermore, such microscope methods are able to distinguish between planktonic and biofilm bacteria and the identification of the biofilm microorganisms in samples may be obtained throughout species-specific fluorescence *in situ* hybridization probes and fluorescence microscopy (Høiby et al., 2015). With this regard, the application of Peptide Nucleic Acid Fluorescence *in situ* Hybridization on urinary catheter using a universal bacterial and a specific for *Enterobacteriaceae* probes revealed single cells and clusters of *Enterobacteriaceae* within the biofilm, which were further identified as *E. faecalis* and *E. coli* by means of culture methods (Donelli and Vuotto, 2014). Likewise, in animal models, scanning electron microscopy and confocal laser scanning microscopy performed on endotracheal tubes were used for biofilm analysis (Berra and Baccarelli, 2004; Fernández-Barat et al., 2012).

Confocal laser scanning microscopy is a high-resolution technique that allows three-dimensional visualization of biofilm architecture and, when combined with live/dead stain, may serve to quantify biofilm viability; in addition, the presence of extracellular DNA and exopolysaccharides may be visualized (Wilson et al., 2017). Frank et al. (2009) analyzed Foley urinary catheters obtained from patients following total prostatectomy with confocal microscopy and found the presence of dense matrices of microbial cells. Interestingly, microorganisms were most often observed in polymicrobial communities (Frank et al., 2009).

All in all, although the above mentioned microscopy methods possess several characteristics that may render them very useful in the setting of IAIs, they are not routinely available in the laboratory due to their cost and the need of experienced and highly trained users for accurate analyses (Wilson et al., 2017; **Table 1**).

CONCLUSION

With the increasing rate of devices implantation for the treatment of several diseases, a parallel increase in the incidence of IAIs has been observed, leading to an excess of morbidity, mortality, and increased costs for the healthcare system. Dealing with IAIs is a rather complex challenge for treating physicians, and their optimal management requires a multidisciplinary approach and a strict collaboration between different specialists such as surgeons, infectious diseases specialists, microbiologists, pathologists, and radiologists. In particular, a correct microbiological diagnosis of IAIs is of crucial importance in order to prompt an appropriate antimicrobial treatment. Currently, the available diagnostic approaches may be summarized in culture- (i.e., TC and SFC) and non-culture-based methods such as metabolic (DTT, RA, XTT, and BTA) and molecular (Broad-range 16S rRNA gene PCR and sequencing, multiplex PCR and IBIS T5000) ones. Overall, different parameters and conditions may affect the diagnostic yield of each method and, therefore, should be taken into account in the optimization of the diagnostic algorithm of IAIs. These factors include (i) a previous antimicrobial treatment, (ii) the procedure of sample collection (pre-operative vs. intra-operative,

number of samples, eventual sample pre-treatment, type of containers), (iii) the used diagnostic method, and (iv) the growth conditions (duration of incubation, type of incubation-aerobic vs. anaerobic-, inoculation into BCBs). As a matter of fact, along with the advantages and disadvantages of each method alone (**Table 1**), a high diagnostic sensitivity may be obtained by combining these methods with each other, similarly to that already demonstrated (Drago et al., 2013).

The concrete indications for the appropriate use of the described different diagnostic methods may be therefore summarized as follows: (i) in the case of suspected/certain IAI, superficial or tissue swabs must be avoided for their low sensitivity and the risk of contamination, (ii) tissue cultures should be performed, (iii) in the case of implant removal, sonication and quantitative cultures should be applied, and (iv) molecular and metabolic assays should be considered as complementary to culture-based methods to shorten the diagnosis, to search for fastidious microorganisms or when antibiotics have been previously administered.

The research in this field is continuously evolving and, accordingly, a further improvement in the etiological diagnosis of IAIs is expected in the near future.

AUTHOR CONTRIBUTIONS

AO, LR, and AC: conceptualization of the narrative review. AO, CMM, DA, FD, MD, LR, and AC: drafting of the manuscript. MV, MTM, PV, and CMM: critical revision of the manuscript for important intellectual content. All authors contributed to the article and approved the submitted version.

FUNDING

This work was granted by the Regione Lazio to PV for the project entitled "Innovazione nell'identificazione ed enumerazione di batteri e virus patogeni nell'uomo e negli alimenti: trasferimento delle metodologie innovative alle strutture sanitarie, alle industrie farmaceutiche e alimentari operanti nel Lazio—DSPMI-INN".

REFERENCES

Achermann, Y., Vogt, M., Leunig, M., Wüst, J., and Trampuz, A. (2010). Improved diagnosis of periprosthetic joint infection by multiplex PCR of sonication fluid from removed implants. *J. Clin. Microbiol.* 48, 1208–1214. doi: 10.1128/JCM.00006-10

Adam, B., Baillie, G. S., and Douglas, L. J. (2002). Mixed species biofilms of *Candida albicans* and *Staphylococcus epidermidis*. *J. Med. Microbiol.* 51, 344–349. doi: 10.1099/0022-1317-51-4-344

Ahn, C. Y., Ko, C. Y., Wagar, E. A., Wong, R. S., and Shaw, W. W. (1996). Microbial evaluation: 139 implants removed from symptomatic patients. *Plast Reconstr. Surg.* 98, 1225–1229.

Apostolakis, S. (2020). Use of focused ultrasound (Sonication) for the diagnosis of infections in neurosurgical operations: A systematic review and meta-analysis. *World Neurosurg.* 136, 364–373. doi: 10.1016/j.wneu.2019.12.143

Aslanzadeh, J. (2004). Preventing PCR amplification carryover contamination in a clinical laboratory. *Ann. Clin. Lab. Sci.* 34, 389–396.

Bacconi, A., Richmond, G. S., Baroldi, M. A., Laffler, T. G., Blyn, L. B., Carolan, H. E., et al. (2014). Improved sensitivity for molecular detection of bacterial and *Candida* infections in blood. *J. Clin. Microbiol.* 52, 3164–3174. doi: 10.1128/JCM.00801-14

Bellova, P., Knop-Hammad, V., Königshausen, M., Mempel, E., Frieler, S., Gessmann, J., et al. (2019). Sonication of retrieved implants improves sensitivity in the diagnosis of periprosthetic joint infection. *BMC Musculoskelet Disord.* 20:623. doi: 10.1186/s12891-019-3006-1

Berlutti, F., Rosso, F., Bosso, P., Giansanti, F., Ajello, M., De Rosa, A., et al. (2003). Quantitative evaluation of bacteria adherent to polyelectrolyte HEMA-based hydrogels. *J. Biomed. Mater. Res. A* 67, 18–25. doi: 10.1002/jbm.a.10026

Berra, L., and Baccarelli, A. (2004). Endotracheal tubes coated with antiseptics decrease bacterial colonization of the ventilator circuits, lungs, and endotracheal tube. *Anesthesiology* 100, 1446–1456.

Bjerkan, G., Witsø, E., and Bergh, K. (2009). Sonication is superior to scraping for retrieval of bacteria in biofilm on titanium and steel surfaces in vitro. *Acta Orthop.* 80, 245–250. doi: 10.3109/17453670902947457

Bjerkan, G., Witsø, E., Nor, A., Viset, T., Løseth, K., Lydersen, S., et al. (2012). A comprehensive microbiological evaluation of fifty-four patients undergoing revision surgery due to prosthetic joint loosening. *J. Med. Microbiol.* 61, 572–581. doi: 10.1099/jmm.0.036087-0

Blomström-Lundqvist, C., Traykov, V., Erba, P. A., Burri, H., Nielsen, J. C., Bongiorni, M. G., et al. (2020). European Heart Rhythm Association (EHRA) international consensus document on how to prevent, diagnose, and treat cardiac implantable electronic device infections—endorsed by the Heart Rhythm Society (HRS), the Asia Pacific Heart Rhythm Society (APHRS), the Latin American Heart Rhythm Society (LAHRS), International Society for Cardiovascular Infectious Diseases (ISCVID) and the European Society of Clinical Microbiology and Infectious Diseases (ESCMID) in collaboration with the European Association for Cardio-Thoracic Surgery (EACTS). *Europace* 22, 515–549. doi: 10.1093/europace/euz246

Bonkat, G., Braissant, O., Rieken, M., Müller, G., Frei, R., van der Merwe, A., et al. (2013). Comparison of the roll-plate and sonication techniques in the diagnosis of microbial ureteral stent colonisation: results of the first prospective randomised study. *World J. Urol.* 31, 579–584. doi: 10.1007/s00345-012-0963-5

Bonkat, G., Rieken, M., Rentsch, C. A., Wyler, S., Feike, A., Schäfer, J., et al. (2011). Improved detection of microbial ureteral stent colonisation by sonication. *World J. Urol.* 29, 133–138. doi: 10.1007/s00345-010-0535-5

Bonkat, G., Rieken, M., Siegel, F. P., Frei, R., Steiger, J., Gröschl, I., et al. (2012). Microbial ureteral stent colonization in renal transplant recipients: frequency and influence on the short-time functional outcome. *Transpl. Infect. Dis.* 14, 57–63. doi: 10.1111/j.1399-3062.2011.00671.x

Borens, O., Yusuf, E., Steinrücken, J., and Trampuz, A. (2013). Accurate and early diagnosis of orthopedic device-related infection by microbial heat production and sonication. *J. Orthop. Res.* 31, 1700–1703. doi: 10.1002/jor.22419

Brownie, J., Shawcross, S., Theaker, J., Whitcombe, D., Ferrie, R., Newton, C., et al. (1997). The elimination of primer-dimer accumulation in PCR. *Nucleic Acids Res.* 25, 3235–3241.

Burmølle, M., Thomsen, T. R., Fazli, M., Dige, I., Christensen, L., Homøe, P., et al. (2010). Biofilms in chronic infections - a matter of opportunity - monospecies biofilms in multispecies infections. *FEMS Immunol. Med. Microbiol.* 59, 324–336. doi: 10.1111/j.1574-695X.2010.00714.x

Butler-Wu, S. M., Burns, E. M., Pottinger, P. S., Magaret, A. S., Rakeman, J. L., Matsen, F. A., et al. (2011). Optimization of periprosthetic culture for diagnosis of propionibacterium acnes prosthetic joint infection. *J. Clin. Microbiol.* 49, 2490–2495. doi: 10.1128/JCM.00450-11

Carmen, J. C., Roeder, B. L., Nelson, J. L., Ogilvie, R. L. R., Robison, R. A., Schaalje, G. B., et al. (2005). Treatment of biofilm infections on implants with low-frequency ultrasound and antibiotics. *Am. J. Infect. Control* 33, 78–82. doi: 10.1016/j.ajic.2004.08.002

Cazanave, C., Greenwood-Quaintance, K. E., Hanssen, A. D., Karau, M. J., Schmidt, S. M., Gomez Urena, E. O., et al. (2013). Rapid molecular microbiologic diagnosis of prosthetic joint infection. *J. Clin. Microbiol.* 51, 2280–2287. doi: 10.1128/JCM.00335-13

Chang, S.-S., Hsu, H.-L., Cheng, J.-C., and Tseng, C.-P. (2011). An efficient strategy for broad-range detection of low abundance bacteria without DNA decontamination of PCR reagents. *PLoS One* 6:e20303. doi: 10.1371/journal.pone.0020303

Clarridge, J. E. (2004). Impact of 16S rRNA gene sequence analysis for identification of bacteria on clinical microbiology and infectious diseases. *Clin. Microbiol. Rev.* 17, 840–862. doi: 10.1128/CMR.17.4.840-862.2004

Conen, A., Raabe, A., Schaller, K., Fux, C. A., Vajkoczy, P., and Trampuz, A. (2020). Management of neurosurgical implant-associated infections. *Swiss Med. Wkly* 150:w20208. doi: 10.4414/smw.2020.20208

Corless, C. E., Guiver, M., Borrow, R., Edwards-Jones, V., Kaczmarski, E. B., and Fox, A. J. (2000). Contamination and sensitivity issues with a real-time universal 16S rRNA PCR. *J. Clin. Microbiol.* 38, 1747–1752.

Costerton, J. W., Post, J. C., Ehrlich, G. D., Hu, F. Z., Kreft, R., Nistico, L., et al. (2011). New methods for the detection of orthopedic and other biofilm infections. *FEMS Immunol. Med. Microbiol.* 61, 133–140. doi: 10.1111/j.1574-695X.2010.00766.x

De Vecchi, E., Bottagisio, M., Bortolin, M., Toscano, M., Lovati, A. B., and Drago, L. (2017). Improving the bacterial recovery by using dithiothreitol with aerobic and anaerobic broth in biofilm-related prosthetic and joint infections. *Adv. Exp. Med. Biol.* 973, 31–39. doi: 10.1007/5584_2016_51

De Vecchi, E., Bortolin, M., Signori, V., Romanò, C. L., and Drago, L. (2016). Treatment with dithiothreitol improves bacterial recovery from tissue samples in osteoarticular and joint infections. *J. Arthroplasty*. 31, 2867–2870. doi: 10.1016/j.arth.2016.05.008

Del Pozo, J. L., Tran, N. V., Petty, P. M., Johnson, C. H., Walsh, M. F., Bite, U., et al. (2009). Pilot study of association of bacteria on breast implants with capsular contracture. *J. Clin. Microbiol.* 47, 1333–1337. doi: 10.1128/JCM.00096-09

Deng, Y., and Lv, W. (2016). *Biofilms and Implantable Medical Devices: Infection and Control*. Available online at: https://books.google.it/books?hl=it&lr=&id=XTHZCgAAQBAJ&oi=fnd&pg=PP1&dq=Deng,+Y.,+and+Lv,+W.+(2017).+Biofilms+and+Implantable+Medical+Devices.+Sawston:+Woodhead+Publishing,+240.&ots=IrUSyG2nne&sig=Pkihz_w4YlkQp-YaQBZx9Y8HV7o#v=onepage&q&f=false

Dobke, M. K., Svahn, J. K., Vastine, V. L., Landon, B. N., Stein, P. C., and Parsons, C. L. (1995). Characterization of microbial presence at the surface of silicone mammary implants. *Ann. Plast Surg.* 34, 563–569. doi: 10.1097/00000637-199506000-00001

Donelli, G., and Vuotto, C. (2014). Biofilm-based infections in long-term care facilities. *Future Microbiol.* 9, 175–188. doi: 10.2217/fmb.13.149

Drago, L. (2017). *A Modern Approach to Biofilm-Related Orthopaedic Implant Infections: Advances in Microbiology, Infectious Diseases and Public Health*, Vol. 5. Cham: Springer International Publishing.

Drago, L., and De Vecchi, E. (2017). Microbiological diagnosis of implant-related infections: scientific evidence and cost/benefit analysis of routine antibiofilm processing. *Adv. Exp. Med. Biol.* 971, 51–67. doi: 10.1007/5584_2016_154

Drago, L., Clerici, P., Morelli, I., Ashok, J., Benzakour, T., Bozhkova, S., et al. (2019). The World Association against Infection in Orthopaedics and Trauma (WAIOT) procedures for microbiological sampling and processing for Periprosthetic Joint Infections (PJIs) and other implant-related infections. *J. Clin. Med.* 8:933. doi: 10.3390/jcm8070933

Drago, L., Romanò, C. L., Mattina, R., Signori, V., and De Vecchi, E. (2012). Does dithiothreitol improve bacterial detection from infected prostheses? A pilot study. *Clin. Orthop. Relat. Res.* 470, 2915–2925. doi: 10.1007/s11999-012-2415-3

Drago, L., Signori, V., Vecchi, E. D., Vassena, C., Palazzi, E., Cappelletti, L., et al. (2013). Use of dithiothreitol to improve the diagnosis of prosthetic joint infections. *J. Orthop. Res.* 31, 1694–1699. doi: 10.1002/jor.22423

Drancourt, M., Berger, P., and Raoult, D. (2004). Systematic 16S rRNA gene sequencing of atypical clinical isolates identified 27 new bacterial species associated with humans. *J. Clin. Microbiol.* 42, 2197–2202. doi: 10.1128/JCM.42.5.2197-2202.2004

Dudareva, M., Barrett, L., Figtree, M., Scarborough, M., Watanabe, M., Newnham, R., et al. (2018). Sonication versus tissue sampling for diagnosis of prosthetic joint and other orthopedic device-related infections. *J. Clin. Microbiol.* 56:e688–18. doi: 10.1128/JCM.00688-18

Dy Chua, J., Abdul-Karim, A., Mawhorter, S., Procop, G. W., Tchou, P., Niebauer, M., et al. (2005). The role of swab and tissue culture in the diagnosis of implantable cardiac device infection. *Pacing Clin. Electrophys.* 28, 1276–1281. doi: 10.1111/j.1540-8159.2005.00268.x

Ecker, D. J., Sampath, R., Massire, C., Blyn, L. B., Hall, T. A., Eshoo, M. W., et al. (2008). Ibis T5000: a universal biosensor approach for microbiology. *Nat. Rev. Microbiol.* 6, 553–558. doi: 10.1038/nrmicro1918

Elnifro, E. M., Ashshi, A. M., Cooper, R. J., and Klapper, P. E. (2000). Multiplex PCR: optimization and application in diagnostic virology. *Clin. Microbiol. Rev.* 13, 559–570. doi: 10.1128/CMR.13.4.559

Esquer Garrigos, Z., Sohail, M. R., Greenwood-Quaintance, K. E., Cunningham, S. A., Vijayvargiya, P., Fida, M., et al. (2020). Molecular approach to diagnosis of cardiovascular implantable electronic device infection. *Clin. Infect. Dis.* 70, 898–906. doi: 10.1093/cid/ciz266

Esteban, J., Alvarez-Alvarez, B., Blanco García, A., Fernandez-Roblas, R., Gadea, I., Garcia-Cañete, J., et al. (2013). Prolonged incubation time does not increase sensitivity for the diagnosis of implantrelated infection using samples prepared by sonication of the implants. *Bone Jt. J.* 95-B, 1001–1006. doi: 10.1302/0301-620X.95B7.31174

Esteban, J., Gomez-Barrena, E., Cordero, J., Martín-de-Hijas, N. Z., Kinnari, T. J., and Fernandez-Roblas, R. (2008). Evaluation of quantitative analysis of cultures from sonicated retrieved orthopedic implants in diagnosis of orthopedic infection. *J. Clin. Microbiol.* 46, 488–492. doi: 10.1128/JCM.01762-07

Fernández-Barat, L., Ferrer, M., Sierra, J. M., Soy, D., Guerrero, L., Vila, J., et al. (2012). Linezolid limits burden of methicillin-resistant *Staphylococcus aureus* in biofilm of tracheal tubes. *Crit. Care Med.* 40, 2385–2389. doi: 10.1097/CCM.0b013e31825332fc

Firoozabadi, R., Alton, T., and Wenke, J. (2015). Novel strategies for the diagnosis of posttraumatic infections in orthopaedic trauma patients. *J. Am. Acad. Orthop. Surg.* 23, 443–451. doi: 10.5435/JAAOS-D-14-00174

Frank, D. N., Wilson, S. S., St. Amand, A. L., and Pace, N. R. (2009). Culture-independent microbiological analysis of foley urinary catheter biofilms. *PLoS One* 4:e7811. doi: 10.1371/journal.pone.0007811

Giusti, M. D., Berlutti, F., Pantanella, F., Marinelli, L., Frioni, A., Natalizi, T., et al. (2011). *A New Biosensor to Enumerate Bacteria in Planktonic and Biofilm Lifestyle*. London: IntechOpen.

Gomez, E., Cazanave, C., Cunningham, S. A., Greenwood-Quaintance, K. E., Steckelberg, J. M., Uhl, J. R., et al. (2012). Prosthetic joint infection diagnosis using broad-range PCR of biofilms dislodged from knee and hip arthroplasty surfaces using sonication. *J. Clin. Microbiol.* 50, 3501–3508. doi: 10.1128/JCM.00834-12

Grossman, A. B., Burgin, D. J., and Rice, K. C. (2021). Quantification of *Staphylococcus aureus* biofilms formation by crystal violet and confocal microscopy. *Methods Mol. Biol.* 2341, 69–78. doi: 10.1007/978-1-0716-1550-8_9

Grosso, M. J., Frangiamore, S. J., Yakubek, G., Bauer, T. W., Iannotti, J. P., and Ricchetti, E. T. (2018). Performance of implant sonication culture for the diagnosis of periprosthetic shoulder infection. *J. Shoulder Elbow Surg.* 27, 211–216. doi: 10.1016/j.jse.2017.08.008

Guerin, T. F., Mondido, M., McClenn, B., and Peasley, B. (2001). Application of resazurin for estimating abundance of contaminant-degrading micro-organisms. *Lett. Appl. Microbiol.* 32, 340–345. doi: 10.1046/j.1472-765x.2001.00916.x

Hamady, M., and Knight, R. (2009). Microbial community profiling for human microbiome projects: Tools, techniques, and challenges. *Genome Res.* 19, 1141–1152. doi: 10.1101/gr.085464.108

Handschur, M., Karlic, H., Hertel, C., Pfeilstöcker, M., and Haslberger, A. G. (2009). Preanalytic removal of human DNA eliminates false signals in general 16S rDNA PCR monitoring of bacterial pathogens in blood. *Comp. Immunol. Microbiol. Infect. Dis.* 32, 207–219. doi: 10.1016/j.cimid.2007.10.005

Harris, L. G., El-Bouri, K., Johnston, S., Rees, E., Frommelt, L., Siemssen, N., et al. (2010). Rapid identification of *Staphylococci* from prosthetic joint infections using MALDI-TOF mass-spectrometry. *Int. J. Artif. Organs.* 33, 568–574. doi: 10.1177/039139881003300902

Hedrick, T. L., Adams, J. D., and Sawyer, R. G. (2006). Implant-associated infections: an overview. *J. Long Term Eff. Med. Implants* 16, 83–99. doi: 10.1615/jlongtermeffmedimplants.v16.i1.90

Hoekstra, M., Veltman, E. S., Nurmohamed, R. F. R. H. A., van Dijk, B., Rentenaar, R. J., Vogely, H. C., et al. (2020). Sonication leads to clinically relevant changes

in treatment of periprosthetic hip or knee joint infection. *J. Bone Jt. Infect.* 5, 128–132. doi: 10.7150/jbji.45006

Høiby, N., Bjarnsholt, T., Moser, C., Bassi, G. L., Coenye, T., Donelli, G., et al. (2015). ESCMID* guideline for the diagnosis and treatment of biofilm infections 2014. *Clin. Microbiol. Infect.* 21, S1–S25. doi: 10.1016/j.cmi.2014.10.024

Holinka, J., Bauer, L., Hirschl, A. M., Graninger, W., Windhager, R., and Presterl, E. (2011). Sonication cultures of explanted components as an add-on test to routinely conducted microbiological diagnostics improve pathogen detection. *J. Orthop. Res.* 29, 617–622. doi: 10.1002/jor.21286

Honraet, K., Goetghebeur, E., and Nelis, H. J. (2005). Comparison of three assays for the quantification of *Candida* biomass in suspension and CDC reactor grown biofilms. *J. Microbiol. Methods* 63, 287–295. doi: 10.1016/j.mimet.2005.03.014

Horz, H.-P., Scheer, S., Huenger, F., Vianna, M. E., and Conrads, G. (2008). Selective isolation of bacterial DNA from human clinical specimens. *J. Microbiol. Methods* 72, 98–102. doi: 10.1016/j.mimet.2007.10.007

Huang, H.-S., Tsai, C.-L., Chang, J., Hsu, T.-C., Lin, S., and Lee, C.-C. (2018). Multiplex PCR system for the rapid diagnosis of respiratory virus infection: systematic review and meta-analysis. *Clin. Microbiol. Infect.* 24, 1055–1063. doi: 10.1016/j.cmi.2017.11.018

Inacio, R. C., Klautau, G. B., Murça, M. A. S., da Silva, C. B., Nigro, S., Rivetti, L. A., et al. (2015). Microbial diagnosis of infection and colonization of cardiac implantable electronic devices by use of sonication. *Int. J. Infect. Dis.* 38, 54–59. doi: 10.1016/j.ijid.2015.07.018

Ivy, M. I., Thoendel, M. J., Jeraldo, P. R., Greenwood-Quaintance, K. E., Hanssen, A. D., Abdel, M. P., et al. (2018). Direct detection and identification of prosthetic joint infection pathogens in synovial fluid by metagenomic shotgun sequencing. *J. Clin. Microbiol.* 56:e402–18. doi: 10.1128/JCM.00402-18

Izakovicova, P., Borens, O., and Trampuz, A. (2019). Periprosthetic joint infection: current concepts and outlook. *EFORT Open Rev.* 4, 482–494. doi: 10.1302/2058-5241.4.180092

Jan, A., Bhat, K. M., Bhat, A. S. J., Mir, M. A., Bhat, M. A., Imtiyaz, A., et al. (2013). Surface sterilization method for reducing microbial contamination of field grown strawberry explants intended for in vitro culture. *Afr. J. Biotechnol.* 12, 5749–5753. doi: 10.5897/AJB2013.12918

Janz, V., Trampuz, A., Perka, C. F., and Wassilew, G. I. (2017). Reduced culture time and improved isolation rate through culture of sonicate fluid in blood culture bottles. *Technol. Health Care* 25, 635–640. doi: 10.3233/THC-160660

Janz, V., Wassilew, G. I., Hasart, O., Matziolis, G., Tohtz, S., and Perka, C. (2013). Evaluation of sonicate fluid cultures in comparison to histological analysis of the periprosthetic membrane for the detection of periprosthetic joint infection. *Int. Orthop.* 37, 931–936. doi: 10.1007/s00264-013-1853-1

Jordana-Lluch, E., Carolan, H. E., Giménez, M., Sampath, R., Ecker, D. J., Quesada, M. D., et al. (2013). Rapid diagnosis of bloodstream infections with PCR followed by mass spectrometry. *PLoS One* 8:e62108. doi: 10.1371/journal.pone.0062108

Joshi, H. B., Stainthorpe, A., MacDONAGH, R. P., Keeley, F. X., and Timoney, A. G. (2003). Indwelling ureteral stents: evaluation of symptoms, quality of life and utility. *J. Urol.* 169, 1065–1069. doi: 10.1097/01.ju.0000048980.33855.90

Jost, G. F., Wasner, M., Taub, E., Walti, L., Mariani, L., and Trampuz, A. (2014). Sonication of catheter tips for improved detection of microorganisms on external ventricular drains and ventriculo-peritoneal shunts. *J. Clin. Neurosci.* 21, 578–582. doi: 10.1016/j.jocn.2013.05.025

Karau, M. J., Greenwood-Quaintance, K. E., Schmidt, S. M., Tran, N. V., Convery, P. A., Jacobson, S. R., et al. (2013). Microbial biofilms and breast tissue expanders. *BioMed. Res. Int.* 2013, 1–6. doi: 10.1155/2013/254940

Klug, D., Wallet, F., Kacet, S., and Courcol, R. J. (2003). Involvement of adherence and adhesion *Staphylococcus epidermidis* genes in pacemaker lead-associated infections. *J. Clin. Microbiol.* 41, 3348–3350. doi: 10.1128/JCM.41.7.3348-3350.2003

Kolenda, C., Josse, J., Batailler, C., Faure, A., Monteix, A., Lustig, S., et al. (2021). Experience with the use of the MicroDTTect device for the diagnosis of low-grade chronic prosthetic joint infections in a routine setting. *Front. Med.* 8:565555. doi: 10.3389/fmed.2021.565555

Kotaskova, I., Obrucova, H., Malisova, B., Videnska, P., Zwinsova, B., Peroutkova, T., et al. (2019). Molecular techniques complement culture-based assessment of bacteria composition in mixed biofilms of urinary tract catheter-related samples. *Front. Microbiol.* 10:462. doi: 10.3389/fmicb.2019.00462

Kristiansson, E., Fick, J., Janzon, A., Grabic, R., Rutgersson, C., Weijdegård, B., et al. (2011). Pyrosequencing of antibiotic-contaminated river sediments reveals high levels of resistance and gene transfer elements. *PLoS One* 6:e17038. doi: 10.1371/journal.pone.0017038

Lausmann, C., Kolle, K. N., Citak, M., Abdelaziz, H., Schulmeyer, J., Delgado, G. D., et al. (2020). How reliable is the next generation of multiplex-PCR for diagnosing prosthetic joint infection compared to the MSIS criteria? Still missing the ideal test. *Hip. Int. J. Clin. Exp. Res. Hip. Pathol. Ther.* 30, 72–77. doi: 10.1177/1120700020938576

Legout, L., D'Elia, P. V., Sarraz-Bournet, B., Haulon, S., Meybeck, A., Senneville, E., et al. (2012). Diagnosis and management of prosthetic vascular graft infections. *Méd. Mal. Infect.* 42, 102–109. doi: 10.1016/j.medmal.2012.01.003

Lescat, M., Poirel, L., Tinguely, C., and Nordmann, P. (2019). A Resazurin reduction-based assay for rapid detection of polymyxin resistance in *Acinetobacter baumannii* and *Pseudomonas aeruginosa*. *J. Clin. Microbiol.* 57:e1563–18. doi: 10.1128/JCM.01563-18

Li, C., Renz, N., Thies, C. O., and Trampuz, A. (2018). Meta-analysis of sonicate fluid in blood culture bottles for diagnosing periprosthetic joint infection. *J. Bone Jt. Infect.* 3, 273–279. doi: 10.7150/jbji.29731

Liu, H., Zhang, Y., Li, L., and Zou, H. C. (2017). The application of sonication in diagnosis of periprosthetic joint infection. *Eur. J. Clin. Microbiol. Infect. Dis.* 36, 1–9. doi: 10.1007/s10096-016-2778-6

Liu, K., Fu, J., Yu, B., Sun, W., Chen, J., and Hao, L. (2018). Meta-analysis of sonication prosthetic fluid PCR for diagnosing periprosthetic joint infection. *PLoS One* 13:e0196418. doi: 10.1371/journal.pone.0196418

Lutz, M.-F., Berthelot, P., Fresard, A., Cazorla, C., Carricajo, A., Vautrin, A.-C., et al. (2005). Arthroplastic and osteosynthetic infections due to Propionibacterium acnes: a retrospective study of 52 cases, 1995–2002. *Eur. J. Clin. Microbiol. Infect. Dis.* 24:739. doi: 10.1007/s10096-005-0040-8

Lyons, O. T. A., Baguneid, M., Barwick, T. D., Bell, R. E., Foster, N., Homer-Vanniasinkam, S., et al. (2016). Diagnosis of aortic graft infection: A case definition by the Management of Aortic Graft Infection Collaboration (MAGIC). *Eur. J. Vasc. Endovasc. Surg.* 52, 758–763. doi: 10.1016/j.ejvs.2016.09.007

Malandain, D., Bémer, P., Leroy, A. G., Léger, J., Plouzeau, C., Valentin, A. S., et al. (2018). Assessment of the automated multiplex-PCR Unyvero i60 ITI® cartridge system to diagnose prosthetic joint infection: a multicentre study. *Clin. Microbiol. Infect.* 24, 83.e1–83.e6. doi: 10.1016/j.cmi.2017.05.017

Mariscal, A., Lopez-Gigosos, R. M., Carnero-Varo, M., and Fernandez-Crehuet, J. (2009). Fluorescent assay based on resazurin for detection of activity of disinfectants against bacterial biofilm. *Appl. Microbiol. Biotechnol.* 82, 773–783. doi: 10.1007/s00253-009-1879-x

Martin, R. M., Zimmermann, L. L., Huynh, M., and Polage, C. R. (2018). Diagnostic approach to health care- and device-associated central nervous system infections. *J Clin Microbiol* 56:e861–18. doi: 10.1128/JCM.00861-18

Mason, P. K., Dimarco, J. P., Ferguson, J. D., Mahapatra, S., Mangrum, J. M., Bilchick, K. C., et al. (2011). Sonication of explanted cardiac rhythm management devices for the diagnosis of pocket infections and asymptomatic bacterial colonization. *Pacing Clin. Electrophysiol.* 34, 143–149. doi: 10.1111/j.1540-8159.2010.02820.x

McDowell, A., and Patrick, S. (2005). Evaluation of nonculture methods for the detection of prosthetic hip biofilms. *Clin. Orthop. Relat. Res.* 437, 74–82. doi: 10.1097/01.blo.0000175123.58428.93

Meddeb, M., Koebel, C., Jaulhac, B., and Schramm, F. (2016). Comparison between a broad-range real-time and a broad-range end-point PCR assays for the detection of bacterial 16S rRNA in clinical samples. *Ann. Clin. Lab. Sci.* 46, 18–25.

Minassian, A. M., Newnham, R., Kalimeris, E., Bejon, P., Atkins, B. L., and Bowler, I. C. (2014). Use of an automated blood culture system (BD BACTEC™) for diagnosis of prosthetic joint infections: easy and fast. *BMC Infect. Dis.* 14:233. doi: 10.1186/1471-2334-14-233

Morgenstern, C., Cabric, S., Perka, C., Trampuz, A., and Renz, N. (2018). Synovial fluid multiplex PCR is superior to culture for detection of low-virulent pathogens causing periprosthetic joint infection. *Diagn. Microbiol. Infect. Dis.* 90, 115–119. doi: 10.1016/j.diagmicrobio.2017.10.016

Moure, R., Muñoz, L., Torres, M., Santin, M., Martín, R., and Alcaide, F. (2011). Rapid detection of Mycobacterium tuberculosis complex and rifampin resistance in smear-negative clinical samples by use of an integrated real-time PCR method. *J. Clin. Microbiol.* 49, 1137–1139. doi: 10.1128/JCM.01831-10

Nagpal, A., Patel, R., Greenwood-Quaintance, K. E., Baddour, L. M., Lynch, D. T., Lahr, B. D., et al. (2015). Usefulness of sonication of cardiovascular implantable electronic devices to enhance microbial detection. *Am. J. Cardiol.* 115, 912–917. doi: 10.1016/j.amjcard.2015.01.017

Nelson, C. L., McLaren, A. C., McLaren, S. G., Johnson, J. W., and Smeltzer, M. S. (2005). Is aseptic loosening truly aseptic? *Clin. Orthop. Relat. Res.* 437, 25–30. doi: 10.1097/01.blo.0000175715.68624.3d

Neut, D., Horn, J. R., Kooten, T. G., Mei, H. C., and Busscher, H. J. (2003). Detection of biomaterial-associated infections in orthopaedic joint implants. *Clin. Orthop. Relat. Res.* 413, 261–268. doi: 10.1097/01.blo.0000073345.50837.84

Nguyen, L. L., Nelson, C. L., Saccente, M., Smeltzer, M. S., Wassell, D. L., and McLaren, S. G. (2002). Detecting bacterial colonization of implanted orthopaedic devices by ultrasonication. *Clin. Orthop. Relat. Res.* 403, 29–37.

O'Brien, J., Wilson, I., Orton, T., and Pognan, F. (2000). Investigation of the Alamar Blue (resazurin) fluorescent dye for the assessment of mammalian cell cytotoxicity. *Eur. J. Biochem.* 267, 5421–5426. doi: 10.1046/j.1432-1327.2000.01606.x

Oliva, A., Mascellino, M., Nguyen, B., De Angelis, M., Cipolla, A., Di Berardino, A., et al. (2018). Detection of biofilm-associated implant pathogens in cardiac device infections: High sensitivity of sonication fluid culture even in the presence of antimicrobials. *J. Glob. Infect. Dis.* 10:74. doi: 10.4103/jgid.jgid_31_17

Oliva, A., Nguyen, B. L., Mascellino, M. T., D'Abramo, A., Iannetta, M., Ciccaglioni, A., et al. (2013). Sonication of explanted cardiac implants improves microbial detection in cardiac device infections. *J. Clin. Microbiol.* 51, 496–502. doi: 10.1128/JCM.02230-12

Oliva, A., Pavone, P., D'Abramo, A., Iannetta, M., Mastroianni, C. M., and Vullo, V. (2016). Role of sonication in the microbiological diagnosis of implant-associated infections: beyond the orthopedic prosthesis. *Adv. Exp. Med. Biol.* 897, 85–102. doi: 10.1007/5584_2015_5007

Olofsson, A.-C., Hermansson, M., and Elwing, H. (2003). N-Acetyl-l-Cysteine affects growth, extracellular polysaccharide production, and bacterial biofilm formation on solid surfaces. *Appl. Environ. Microbiol.* 69, 4814–4822. doi: 10.1128/AEM.69.8.4814-4822.2003

Osmon, D. R., Berbari, E. F., Berendt, A. R., Lew, D., Zimmerli, W., Steckelberg, J. M., et al. (2013). Diagnosis and management of prosthetic joint infection: clinical practice guidelines by the infectious diseases society of americaa. *Clin. Infect. Dis.* 56, e1–e25. doi: 10.1093/cid/cis803

Ouyang, Z., Zhai, Z., Qin, A., Li, H., Liu, X., Qu, X., et al. (2015). Limitations of Gram staining for the diagnosis of infections following total hip or knee arthroplasty. *Exp. Ther. Med.* 9, 1857–1864. doi: 10.3892/etm.2015.2315

Pajkos, A., Deva, A. K., Vickery, K., Cope, C., Chang, L., and Cossart, Y. E. (2003). Detection of subclinical infection in significant breast implant capsules. *Plast Reconstr. Surg.* 111, 1605–1611. doi: 10.1097/01.PRS.0000054768.14922.44

Pantanella, F., Valenti, P., Frioni, A., Natalizi, T., Coltella, L., and Berlutti, F. (2008). BioTimer Assay, a new method for counting Staphylococcus spp. in biofilm without sample manipulation applied to evaluate antibiotic susceptibility of biofilm. *J. Microbiol. Methods* 75, 478–484. doi: 10.1016/j.mimet.2008.07.027

Pantanella, F., Valenti, P., Natalizi, T., Passeri, D., and Berlutti, F. (2013). Analytical techniques to study microbial biofilm on abiotic surfaces: pros and cons of the main techniques currently in use. *Ann. Ig. Med. Prev. E Comunita.* 25, 31–42. doi: 10.7416/ai.2013.1904

Parvizi, J., Ghanem, E., Menashe, S., Barrack, R. L., and Bauer, T. W. (2006). Periprosthetic infection: what are the diagnostic challenges? *JBJS* 88, 138–147. doi: 10.2106/JBJS.F.00609

Parvizi, J., Tan, T. L., Goswami, K., Higuera, C., Della Valle, C., Chen, A. F., et al. (2018). The 2018 definition of periprosthetic hip and knee infection: An evidence-based and validated criteria. *J. Arthrop.* 33, 1309–1314. doi: 10.1016/j.arth.2018.02.078

Peel, T. N., Spelman, T., Dylla, B. L., Hughes, J. G., Greenwood-Quaintance, K. E., Cheng, A. C., et al. (2017). Optimal periprosthetic tissue specimen number for diagnosis of prosthetic joint infection. *J. Clin. Microbiol.* 55, 234–243. doi: 10.1128/JCM.01914-16

Peeters, E., Nelis, H. J., and Coenye, T. (2008). Evaluation of the efficacy of disinfection procedures against Burkholderia cenocepacia biofilms. *J. Hosp. Infect.* 70, 361–368. doi: 10.1016/j.jhin.2008.08.015

Petti, C. A., Polage, C. R., and Schreckenberger, P. (2005). The role of 16S rRNA gene sequencing in identification of microorganisms misidentified by conventional methods. *J. Clin. Microbiol.* 43, 6123–6125. doi: 10.1128/JCM.43.12.6123-6125.2005

Piper, K. E., Jacobson, M. J., Cofield, R. H., Sperling, J. W., Sanchez-Sotelo, J., Osmon, D. R., et al. (2009). Microbiologic diagnosis of prosthetic shoulder infection by use of implant sonication. *J. Clin. Microbiol.* 47, 1878–1884. doi: 10.1128/JCM.01686-08

Pitt, W. G., and Ross, S. A. (2003). Ultrasound increases the rate of bacterial cell growth. *Biotechnol. Prog.* 19, 1038–1044. doi: 10.1021/bp0340685

Portillo, M. E., Salvadó, M., Alier, A., Martínez, S., Sorli, L., Horcajada, J. P., et al. (2014). Advantages of sonication fluid culture for the diagnosis of prosthetic joint infection. *J. Infect.* 69, 35–41. doi: 10.1016/j.jinf.2014.03.002

Portillo, M. E., Salvadó, M., Sorli, L., Alier, A., Martínez, S., Trampuz, A., et al. (2012). Multiplex PCR of sonication fluid accurately differentiates between prosthetic joint infection and aseptic failure. *J. Infect.* 65, 541–548. doi: 10.1016/j.jinf.2012.08.018

Portillo, M. E., Salvado, M., Trampuz, A., Plasencia, V., Rodriguez-Villasante, M., Sorli, L., et al. (2013). Sonication versus vortexing of implants for diagnosis of prosthetic joint infection. *J. Clin. Microbiol.* 51, 591–594. doi: 10.1128/JCM.02482-12

Portillo, M. E., Salvadó, M., Trampuz, A., Siverio, A., Alier, A., Sorli, L., et al. (2015). Improved diagnosis of orthopedic implant-associated infection by inoculation of sonication fluid into blood culture bottles. *J. Clin. Microbiol.* 53, 1622–1627. doi: 10.1128/JCM.03683-14

Prinz, V., Bayerl, S., Renz, N., Trampuz, A., Vajkoczy, P., and Finger, T. (2019). Sonication improves pathogen detection in ventriculoperitoneal shunt-associated infections. *Neurosurgery* 85, 516–523. doi: 10.1093/neuros/nyy383

Puges, M., Pereyre, S., Bérard, X., Accoceberry, I., Roy, C. L., Stecken, L., et al. (2018). Comparison of genus specific PCR and culture with or without sonication for microbiological diagnosis of vascular graft infection. *Eur. J. Vasc. Endovasc. Surg.* 56, 562–571. doi: 10.1016/j.ejvs.2018.06.064

Randau, T. M., Molitor, E., Fröschen, F. S., Hörauf, A., Kohlhof, H., Scheidt, S., et al. (2020). The performance of a dithiothreitol-based diagnostic system in diagnosing periprosthetic joint infection compared to sonication fluid cultures and tissue biopsies. *Z. Orthop. Unfall.* 159, 447–453. doi: 10.1055/a-1150-8396

Reischies, F. M. J., Krause, R., Holzer, J., Tiefenbacher, F., Winter, R., Eylert, G., et al. (2017). What can we learn from sonication results of breast implants? *PLoS One* 12:e0182267. doi: 10.1371/journal.pone.0182267

Relman, D. A., Schmidt, T. M., MacDermott, R. P., and Falkow, S. (1992). Identification of the uncultured bacillus of Whipple's disease. *N. Engl. J. Med.* 327, 293–301. doi: 10.1056/NEJM199207303270501

Renz, N., Feihl, S., Cabric, S., and Trampuz, A. (2017). Performance of automated multiplex PCR using sonication fluid for diagnosis of periprosthetic joint infection: a prospective cohort. *Infection* 45, 877–884. doi: 10.1007/s15010-017-1073-5

Renz, N., Mudrovcic, S., Perka, C., and Trampuz, A. (2018). Orthopedic implant-associated infections caused by *Cutibacterium* spp. – A remaining diagnostic challenge. *PLoS One* 13:e0202639. doi: 10.1371/journal.pone.0202639

Rieber, H., Frontzek, A., Heinrich, S., Breil-Wirth, A., Messler, J., Hegermann, S., et al. (2021). Microbiological diagnosis of polymicrobial periprosthetic joint infection revealed superiority of investigated tissue samples compared to sonicate fluid generated from the implant surface. *Int. J. Infect. Dis.* 106, 302–307. doi: 10.1016/j.ijid.2021.03.085

Rieger, U. M., Djedovic, G., Pattiss, A., Raschke, G. F., Frei, R., Pierer, G., et al. (2016). Presence of biofilms on polyurethane-coated breast implants: preliminary results. *J. Long Term Eff. Med. Implants* 26, 237–243. doi: 10.1615/JLongTermEffMedImplants.2016016851

Rieger, U. M., Mesina, J., Kalbermatten, D. F., Haug, M., Frey, H. P., Pico, R., et al. (2013). Bacterial biofilms and capsular contracture in patients with breast implants. *Br. J. Surg.* 100, 768–774. doi: 10.1002/bjs.9084

Rieger, U. M., Pierer, G., Lüscher, N. J., and Trampuz, A. (2009). Sonication of removed breast implants for improved detection of subclinical infection. *Aesthetic Plast Surg.* 33, 404–408. doi: 10.1007/s00266-009-9333-0

Roethlisberger, M., Moffa, G., Fisch, U., Wiggli, B., Schoen, S., Kelly, C., et al. (2018). Effectiveness of a chlorhexidine dressing on silver-coated external ventricular drain–associated colonization and infection: A prospective single-blinded randomized controlled clinical trial. *Clin. Infect. Dis.* 67, 1868–1877. doi: 10.1093/cid/ciy393

Rohacek, M., Erne, P., Kobza, R., Pfyffer, G. E., Frei, R., and Weisser, M. (2015). Infection of cardiovascular implantable electronic devices: detection with sonication, swab cultures, and blood cultures. *Pacing Clin. Electrophysiol.* 38, 247–253. doi: 10.1111/pace.12529

Rohacek, M., Weisser, M., Kobza, R., Schoenenberger, A. W., Pfyffer, G. E., Frei, R., et al. (2010). Bacterial colonization and infection of electrophysiological cardiac devices detected with sonication and swab culture. *Circulation* 121, 1691–1697. doi: 10.1161/CIRCULATIONAHA.109.906461

Rosa, L., Cutone, A., Coletti, M., Lepanto, M. S., Scotti, M., Valenti, P., et al. (2017). Biotimer assay: A reliable and rapid method for the evaluation of central venous catheter microbial colonization. *J. Microbiol. Methods* 143, 20–25. doi: 10.1016/j.mimet.2017.09.016

Rosa, L., Lepanto, M. S., Cutone, A., Berlutti, F., De Angelis, M., Vullo, V., et al. (2019). BioTimer assay as complementary method to vortex-sonication-vortex technique for the microbiological diagnosis of implant associated infections. *Sci. Rep.* 9:7534. doi: 10.1038/s41598-019-44045-1

Rothenberg, A. C., Wilson, A. E., Hayes, J. P., O'Malley, M. J., and Klatt, B. A. (2017). Sonication of arthroplasty implants improves accuracy of periprosthetic joint infection cultures. *Clin. Orthop. Relat. Res.* 475, 1827–1836. doi: 10.1007/s11999-017-5315-8

Rothman, R., Ramachandran, P., Yang, S., Hardick, A., Won, H., Kecojevic, A., et al. (2010). Use of quantitative broad-based polymerase chain reaction for detection and identification of common bacterial pathogens in cerebrospinal fluid. *Acad. Emerg. Med.* 17, 741–747. doi: 10.1111/j.1553-2712.2010.00790.x

Ryu, S. Y., Greenwood-Quaintance, K. E., Hanssen, A. D., Mandrekar, J. N., and Patel, R. (2014). Low sensitivity of periprosthetic tissue PCR for prosthetic knee infection diagnosis. *Diagn. Microbiol. Infect. Dis.* 79, 448–453. doi: 10.1016/j.diagmicrobio.2014.03.021

Sambri, A., Cadossi, M., Giannini, S., Pignatti, G., Marcacci, M., Neri, M. P., et al. (2018). Is treatment with dithiothreitol more effective than sonication for the diagnosis of prosthetic joint infection? *Clin. Orthop. Relat. Res.* 476, 137–145. doi: 10.1007/s11999.0000000000000060

Sampedro, M. F., Huddleston, P. M., Piper, K. E., Karau, M. J., Dekutoski, M. B., Yaszemski, M. J., et al. (2010). A biofilm approach to detect bacteria on removed spinal implants. *Spine* 35, 1218–1224. doi: 10.1097/BRS.0b013e3181c3b2f3

Sandbakken, E. T., Witsø, E., Sporsheim, B., Egeberg, K. W., Foss, O. A., Hoang, L., et al. (2020). Highly variable effect of sonication to dislodge biofilm-embedded Staphylococcus epidermidis directly quantified by epifluorescence microscopy: an in vitro model study. *J. Orthop. Surg.* 15:522. doi: 10.1186/s13018-020-02052-3

Sandberg, M. E., Schellmann, D., Brunhofer, G., Erker, T., Busygin, I., Leino, R., et al. (2009). Pros and cons of using resazurin staining for quantification of viable Staphylococcus aureus biofilms in a screening assay. *J. Microbiol. Methods* 78, 104–106. doi: 10.1016/j.mimet.2009.04.014

Schäfer, P., Fink, B., Sandow, D., Margull, A., Berger, I., and Frommelt, L. (2008). Prolonged bacterial culture to identify late periprosthetic joint infection: a promising strategy. *Clin. Infect. Dis.* 47, 1403–1409. doi: 10.1086/592973

Schulz, P., Dlaska, C. E., Perka, C., Trampuz, A., and Renz, N. (2021). Preoperative synovial fluid culture poorly predicts the pathogen causing periprosthetic joint infection. *Infection* 49, 427–436. doi: 10.1007/s15010-020-01540-2

Scotland, K. B., Lo, J., Grgic, T., and Lange, D. (2019). Ureteral stent-associated infection and sepsis: pathogenesis and prevention: a review. *Biofouling* 35, 117–127. doi: 10.1080/08927014.2018.1562549

Seng, P., Drancourt, M., Gouriet, F., La Scola, B., Fournier, P., Rolain, J. M., et al. (2009). Ongoing revolution in bacteriology: routine identification of bacteria by matrix-assisted laser desorption ionization time-of-flight mass spectrometry. *Clin. Infect. Dis.* 49, 543–551. doi: 10.1086/600885

Shen, H., Tang, J., Wang, Q., Jiang, Y., and Zhang, X. (2015). Sonication of explanted prosthesis combined with incubation in BD bactec bottles for pathogen-based diagnosis of prosthetic joint infection. *J. Clin. Microbiol.* 53, 777–781. doi: 10.1128/JCM.02863-14

Skogman, M. E., Vuorela, P. M., and Fallarero, A. (2012). Combining biofilm matrix measurements with biomass and viability assays in susceptibility assessments of antimicrobials against *Staphylococcus aureus* biofilms. *J. Antibiot. (Tokyo)* 65, 453–459. doi: 10.1038/ja.2012.49

Spear, S. L., and Baker, J. L. (1995). Classification of capsular contracture after prosthetic breast reconstruction. *Plast Reconstr. Surg.* 96, 1119–1123.

Stoodley, P., Conti, S. F., DeMeo, P. J., Nistico, L., Melton-Kreft, R., Johnson, S., et al. (2011). Characterization of a mixed MRSA/MRSE biofilm in an explanted total ankle arthroplasty. *FEMS Immunol. Med. Microbiol.* 62, 66–74. doi: 10.1111/j.1574-695X.2011.00793.x

Stylianakis, A., Schinas, G., Thomaidis, P. C., Papaparaskevas, J., Ziogas, D. C., Gamaletsou, M. N., et al. (2018). Combination of conventional culture, vial culture, and broad-range PCR of sonication fluid for the diagnosis of prosthetic joint infection. *Diagn. Microbiol. Infect. Dis.* 92, 13–18. doi: 10.1016/j.diagmicrobio.2018.04.008

Swearingen, M. C., DiBartola, A. C., Dusane, D., Granger, J., and Stoodley, P. (2016). 16S rRNA analysis provides evidence of biofilms on all components of three infected periprosthetic knees including permanent braided suture. *Pathog. Dis.* 74:ftw083. doi: 10.1093/femspd/ftw083

Talsma, D. T., Ploegmakers, J. J. W., Jutte, P. C., Kampinga, G., and Wouthuyzen-Bakker, M. (2021). Time to positivity of acute and chronic periprosthetic joint infection cultures. *Diagn. Microbiol. Infect. Dis.* 99:115178. doi: 10.1016/j.diagmicrobio.2020.115178

Tande, A. J., and Patel, R. (2014). Prosthetic Joint Infection. *Clin. Microbiol. Rev.* 27, 302–345. doi: 10.1128/CMR.00111-13

Tascini, C., Cardinali, G., Barletta, V., Di Paolo, A., Leonildi, A., Zucchelli, G., et al. (2016). First case of trichoderma longibrachiatum CIED (Cardiac Implantable Electronic Device)-associated endocarditis in a Non-immunocompromised Host: biofilm removal and diagnostic problems in the light of the current literature. *Mycopathologia* 181, 297–303. doi: 10.1007/s11046-015-9961-7

Thoendel, M. J., Jeraldo, P. R., Greenwood-Quaintance, K. E., Yao, J. Z., Chia, N., Hanssen, A. D., et al. (2018). Identification of prosthetic joint infection pathogens using a shotgun metagenomics approach. *Clin Infect. Dis.* 67, 1333–1338. doi: 10.1093/cid/ciy303

Tollefson, D. F., Bandyk, D. F., Kaebnick, H. W., Seabrook, G. R., and Towne, J. B. (1987). Surface biofilm disruption: enhanced recovery of microorganisms from vascular prostheses. *Arch. Surg.* 122, 38–43. doi: 10.1001/archsurg.1987.01400130044006

Trampuz, A., and Widmer, A. F. (2006). Infections associated with orthopedic implants. *Curr. Opin. Infect. Dis.* 19, 349–356. doi: 10.1097/01.qco.0000235161.85925.e8

Trampuz, A., Osmon, D. R., Hanssen, A. D., Steckelberg, J. M., and Patel, R. (2003). Molecular and antibiofilm approaches to prosthetic joint infection. *Clin. Orthop. Relat. Res.* 414, 69–88. doi: 10.1097/01.blo.0000087324.60612.93

Trampuz, A., Piper, K. E., Jacobson, M. J., Hanssen, A. D., Unni, K. K., Osmon, D. R., et al. (2007). Sonication of removed hip and knee prostheses for diagnosis of infection. *N. Engl. J. Med.* 357, 654–663. doi: 10.1056/NEJMoa061588

Travnickova, E., Mikula, P., Oprsal, J., Bohacova, M., Kubac, L., Kimmer, D., et al. (2019). Resazurin assay for assessment of antimicrobial properties of electrospun nanofiber filtration membranes. *AMB Express* 9:183. doi: 10.1186/s13568-019-0909-z

Tzeng, A., Tzeng, T. H., Vasdev, S., Korth, K., Healey, T., Parvizi, J., et al. (2015). Treating periprosthetic joint infections as biofilms: key diagnosis and management strategies. *Diagn. Microbiol. Infect. Dis.* 81, 192–200. doi: 10.1016/j.diagmicrobio.2014.08.018

Ulcar, B. K., Lakic, N., Jeverica, S., Pecavar, B., Logar, M., Cerar, T. K., et al. (2018). Contribution of sonicate-fluid cultures and broad-range PCR to microbiological diagnosis in vascular graft infections. *Infect. Dis.* 50, 429–435. doi: 10.1080/23744235.2017.1418529

Van Diek, F. M., Albers, C. G. M., Van Hooff, M. L., Meis, J. F., and Goosen, J. H. M. (2017). Low sensitivity of implant sonication when screening for infection in revision surgery. *Acta Orthop.* 88, 294–299. doi: 10.1080/17453674.2017.1300021

Viola, G. M., Mansouri, M. D., Nasir, N., and Darouiche, R. O. (2009). Incubation alone is adequate as a culturing technique for cardiac rhythm management devices. *J. Clin. Microbiol.* 47, 4168–4170. doi: 10.1128/JCM.01354-09

Virden, C. P., Frank, D. H., and Diego, S. (2020). Subclinical infection of the silicone breast implant surface as a possible cause of capsular contracture. *Aesthetic. Plast Surg.* 44, 1141–1147.

Virolainen, P., Lähteenmäki, H., Hiltunen, A., Sipola, E., Meurman, O., and Nelimarkka, O. (2002). The reliability of diagnosis of infection during revision arthroplasties. *Scand. J. Surg.* 91, 178–181. doi: 10.1177/145749690209100208

Williams, J. L., Norman, P., and Stockley, I. (2004). The value of hip aspiration versus tissue biopsy in diagnosing infection before exchange hip arthroplasty surgery. *J. Arthrop.* 19, 582–586. doi: 10.1016/j.arth.2003.11.011

Wilson, C., Lukowicz, R., Merchant, S., Valquier-Flynn, H., Caballero, J., Sandoval, J., et al. (2017). Quantitative and qualitative assessment methods for biofilm growth: A mini-review. *Res. Rev. J. Eng. Technol.* 6, 1–25.

Wouthuyzen-Bakker, M., Shohat, N., Sebillotte, M., Arvieux, C., Parvizi, J., and Soriano, A. (2019). Is Gram staining still useful in prosthetic joint infections? *J. Bone Jt. Infect.* 4, 56–59. doi: 10.7150/jbji.31312

Xu, Y., Larsen, L. H., Lorenzen, J., Hall-Stoodley, L., Kikhney, J., Moter, A., et al. (2017). Microbiological diagnosis of device-related biofilm infections. *APMIS* 125, 289–303. doi: 10.1111/apm.12676

Xu, Y., Rudkjøbing, V. B., Simonsen, O., Pedersen, C., Lorenzen, J., Schønheyder, H. C., et al. (2012). Bacterial diversity in suspected prosthetic joint infections: an exploratory study using 16S rRNA gene analysis. *FEMS Immunol. Med. Microbiol.* 65, 291–304. doi: 10.1111/j.1574-695X.2012.00949.x

Xu, Z., Liang, Y., Lin, S., Chen, D., Li, B., Li, L., et al. (2016). Crystal violet and XTT assays on *Staphylococcus aureus* biofilm quantification. *Curr. Microbiol.* 73, 474–482. doi: 10.1007/s00284-016-1081-1

Yan, Q., Karau, M. J., Greenwood-Quaintance, K. E., Mandrekar, J. N., Osmon, D. R., Abdel, M. P., et al. (2018). Comparison of diagnostic accuracy of periprosthetic tissue culture in blood culture bottles to that of prosthesis sonication fluid culture for diagnosis of Prosthetic Joint Infection (PJI) by use of bayesian latent class modeling and IDSA PJI criteria for classification. *J. Clin. Microbiol.* 56:e319–18. doi: 10.1128/JCM.00319-18

Zabramski, J. M., Whiting, D., Darouiche, R. O., Horner, T. G., Olson, J., Robertson, C., et al. (2003). Efficacy of antimicrobial-impregnated external ventricular drain catheters: a prospective, randomized, controlled trial. *J. Neurosurg.* 98, 725–730. doi: 10.3171/jns.2003.98.4.0725

Zhai, Z., Li, H., Qin, A., Liu, G., Liu, X., Wu, C., et al. (2014). Meta-analysis of sonication fluid samples from prosthetic components for diagnosis of infection after total joint arthroplasty. *J. Clin. Microbiol.* 52, 1730–1736. doi: 10.1128/JCM.03138-13

Zhang, H., Morrison, S., and Tang, Y.-W. (2015). Multiplex polymerase chain reaction tests for detection of pathogens associated with gastroenteritis. *Clin. Lab. Med.* 35, 461–486. doi: 10.1016/j.cll.2015.02.006

Zimmerli, W., and Sendi, P. (2011). Pathogenesis of implant-associated infection: the role of the host. *Semin. Immunopathol.* 33, 295–306. doi: 10.1007/s00281-011-0275-7

Conflict of Interest: The authors declare that the research was conducted in the absence of any commercial or financial relationships that could be construed as a potential conflict of interest.

Publisher's Note: All claims expressed in this article are solely those of the authors and do not necessarily represent those of their affiliated organizations, or those of the publisher, the editors and the reviewers. Any product that may be evaluated in this article, or claim that may be made by its manufacturer, is not guaranteed or endorsed by the publisher.

frontiers in Microbiology

ORIGINAL RESEARCH
published: 05 November 2021
doi: 10.3389/fmicb.2021.761111

Bacterial and Fungal Infections Promote the Bone Erosion Progression in Acquired Cholesteatoma Revealed by Metagenomic Next-Generation Sequencing

Hua Jiang[1†], Chengpeng Wu[2†], Jingjie Xu[2], Qi Wang[1], Lei Shen[1], Xunyan Ou[1], Hongyan Liu[1], Xu Han[3], Jun Wang[3], Wenchao Ding[3], Lidan Hu[4] and Xiangjun Chen[1,2]**

[1] Department of Otolaryngology, The Second Affiliated Hospital, Zhejiang University School of Medicine, Hangzhou, China, [2] Eye Center of the Second Affiliated Hospital, Institute of Translational Medicine, Zhejiang University School of Medicine, Hangzhou, China, [3] Hangzhou Matridx Biotechnology Co., Ltd., Hangzhou, China, [4] The Children's Hospital, Zhejiang University School of Medicine, National Clinical Research Center for Child Health, Hangzhou, China

OPEN ACCESS

Edited by:
María Guembe, Gregorio Marañón Hospital, Spain

Reviewed by:
Bernard Joseph Hudson, New South Wales Health Pathology, Australia
Aldert Zomer, Utrecht University, Netherlands

***Correspondence:**
Lidan Hu
hulidan@zju.edu.cn
Xiangjun Chen
chenxiangjun@zju.edu.cn

† These authors have contributed equally to this work

Specialty section:
This article was submitted to Infectious Agents and Disease, a section of the journal Frontiers in Microbiology

Received: *19 August 2021*
Accepted: *11 October 2021*
Published: *05 November 2021*

Citation:
Jiang H, Wu C, Xu J, Wang Q, Shen L, Ou X, Liu H, Han X, Wang J, Ding W, Hu L and Chen X (2021) Bacterial and Fungal Infections Promote the Bone Erosion Progression in Acquired Cholesteatoma Revealed by Metagenomic Next-Generation Sequencing. Front. Microbiol. 12:761111. doi: 10.3389/fmicb.2021.761111

An acquired cholesteatoma generally occurs as a consequence of otitis media and eustachian tube dysfunction. Patients with acquired cholesteatoma generally present with chronic otorrhea and progressive conductive hearing loss. There are many microbes reportedly associated with acquired cholesteatoma. However, conventional culture-based techniques show a typically low detection rate for various pathogenetic bacteria and fungi. Metagenomic next-generation sequencing (mNGS), an emerging powerful platform offering higher sensitivity and higher throughput for evaluating many samples at once, remains to be studied in acquired cholesteatoma. In this study, 16 consecutive patients from January 2020 to January 2021 at the Second Affiliated Hospital of Zhejiang University School of Medicine (SAHZU) were reviewed. We detected a total of 31 microbial species in patients, mNGS provided a higher detection rate compared to culture (100% vs. 31.25%, $p = 0.000034$). As the severity of the patient's pathological condition worsens, the more complex types of microbes were identified. The most commonly detected microbial genus was *Aspergillus* (9/16, 56.25%), especially in patients suffering from severe bone erosion. In summary, mNGS improves the sensibility to identify pathogens of cholesteatoma patients, and *Aspergillus* infections increase bone destruction in acquired cholesteatoma.

Keywords: acquired cholesteatoma, metagenomic next-generation sequencing (mNGS), microbes, infection, *Aspergillus*

INTRODUCTION

An acquired cholesteatoma generally occurs as a consequence of otitis media and eustachian tube dysfunction. It is characterized by chronic infection and temporal bone deterioration (Parisier, 1989). Patients with acquired cholesteatoma generally present with chronic otorrhea and progressive conductive hearing loss. In addition to hearing loss, the damaging effects of cholesteatoma can lead to serious complications, such as labyrinthitis, facial paralysis, and brain

abscess (Inagaki and Paparella, 2009). Surgery is currently regarded as the only clinical treatment option for cholesteatoma patients, which is directed at eradication of the entrapped keratinized epithelium and keratin from the middle ear and mastoid spaces. The primary goal of surgery is to create a disease-free, or risk-free ears. Nevertheless, medical management is indicated in preparation for a definitive surgical procedure, with no recommendations available to either prevent or cure the disease (Welkoborsky, 2011).

There are various microbes reportedly closely linked to acquired cholesteatoma, most commonly such as *Pseudomonas aeruginosa* and *Staphylococcus aureus* (Ricciardiello et al., 2009). Although the etiology of cholesteatoma remains unknown, previous studies have demonstrated that microbial activity may contribute to the pathogenesis and clinical behavior of cholesteatoma (Likus et al., 2016; Kalcioglu et al., 2018). However, to date, studies on the microbes associated with cholesteatoma have relied on traditional culture-based techniques for characterizing the microbiota. Since conventional culture-based techniques have a typically low detection rate due to the unculturability of many bacteria and fungi, more sensitive methods, such as 16S rRNA gene sequencing for bacteria identification have been developed to characterize microbiota (Liu et al., 2011; Kalcioglu et al., 2018; Weiss et al., 2019). The limitation of these studies based on 16S rRNA is obvious, the fungi, viruses and parasites were not considered. More recently, metagenomic next-generation sequencing (mNGS) based on the shotgun approach has been surging used for clinical diagnosis of infections (Mai et al., 2017; Wilson et al., 2017; Fan et al., 2018). Notably, mNGS offers higher sensitivity and high-throughput for evaluating many samples at once, and can provide more (and more reliable) information through sequence data than that is available through traditional culture-based analysis.

To our knowledge, no published study has yet described a mNGS-based evaluation of cholesteatoma-associated microbial communities. In this study, we apply this novel technique to investigate the diversity and composition of microbiota that accompany with cholesteatoma in order to provide insight into how these microbes contribute to the pathogenesis of cholesteatoma.

MATERIALS AND METHODS

Ethics Statement

This study was reviewed and approved by the Institutional Review Board of SAHZU. Written informed consent was obtained from every patient and all procedures were conducted in accordance with the Declaration of Helsinki.

Case Series

A total of 16 consecutive patients with cholesteatoma received surgery in the otolaryngology department of the Second Affiliated Hospital of Zhejiang University School of Medicine (SAHZU) from January 2020 to January 2021. The cholesteatoma tissue samples were obtained from patients during surgery and were collected in a sterile container. The specimens were sent for microbial bacterial and fungal smear and in our microbiological laboratory and mNGS sequencings and bioinformatic analysis by *Hangzhou Matridx Biotechnology Co*. All patients received pre-operative temporal bone CT scan and CT scores based on bone erosion (**Table 1**) were recorded.

Microbial Culture

Mycological analysis was carried out in the Microbiology Department of our hospital. Microscopic examination was performed by Zeiss Axiovert 200 under 40×, to initially detect any direct signs of bacterial or fungal infection in the debris. The remaining tissue samples were cultured on Sabouraud's Dextrose Agar for assessment of fungal growth and on blood Agar and Mac Conkey's Agar for bacterial growth. Identification of isolated colonies was based on colony morphology, pigmentation, microscopy, and other standard physiological and biochemical assays (Procop et al., 2017).

DNA Extraction, Metagenomic Sequencing, and Data Analysis

All samples were subjected to DNA extraction (each patient and "no-template" as negative control), library preparation, and next-generation sequencing (NGS). DNA extraction and library preparation were conducted using an NGS Automatic Library Preparation System (Cat. MAR002, MatriDx Biotech Corp., Hangzhou). The reagents included a Nucleic Acid Extraction Kit (Cat. MD013, MatriDx Biotech Corp., Hangzhou) and a Total DNA Library Preparation Kit (other samples) (Cat. MD001T, MatriDx Biotech Corp., Hangzhou). To control the contamination of each sequencing run, each sequencing run on Illumina Next Seq instrument included "no template" as negative control. Quality control was carried out using a bioanalyzer (Agilent 2100, Agilent Technologies, Santa Clara, CA, United States) combined with quantitative PCR to measure the adapters before sequencing. Libraries were pooled and then sequenced on an Illumina NextSeq500 system using a 75-cycle sequencing kit. A total of 10–20 million reads were obtained for each sample.

Metagenomic Next-Generation Sequencing Data Analysis

High quality sequencing data was generated after removal of short (<35 bp) reads, low quality and low complexity reads. The sequencing data was firstly demultiplexed to get the sequence reads of each sample in fastq format. Then, sequence

TABLE 1 | Scores of temporal CT scan.

Score	Pathological phenotype of CT scan	Estimated lesion area
1	Scutum and/or auditory ossicles erosion	Cholesteatoma confined to middle ear or mastoid cavity
2	Tegmen tympani erosion and/or Lateral semicircular canal erosion and/or facial nerve canal erosion and/or sigmoid sinus bone plate erosion	Cholesteatoma exceeds middle ear/mastoid cavity, or invades facial nerve

CT, computed tomography.

reads of each sample were aligned to human-specific database constructed from Homo sapiens sequences in NCBI nucleotide (nt) database using bowtie2 (Langmead and Salzberg, 2012; Wood et al., 2019) (version 2.3.5.1) for eliminating the human sequences. The remaining reads were aligned to a manual-curated microbial database using kraken2 (confidence = 0.5) for quickly classification and the classified reads of interested microorganisms were aligned again using bowtie2 for validation. Additionally, the result of microorganism classification was used to identify the potential pathogens.

Statistical Analysis

Significant differences in the relative abundance of microbial taxa (i.e., the proportions of each microbe) between patient groups (categorized by CT score) were determined using *t*-tests. Fisher's exact test were used to evaluate independent binomial variables (SPSS version 20). The p-value of ≤ 0.05 was considered statistically significant.

RESULTS

Clinical Findings

Sixteen patients with cholesteatoma were enrolled in this study. Ten were male and six were female, with an age range of 17 to 75 years. Clinical data are shown in **Table 2**. All patients showed purulent discharge and hearing loss. Two of them presented with otalgia, and two other patients displayed facial paralysis. Most frequently, pre-operation otoscopic findings were pars flaccida retraction (12/16) and three of them had granulation in the retraction pocket. Pars tensa perforation was found in two patients. The two patients who complained of otalgia had external

TABLE 2 | The demographic data and clinical features of patients with cholesteatoma.

Patients No.	Age (years)	Gender	Affected ear	Clinical presentation	Otoscopic findings	CT scores
1	44	M	R	Pulurent discharge + otalgia + HL	Postero-superior CW collapse	2
2	58	F	L	Pulurent discharge + HL	Pars flaccida retraction	2
3	17	F	R	Pulurent discharge + HL	Pars flaccida retraction	1
4	20	M	L	Pulurent discharge + HL	Pars flaccida retraction + granulation	1
5	21	M	R	Pulurent discharge + HL + FP	Pars flaccida retraction	1
6	75	F	R	Pulurent discharge + HL + FP	Pars tensa perforation	2
7	49	M	R	Pulurent discharge + HL	Pars flaccida retraction	1
8	55	M	L	Pulurent discharge + HL	Pars flaccida retraction + granulation	1
9	64	M	R	Pulurent discharge + HL	Pars flaccida retraction	2
10	62	F	R	Pulurent discharge + HL	Pars tensa perforation + granulation	1
11	74	F	L	Pulurent discharge + HL	Pars flaccida retraction	1
12	45	M	L	Pulurent discharge + otalgia + HL	Postero-superior CW collapse	2
13	43	M	R	Pulurent discharge + HL	Pars flaccida retraction	2
14	23	M	L	Pulurent discharge + HL	Pars flaccida retraction	1
15	57	F	R	Pulurent discharge + HL	Pars flaccida retraction	1
16	72	M	R	Pulurent discharge + HL	Pars flaccida retraction + granulation	2

No, number; M, male; F, female; R, right; L, left; HL, hearing loss; FP, facial paralysis; CW, canal wall.

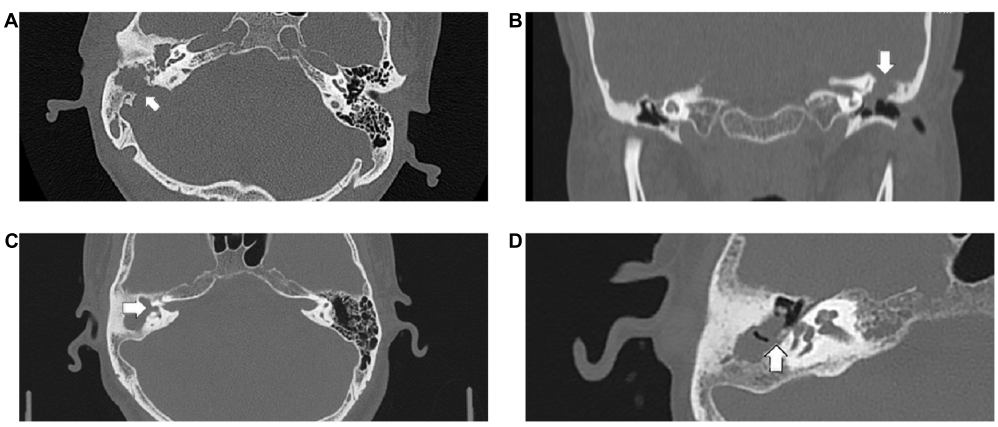

FIGURE 1 | The following CT scan findings were recorded as score 2: **(A)** the sigmoid sinus bone plate eroded (arrowed), **(B)** coronal section of the left epitympanum demonstrating a tegmen tympani defect (arrowed), **(C)** a large defect of the lateral semicircular canal (arrowed), **(D)** the pyramid segment of facial canal eroded (arrowed).

canal collapse, which precluded observation of the tympanic membrane. Seven patients with severe temporal bone erosion were recorded as CT score 2 (**Table 2** and **Figure 1**).

Microbial Culture Results

Eleven (68.75%) of the 16 patients, were negative for culturable bacteria or fungi (**Table 3**). In the remaining five patients, bacterial species were successfully cultured and identified in four cholesteatoma specimens, and fungal species were detected in only one specimen. *Staphylococcus* was the most common bacterial species (75%).

Metagenomic Next-Generation Sequencing Results

Our mNGS reads showed a 100% detection rate of potential pathogens in all cholesteatoma samples (**Table 3**). After excluding the microbial taxa that obviously originated from the environment or a background source, a total of 31 microbial species, including fungi and bacteria were recognized. Eleven samples (68.75%) had more than two different species, and cholesteatoma-specific microbiota were comprised of 2 to 8 taxa. The most commonly detected microbial genus was *Aspergillus* (11/16, 68.75%), with a huge variation in read counts (1 to 2882) and relative abundances (0.01% to 90.34%) (**Table 3**). The second most common genus was *Staphylococcus* (7/16, 43.75%), with the reads counts ranging from 113 to 1435881 and relative abundances between 1.06% and 90.99% across samples in which was detected (**Table 3**). The relative abundances of *Aspergillus* significantly varied between patient groups. Patients with the high CT scores have significantly higher relative abundances of *Aspergillus* than those with low CT scores (p = 0.023) (**Table 4** and **Figure 2**).

DISCUSSION

Several studies have used mNGS as a tool for universal pathogen detection in infectious disease, thus indicating its potential in clinical diagnoses, particularly in microbiota-associated disorders (Hu et al., 2018; Zhu et al., 2018). The advantages of mNGS sequence-based detection of microbes associated with a disease state include high throughput evaluation that can accommodate many samples at once compared to traditional PCR-based detection, the quantity of data provided by sequence is potentially much higher because bacterial, fungal, and viral community members can be detected simultaneously, and the reliability of sequence data surpasses that of traditional morphological and physiological assays (i.e., Biolog plates) for microbial identification (Jacob, 2013).

It is noteworthy that mNGS successfully identified pathogenic fungi or bacteria in all cases, whereas traditional culture-based identification found pathogenic microbes in only 31.25% of our cholesteatoma cohort. The presence and high relative abundance of microbes found by culture-based methods was confirmed by mNGS data, thereby illustrating the suitability of mNGS for detection of pathogens in cholesteatoma debris. However, the two techniques differed in the most commonly detected microbes,

TABLE 3 | Microbiological culture results and mNGS results of 16 cholesteatoma samples.

Patients No.	Microbiological culture	mNGS Organism	Reads	Relative abundance
1	Negative	*Bacteroides fragilis*	551	53.08%
2	Aspergillus flavus	*Aspergillus flavus*	2882	90.34%
3	Negative	*Enterobacter cloacae complex*	6	2.39%
4	Negative	*Candida parapsilosis*	164312	16.52%
		Mobiluncus curtisii	45456	4.61%
		Porphyromonas asaccharolytica	27033	2.74%
		Campylobacter ureolyticus	21601	2.19%
		Anaerococcus prevotii	10743	1.09%
		Staphylococcus	10485	1.06%
		Streptococcus pseudoporcinus	8225	0.83%
		Finegoldia magna	6445	0.65%
5	Negative	*Campylobacter ureolyticus*	42466	33.79%
		Finegoldia magna	11000	26.49%
		Enterococcus faecalis	2873	2.29%
6	Negative	*Aspergillus terreus*	73	15.87%
		Lactobacillus iners	86	8.74%
7	Negative	*Staphylococcus aureus*	989	75.44%
		Aspergillus	58	4.42%
		Nocardiopsis dassonvillei	13	0.99%
8	Proteus mirabilis	*Proteus mirabilis*	48358	39.87%
		Prevotella oris	19821	16.34%
		Parvimonas micra	8289	6.83%
		Campylobacter showae	7451	6.14%
		Aspergillus	2123	1.75%
9	Negative	*Aspergillus*	452	20.28%
		Streptomyces	277	12.43%
		Pseudomonas stutzeri	259	11.62%
		Nocardiopsis dassonvillei	87	3.9%
10	Corynebacterium segmentosum	*Corynebacterium segmentosum*	4541295	87.24%
		Staphylococcus	241076	4.63%
		Aspergillus	8847	0.17%
11	Staphylococcus epidermidis	*Staphylococcus epidermidis*	1435881	90.15%
		Aspergillus	792	0.05%
		Pseudomonas stutzeri	504	0.03%
12	Negative	*Anaerococcus*	288	24.26%
		Staphylococcus caprae	113	9.52%
		Peptoniphilus harei	102	8.51%
		Aspergillus	6	0.51%
13	Staphylococcus aureus	*Staphylococcus aureus*	37824	90.99%

(Continued)

TABLE 3 | (Continued)

Patients No.	Microbiological culture	mNGS Organism	Reads	Relative abundance
14	Negative	*Prevotella buccalis*	25447	31.99%
		Anaerococcus hydrogenalis	15306	19.24%
		Pseudomonas aeruginosa	6468	8.13%
		Finegoldia magna	4354	5.47%
		Trichophyton rubrum	285	0.36%
		Aspergillus	1	0.01%
15	Negative	*Aspergillus*	1	2.08%
16	Negative	*Staphylococcus caprae*	110286	64.73%
		Corynebacterium jeikeium	34988	20.54%
		Aspergillus	14	0.01%

TABLE 4 | Relative abundances of *Aspergillus* in patients with different CT scores.

CT scores	Patients No.	Relative abundances (%)	Reads
2	1	0	0
	2	90.34	2882
	6	15.87	73
	9	20.28	452
	12	0.51	6
	13	0	0
	16	0.01	14
1	3	0	0
	4	0	0
	5	0	0
	7	4.42	58
	8	1.75	2123
	10	0.17	8847
	11	0.05	792
	14	0.01	1
	15	2.08	1

CT, computed tomography.

since culture methods showed *Staphylococcus* as a predominant taxon, while mNGS showed *Aspergillus* as the most common pathogen associated with cholesteatoma. Besides, *Staphylococcus* was still the second most common pathogens by mNGS. These mNGS results thus offer a new perspective on the effects incurred by microbiota on the development of cholesteatoma.

Standard textbook descriptions of cholesteatoma have historically included bacteria associated with this disorder, but have almost completely neglected the fungal constituents of the debris. Previous studies of chronic rhinosinusitis biofilms have revealed the presence of fungal constituents (Healy et al., 2008), alternatively, fungal colonization of cholesteatoma had been sparsely studied. Especially two studies cultured the fungi from cholesteatoma tissue (Effat and Madany, 2014; Singh et al., 2018). Singh et al. (2018) cultured 40 cholesteatoma samples and successfully isolated fungi from 17 of the specimens (42.5%).

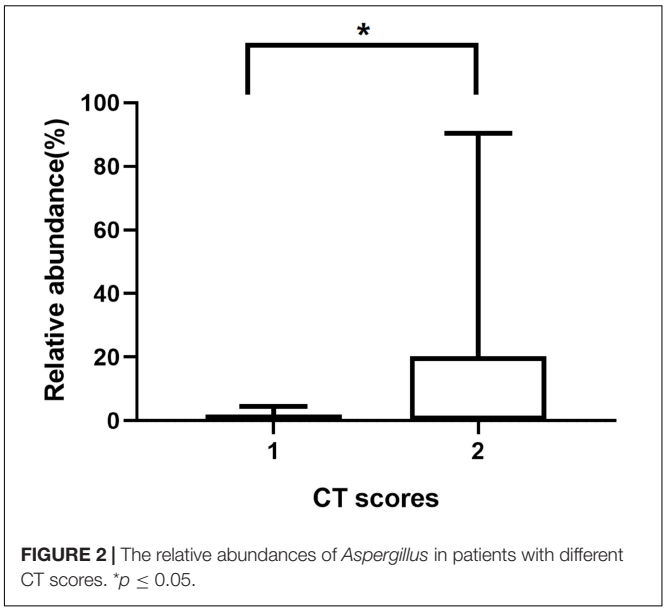

FIGURE 2 | The relative abundances of *Aspergillus* in patients with different CT scores. *$p \leq 0.05$.

Among these 17 cases, 6 cases had detectable grown of both fungi and bacteria. Effat and Madany (2014) obtained keratinous debris from 18 patients (19 ears) with cholesteatoma and found culturable fungi in 17 of the samples (89%), but reported no data on culturable bacterial. More recently, Weiss et al. (2019) evaluated the microbiota associated with cholesteatoma by 16S rDNA gene sequencing in 19 patients. A total of 96 bacterial species and 34 fungal species were identified in association with the cholesteatoma matrix, but no difference was found between the relative abundance of fungal and bacterial taxa prevalent in the diseased tissue compared with that of the adjacent, uninvolved middle ear.

In our study, we used mNGS to analyze the cholesteatoma microbiome for the presence of pathogens. In contrast with conventional culture methods and 16S rDNA gene sequencing, mNGS offers higher sensitivity and throughput microbial pathogen detection and microbiome analyses due to its capacity for simultaneous detection of bacteria and fungi. In our case series, a total of 12 cases (12/16, 75%) exhibited detectable fungal infection, among which 10 cases (10/16, 62.5%) had both bacterial and fungal microbes, a substantially higher proportion than that reported through culture-based investigation (6/17, 35.3%) (Singh et al., 2018). The common fungal genus specifically associated with cholesteatoma in our cholesteatoma cohort was *Aspergillus*, differing from the consistent prevalence of *Alternaria* reported by Weiss et al. (2019). Moreover, only two cases in this study had *Aspergillus* in the absence of any significant bacterial taxa.

As discussed above, fungi have been found to colonize bacterial biofilms in chronic rhinosinusitis. In cholesteatomas, bacterial biofilms were also detected by electron microscopy (Saunders et al., 2011). In the current study, both bacterial and fungal growth was detected in more than half of the samples, consistent with that fungi also likely reside in bacterial biofilms related to cholesteatomas. Some studies have investigated the

interactions between bacteria and fungi and their impact on the efficacy of antimicrobial agents. In chronic rhinosinusitis, for example, fungi and bacteria were found to act synergistically against host defenses and antibiotics (Healy et al., 2008). Studies exploring the mechanism underpinning this phenomenon proposed that fungi could interact with bacteria to become coated in the biofilm matrix which subsequently served as a barrier preventing diffusion of antimicrobial agents and facilitating the secretion and diffusion of polysaccharides by fungal cells (Harriott and Noverr, 2010; Kong et al., 2016). The interaction between fungi and bacteria may be also associated with poor response to antibiotic therapy in cholesteatoma. In future studies, we will explore the mechanism behind this phenomenon of the relationship between *Aspergillus* and cholesteatoma.

A study by Kauffman et al. (2000) using airway-derived epithelial cell line A549 and primary epithelial nasal cells found that exposure to *Aspergillus* extracts resulted in cell shrinking, cell desquamation, and proinflammatory cytokine production. More recently, Patel et al. (2019) demonstrated that *Aspergillus* could stimulate IL-25 secretion and elicit type 2 inflammation in non-invasive fungal rhinosinusitis. It is therefore plausible that *Aspergillus* could play a role in cholesteatoma progression. To explore this possibility in our study, we used CT scans to evaluate bone erosion related to cholesteatoma and found that *Aspergillus* infection was identified more often in cases with severe bone erosion, compared with its prevalence in cases with minor bone erosion. Similarly, in allergic fungal rhinosinusitis, *Aspergillus* was also reportedly associated with bone destruction (Marfani et al., 2010). Many studies have focused on osteoprotegerin (OPG), a receptor activator of nuclear factor κB (RANK) and RANK ligand (RANKL), in cholesteatoma-related bone erosion (Jeong et al., 2006; Kuczkowski et al., 2010; Likus et al., 2016). However, some inconsistencies remain in the relationship between these proteins and cholesteatoma. Specifically, although inflammatory cytokines and bacteria were thought to be correlated with OPG and RANKL expression and bone destruction in cholesteatoma (Haruyama et al., 2010; Kalcioglu et al., 2018), no significant differences were observed in the expression of OPG and RANKL between the cholesteatoma cases with and without bacterial infections (Kalcioglu et al., 2018). Thus, further study the role of fungi and bacteria in bone erosion in cholesteatoma is warranted.

In conclusion, this study represents the first report to our knowledge using mNGS to detect microbes in cholesteatoma samples. It is noteworthy that the most commonly detected microbe specifically associated with cholesteatoma is *Aspergillus* and its presence is apparently related to increase the degree of bone destruction. This study had some limitations, such as relatively small sample size and use of CT scoring to differentiate disease states instead of healthy control subjects. In addition, the read counts varied greatly between samples. It is possible that water lavage during oto-surgery may have resulted in the loss or reduction in microbial load during surgery. To accommodate this issue in the present study, the cut-off value for potential pathogen detection was set low and at least one unique read was used as a threshold. However, similar methods have been used by other mNGS studies (Miao et al., 2018; Wang et al., 2019). Regardless of its limitations, the results provided by this mNGS analysis likely represent the most accurate characterization of the cholesteatoma microbiota to date and provide insight into how microbial taxa may contribute to the severity of this disease.

DATA AVAILABILITY STATEMENT

The datasets presented in this study can be found in online repositories. The names of the repository/repositories and accession number(s) can be found below: NCBI (accession: PRJNA768391).

ETHICS STATEMENT

The studies involving human participants were reviewed and approved by The Second Affiliated Hospital, Zhejiang University School of Medicine. The patients/participants provided their written informed consent to participate in this study. Written informed consent was obtained from the individual(s) for the publication of any potentially identifiable images or data included in this article.

AUTHOR CONTRIBUTIONS

XC and HJ conceived and designed the study. XC, HJ, and LH analyzed the data. HJ, QW, LS, XO, and HL collected the related clinical information. HJ, CW, JX, XH, JW, and WD conducted the infection samples associated with the study. XH, JW, and WD provided the technical support. XC and HJ wrote the draft. LH, JX, and CW revised the draft. All authors approved the final version. All authors contributed to the article and approved the submitted version.

FUNDING

This work was supported by grants from the Science Technology Project of Zhejiang Province (Grant Numbers 2018C37058 and LGC19H120002) and the Natural Science Foundation of Zhejiang Province for Distinguished Young Scholar (Grant Number LR21H120001).

ACKNOWLEDGMENTS

We thank the patient for cooperating with our investigation and acknowledge Hangzhou Matridx Biotechnology Company for performing mNGS.

SUPPLEMENTARY MATERIAL

The Supplementary Material for this article can be found online at: https://www.frontiersin.org/articles/10.3389/fmicb.2021.761111/full#supplementary-material

REFERENCES

Effat, K., and Madany, N. (2014). Mycological study on cholesteatoma keratin obtained during primary mastoid surgery. *J. Laryngol. Otol.* 128:881. doi: 10.1017/S0022215114002059

Fan, S., Ren, H., Wei, Y., Mao, C., Ma, Z., Zhang, L., et al. (2018). Next-generation sequencing of the cerebrospinal fluid in the diagnosis of neurobrucellosis. *Int. J. Infect. Dis.* 67, 20–24. doi: 10.1016/j.ijid.2017.11.028

Harriott, M. M., and Noverr, M. C. (2010). Ability of Candida albicans mutants to induce Staphylococcus aureus vancomycin resistance during polymicrobial biofilm formation. *Antimicrob. Agents Chemother.* 54, 3746–3755. doi: 10.1128/AAC.00573-10

Haruyama, T., Furukawa, M., Kusunoki, T., Onoda, J., and Ikeda, K. (2010). Expression of IL-17 and its role in bone destruction in human middle ear cholesteatoma. *ORL J. Otorhinolaryngol. Relat. Spec.* 72, 325–331. doi: 10.1159/000319897

Healy, D. Y., Leid, J. G., Sanderson, A. R., and Hunsaker, D. H. (2008). Biofilms with fungi in chronic rhinosinusitis. *Otolaryngol. Head Neck Surg.* 138, 641–647. doi: 10.1016/j.otohns.2008.02.002

Hu, Z., Weng, X., Xu, C., Lin, Y., Cheng, C., Wei, H., et al. (2018). Metagenomic next-generation sequencing as a diagnostic tool for toxoplasmic encephalitis. *Ann. Clin. Microbiol. Antimicrob.* 17:45. doi: 10.1186/s12941-018-0298-1

Inagaki, T., and Paparella, M. M. (2009). Chronic otitis media with cholesteatoma: middle ear/inner ear interaction. *Otol. Neurotol.* 30, 430–431. doi: 10.1097/MAO.0b013e31818600db

Jacob, H. J. (2013). Next-generation sequencing for clinical diagnostics. *N. Engl. J. Med.* 369, 1557–1558. doi: 10.1056/NEJMe1310846

Jeong, J. H., Park, C. W., Tae, K., Lee, S. H., Shin, D. H., Kim, K. R., et al. (2006). Expression of RANKL and OPG in middle ear cholesteatoma tissue. *Laryngoscope* 116, 1180–1184. doi: 10.1097/01.mlg.0000224345.59291.da

Kalcioglu, M. T., Guldemir, D., Unaldi, O., Egilmez, O. K., Celebi, B., and Durmaz, R. (2018). Metagenomics analysis of bacterial population of tympanosclerotic plaques and cholesteatomas. *Otolaryngol. Head Neck Surg.* 159, 724–732. doi: 10.1177/0194599818772039

Kauffman, H. F., Tomee, J. C., Van De Riet, M. A., Timmerman, A. J., and Borger, P. (2000). Protease-dependent activation of epithelial cells by fungal allergens leads to morphologic changes and cytokine production. *J. Allergy Clin. Immunol.* 105, 1185–1193. doi: 10.1067/mai.2000.106210

Kong, E. F., Tsui, C., Kucharíková, S., Andes, D., Van Dijck, P., and Jabra-Rizk, M. A. (2016). Commensal protection of Staphylococcus aureus against antimicrobials by Candida albicans biofilm matrix. *MBio* 7, e1365–16. doi: 10.1128/mBio.01365-16

Kuczkowski, J., Sakowicz-Burkiewicz, M., and Iżycka-Świeszewska, E. (2010). Expression of the receptor activator for nuclear factor-κB ligand and osteoprotegerin in chronic otitis media. *Am. J. Otolaryngol.* 31, 404–409. doi: 10.1016/j.amjoto.2009.06.004

Langmead, B., and Salzberg, S. L. (2012). Fast gapped-read alignment with Bowtie 2. *Nat. Methods* 9:357. doi: 10.1038/nmeth.1923

Likus, W., Siemianowicz, K., Markowski, J., Wiaderkiewicz, J., Kostrząb-Zdebel, A., Jura-Szołtys, E., et al. (2016). Bacterial infections and osteoclastogenesis regulators in men and women with cholesteatoma. *Arch. Immunol. Ther. Exp.* 64, 241–247. doi: 10.1007/s00005-015-0373-7

Liu, C. M., Cosetti, M. K., Aziz, M., Buchhagen, J. L., Contente-Cuomo, T. L., Price, L. B., et al. (2011). The otologic microbiome: a study of the bacterial microbiota in a pediatric patient with chronic serous otitis media using 16SrRNA gene-based pyrosequencing. *Arch. Otolaryngol. Head Neck Surg.* 137, 664–668. doi: 10.1001/archoto.2011.116

Mai, N. T. H., Phu, N. H., Nhu, L. N. T., Hong, N. T. T., Hanh, N. H. H., Nguyet, L. A., et al. (2017). Central nervous system infection diagnosis by next-generation sequencing: a glimpse into the future?. *Open Forum Infect. Dis.* 4:ofx046. doi: 10.1093/ofid/ofx046

Marfani, M., Jawaid, M., Shaikh, S., and Thaheem, K. (2010). Allergic fungal rhinosinusitis with skull base and orbital erosion. *J. Laryngol. Otol.* 124:161. doi: 10.1017/S0022215109991253

Miao, Q., Ma, Y., Wang, Q., Pan, J., Zhang, Y., Jin, W., et al. (2018). Microbiological diagnostic performance of metagenomic next-generation sequencing when applied to clinical practice. *Clin. Infect. Dis.* 67, S231–S240. doi: 10.1093/cid/ciy693

Parisier, S. C. (1989). Management of cholesteatoma. *Otolaryngol. Clin. North Am.* 22, 927–940. doi: 10.1016/S0030-6665(20)31368-2

Patel, N. N., Triantafillou, V., Maina, I. W., Workman, A. D., Tong, C. C., Kuan, E. C., et al. (2019). Fungal extracts stimulate solitary chemosensory cell expansion in noninvasive fungal rhinosinusitis. *Int. Forum Allergy Rhinol.* 9, 730–737. doi: 10.1002/alr.22334

Procop, G. W., Church, D., Hall, G., and Janda, W. (2017). *Koneman's Color Atlas and Textbook of Diagnostic*. Philadelphia: Wolters Kluwer.

Ricciardiello, F., Cavaliere, M., Mesolella, M., and Iengo, M. (2009). Notes on the microbiology of cholesteatoma: clinical findings and treatment. *Acta Otorhinolaryngol. Ital.* 29:197.

Saunders, J., Murray, M., and Alleman, A. (2011). Biofilms in chronic suppurative otitis media and cholesteatoma: scanning electron microscopy findings. *Am. J. Otolaryngol.* 32, 32–37. doi: 10.1016/j.amjoto.2009.09.010

Singh, G. B., Solo, M., Kaur, R., Arora, R., and Kumar, S. (2018). Mycology of chronic suppurative otitis media-cholesteatoma disease: an evaluative study. *Am. J. Otolaryngol.* 39, 157–161. doi: 10.1016/j.amjoto.2017.12.001

Wang, S., Chen, Y., Wang, D., Wu, Y., Zhao, D., Zhang, J., et al. (2019). The feasibility of metagenomic next-generation sequencing to identify pathogens causing tuberculous meningitis in cerebrospinal fluid. *Front. Microbiol.* 10:1993. doi: 10.3389/fmicb.2019.01993

Weiss, J. P., Antonelli, P. J., and Dirain, C. O. (2019). Microbiome Analysis of Cholesteatoma by Gene Sequencing. *Otol. Neurotol.* 40, 1186–1193. doi: 10.1097/MAO.0000000000002355

Welkoborsky, H. (2011). Current concepts of the pathogenesis of acquired middle ear cholesteatoma. *Laryngorhinootologie* 90, 38–48. doi: 10.1055/s-0030-1268464

Wilson, M. R., Suan, D., Duggins, A., Schubert, R. D., Khan, L. M., Sample, H. A., et al. (2017). A novel cause of chronic viral meningoencephalitis: cache Valley virus. *Ann. Neurol.* 82, 105–114. doi: 10.1002/ana.24982

Wood, D. E., Lu, J., and Langmead, B. (2019). Improved metagenomic analysis with Kraken 2. *Genome Biol.* 20:257. doi: 10.1186/s13059-019-1891-0

Zhu, Y.-M., Ai, J.-W., Xu, B., Cui, P., Cheng, Q., Wu, H., et al. (2018). Rapid and precise diagnosis of disseminated T. marneffei infection assisted by high-throughput sequencing of multifarious specimens in a HIV-negative patient: a case report. *BMC Infect. Dis.* 18:379. doi: 10.1186/s12879-018-3276-5

Conflict of Interest: XH, JW, and WD are employed by "Matridx Biotechnology Co., Ltd."

The remaining authors declare that the research was conducted in the absence of any commercial or financial relationships that could be construed as a potential conflict of interest.

Publisher's Note: All claims expressed in this article are solely those of the authors and do not necessarily represent those of their affiliated organizations, or those of the publisher, the editors and the reviewers. Any product that may be evaluated in this article, or claim that may be made by its manufacturer, is not guaranteed or endorsed by the publisher.

Advantages of publishing in Frontiers

OPEN ACCESS
Articles are free to read for greatest visibility and readership

FAST PUBLICATION
Around 90 days from submission to decision

HIGH QUALITY PEER-REVIEW
Rigorous, collaborative, and constructive peer-review

TRANSPARENT PEER-REVIEW
Editors and reviewers acknowledged by name on published articles

Frontiers
Avenue du Tribunal-Fédéral 34
1005 Lausanne | Switzerland

Visit us: www.frontiersin.org
Contact us: frontiersin.org/about/contact

REPRODUCIBILITY OF RESEARCH
Support open data and methods to enhance research reproducibility

DIGITAL PUBLISHING
Articles designed for optimal readership across devices

FOLLOW US
@frontiersin

IMPACT METRICS
Advanced article metrics track visibility across digital media

EXTENSIVE PROMOTION
Marketing and promotion of impactful research

LOOP RESEARCH NETWORK
Our network increases your article's readership